1871
ИнБЮМ – IBSS

ISSN 2499-9768 print

МОРСКОЙ БИОЛОГИЧЕСКИЙ ЖУРНАЛ

MARINE BIOLOGICAL JOURNAL

Vol. 8 No. 1
2023

300 years
Russian Academy of Sciences

МОРСКОЙ БИОЛОГИЧЕСКИЙ ЖУРНАЛ
MARINE BIOLOGICAL JOURNAL
Выпуск посвящён 300-летию Российской академии наук.
Журнал включён в перечень рецензируемых научных изданий, рекомендованных ВАК Российской Федерации, а также в базу данных Russian Science Citation Index (RSCI).
Журнал реферируется международной библиографической и реферативной базой данных Scopus (Elsevier), международной информационной системой по водным наукам и рыболовству ASFA (ProQuest), Всероссийским институтом научно-технической информации (ВИНИТИ), а также Российским индексом научного цитирования (РИНЦ) на базе Научной электронной библиотеки elibrary.ru.
Все материалы проходят независимое двойное слепое рецензирование.

Адрес учредителя, издателя и редакции:
ФИЦ «Институт биологии южных морей имени А. О. Ковалевского РАН».
Пр-т Нахимова, 2, Севастополь, 299011, РФ.
Тел.: +7 8692 54-41-10. E-mail: *mbj@imbr-ras.ru*.
Сайт журнала: https://marine-biology.ru.

Адрес соиздателя:
Зоологический институт РАН.
Университетская наб., 1, Санкт-Петербург, 199034, РФ.

Founder, Publisher, and Editorial Office address:
A. O. Kovalevsky Institute of Biology of the Southern Seas of Russian Academy of Sciences.
2 Nakhimov ave., Sevastopol, 299011, Russia.
Tel.: +7 8692 54-41-10. E-mail: *mbj@imbr-ras.ru*.
Journal website: https://marine-biology.ru.

Co-publisher address:
Zoological Institute Russian Academy of Sciences.
1 Universitetskaya emb., Saint Petersburg, 199034, Russia.

A. O. KOVALEVSKY INSTITUTE OF BIOLOGY OF THE SOUTHERN SEAS OF RAS
ZOOLOGICAL INSTITUTE OF RAS

МОРСКОЙ БИОЛОГИЧЕСКИЙ ЖУРНАЛ

MARINE BIOLOGICAL JOURNAL

2023 Vol. 8 no. 1

Established in February 2016 SCIENTIFIC JOURNAL *4 issues per year*

CONTENTS

1871
ИнБЮМ – IBSS

Морской биологический журнал
Marine Biological Journal
2023, vol. 8, no. 1, pp. 3–15
https://marine-biology.ru

SCIENTIFIC COMMUNICATIONS

UDC 598.231.25-154(292.471-13)“2019/2020”

FEATURES OF HYDROPHILIC BIRDS WINTERING AT SEA COASTS OF SOUTHERN CRIMEA UNDER CONDITIONS OF THE MILD WINTER 2019/2020

© 2023 **M. M. Beskaravayny[1] and V. E. Giragosov[2]**

[1]T. I. Vyazemsky Karadag Scientific Station – Nature Reserve of RAS – Branch of IBSS, Feodosiya, Russian Federation

[2]A. O. Kovalevsky Institute of Biology of the Southern Seas of RAS, Sevastopol, Russian Federation

E-mail: *karavay54@mail.ru*

Received by the Editor 30.07.2020; after reviewing 11.01.2021;
accepted for publication 20.10.2022; published online 14.03.2023.

In the Southern Crimea, the main winter habitat for hydrophilic birds is the coastal zone. In this area, species and quantitative composition of birds has been studied quite fully, *inter alia* under extreme cold conditions. A comparison of features of bird wintering in warm and cold winters is of interest since it allows to clarify the effect of weather conditions on the state of ornithological complexes and dynamics of intra-regional bird migrations. The aim of this research was to identify the species composition, abundance, and biotopic distribution of hydrophilic birds in the Southern Crimea under mild winter conditions. The study was carried out in the area from the Primorsky village near Feodosiya to Sevastopol (about 250 km) in the winter 2019/2020 characterized by prevalence of positive temperatures. The main coastal biotopes were surveyed: water areas off the open sea coasts, closed bays, and liman lakes. Off the open coasts, 24 species were revealed; this is significantly less than in cold seasons (for comparison: 41 species wintered there in the cold winter 2012). Lari and Anseriformes prevailed in species diversity. High abundance and active longshore migration of Levantine shearwater and great cormorant were recorded. The abundance of Anseriformes, coot, and some gull species was lower than in cold winters. In Sevastopol bays, 29 species were registered (for comparison: 35 species wintered there in cold January 2008). Anseriformes and Lari prevailed in species diversity, while coot and black-headed gull prevailed in abundance. On liman lakes, 24 wintering species were noted; coot and Anseriformes, mainly common pochard, prevailed in abundance. In total, 44 bird species (61.1% of wintering in the area) representing 11 orders were recorded in all the studied biotopes in the mild winter 2019/2020. The features of this winter were high abundance of Levantine shearwater and wintering of red-throated diver, parasitic jaeger, and Bewick’s swan.

Keywords: hydrophilic birds, Southern Crimea, wintering, mild winter, open coasts, closed bays, liman lakes, species composition, abundance

The coastal zone of the Southern Crimea with the adjacent marine area is the main winter habitat for hydrophilic birds. Weather conditions in the Northern Black Sea Region determining the nature and intensity of intra-regional bird migrations are among the key factors affecting quantitative

and qualitative composition of winter ornithological complexes in this zone. Specifically, during extreme cold snaps accompanied by freeze-up and snowfalls in the Northern Crimea and Sivash area, a mass bird migration to non-freezing water areas off the southern coasts occurs, and this is a characteristic feature of wintering in Crimea [Pusanow, 1933]. In winter seasons with moderate temperature, the coasts of the Southern Crimea are significantly inferior to the coasts of the Northern Crimea both in species diversity and abundance of wintering birds.

To date, the species composition and quantitative characteristics of winter ornithological complexes off the coast of the Southern Crimea have been studied quite fully [Andryushchenko et al., 2012; Beskaravayny, 2008, 2013; Beskaravayny, Kostin S., 1999; Mosalov et al., 2002], with the focus on wintering under cold conditions [Andryushchenko et al., 2012; Beskaravayny, 2010]. To clarify the effect of weather conditions on the species composition and abundance of wintering birds, as well as to reveal the patterns of their long-term dynamics, it is interesting to compare the features of wintering in cold and warm winters. The aim of this work is to identify the species composition, abundance, and biotopic distribution of hydrophilic birds wintering off the coast of the Southern Crimea under mild weather conditions, on the example of the winter season 2019/2020.

MATERIAL AND METHODS

The material was collected in 2019/2020 in the Southern Crimea area from the Primorsky village near Feodosiya to Sevastopol (about 250 km along the coastline). All the main biotopes of marine origin where hydrophilic birds use to winter were covered with observations – water areas off the open sea coasts, closed bays, and liman lakes. The objects of observations and counting were mainly representatives of the orders Gaviiformes, Podicipediformes, Procellariiformes, Pelecaniformes, Ciconiiformes, Anseriformes, Gruiformes, and Charadriiformes. We also counted some species from other orders that are ecologically closely related to near-aquatic biotopes: the marsh harrier *Circus aeruginosus* (Linnaeus, 1758), common kingfisher *Alcedo atthis* (Linnaeus, 1758), and reed bunting *Emberiza schoeniclus* (Linnaeus, 1758).

Species counted from the second half of December to the first decade of February (the period when the autumn migration is over and the spring migration has not yet begun) were attributed to wintering species. Observations and quantitative counting were carried out mainly in January. Three areas were covered (Fig. 1): eastern (waters of the western Feodosiya Gulf, vicinity of Feodosiya, the Karadag Nature Reserve, and the Kurortnoye village), central (vicinity of Yalta and the Cape Martyan Nature Reserve), and western (Sevastopol). On the water areas off the open sea coasts, birds were counted on six alongshore routes 1–4.2 km long, with a coastal strip analyzed about 1 km wide. Individuals sitting on the water area and on the coast and individuals migrating along the coastline were counted separately.

On the water areas of coastal liman lakes and closed bays, all the observed individuals were counted. In total, 2 lakes and 5 bays were surveyed. To compare quantitative characteristics of ornithological complexes, we used such parameters as the relative abundance (*per* 1 km^2 of a water area) and the Shannon diversity index (H) [Pesenko, 1982]. Calculations were carried out in Microsoft Excel.

Binoculars with 10× magnification were used for observations and counting. In some cases, photographing was used. The weather conditions are characterized according to the data of the website [Weather Forecast and Archive, 2020].

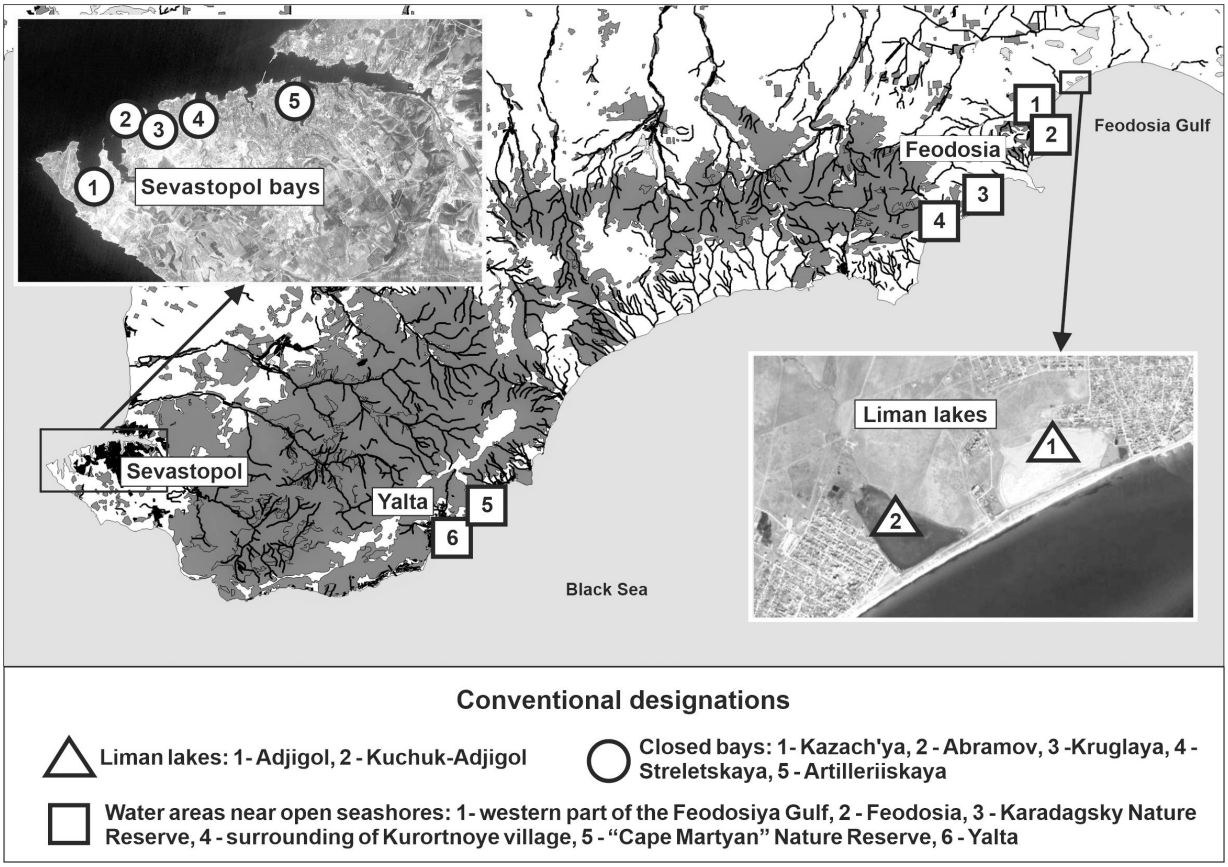

Fig. 1. Schematic map of the area with the spots of bird counting

Wintering conditions for hydrophilic birds in 2019/2020. The coastal zone of the Southern Crimea includes a wide range of stations of marine origin; those have been classified and described in detail in the work published earlier [Beskaravayny, 2008]. Within the boundaries of the studied area, we consider the following main types of habitats for hydrophilic birds.

1. Water areas off the open sea coasts.

1.1. Water area near deeper coasts. For a considerable distance, it is adjacent to the coastline of the Southern Crimea. This water area is characterized by the largest bottom slope (usually 1–2°; the depth within the coastal strip analyzed reaches 30–50 m) and prevalence of pebble bottom substrate and pebble beaches.

1.2. Water area near shallow coasts. It washes the Feodosiya Gulf which is characterized by sand-and-shell beaches and a slight slope (< 1°) of the silty-sand bottom (the depth within the coastal strip analyzed reaches 14–15 m).

Specific biotopes are water areas adjacent to the coasts of large cities – Feodosiya in the western Feodosiya Gulf and Yalta in the central Southern coast. The sea pollution and the construction of artificial beaches result in the change or destruction of benthic communities which form a natural food base. On the other hand, birds find alternative food sources in cities – food waste and feeding.

2. Closed bays. Birds were counted in the Kazachya, Abramov, Kruglaya, Streletskaya, and Artilleriiskaya bays located on the northern coast of the Heracles Peninsula, within the city of Sevastopol. With a width of 0.2–1.9 km, these bays are cut into the coastline for 0.4–2.2 km. In mouth areas, the depth is 15–20 m; in upper areas inhabited by at least 90% of birds, the depth does not exceed 3 m. In some bays, there are fragments of reed communities.

3. Liman salt lakes Adzhigol and Kuchuk-Adzhigol near the eastern Feodosiya. They are separated from the sea by sandy barriers 100–120 m wide. Due to low precipitation in 2019, the area of these lakes was relatively small in the winter 2019/2020 (Adzhigol Lake, 0.25 km^2; Kuchuk-Adzhigol Lake, 0.30 km^2), and the depth was about 0.5 m. These lakes can serve as winter habitats for birds only during frost-free periods, when they are not covered in ice.

After the most significant cold snap of the early XXI century (in late January–February 2012) [Andryushchenko et al., 2012], winter seasons were characterized by the lack of deep and prolonged temperature drops. Over the past seven years (2014–2020), average air and sea surface temperature in January in bird counting areas was as follows: in Feodosiya, + 2.2 and +8.9 °C, respectively; in Yalta, +4.2 and +9.8 °C; in Sevastopol, +3.8 and +9.4 °C. On average for three areas, the values were +3.4 and +9.4 °C, respectively. In the main period of bird counting (January 2020), the results of which are given in this article, the average air temperature for the area was +4.0 °C; water temperature was +10.1 °C [Weather Forecast and Archive, 2020]. These values correspond to indicators of a mild winter for the Southern coast of Crimea. Positive temperature prevailed in the Northern Crimea and Sivash area as well – in the areas of mass wintering of hydrophilic birds. The periods with sub-zero air temperature were short; those occurred mainly in January and February (as a rule, not lower than –2 °C and no more than 3 consecutive days). A cold snap with snowfall in the Southern Crimea (–6…–9 °C) and in northern areas (down to –12 °C) occurred on 7–10 February.

RESULTS AND DISCUSSION

Ornithological complex of the water area off the open coasts. In this biotope, the formation of the winter ornithological complex began in mid-September, with the arrival of regular small aggregations of the mallard *Anas platyrhynchos* Linnaeus, 1758 (13 individuals) and black-headed gull *Larus ridibundus* Linnaeus, 1766 (30) in the vicinity of Feodosiya. In October, the great crested grebe *Podiceps cristatus* (Linnaeus, 1758) was recorded (first date was 14 October), and the black-throated diver *Gavia arctica* Linnaeus, 1758 was noted (20 October). On 10 November, the mute swan *Cygnus olor* (Gmelin, 1789) and coot *Fulica atra* Linnaeus, 1758 were registered in the vicinity of Feodosiya. With a significant delay, compared to the arrival in previous years, the arrival of the black-necked grebe *Podiceps nigricollis* Brehm, 1831 was recorded – on 8 November (the average long-term date is 5 October [Beskaravayny, 2008]). In the period from mid-December to late January, the maximum abundance of the Levantine shearwater *Puffinus yelkouan* (Acerbi, 1827) was noted. By mid-March, the mute swan and mallard mostly left their wintering grounds. From the second half to the end of this month, there was the gradual departure of the black-headed gull.

In total, 24 species were revealed off the open sea coasts in winter 2019/2020 (taking into account the Arctic skua *Stercorarius parasiticus* (Linnaeus, 1758) registered near Sevastopol on 19.12.2019 and the Levantine shearwater and common shelduck *Tadorna tadorna* (Linnaeus, 1758) observed only flying over the water area). Out of them, 4 species (the red-necked grebe *Podiceps grisegena* (Boddaert, 1783), Levantine shearwater, Arctic skua, and little gull *Larus minutus* Pallas, 1776) were specific for this ornithological complex (Table 1). This accounts for 37.5% of the total number of species known for this biotope (at least 64) [Andryushchenko et al., 2012; Beskaravayny, 2008; Beskaravayny, Kostin S., 1999; Mosalov et al., 2002], and the value is much lower than in seasons with extreme cold snaps. Specifically, during the latest cold snap (January–February 2012), wintering of 41 species was recorded in this biotope [Andryushchenko et al., 2012].

Table 1. Abundance of wintering birds off the open sea coasts in 2019/2020

Species	Coastal water areas with great depths (Southern coast)			Coastal water areas with shallow depths (Feodosiya Gulf)		Counted in total, 14.5 km
	Eastern area – the Karadag Nature Reserve and the vicinity of the Kurortnoye village, 5 km	Central area		Vicinity of the Primorsky village, 4.2 km	Feodosiya, 2.3 km	
		The Cape Martyan Nature Reserve, 2 km	Yalta, 1 km			
Gavia arctica	15 / 3.0	–	–	47 / 11.2 (11)	1 / 0.4	63 (11)
Podiceps nigricollis	21 / 4.2	–	3 / 3.0	7 / 1.7	28 / 12.2	59
Podiceps grisegena	–	–	–	1 / 0.2	–	1
Podiceps cristatus	2 / 0.4 (3)	24 / 12.0	10 / 10.0	4 / 1.0	4 / 1.7	44
Puffinus yelkouan	–	(~ 4,000)	–	–	–	(4,000)
Phalacrocorax carbo	(4)	590 / 295 (855)	1 / 1.0	96 / 22.9 (11)	1 / 0.4	688 (870)
Phalacrocorax aristotelis	68 / 13.6	60 / 30.0 (90)	10 / 10.0	–	1 / 0.4	139 (90)
Cygnus olor	–	–	–	3 / 0.7	13 / 5.7	16
Tadorna tadorna	–	–	–	(20)	–	(20)
Anas platyrhynchos	110 / 22.0	2 / 1.0	37 / 37.0	–	160 / 69.6	309
Aythya ferina	–	–	18 / 18.0	–	–	18
Aythya fuligula	–	–	5 / 5.0	–	70 / 30.4	75
Mergus serrator	5 / 1.0	–	–	–	–	5
Fulica atra	–	–	74 / 74.0	–	228 / 99.1	302
Gallinula chloropus	–	–	–	–	1 / 0.4	1
Larus minutus	1 / 0.2	–	–	–	–	1
Larus melanocephalus	1 / 0.2	–	–	–	–	1
Larus ridibundus	–	–	~ 2,500 / 2,500.0	41 / 9.8	439 / 190.9	2,980
Larus cachinnans / *Larus michahellis*	19 / 3.8	~ 400 / 200.0	5 / 5.0	15 / 3.6 (10)	25 / 10.9	464 (10)
Larus canus	–	–	20 / 20.0	5 / 1.2	28 / 12.2	53
Thalasseus sandvicensis	–	–	4 / 4.0	3 / 0.7	–	7
Alcedo atthis	–	–	–	–	1 / 0.4	1
Total number of species (excluding flying birds)	10	6	13	11	15	21
Total number of individuals (excluding flying birds)	242	1,076	2,687	222	1,000	5,227
Abundance *per* 1 km^2 (excluding flying birds)	48	538	2,687	53	435	360
The Shannon index	1.46	0.95	0.38	1.59	1.58	1.54

Note. Data on the abundance are given as follows: counted individuals, in total / in terms of 1 km^2 of water area; in brackets, individuals flying over the sea and the coast. Data on the abundance of two closely related gull species, *Larus cachinnans* and *L. michahellis*, are summarized due to the difficulty of their identification from a long distance.

In terms of species richness, Lari prevailed (8 species out of 12 known for this biotope), as well as Anseriformes (6 out of 28; during the cold snap in 2012, 20 species were recorded). Other orders were represented by 1–3 species. A characteristic feature of this and other winters similar in terms of weather conditions was the absence of most Anseriformes (the whooper swan *Cygnus cygnus* (Linnaeus, 1758), Eurasian teal *Anas crecca* Linnaeus, 1758, red-crested pochard *Netta rufina* (Pallas, 1773), greater scaup *Aythya marila* (Linnaeus, 1761), common goldeneye *Bucephala clangula* (Linnaeus, 1758), smew *Mergellus albellus* (Linnaeus, 1758), *etc.*) which winter off the southern coasts only during extreme cold snaps and freezing of shallow waters at their traditional wintering grounds in the Northern Black Sea Region. The absence of several species in some areas of the central Southern coast, where they used to winter regularly, is worth noting as well. Specifically, the black-throated diver and red-breasted merganser *Mergus serrator* Linnaeus, 1758 were not revealed in the coastal water areas of the Cape Martyan Nature Reserve and Yalta (the average long-term winter density in previous periods was 3.1 and 3.9 ind.·km^{-1}, respectively [Beskaravayny, 2008]). These species were registered only in the east of the region. In the Cape Martyan vicinity, the black-necked grebe was not recorded either, though it used to be one of the most permanent elements of the winter ornithological complex (the average long-term density is 4.1 ind.·km^{-1}).

In terms of abundance, fish-feeding or predominantly fish-feeding species (the Levantine shearwater and cormorants; off the eastern coasts, the black-throated diver) prevailed in different spots of the water area, as well as species of a wide trophic spectrum (the yellow-legged gull *Larus michahellis* J. F. Naumann, 1840 and Caspian gull *Larus cachinnans* Pallas, 1811). In the central Southern coast, due to significant aggregations of these species (except for the black-throated diver), the total abundance of wintering birds was maximum. A noticeable increase in the abundance of the black-headed gull in the vicinity of Yalta compared to the value in the period of depression in the late 1990s–early 2000s was registered, when 68–306 individuals wintered there [Beskaravayny, 2008; Kostin S. et al., 1998]. An aggregation of several tens of thousands of the Levantine shearwater was also observed in the open sea near Sevastopol on 23.01.2020 (M. Stefanovich, personal communication).

Quantitative prevalence of several species, characteristic of the open sea coasts, determined the low value of the Shannon index (1.54) – the indicator reflecting diversity and evenness of the ornithological complex. The minimum value was recorded in the vicinity of Yalta (0.38) because of a sharp prevalence of the black-headed gull. High variability in the relative abundance and diversity of ornithological complexes in the open water areas is due to a relatively short stay of flocks of migratory birds there, especially the Levantine shearwater, great cormorant *Phalacrocorax carbo* (Linnaeus, 1758), yellow-legged gull, and Caspian gull.

Out of abundant bird species in the open water areas, the great cormorant and Levantine shearwater should be noted, which performed active longshore migrations throughout the winter season. Specifically, longshore feeding migrations of cormorants were observed in the area from Yalta, where in January their intensity was more than 500 ind.·h^{-1}, to Sevastopol, where the abundance off the open sea coasts reached 2.2 thousand individuals. The following observations can illustrate the intensity of shearwater migrations: on 20 December, in 5 minutes, about 3 thousand birds flew south-westward off the coast of Karadag; on 27 January, the flight intensity eastward and westward in the vicinity of Yalta was 1,240 and 2,270 ind.·h^{-1}, respectively.

In the east of the region, a relatively high abundance of the black-throated diver was recorded. In the vicinity of Feodosiya and in some areas of the wild coast (the Karadag Nature Reserve), high concentrations of the mallard were registered. The group of dominants near the large cities – Feodosiya and Yalta – was supplemented by the coot and black-headed gull. These species, as well as the mute swan, common pochard *Aythya ferina* (Linnaeus, 1758), tufted duck *Aythya fuligula* (Linnaeus, 1758), and common gull *Larus canus* Linnaeus, 1758, occurred only or mainly within the city water areas (see Table 1).

In general, during a mild winter, the ornithological complex of open coasts is characterized by a relative scarcity of species composition, sporadic distribution, and low, compared to that for cold winters, abundance of most Anseriformes, coot, and some gulls. To confirm, let us compare the abundance of several species in the central area, the vicinity of Yalta (Fig. 2), during a mild winter (2020) and an extremely cold winter (2012) [Andryushchenko et al., 2012]. In 2012, cold span lasted from late January to mid-February (in the Northern Black Sea Region, the temperature dropped to −18…−27 °C). Water bodies were covered with ice until mid-March, and this caused a mass bird migration to southern coasts [Andryushchenko et al., 2012].

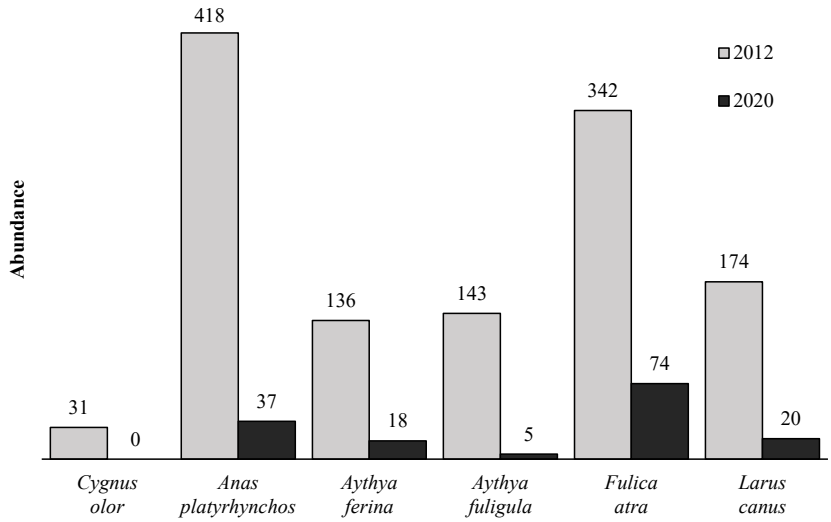

Fig. 2. Comparison of the abundance of several most common bird species wintering near Yalta under extreme cold winter conditions (January–early February 2012) [Andryushchenko et al., 2012] and mild winter conditions (January 2020)

Ornithological complex of closed Sevastopol bays. In the bays of the northern Heracles Peninsula, the formation of the winter ornithological complex began with an arrival of the great crested grebe (21 September) and a noticeable increase in the abundance of the mallard in September. Next month, the tufted duck (6 October) and common pochard (13 October) arrived. In the middle – the second half of this month, the abundance of the coot and black-headed gull (the second species is known to summer there) increased significantly. In November, there were the first records of the mute swan (6 November) and common gull (24 November). In the first half of December, the abundance of these two species, as well as the great crested grebe and great cormorant, increased noticeably; the abundance of the mallard, common pochard, and black-headed gull reached its maximum. In January, the highest abundance of the great cormorant and tufted duck was recorded. At the end of the first decade of February, which coincided with a short-term cold snap, the abundance of the great crested grebe, coot, and common gull was maximum. In February, the departure of the great cormorant, common

pochard, tufted duck (the last date was 10 March), and coot began. The great crested grebe, mute swan, and mallard began to leave the bays in the second half of February. The departure of the black-headed gull and common gull began in March, and the last date was 4 April. In the middle – the second half of March, most of the birds left the bays.

In the composition of the ornithological complex of Sevastopol bays, 29 species were registered in the winter 2019/2020 (Table 2), or 59.2% of the total number of species (49) recorded in this biotope for all the years of observations [Beskaravayny, 2013; Giragosov et al., 2015, 2021; our unpublished data]. For comparison: after a long cold snap in Crimea in the first half of January 2008 (down to −14 °C in Simferopol) [Weather Forecast and Archive, 2020], at least 35 species wintered in this area [Beskaravayny, 2013].

Table 2. Abundance of wintering birds in closed Sevastopol bays and on liman lakes near Feodosiya in the winter 2019/2020

Species	Sevastopol bays						Liman lakes near Feodosiya		
	Kaz., 1.14 km^2	Abr., 0.05 km^2	Kr., 0.66 km^2	Str., 0.78 km^2	Art., 0.13 km^2	Counted in total, 2.75 km^2	Kuchuk-Adzhigol, 0.3 km^2	Adzhigol, 0.25 km^2	Counted in total, 0.55 km^2
Gavia stellata	–	–	1	–	–	1	–	–	–
Gavia arctica	–	10	1	1	–	12	–	–	–
Podiceps ruficollis	16	–	3	6	–	25	–	–	–
Podiceps nigricollis	1	3	6	–	–	11	5	–	5
Podiceps auritus	1	–	1	–	–	2	–	–	–
Podiceps cristatus	317	–	90	1	–	408	14	–	14
Phalacrocorax carbo	153	4	13	19	5	189	–	–	–
Phalacrocorax aristotelis	1	2	–	–	–	3	–	–	–
Botaurus stellaris	–	–	–	–	–	–	1	–	1
Egretta alba	–	–	–	–	–	–	6	–	6
Ardea cinerea	2	–	1	1	–	4	6	–	6
Anser anser	–	–	–	–	–	–	50	–	50
Cygnus olor	2	–	18	–	–	20	71	1	72
Cygnus cygnus	–	–	–	–	–	–	14	–	14
Cygnus bewickii	–	–	–	–	–	–	5	–	5
Tadorna tadorna	–	–	–	–	–	–	48	21	69
Anas platyrhynchos	44	–	145	2	–	191	160	21	6
Anas crecca	14	–	1	–	–	15	2	–	2
Anas strepera	–	–	–	–	–	–	~40	–	~40
Anas penelope	1	–	–	–	–	1	2	–	2
Anas clypeata	–	–	–	–	–	–	15	–	15
Netta rufina	–	–	1	–	–	1	50	–	50
Aythya ferina	47	–	41	8	–	96	470	–	470
Aythya fuligula	64	–	46	10	97	217	39	–	39
Mergus serrator	3	–	–	–	–	3	–	–	–

Continue on the next page…

Species	Sevastopol bays						Liman lakes near Feodosiya		
	Kaz., 1.14 km^2	Abr., 0.05 km^2	Kr., 0.66 km^2	Str., 0.78 km^2	Art., 0.13 km^2	Counted in total, 2.75 km^2	Kuchuk-Adzhigol, 0.3 km^2	Adzhigol, 0.25 km^2	Counted in total, 0.55 km^2
Circus aeruginosus	–	–	–	–	–	–	1	–	1
Rallus aquaticus	–	–	1	–	–	1	–	–	–
Gallinula chloropus	2	–	5	7	–	14	–	–	–
Fulica atra	1,150	–	306	187	362	2,005	670	6	676
Tringa totanus	1	–	–	–	–	1	–	–	–
Calidris alpina	3	–	–	–	–	3	–	–	–
Gallinago gallinago	–	–	–	–	–	–	1	6	7
Larus melanocephalus	–	–	8	2	–	10	–	–	–
Larus ridibundus	40	2	245	194	121	602	18	32	50
Larus cachinnans	25	9	78	53	5	170	–	2	2
Larus michahellis								–	–
Larus canus	61	2	66	6	13	148	–	–	–
Thalasseus sandvicensis	4	–	1	–	–	5	–	–	–
Alcedo atthis	–	–	–	1	–	1	–	–	–
Emberiza schoeniclus	–	–	–	–	–	–	–	≥ 20	≥ 20
Total number of species	23	8	23	16	7	29	22	8	24
Total number of individuals	1,953	32	1,078	498	603	4,164	1,688	109	1,797
Abundance *per* 1 km^2	1,715	696	1,624	643	4,674	1,513	5,627	436	3,267
The Shannon index	1.49	1.72	2.07	1.50	1.09	1.82	1.84	1.74	1.96

Note. Sevastopol bays: Kazachya (Kaz.); Abramov (Abr.); Kruglaya (Kr.); Streletskaya (Str.); Artilleriiskaya (Art.).

Relatively high ecological diversity of the ornithological complex of the bays, which includes species typical of shallow waters (many Anseriformes and waders), reed beds (grebes, herons, coot, *etc.*), and open water areas (cormorants and gulls), is due to both significant intrabiotopic differentiation and their connection with the open sea. Six species were specific: the red-throated diver *Gavia stellata* (Pontoppidan, 1763), little grebe *Podiceps ruficollis* (Pallas, 1764), Slavonian grebe *Podiceps auritus* (Linnaeus, 1758), water rail *Rallus aquaticus* Linnaeus, 1758, common redshank *Tringa totanus* (Linnaeus, 1758), and dunlin *Calidris alpina* (Linnaeus, 1758).

In terms of the number of species, Anseriformes (8 out of 22 known here) and Lari (6 out of 8) prevailed. The whooper swan, Eurasian wigeon *Anas penelope* Linnaeus, 1758, red-crested pochard, common goldeneye, smew, *etc.*, which are common only during cold snaps, were not recorded at all or were rare. Compared to the data of counting after the cold snap in January 2008, the abundance of the common pochard, coot, and common gull in January 2020 was 2.5–3 times lower, and the abundance of the mute swan was 7 times lower.

In most bays, the coot and black-headed gull significantly prevailed. In the Kazachya Bay, the group of dominants was supplemented by the great crested grebe and great cormorant; in the Kruglaya Bay, by the mallard.

Conditions for birds were the most favorable in the Kazachya and Kruglyaya bays, which are distinguished by a variety of biotopes (reed beds and vast shallow waters with different types of sediments), variety of food resources (communities of phyto- and zoobenthos and rich ichthyofauna), and presence of rarely visited coastal areas within the boundaries of regime enterprises. For these reasons, the ornithological complexes of these two bays were characterized by high levels of diversity and were the leading ones both in terms of species richness and absolute abundance of birds (see Table 2).

A small number of wintering species in the Artilleriiskaya Bay results from the lack of shallow waters and riparian vegetation at the concreted shores, as well as from intensive shipping there. However, with a rather low abundance of individuals, the relative abundance (density) of birds in this bay was the highest – due to its small area.

In the Streletskaya Bay, the second largest among the surveyed bays, but subjected to negative factors (intensive shipping and arrangement of most of the coastline with berths), the relative abundance of birds was the lowest. Similar conditions determined the scarcity of the species composition and low relative abundance of birds in the small and more open, compared to others, Abramov Bay. In the composition of its ornithological complex, species typical of open coasts prevailed quantitatively (see Table 2).

Ornithological complex of liman lakes. On the lakes in the vicinity of Feodosiya, an increase in the abundance of the mute swan, common pochard, and tufted duck became noticeable in the first decade of October; of the mallard, in the middle of this month. In early January, the maximum abundance of the red-crested pochard was recorded, and the arrival of graylag goose *Anser anser* (Linnaeus, 1758) was established. In mid-January, the maximum abundance of the mute swan, mallard, common pochard, and coot was noted, and the first arrivals of the whooper swan and Bewick's swan *Cygnus bewickii* were registered (Fig. 3). By late January, the abundance of the tufted duck reached its maximum; in early February, Eurasian teal and common shelduck had the highest abundance. At the same time, the arrival of the gadwall *Anas strepera* Linnaeus, 1758 and Eurasian wigeon was registered. By the first decade of March, the abundance of the common pochard and coot decreased noticeably; by mid-March, the abundance of the mute swan and red-crested pochard dropped.

Fig. 3. Bewick's swans (*Cygnus bewickii*) and whooper swan (*Cygnus cygnus*) on Kuchuk-Adzhigol Lake near Feodosiya, 27.01.2020, photo by M. Kosareva

A total of 24 species were registered on the lakes during the winter 2019/2020 (see Table 2), or 58.5% of the total number of species recorded during wintering (41). The species composition was characterized by a significant number of species of the reed complex (13) and by high specificity (10 species: the Eurasian bittern *Botaurus stellaris* (Linnaeus, 1758), great egret *Egretta alba* (Linnaeus, 1758), greylag goose, whooper swan, Bewick's swan, gadwall, Northern shoveler *Anas clypeata* Linnaeus, 1758, marsh harrier, common snipe *Gallinago gallinago* (Linnaeus, 1758), and reed bunting).

The number of species, absolute abundance, and relative abundance of birds on the more full-flowing Kuchuk-Adzhigol Lake were significantly higher than on Adzhigol Lake. The ornithological complex was formed mostly by Anseriformes (11 species). In terms of abundance, throughout the wintering period, the common pochard, mallard, and coot prevailed. Short-term aggregations of the gadwall and Bewick's swan were the largest known for these species in the Southern Crimea.

Conclusion. Under the conditions of mild winter prevailing in the Northern Black Sea Region in 2019/2020, at least 44 species of hydrophilic birds from 11 orders, or 61.1% of all species known to winter in this area (72), wintered off the sea coasts of the Southern Crimea [Andryushchenko et al., 2012; Beskaravayny, 2008; Beskaravayny, Kostin S., 1999; Kostin Yu., 1983; Mosalov et al., 2002].

The qualitative and quantitative scarcity of ornithological complexes in such winters is most noticeable on water areas off the open sea coasts. This, along with the weather factor, is due to relative monotony and low food supply of biotopes. There, less than half of the species known for these biotopes is recorded. The abundance of most Anseriformes, the coot and some gulls is lower compared to that in cold winters. In some areas, several regularly wintering species are not registered at all (the black-throated diver, black-necked grebe, and red-breasted merganser).

The role of these water areas as a winter habitat for hydrophilic birds increases only during cold snaps, when the freezing of water bodies in the north of the peninsula and in continental areas causes a mass bird migration to southern coasts. Specifically, in some areas of the central Southern coast, the abundance of background species in the warm winter 2019/2020 was 8 times lower than that during the extremely cold winter 2011/2012.

Ornithological complexes associated with water areas more or less isolated from the open sea were represented more fully (about 60% of the total species composition). The maximum species and ecological diversity of birds was established for closed Sevastopol bays, which are protected from winter storms and are characterized by diversity of biotopes. However, with a rather high abundance in 2020, the abundance of some background species compared to that for the cold winter 2008 was 2.5–7 times lower. A large number of species of the reed complex and the highest specificity of the species composition can be considered as characteristic features of the ornithological complex of liman lakes which are completely isolated from the sea.

Anseriformes, with their relative qualitative scarcity (14 species, or 50% known in the area), however, prevailed in the number of species (except for water areas near open shallow coasts). By the abundance, representatives of this order – the mallard and common pochard – were in the group of dominants on the Kuchuk-Adzhigol Lake near Feodosiya and in most Sevastopol bays. Lari – the second group in terms of species diversity – were presented more fully (8 species, or 61.5%). Their abundance was high in Sevastopol bays, in the vicinity of other large cities (the black-headed gull), and in some non-urbanized areas of the coast (the yellow-legged gull and Caspian gull). Among the prevailing species, there were also the great cormorant, Levantine shearwater (on open water areas), and coot (in bays and on liman lakes).

A very high abundance of the Levantine shearwater and a significant increase in the abundance of the black-headed gull in the vicinity of Yalta were characteristic features of the winter period 2019/2020. Of interest are the registrations of the red-throated diver and Arctic skua which are known in winter in Crimea from single observations [Kostin Yu., 1983]. Wintering of five Bewick's swans in the south of the peninsula confirms the tendency for this species to increase in the abundance in the south of Russia and Ukraine since the first half of the1980s [Belik et al., 2012].

This work was carried out within the framework of KSS – Nature Reserve of RAS – Branch of IBSS state research assignment No. 121032300023-7 and IBSS state research assignment No. 121030100028-0.

Acknowledgment. The authors express their sincere gratitude to A. Grinchenko, M. Kosareva, and M. Stefanovich, who kindly provided information about their observations used in this work, as well as to anonymous reviewers for their valuable comments that made it possible to improve the article.

REFERENCES

1. Andryushchenko Yu. A., Beskaravayny M. M., Kostin S. Yu., Popenko V. M., Prokopenko S. P. On the bird wintering in the south of the Crimea under extreme winter conditions of 2011/2012. *Branta* : sbornik nauchnykh trudov Azovo-Chernomorskoi ornitologicheskoi stantsii, 2012, iss. 15, pp. 140–147. (in Russ.). https://branta.org.ua/en/branta-issues/branta-15/15-11.html
2. Belik V. P., Gugueva E. V., Vetrov V. V., Makhmutov R. Sh. Migration of the Bewick's swan (*Cygnus bewickii*) in the Volga–Akhtuba floodplain. *Kazarka* : byulleten' rabochei gruppy po guseobraznym Severnoi Evrazii, 2012, vol. 15, no. 1, pp. 13–29. (in Russ.)
3. Beskaravayny M. M. *Ptitsy morskikh beregov Yuzhnogo Kryma.* Simferopol : N.Orianda, 2008, 160 p. (in Russ.)
4. Beskaravayny M. M. Extreme falls of temperature as a factor of formation of hydrophilic birds winterings in the South Crimea. *Branta* : sbornik nauchnykh trudov Azovo-Chernomorskoi ornitologicheskoi stantsii, 2010, iss. 13, pp. 21–32. (in Russ.). https://branta.org.ua/en/branta-issues/branta-13/13-03.html
5. Beskaravayny M. M. Zimovka ptits v sevastopol'skikh bukhtakh. In: *Ptitsy i okruzhayushchaya sreda* : sbornik nauchnykh trudov / I. T. Rusev, V. P. Stoilovskii, A. I. Korzyukov, D. A. Kivganov (Eds). Odesa : Aprel', 2013, pp. 24–29. (in Russ.)
6. Beskaravayny M. M., Kostin S. Yu. Struktura i raspredelenie zimnei gidrofil'noi ornitofauny Yuzhnogo berega Kryma. In: *Problemy izucheniya fauny Yuga Ukrainy*. Odesa : Astroprint ; Melitopol : Branta, 1999, pp. 19–33. (in Russ.)
7. Giragosov V. E., Beskaravayny M. M., Kostin S. Yu. New data on some rare and poor studied bird species of the Crimea from observations in Sevastopol Region. *Branta* : sbornik nauchnykh trudov Azovo-Chernomorskoi ornitologicheskoi stantsii, 2015, iss. 18, pp. 24–30. (in Russ.). https://branta.org.ua/en/branta-issues/branta-18/branta18-03.html
8. Giragosov V. E., Beskaravayny M. M., Drapun I. E. New information on the bar-tailed godwit *Limosa lapponica* (Linnaeus, 1758) and red-throated diver *Gavia stellata* (Pontoppidan, 1763) on the Crimean Peninsula (the Black Sea). *Morskoj biologicheskij zhurnal*, 2021, vol. 6, no. 3, pp. 44–49. (in Russ.). https://doi.org/10.21072/mbj.2021.06.3.05
9. Kostin Yu. V. *Ptitsy Kryma.* Moscow : Nauka, 1983, 240 p. (in Russ.)
10. Kostin S. Yu., Appak B. A., Beskaravayny M. M. Results of bird surveys in winter in the southern coastal part of the Crimea // *Zimnie uchety ptits na Azovo-Chernomorskom poberezh'e Ukrainy* : sbornik materialov XVIII rabochego soveshchaniya Azovo-Chernomorskoi ornitologicheskoi rabochei gruppy, 4–6 February, 1998. Alushta ; Kyiv : Wetlands International, 1998, [iss. 1], pp. 14–18. (in Russ.)

11. Mosalov A. A., Ganitsky I. V., Koblik E. A., Glukhovsky M. V., Red'kin Ya. A., Sharikov A. V., Shitikov D. A. Winter avifauna of some coastal areas of the Crimea. *Russkii ornitologicheskii zhurnal*, 2002, vol. 11, iss. 182, pp. 315–329. (in Russ.)
12. Pesenko Yu. A. *Printsipy i metody kolichestvennogo analiza v faunisticheskikh issledovaniyakh.* Moscow : Nauka, 1982, 288 p. (in Russ.)
13. *Weather Forecast and Archive* : [site]. (in Russ.). URL: http://weatherarchive.ru/ [accessed: 25.07.2020].
14. Pusanow I. Versuch einer Revision der taurischen Ornis. *Bulletin de la Société des naturalistes de Moscou. Section biologique*, 1933, t. 42, livr. 1, pp. 3–41.

ОСОБЕННОСТИ ЗИМОВКИ ГИДРОФИЛЬНЫХ ПТИЦ У МОРСКИХ БЕРЕГОВ ЮЖНОГО КРЫМА В УСЛОВИЯХ МЯГКОЙ ЗИМЫ 2019/2020 Г.

М. М. Бескаравайный[1], В. Е. Гирагосов[2]

[1]Карадагская научная станция имени Т. И. Вяземского — природный заповедник РАН — филиал ФИЦ ИнБЮМ, Феодосия, Российская Федерация

[2]ФГБУН ФИЦ «Институт биологии южных морей имени А. О. Ковалевского РАН», Севастополь, Российская Федерация

E-mail: *karavay54@mail.ru*

Береговая зона — основное на юге Крыма зимнее местообитание гидрофильных птиц, видовой и количественный состав которых изучены достаточно полно, в том числе в условиях экстремальных похолоданий. Для выяснения влияния погодных условий на состояние орнитокомплексов и динамику внутрирегиональных перемещений птиц интерес представляет сравнение особенностей зимовки в тёплые и холодные зимы. Цель данной работы — выявить видовой состав, численность и биотопическое распределение гидрофильных птиц в южной части Крымского полуострова в условиях мягкой зимы. Исследования проведены в районе от посёлка Приморский у Феодосии до Севастополя (около 250 км) зимой 2019/2020 г., отличающейся преобладанием положительных температур. Обследованы основные береговые биотопы — акватории у открытых берегов, закрытые бухты и лиманные озёра. У открытых берегов выявлено 24 вида, что значительно меньше, чем в холодные сезоны (для сравнения: в холодную зиму 2012 г. здесь зимовал 41 вид). По разнообразию доминировали чайковые и гусеобразные; отмечены высокая численность и активная вдольбереговая миграция левантского буревестника и большого баклана, а также более низкая, чем в холодные зимы, численность гусеобразных, лысухи и некоторых чаек. В севастопольских бухтах выявлено 29 видов (для сравнения: в холодном январе 2008 г. — 35 видов). По разнообразию лидировали гусеобразные и чайковые, по численности — лысуха и озёрная чайка. На лиманных озёрах зимовало 24 вида, доминировали лысуха и гусеобразные, в основном красноголовая чернеть. Всего во всех исследованных биотопах в период мягкой зимы 2019/2020 г. обнаружено 44 вида птиц (61,1 % зимующих в регионе) из 11 отрядов. К особенностям зимы 2019/2020 г. относится высокая численность левантского буревестника; отмечена зимовка краснозобой гагары, короткохвостого поморника и малых лебедей.

Ключевые слова: гидрофильные птицы, Южный Крым, зимовка, мягкая зима, открытый берег, закрытые бухты, лиманные озёра, видовой состав, численность

1871
ИнБЮМ – IBSS

Морской биологический журнал
Marine Biological Journal
2023, vol. 8, no. 1, pp. 16–26
https://marine-biology.ru

UDC [582.263-155.7:579.2]:665.61

THE EFFECT OF CRUDE OIL ON THE SYMBIOTIC ASSOCIATION OF THE GREEN ALGA *ACROSIPHONIA ARCTA* (DILLWYN) GAIN AND EPIPHYTIC BACTERIA

© 2023 **G. M. Voskoboinikov[1], L. O. Metelkova[2], D. V. Pugovkin[1], and D. O. Salakhov[1]**

[1]Murmansk Marine Biological Institute of the Russian Academy of Sciences, Murmansk, Russian Federation
[2]D. I. Mendeleyev Institute for Metrology, Saint Petersburg, Russian Federation
E-mail: *grvosk@mail.ru*

Received by the Editor 01.04.2022; after reviewing 07.07.2022;
accepted for publication 20.10.2022; published online 14.03.2023.

It was experimentally shown that the green alga *Acrosiphonia arcta*, inhabiting the Barents Sea littoral zone, remains viable for 10 days in case of exposure to crude oil introduced into seawater at a concentration of 5 mg·L^{-1}. This concentration corresponds to a weak oil spill in the marine environment. Morphological and functional changes in the symbiotic association of *A. arcta* and epiphytic bacteria on its surface were traced by the techniques of microbiology, light and electron microscopy, and physiology. During the experiment, most algal cells maintained a high level of photosynthesis, and their ultrastructure was preserved. Interestingly, by the end of the exposure, under the effect of crude oil, the proportion of chloroplasts decreased in algal cells, and the pyrenoid and starch granules disappeared. The dynamics of the number of epiphytic bacteria in the experiment and the proportion of hydrocarbon-oxidizing bacteria in the total number of cultivated heterotrophs were traced. The capability of *A. arcta* to absorb and transform oil products was shown. This algal species is capable of developing in oil-contaminated water areas on any substrate, preparing it for colonization by larger perennial macrophyte algae, and this determines the significant role of *A. arcta* in the restoration of coastal phytocoenoses.

Keywords: *Acrosiphonia arcta*, oil, seawater bioremediation, symbiotic association, epiphytic bacteria, photosynthesis, ultrastructure

As found earlier, macrophyte algae, inhabiting the Barents Sea and representing various systematic groups, are capable of absorbing diesel fuel [Pilatti et al., 2016; Voskoboinikov et al., 2018, 2020a]. In experiments on seawater purification from diesel fuel using algae, it was shown that a decrease in the content of oil products (hereinafter OP) in water occurred in parallel with their accumulation in plants. At the same time, on algae surface, degradation of OP occurred due to epiphytic hydrocarbon-oxidizing bacteria (hereinafter HOB), and this ensured their absorption and diesel fuel neutralization by plant cells. As known, HOB, that are in a mutualistic relationship with macrophyte algae, are able to oxidize almost all OP, with the degradation rate depending on the ratio of their constituent hydrocarbons [Atlas, 1978; Heitkamp, Cerniglia, 1987; Pirnik, 1977; Pugovkin, 2017]. Scant data on this issue have been obtained on algae representatives with lamellar thallus [Pugovkin, 2017; Ryzhik et al., 2019; Voskoboinikov et al., 2018, 2020b]. Interestingly, *Acrosiphonia arcta* (Dillwyn) Gain, 1912 belongs to pioneer species that prepare the substrate for its colonization by perennial dominant species [Malavenda et al., 2017].

The aim of this study is to identify morpho-functional changes, caused by the effect of crude oil, in the green alga *A. arcta* (a species with a siphonaceous thallus; an inhabitant of the littoral zone), to analyze the toxicant transformation by the symbiotic association of this alga and bacteria, and to determine the potential role of the species in seawater purification.

MATERIAL AND METHODS

A. arcta vegetative thalli, approximately equal in size and weight, were sampled on the coast of the Zelenetskaya Bay of the Barents Sea (69°07′09″N, 36°05′35″E) in summer. Foulers were removed, and thalli were placed in glass containers with 1.3 L of seawater. Seawater (salinity of 33‰) sampled in the alga habitat was pre-filtered through a cotton-gauze filter to remove large (visible) suspended matter. Then, oil from the field on Kolguev Island (Peschanoozerskoye oil and gas condensate field) was introduced into seawater at a concentration of 5 mg·L^{-1}, which corresponds to a weak oil spill in the marine environment and is 100 MPC (maximum permissible concentration) for water in terms of the total content of OP. According to regulatory documents, MPC for the total content of OP corresponds to 0.05 mg·L^{-1} [Normativy, 2020]. The experiment was carried out in a thermostatic box at a temperature of +7…+8 °C, irradiance of 16–18 W·m^{-2}, with a photoperiod 24L : 0D (it corresponds to the natural habitat of the alga in summer), and constant water aeration with air. Control (in containers with seawater with no oil) and experimental (in containers with introduced oil, 5 mg·L^{-1}) samples of the alga and water were taken for investigation at the beginning of the exposure (initial samples) and in 5 and 10 days. Changes in cell morphology were analyzed under a Mikmed-6 light microscope (LOMO, Russia) and a JEM-100C transmission electron microscope (Jeol, Japan). Under a light microscope, samples were examined *in vivo*. Samples for examining under an electron microscope (20–30-nm thick sections stained with toluidine blue) were prepared according to the standard technique [Voskoboinikov, Titlyanov, 1978]. The intensity of visible photosynthesis of the alga during the experiment was determined by the change in the oxygen content in water before and after thalli incubation using a HI 9141 oximeter (Hanna Instruments, Germany) and by the Winkler titration. The calculation was carried out in μg O_2 *per* 1 g wet weight of thallus *per* hour [Salakhov et al., 2020]. The total content of OP and concentrations of alkanes in water and the alga were determined by gas chromatography–mass spectrometry. Sample preparation and instrumental analysis were carried out according to EPA method 8270 (Semivolatile Organic Compounds by GC/MS) described in detail earlier [Voskoboinikov et al., 2018]. The mass fraction of crude oil components was calculated by the internal standard calibration. For water, the results are given in μg·L^{-1}; for the alga, in μg·g^{-1} dry weight.

The number of cultivated heterotrophic bacteria was determined by the limiting dilution analysis [Rukovodstvo, 1980] using liquid Zobell media for common heterotrophs [Prakticheskaya gidrobiologiya. Presnovodnye ekosistemy, 2006] and MMS medium for HOB [Koronelli, Iljinsky, 1984; Mills et al., 1978]. Obtained number of cultivated bacteria was recalculated *per* 1 g wet weight of the alga thallus.

RESULTS

Changes in the oil product content in water and the alga during the experiment. The fraction of Kolguev crude oil dissolved in dichloromethane, was characterized by the predominance of n-alkanes in the C_8–C_{30} range with maximums in the C_{14}–C_{16} range. The content of isoprenoids (pristane and phytane) was no more than 7% of the total sum of n-alkanes. Initial seawater contained 495 μg·L^{-1} of OP,

which is 10 MPC (Table 1). During the experiment (10 days), the content of OP in initial seawater with no oil increased to 1,527 μg·L^{-1} ("water + *A. arcta*"). The value of the indicator reflecting the degree of hydrocarbon transformation (∑n-alkanes / ∑OP) increased as well – from 0.06 to 0.10–0.12.

Table 1. Content and proportion of alkanes and oil products (OP) in water samples during the experiment, μg·L^{-1}

	Water	Water + *A. arcta*	Water + OP			Water + *A. arcta* + OP		
	0 days	10 days	0 days	5 days	10 days	0 days	5 days	10 days
Sum of n-alkanes	28.6	185	1,569	247	185	1,569	54	95
∑n-alkanes / ∑OP	0.06	0.12	0.28	0.13	0.16	0.28	0.09	0.08
Total content of OP	495	1,527	5,552	1,954	1,158	5,552	628	1,166

When oil was introduced, the content of OP (on the 1st day) was 5,552 μg·L^{-1}. By the 10th day of the experiment, the total content of OP in water samples decreased by 79%. With the presence of *A. arcta*, the total content of OP in water decreased by 88% on the 5th day and increased to 1,166 μg·g^{-1} on the 10th day of the exposure.

The total content of oil hydrocarbons (hereinafter OH) in *A. arcta* control sample (0 days) was 2,686 μg·g^{-1} (Table 2). By the 10th day, the value decreased by almost 30%.

With the presence of *A. arcta* in the medium with OP, the content of OH in the alga thallus increased significantly on the 5th day of the experiment but decreased on the 10th day.

Table 2. Content and proportion of alkanes and oil products (OP) in *Acrosiphonia arcta* samples during the experiment, μg·g^{-1} dry weight

	Control		Experiment		
	0 days	10 days	0 days	5 days	10 days
Sum of n-alkanes	102	156	102	1,482	867
∑n-alkanes / ∑OP	0.04	0.08	0.04	0.19	0.16
Total content of OP	2,686	1,929	2,686	7,930	5,395

Changes in the alga viability, morphology, and physiology during the experiment. Both control (with no oil) and experimental algae (with introduced oil) remained viable until the end of the exposure. In the control sample, thalli had an intense green color. In the experiment sample, the color intensity in some thalli decreased by the 10th day.

Light-optical and electron microscopic observations in 5 and 10 days of the experiment did not reveal any morphological changes in the alga cells with no oil (the control sample) compared to the initial variant.

The cell cytoplasm adhered tightly to the inner side of the plasma membrane. On cell sections, oval-shaped chloroplasts were detected (1 in Fig. 1a), located close to the plasmalemma.

In most cells, chloroplasts were combined into the photosynthetic reticulum. Chloroplasts contained thylakoids running parallel to each other along the long axis and a submerged pyrenoid with starch granules (2 in Fig. 1a) forming a sheath. Starch granules were abundant outside the pyrenoid as well – in the stroma of chloroplasts (3 in Fig. 1a). In the cytoplasm, there were up to three mitochondria

per cell section, 1–2 μm in size, with single cristae; moreover, several electron-dense granules were recorded, mostly rounded, 1.5–3 μm in diameter. On the outer side of the shell of *A. arcta* thallus, there were single bacteria in the initial variant.

In the experiment, 10 days after oil introduction, plasmolysis was observed in single cells of *A. arcta* thallus in *in vivo* samples. The plasmalemma separation from the inner surface of the thallus cell membrane was recorded not only under a light microscope, but also on sections under electron microscope. At this stage of the experiment, a degrading pyrenoid was observed in chloroplasts of single cells; it was not revealed in most cells. There were no starch granules. At the same time, there were no signs of damage to the lamellar system of chloroplasts (1 in Fig. 1b). The chloroplast stroma was quite dense, with abundant thylakoids. In the cytoplasm, compared to that of the control sample, on cell sections, there was an increase in number (up to 4–7) and size (up to 2.5 μm) of mitochondria, as well as in size of electron-dense globules (up to 4 μm) (4 in Fig. 1b). On the outer side of *A. arcta* shell, there were abundant microorganisms of various shape and density forming a continuous layer in some areas (7 in Fig. 1c).

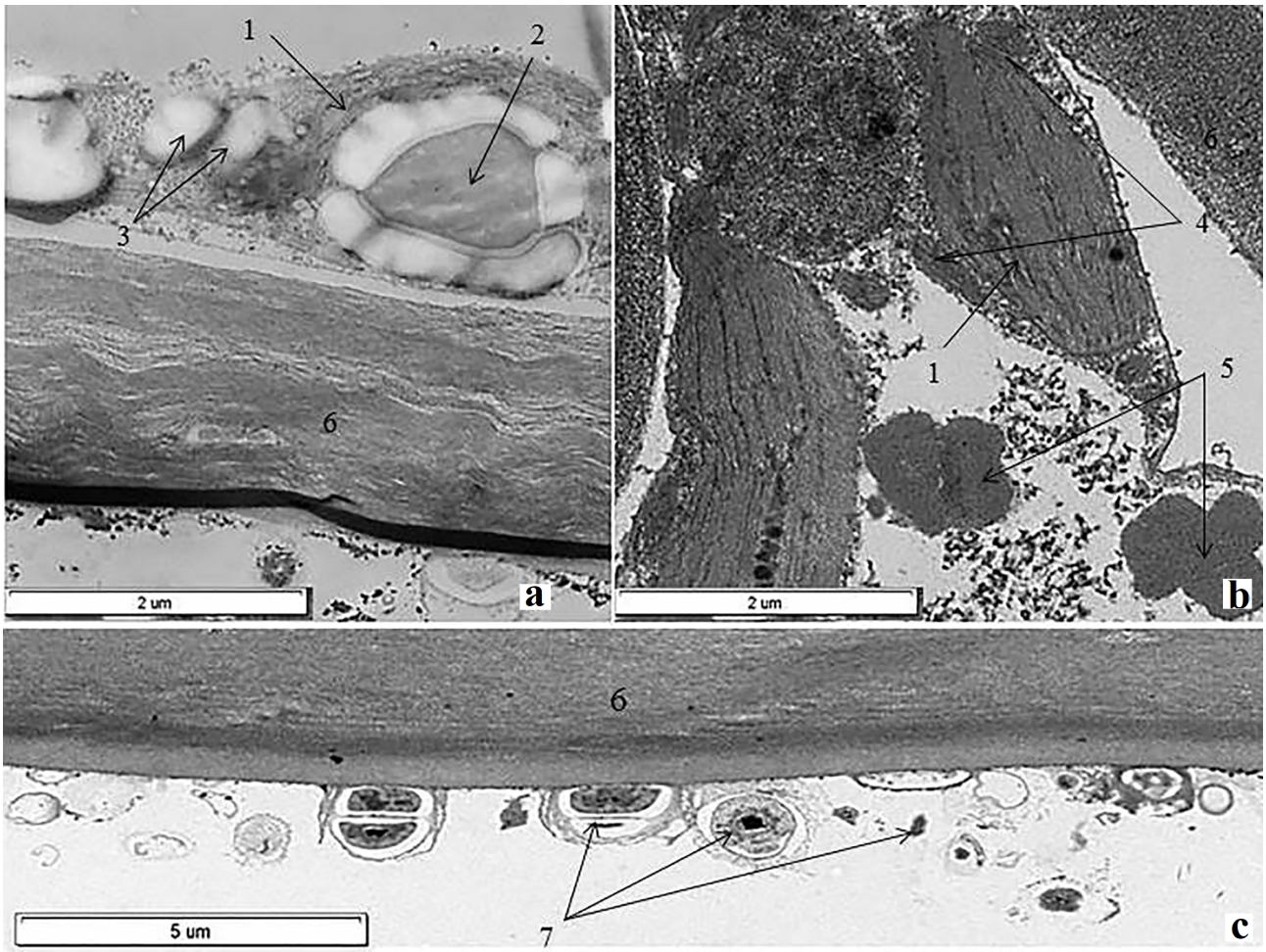

Fig. 1. Cell structure of *Acrosiphonia arcta* under oil contamination: a, control; b, c, experimental sample after 10 days of exposure. Legend: 1, chloroplast; 2, pyrenoid with starch granules; 3, starch granules in the chloroplast stroma; 4, mitochondria; 5, electron-dense globules; 6, algal shell; 7, epiphytic microorganisms on the surface of the alga

The intensity of photosynthesis in the initial samples of *A. arcta* was 0.42 μg O_2 *per* 1 g wet weight *per* hour (Fig. 2).

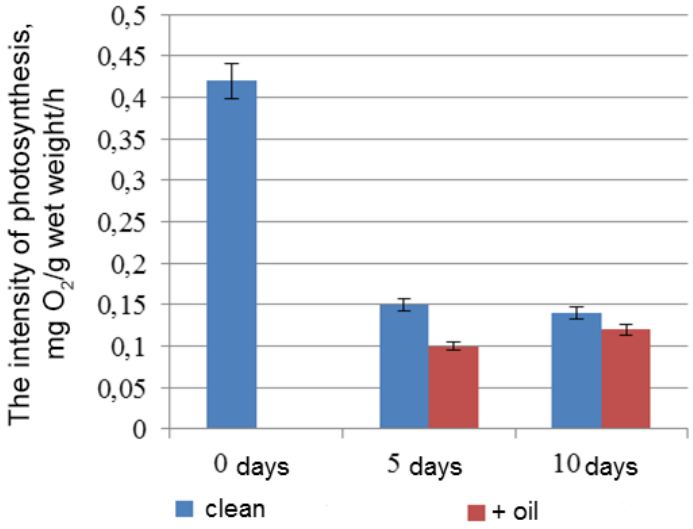

Fig. 2. Intensity of *Acrosiphonia arcta* photosynthesis during the experiment

In 5 days, in the alga of the control sample, the intensity of photosynthesis decreased by 2.8 times and did not change until the end of the exposure. In experimental samples of *A. arcta*, on the 5th day, there was a decrease in the intensity of photosynthesis by 1.5 times compared to the control variant. By the end of the exposure, the value almost did not differ from the control one.

Change in the number of epiphytic bacteria. During the experiment, a significant change in the number of cultivated heterotrophic bacteria was recorded – within several orders of magnitude. *Prior* to being placed under experimental conditions, *A. arcta* had a rather high (up to 9 orders of magnitude) number of cultivated epiphytic bacteria – more than 20 million cells·g^{-1} for heterotrophs and 4.3 thousand cells·g^{-1} for HOB (Fig. 3).

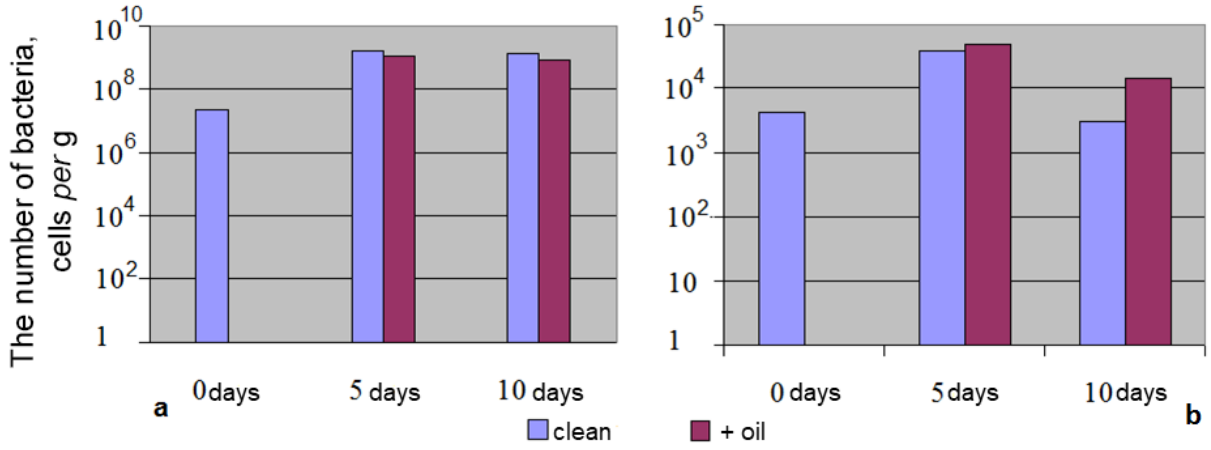

Fig. 3. Number of cultivated epiphytic heterotrophic (a) and hydrocarbon-oxidizing (b) bacteria in the experiment

By the 5th day of the exposure, in the control sample, the number of epiphytic bacteria of *A. arcta* was approximately 81.5 times higher (1.6×10^9 cells·g^{-1}) than in the initial variant (2.2×10^7 cells·g^{-1}). After oil introduction (100 MPC), their number increased by about 53.5 times – up to 1.1×10^9 cells·g^{-1} (the number of bacteria rose by more than 2 orders of magnitude). By the 10th day, there was a decrease in the number of epiphytic bacteria compared to previous values – by 1.2 times in the sample with oil and by 1.4 times in the control variant (up to 7.8×10^8 and 1.3×10^9 cells·g^{-1}, respectively).

The proportion of HOB in the alga before the experiment accounted for 0.02% of the total number of cultivated bacteria (4.3×10^3 cells·g^{-1}). By the 5th day, their proportion in the control sample decreased to 0.002% (3.02×10^4 cells·g^{-1}); in the experimental sample, the value was 0.005% (4.9×10^4 cells·g^{-1}). By the 10th day, with a decrease in the number of cultivated bacteria compared to that on the 5th day, the proportion of HOB decreased as well – to 0.0002% in the control and to 0.002% in the experiment (3.1×10^3 and 1.5×10^4 cells·g^{-1}, respectively).

DISCUSSION

The experiments have shown as follows: *A. arcta* remains viable for 10 days at such a content of OP in water, which is 10 times higher than the MPC and 100 times higher than 0.05 mg·L^{-1} (the value taken as 1 MPC for fishery reservoirs) [Normativy, 2020]. According to this study and previous ones, the level of seawater contamination by OP at the sampling site ranges from 2 MPC in winter and spring to 10 MPC in summer [Voskoboinikov et al., 2018, 2020b]. In the water area of the Zelenetskaya Bay, there is a diving center; therefore, an increase in contamination may result from the intensified navigation of small vessels with the onset of the season in July. Apparently, the development of the alga under low contamination by OP ensured its resistance to this factor.

The changes in the mass fraction of alkanes and the total content of OP in water in experiments with crude oil and the green alga, as well as without the alga, are shown in Tables 1 and 2. As already noted, in 10 days of the experiment, the content of OP in the initial water with no OP increased to 1,527 μg·L^{-1} ("water + *A. arcta*"). The value of the indicator reflecting the degree of hydrocarbon transformation (∑n-alkanes / ∑OP) increased as well – from 0.06 to 0.10–0.12. This indicates slight "introduced" oil contamination. The alga itself may initially contain a significant amount of OH on the surface.

As also mentioned earlier, when oil was introduced at a concentration of 5 mg·L^{-1}, the measured OP content (on the 1st day) was 5,552 μg·L^{-1}. During the experiment, the total content of OP in water samples without the macrophyte alga gradually decreased; on the 10th day, the value was 1,158 μg·L^{-1} (*i. e.*, it dropped by 79%). With the presence of *A. arcta*, a decrease in the total content of OP to 628 μg·L^{-1} (by 88%) on the 5th day was followed by an increase to 1,166 μg·L^{-1}. On the 10th day of the exposure, the content of OP in water with the macroalga was higher than in control samples (without the alga). This can be explained by the fact that the alga does not consistently absorb OP: there are periods of "returning" absorbed hydrocarbons to the environment until a certain equilibrium is established. Apparently, this is due to the life cycles of bacteria inhabiting surface of macrophyte algae. The concentrations of n-alkanes and isoprenoids (phytane and pristane) changed throughout the experiment, in general, in proportion to the total content of OP.

Initially, *A. arcta* thallus contained 2,686 μg·g^{-1} of OP. On the 10th day of the experiment, the content of hydrocarbons in *A. arcta* decreased to 1,929 μg·g^{-1}. It can be assumed that one part of OP was transformed in the thallus cells, and another part returned to the aquatic environment.

In the experiment with oil introduction, the absorption of OH by the alga surface was registered. The maximum content of OP in the alga cells was recorded on the 5th day of the exposure – 7,930 μg·g^{-1}. On the 10th day, the total content of OP in the alga decreased to 5,395 μg·g^{-1}. Given the data on water, we may assume that some of the hydrocarbons diffused back into water.

The processes of transformation of hydrocarbons in *A. arcta* can be traced by the changes in the values of the indicator ∑n-alkanes / ∑OP. Its decrease by the 10th day reflects active destruction of the main oil components – n-alkanes. However, by the 10th day, these processes were not fully completed. Changes in the total content of OH in water and simultaneously in the alga indicate that *A. arcta* purifies water by absorbing OH.

Visual and microscopic observations of the changes in *A. arcta* throughout the experiment showed as follows. Despite the fact that the alga remained viable under oil contamination corresponding to 100 MPC, destructive changes were registered in single thallus cells – enlightened protoplasm, reduction of the formed pyrenoid in chloroplasts and its starch sheath, and a decrease in the number and partial volume of starch granules on cell section followed by their disappearance. However, until the end of the exposure, chloroplasts in most thallus cells retained their integrity, and there were no signs of damage to the internal membrane structure. At all the stages of the experiment, electron-dense globules were registered in the cytoplasm. We cannot be sure in the nature of these formations, but we do not exclude that the globules are the product of the transformation of absorbed OP. Their presence in the alga cells, not only in the experiment with oil introduced into seawater, but also in the initial sample, may be due to the long-term habitation of the alga in an environment contaminated with OP (10 MPC) before our study. Moreover, the alga itself can synthesize hydrocarbons, *e. g.*, phytane. The intensity of photosynthesis decreased in the alga of both the control (with no OP) and experimental (with introduced OP) samples in 5 days by almost 3 times compared to that of the initial variant. However, in 10 days of the exposure, the values of photosynthesis in the sample with introduced oil did not differ from those registered in the initial variant. This fact may reflect the adaptive capacity of the alga photosynthetic apparatus to oil contamination. It is confirmed by minimal changes in the photosynthetic apparatus throughout the exposure. An increase in the intensity of photosynthesis in the presence of small doses of oil in the environment was revealed in experiments with other algae species, and this confirms the possibility of OH absorption by macrophyte algae and OH inclusion in the metabolism [Salakhov et al., 2020, 2021; Stepanyan, Voskoboinikov, 2006]. Possible changes in metabolism are evidenced by an increase in the number and size of mitochondria and the number of mitochondrial cristae on cell sections during the experiment.

The number of epiphytic bacteria correlated with changes in the concentrations of OH in the alga. By the 5th day, there was an increase in the number of heterotrophic bacteria, *inter alia* HOB. By the end of the exposure, their number decreased compared to the value on the 5th day. OH, which are accumulated in algae, can be a growth factor for microorganisms. Moreover, a sharp rise in the number of heterotrophic bacteria both in the experiment and in the control may be due to the fact as follows: during the vital activity of macrophytes, substances are released into the environment that contribute to the development of heterotrophic microorganisms.

Interestingly, with a significant increase in the number of HOB, their proportion relative to the total number of heterotrophic bacteria in the experiment remained quite low, in the presence of oil as well. The maximum proportion of HOB was observed in the alga *prior* to oil introduction into the medium; then, the value decreased. This was especially noticeable on the 10th day of the exposure: the difference was about an order of magnitude.

When estimating the number of cultivated heterotrophic bacteria in the control and experiment, some discrepancies arose with the results of electron microscopic analysis, in which significantly more bacteria were registered on the alga surface in the presence of oil than in the control (Fig. 1a, c). This can be explained by the fact that most of the bacterial community does not grow on nutrient media [Meyer-Reil, 1977; van Es, Meyer-Reil, 1982; ZoBell, 1946]. It is believed that about 10% of the entire community is capable of cultivating on media, with from 40% to more than 70% of the community being able to use OH as a nutrient substrate [Buckley et al., 1976; Panov, 1990]. However, this does not mean that other ("unaccounted") bacteria present in the environment are not capable of destructing OP. Cultivation on nutrient media allows to identify bacteria that can quickly adapt to conditions of contamination (within the framework of a laboratory experiment as well), to obtain quite reliable results, and to follow the trends occurring in bacterial communities under the effect of various contaminants (in our case, oil).

Conclusion. The obtained results showed the ability of the green alga *Acrosiphonia arcta* not only to withstand oil contamination of 100 MPC for 10 days (in terms of level, it is comparable to a weak oil spill), but also to participate in the purification of seawater from oil products. The first revealed fact is likely to be due to the formation of adaptive reactions during the development of the alga under low contamination by oil products, while the second, by analogy with characteristics of other studied representatives of phytobenthos, can be due to the formation of a symbiotic association of algae and hydrocarbon-oxidizing bacteria. These facts are supported both by the preservation of the structure and function of the photosynthetic apparatus at an oil contamination of 100 MPC and the presence of abundant microorganisms on the alga surface. With an extremely low biomass of *A. arcta*, its percentage contribution to the volume of neutralized oil products in the Barents Sea coast is much lower than that of *Laminaria* or *Fucus* algae [Voskoboinikov et al., 2020a]. However, *A. arcta* occurs in all latitudes of the World Ocean, is highly resistant to the environmental factors of the Barents Sea coast [Lüning, 1984; Wiencke et al., 1993], and is capable of developing in oil-contaminated water areas on any substrate, preparing it for colonization by larger perennial macrophyte algae and their passage through early developmental stages, at the same time participating in the bioremediation of the marine environment from oil. Thus, the role of *A. arcta* in the restoration of coastal phytocoenoses is quite significant.

This work was carried out within the framework of the state research assignment "Bottom biocenoses of the Barents Sea, its drainage basin, and adjacent waters in modern conditions" (No. 122020900044-2).

REFERENCES

1. Voskoboinikov G. M., Matishov G. G., Metelkova L. O., Zhakovskaia Z. A., Lopushanskaia E. M. The participating of the green algae *Ulvaria obscura* in the bioremediation of the sea water from oil products. *Doklady Akademii nauk*, 2018, vol. 481, no. 1, pp. 111–113. (in Russ.). https://doi.org/10.31857/S086956520000064-3
2. Voskoboinikov G. M., Malavenda S. V., Metelkova L. O. Rol' fukusovykh vodoroslei v bioremediatsii pribrezhnykh akvatorii ot nefteproduktov na primere Kol'skogo zaliva. In: *Morskie issledovaniya i obrazovanie*

(MARESEDU-2020) : trudy IX Mezhdunarodnoi nauchno-prakticheskoi konferentsii. Tver : PoliPRESS, 2020a, vol. 3, pp. 320–323. (in Russ.)

3. Voskoboinikov G. M., Ryzhik I. V., Salakhov D. O., Metelkova L. O., Zhakovskaya Z. A., Lopushanskaya E. M. Absorption and conversion of the diesel fuel by the red alga *Palmaria palmata* (Linnaeus) F. Weber et D. Mohr, 1805 (Rhodophyta): The potential role of the alga in bioremediation of sea water. *Biologiya morya*, 2020b, vol. 46, no. 2, pp. 135–141. (in Russ.). https://doi.org/10.31857/S0134347520020102
4. Voskoboinikov G. M., Titlyanov E. A. A study on the anatomy and ultrastructure of the red alga *Grateloupia turuturu* from habitats of different illumination. In: *Ekologicheskie aspekty fotosinteza morskikh makrovodoroslei*. Vladivostok : Izd-vo DVNTs AN SSSR, 1978, pp. 83–87. (in Russ.)
5. Koronelli T. V., Iljinsky V. V. About the enumeration of hydrocarbon-oxidizing bacteria in seawater by a considered method. *Vestnik Moskovskogo universiteta. Seriya 16. Biologiya*, 1984, no. 3, pp. 54–56. (in Russ.)
6. Panov G. V. *Sostoyanie mikrobiologicheskikh protsessov v impaktnykh i fonovykh raionakh Mirovogo okeana (na primere Baltiiskogo i Beringova morei)* : avtoref. dis. … kand. biol. nauk : 03.00.16. Moscow, 1990, 22 p. (in Russ.)
7. *Prakticheskaya gidrobiologiya. Presnovodnye ekosistemy* / V. D. Fedorov, V. I. Kapkov (Eds). Moscow : PIM, 2006, 367 p. (in Russ.)
8. Pugovkin D. V. *Epifitnye bakteriotsenozy Fucus vesiculosus L. Barentseva morya i ikh rol' v degradatsii neftyanykh zagryaznenii* : avtoref. dis. … kand. biol. nauk : 25.00.28. Murmansk, 2017, 26 p. (in Russ.)
9. *Rukovodstvo po metodam biologicheskogo analiza morskoi vody i donnykh otlozhenii* / A. V. Tsyban (Ed.). Leningrad : Gidrometeoizdat, 1980, 191 p. (in Russ.)
10. Stepanyan O. V., Voskoboinikov G. M. The effects of oil and oil products on the morphofunctional characteristics of marine macroalgae. *Biologiya morya*, 2006, vol. 32, no. 4, pp. 241–248. (in Russ.)
11. Normativy predel'no dopustimykh kontsentratsii vrednykh veshchestv v vodakh vodnykh ob"ektov rybokhozyaistvennogo znacheniya. Prilozhenie. Tabl. no. 2. In: *Ob utverzhdenii normativov kachestva vody vodnykh ob"ektov rybokhozyaistvennogo znacheniya, v tom chisle normativov predel'no dopustimykh kontsentratsii vrednykh veshchestv v vodakh vodnykh ob"ektov rybokhozyaistvennogo znacheniya* : prikaz Minsel'khoza Rossii ot 13.12.2016 no. 552 [v red. ot 10.03.2020]. (in Russ.). URL: https://sudact.ru/law/prikaz-minselkhoza-rossii-ot-13122016-n-552/prilozhenie/tablitsa-n-2/ [accessed: 21.03.2022].
12. Atlas R. M. Microorganisms and petroleum pollutants. *BioScience*, 1978, vol. 28, iss. 6, pp. 387–391. https://doi.org/10.2307/1307454
13. Buckley E. N., Jonas R. B., Fraender F. K. Characterization of microbial isolates from an estuarine ecosystem: Relationship of hydrocarbon utilization to ambient hydrocarbon concentrations. *Applied and Environmental Microbiology*, 1976, vol. 32, no. 2, pp. 232–237. https://doi.org/10.1128/aem.32.2.232-237.1976
14. Heitkamp M. A., Cerniglia C. E. Effects of chemical structure and exposure on the microbial degradation of polycyclic aromatic hydrocarbons in freshwater and estuarine ecosystems. *Environmental Toxicology and Chemistry*, 1987, vol. 6, iss. 7, pp. 535–546. https://doi.org/10.1002/etc.5620060706
15. Lüning K. Temperature tolerance and biogeography of seaweeds: The marine algal flora of Helgoland (North Sea) as an example. *Helgoländer Meeresuntersuchungen*, 1984, vol. 38, iss. 2, pp. 305–317. https://doi.org/10.1007/BF01997486
16. Malavenda S. V., Mitayev M. V., Malavenda S. S., Gerasimova M. V. Fouling of coarse-clastic sediments with macrophytes depending on the rate of abrasion, Murmansk coast. *Doklady Earth Sciences*, 2017, vol. 474, iss. 1, pp. 557–560. https://doi.org/10.1134/S1028334X17050063
17. Meyer-Reil L.-A. Bacterial growth rates and biomass production. In: *Microbial Ecology*

of a Brackish Water Environment / G. Rheinheimer (Ed.). Berlin ; Heidelberg : Springer-Verlag, 1977, pp. 223–235. https://doi.org/10.1007/978-3-642-66791-6_16

18. Mills A. L., Breul C., Colwell R. R. Enumeration of petroleum-degrading marine and estuarine microorganisms by the most probable number method. *Canadian Journal of Microbiology*, 1978, vol. 24, pp. 552–557. https://doi.org/10.1139/m78-089
19. Pilatti F., Ramlov F., Schmidt E., Kreusch M., Pereira D., Costa Ch., de Oliveira E., Bauer C., Rocha M., Bouzon Z., Maraschin M. *In vitro* exposure of *Ulva lactuca* Linnaeus (Chlorophyta) to gasoline – Biochemical and morphological alterations. *Chemosphere*, 2016, vol. 156, pp. 428–437. https://doi.org/10.1016/j.chemosphere.2016.04.126
20. Pirnik M. P. Microbial oxidation of methyl branched alkanes. *Critical Reviews in Microbiology*, 1977, vol. 5, iss. 4, pp. 413–422. https://doi.org/10.3109/10408417709102812
21. Ryzhik I., Pugovkin D., Makarov M., Roleda M. Y., Basova L., Voskoboynikov G. Tolerance of *Fucus vesiculosus* exposed to diesel water-accommodated fraction (WAF) and degradation of hydrocarbons by the associated bacteria. *Environmental Pollution*, 2019, vol. 254 (Pt. B), art. no. 113072 (6 p.). https://doi.org/10.1016/j.envpol.2019.113072
22. Salakhov D., Pugovkin D., Ryzhik I., Voskoboinikov G. The influence of diesel fuel on morpho-functional state of *Ulvaria obscura* (Chlorophyta). *IOP Conference Series: Earth and Environmental Science*, 2020, vol. 539, iss. 1, art. no. 012202 (7 p.). https://doi.org/10.1088/1755-1315/539/1/012202
23. Salakhov D., Pugovkin D., Ryzhik I., Voskoboinikov G. The changes in the morpho-functional state of the green alga *Ulva intestinalis* L. in the Barents Sea under the influence of diesel fuel. *IOP Conference Series: Earth and Environmental Science*, 2021, vol. 937, iss. 2, art. no. 022059 (8 p.). https://doi.org/10.1088/1755-1315/937/2/022059
24. van Es F. B., Meyer-Reil L.-A. Biomass and metabolic activity of heterotrophic marine bacteria. In: *Advances in Microbial Ecology* / K. C. Marshall (Ed.). New York ; London : Plenum Press, 1982, vol. 6, pp. 111–170. https://doi.org/10.1007/978-1-4615-8318-9_4
25. Wiencke C., Rahmel J., Karsten U., Weykam G., Kirst G. O. Photosynthesis of marine macroalgae from Antarctica: Light and temperature requirements. *Botanica Acta*, 1993, vol. 106, iss. 1, pp. 78–87. https://doi.org/10.1111/j.1438-8677.1993.tb00341.x
26. ZoBell C. E. *Marine Microbiology. A Monograph on Hydrobacteriology*. Waltham, MA : Chronica Botanica Co., 1946, 240 p.

ВЛИЯНИЕ СЫРОЙ НЕФТИ НА СИМБИОТИЧЕСКУЮ АССОЦИАЦИЮ ЗЕЛЁНОЙ ВОДОРОСЛИ *ACROSIPHONIA ARCTA* (DILLWYN) GAIN И ЭПИФИТНЫХ БАКТЕРИЙ

Г. М. Воскобойников[1], Л. О. Метелькова[2], Д. В. Пуговкин[1], Д. О. Салахов[1]

[1]Мурманский морской биологический институт Российской академии наук, Мурманск, Российская Федерация

[2]Федеральное государственное унитарное предприятие «Всероссийский научно-исследовательский институт метрологии имени Д. И. Менделеева», Санкт-Петербург, Российская Федерация

E-mail: *grvosk@mail.ru*

Экспериментально показано, что зелёная водоросль *Acrosiphonia arcta*, обитающая на литорали Баренцева моря, сохраняет жизнеспособность в течение 10 дней при воздействии сырой нефти, введённой в концентрации 5 мг·л$^{-1}$ в морскую воду. Данная концентрация соответствует слабому разливу нефти. Методами микробиологии, световой и электронной микроскопии,

а также физиологии проанализированы морфофункциональные изменения у симбиотической ассоциации акросифонии и эпифитных бактерий на её поверхности. Показано сохранение высокого уровня фотосинтеза и неповреждённой ультраструктуры у большинства клеток водорослей в течение всего эксперимента. Вместе с тем к концу опыта под воздействием нефти в клетках водорослей уменьшается доля хлоропластов, исчезают пиреноид и гранулы крахмала. Прослежена динамика численности эпифитных бактерий в эксперименте и доля углеводородокисляющих бактерий в общем количестве культивируемых гетеротрофов. Продемонстрирована способность акросифонии поглощать и трансформировать нефтепродукты. Способность данного вида водорослей развиваться в загрязнённых нефтью акваториях на любом субстрате, подготавливая его для заселения более крупными многолетними водорослями-макрофитами, определяет важную роль *A. arcta* в восстановлении прибрежных фитоценозов.

Ключевые слова: *Acrosiphonia arcta*, нефть, биоремедиация морской воды, симбиотическая ассоциация, эпифитные бактерии, фотосинтез, ультраструктура

1871
ИнБЮМ – IBSS

Морской биологический журнал
Marine Biological Journal
2023, vol. 8, no. 1, pp. 27–50
https://marine-biology.ru

UDC [582.261.1:57.086.83]:519.6

PRODUCTION CHARACTERISTICS OF A CULTURE OF THE DIATOM *CYLINDROTHECA CLOSTERIUM* (EHRENBERG) REIMANN ET LEWIN IN A TWO-STAGE CHEMOSTAT

© 2023 **R. G. Gevorgiz[1], S. N. Zheleznova[1], and A. S. Malakhov[2]**

[1]A. O. Kovalevsky Institute of Biology of the Southern Seas of RAS, Sevastopol, Russian Federation
[2]National Research Tomsk Polytechnic University, Tomsk, Russian Federation
E-mail: *r.gevorgiz@yandex.ru*

Received by the Editor 06.10.2020; after reviewing 16.01.2021;
accepted for publication 20.10.2022; published online 14.03.2023.

The advantages and disadvantages of flow and batch microalgae cultivation are discussed. The benefits of the flow cultivation are indicated, in particular in a quasi-continuous mode in a two-stage chemostat. It is proposed to use the culture of the benthic diatom *Cylindrotheca closterium* as a producer of valuable substances since this species has several useful properties of both biological and technological nature. Specifically: 1) *C. closterium* is characterized by relatively high production rates; 2) it efficiently utilizes light energy which removes restrictions on the location of production in areas with a small number of sunny days *per* year; 3) it has a rather low temperature optimum for growth which is significant for the implementation of industrial technologies in Russian Federation; and 4) it has the specific density of cells of more than one, therefore, cells quickly enough sink to the photobioreactor bottom in the absence of the culture aeration (this simplifies the separation of biomass from the culture medium and reduces its cost). The aim of this work is to analyze the production characteristics of the quasi-continuous *C. closterium* culture in the two-stage chemostat. The studies were carried out at a temperature of (20 ± 1) °C and irradiation of 150 μmol quanta·m^{-2}·s^{-1}. The chemostat for *C. closterium* cultivation consisted of two glass 3-L photobioreactors of the plane-parallel type, each having a working thickness of 5 cm and a working surface of 0.03 m^2. The cultivation was carried out on the nutrient medium RS with a constant aeration (the speed was of 1.5 L of air *per* 1 L of culture *per* min). The culture was examined at different dilution rates of the nutrient medium: 0.1; 0.3; 0.5; 0.7; and 0.9 day^{-1}. The growth parameters of the batch culture were calculated: the specific growth rate μ_b = 0.7 day^{-1}; the time for doubling the biomass t_d = 0.987 days. The maximum productivity of a one- and two-stage chemostat was registered at the optimal dilution rate of 0.59 day^{-1}; the values were 1.348 and 1.498 g·L^{-1}·day^{-1}, respectively. As found experimentally, *C. closterium* productivity in the flow culture is 2.2 times higher than in the batch culture. The experimental data were used to calculate the maximum specific growth rate μ_m and the saturation constant K_S with limiting *C. closterium* growth by silicon; the values were 1.05 day^{-1} and 0.028 g·L^{-1}, respectively. It was shown that the observed need for silicon in the flow culture (Y_{fl} = 35 mg·g^{-1}) is lower by 7.9% than in the batch culture (Y_b = 38 mg·g^{-1}). For the diatom *C. closterium*, μ_m, K_S, and Y_{fl} are important physiological characteristics; those play the key role in the design of industrial systems for intensive microalgae cultivation.

Keywords: *Cylindrotheca closterium*, chemostat, mathematical model

Microalgae are widely used in modern biotechnology [Bozarth et al., 2009]. Their biomass and waste products have found an application in food industry, agriculture, and aquaculture [Creswell, 2010; Sathasivam et al., 2019]. Microalgae play an important role in technologies of wastewater treatment [Abinandan et al., 2018; Wollmann et al., 2019], rehabilitation of water basins by preventing blooming [Kiran et al., 2016], CO_2 utilization [Singh, Dhar, 2019], algolization of soils, and green manuring. On their basis, industrial technologies are created for obtaining unique biologically active compounds applied in medicine, perfumery [Lauritano et al., 2016; Lincoln et al., 1990; Patras et al., 2018], *etc.* Microalgae are actively used in various human activity, but their potential is far from being exhausted. Selection of new objects for intensive cultivation from natural populations and production of genetically modified strains with desired properties constantly expand the possibilities for creating new biotechnologies based on microalgae. In this field, there is a considerable progress; however, the search for new producers is ongoing.

Microalgae are known to accumulate many valuable substances precisely under stressful conditions, for example, when their growth is limited by biogenic elements. Accordingly, various methods of two-stage batch cultivation have been developed: at the first stage, the accumulation of biomass occurs, and at the second one, the accumulation of valuable substances, *e. g.*, lipids and carotenoids [Lu et al., 2018; Minyuk et al., 2014; Nagappan et al., 2019]. A significant disadvantage of the two-stage batch cultivation is the death of a considerable part of microalgal cells at the second stage, under stress conditions; this notably reduces the efficiency of obtaining the target product [Minyuk et al., 2014]. The most promising alternative to the two-stage batch cultivation is the flow cultivation, in particular, a usage of a two-stage chemostat with equal or different specific flow rates for each stage.

From the standpoint of obtaining valuable biologically active compounds on an industrial scale, the most promising cultivation objects are benthic species of microalgae. Those are distinguished by several useful properties of both biological and technological nature. Specifically:

1) benthic microalgae are characterized by relatively high production rates [Zheleznova, 2019];
2) those efficiently utilize light energy [Baldisserotto et al., 2019], and this removes restrictions on the location of production in areas with a small number of sunny days *per* year;
3) benthic microalgae are characterized by a rather low temperature optimum for growth [Salleh, McMinn, 2011; Stock et al., 2019], which is significant for the implementation of technologies in Russian Federation;
4) those have the specific density of cells of more than one, therefore, cells quickly enough sink to the photobioreactor bottom in the absence of the culture aeration (this simplifies the separation of biomass from the culture medium, reduces its cost, *etc.*).

In literature, data on intensive cultivation of benthic microalgae are scarce. The studies on benthic diatoms in a flow culture are practically not described as well. Out of many species of benthic microalgae for intensive cultivation on an industrial scale, the diatom *Cylindrotheca closterium* (Ehrenberg) Reimann et Lewin, 1964 is of the greatest interest [Gevorgiz et al., 2016; Wang et al., 2018]. It is capable of accumulating valuable polyunsaturated fatty acids and fucoxanthin [Wang et al., 2015; Zheleznova et al., 2017], as well as iodine, iron, and other trace elements in organic form [de la Cuesta, Manley, 2009; Zheleznova et al., 2015a].

The aim of this work is to analyze the production characteristics of a quasi-continuous *C. closterium* culture in a two-stage chemostat.

MATERIAL AND METHODS

We studied the culture of the diatom *C. closterium* from the IBSS collection of microalgae cultures. For two weeks, the culture obtained from this collection was adapted to the concentrated nutrient medium RS [Zheleznova et al., 2015b] and to conditions of intensive cultivation. The adapted culture was centrifuged (at 1,600 g for 1 min); then, the supernatant was removed, and algal raw mass was used as an inoculum to analyze the production characteristics of a quasi-continuous culture in a chemostat. When working with the chemostat, the nutrient medium RS was used with a 3-fold increase in the concentration of each component; it was prepared on sterile Black Sea water. The composition of the nutrient medium is given in Table 1.

Table 1. Composition of the nutrient medium RS [Zheleznova et al., 2015b] used in the experiment

No.	Component	Content, $g \cdot L^{-1}$
1	$NaNO_3$	2.331
2	$NaH_2PO_4 \cdot 2H_2O$	0.665
3	$Na_2SiO_3 \cdot 9H_2O$	1.158
4	Na_2EDTA	0.792
5	$FeSO_4 \cdot 7H_2O$	0.192
6	$CuSO_4 \cdot 5H_2O$	0.0006
7	$ZnSO_4 \cdot 7H_2O$	0.001 32
8	$CoCl_2 \cdot 6H_2O$	0.0006
9	$MnCl_2 \cdot 4H_2O$	0.001 08
10	$NaMoO_4 \cdot H_2O$	0.000 36

C. closterium production characteristics were studied under optimal light conditions, at optimal temperature and nutrient availability. The chemostat for *C. closterium* cultivation (Fig. 1) consisted of two glass 3-L photobioreactors (the two-stage chemostat) of the plane-parallel type, each having a working thickness of 5 cm. The working volume of the suspension in each photobioreactor was maintained at a constant level, 2 L. The experiment was carried out with uniform day-and-night one-sided irradiation of photobioreactors. As a source of irradiation, luminescent lamps CE-PIL-1-LF 46W/54-765 (Poland) were used. On the working surface of each photobioreactor (0.03 m^2), those gave an average of 150 $\mu mol\,quanta \cdot m^{-2} \cdot s^{-1}$ (33 $W \cdot m^{-2}$). To measure irradiation, a TKA-Spectr spectrophotometer (PAR) was applied. Throughout the experiment, the temperature of the algal suspension was maintained at a constant level of (20 ± 1) °C. To provide cells with carbon, the culture in both photobioreactors was aerated (1.5 L of air *per* 1 L of culture *per* min) with a compressor unit. To increase CO_2 solubility in the culture medium, air was supplied to the suspension *via* a dispensing nozzle.

At the first stage of the experiment, the culture was grown in a batch mode, and at the second stage, in a quasi-continuous one. *C. closterium* proportional-flow quasi-continuous cultivation was carried out in a single-flow mode as follows:

1) for yield, a part of the working volume was withdrawn daily from the second photobioreactor (the second stage of the chemostat);

2) the same part of the working volume was withdrawn from the first photobioreactor (the first stage of the chemostat) and transferred to the second photobioreactor – to restore the working volume in the second photobioreactor;
3) the working volume in the first photobioreactor was restored by adding fresh nutrient medium. The culture was diluted every day.

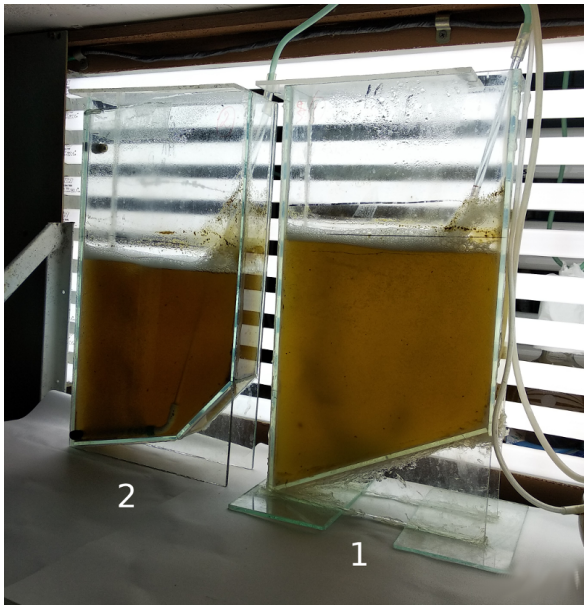

Fig. 1. *Cylindrotheca closterium* culture in a two-stage chemostat (stages are indicated by numbers)

After the batch cultivation, since the 6th day of the experiment, the culture was grown in the quasi-continuous mode with a flow rate of the nutrient medium through the working volume of the microalgal suspension of 0.6 L·day^{-1} (dilution rate, or specific flow rate, ω = 0.6 / 2 = 0.3 day^{-1}). From the 17th to the 27th day of the experiment, the specific flow rate was set as 0.1 day^{-1}; from the 27th to the 35th, 0.5 day^{-1}; from the 35th to the 40th, 0.7 day^{-1}; and from the 40th to 44th, 0.9 day^{-1}.

To determine the culture density, two methods were applied – the method of iodate oxidation [Gevorgiz et al., 2015] and direct weighing of *C. closterium* raw mass in polypropylene test tubes on an analytical balance with an error of 0.1 mg after cell sedimentation by centrifugation (at 1,600 g for 2 min). To calculate the data obtained for wet mass in terms of dry, the conversion factor (k = 0.1) was used [Zheleznova, Gevorgiz, 2020].

RESULTS AND DISCUSSION

The dynamics of the density of *C. closterium* culture in the batch and flow modes of cultivation is shown in Fig. 2. In the experiment, the adapted culture was used; therefore, there was no lag phase for an accumulation curve. The exponential growth phase lasted four days. In the stationary phase, the culture density practically did not change. Upon transition to the quasi-continuous mode of cultivation, rapid adaptation to the conditions of flow cultivation was observed. With a change in the specific flow rate, the transition processes lasted for a short time (no more than 2–3 days), and the culture density value quickly reached a new stationary dynamic equilibrium (Fig. 2).

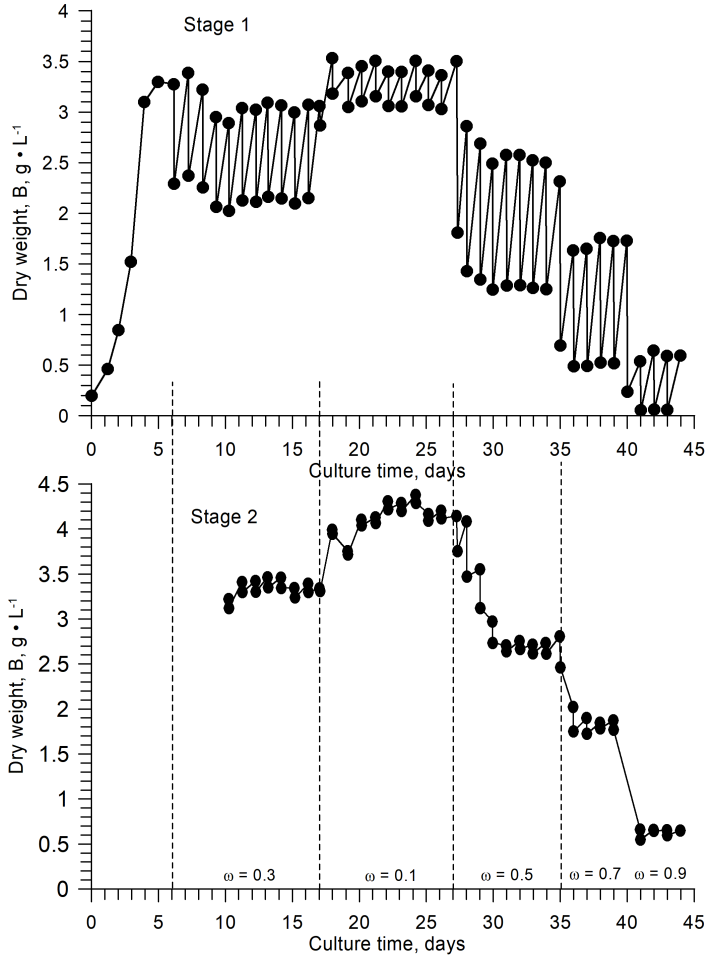

Fig. 2. Dynamics of *Cylindrotheca closterium* density in the batch culture and in the two-stage chemostat at different dilution rates ω (the boundaries are indicated by the dotted lines)

In both the first and second chemostat stages, at a specific flow rate of 0.1 day^{-1}, insignificant cell agglutination was recorded; it caused difficulties in sampling when measuring the culture density and contributed to an increase in data scatter. In both chemostat stages, almost at any flow rate, cells were evenly distributed throughout the entire working volume. At a specific flow rate of 0.9 day^{-1}, a near-wall culture growth was observed, and the aeration was not enough to mix the suspension. Even after mixing the culture with a manual stirrer, some biomass quickly sank to the photobioreactor bottom or walls.

Growth parameters. At the beginning of the batch cultivation, when introducing inoculum into the nutrient medium, the culture density (B_0) was 0.2 g·L^{-1}. In the batch culture, there was no lag phase, since it was adapted to the experimental conditions earlier. The exponential phase of the accumulation curve was characterized by a constant specific growth rate and was described with high accuracy (R^2 = 0.99) by equation (1) (Fig. 3):

$$\ln B = \mu_b (t - t_0) + \ln B_0; \qquad \ln B = 0.7\, t - 1.61, \tag{1}$$

where μ_b is the specific growth rate in the batch culture, day^{-1};

B_0 is the culture density at the initial moment of time t_0 (t_0 = 0).

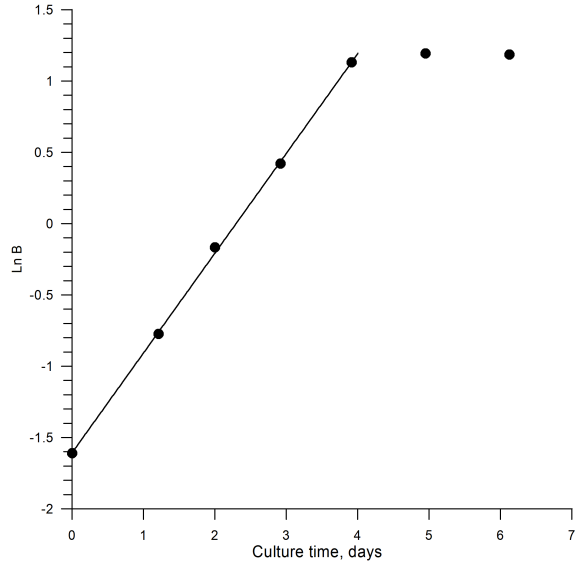

Fig. 3. Dynamics of *Cylindrotheca closterium* density in the batch culture in semi-logarithmic coordinates. Approximation of experimental points by equation (1), R^2 = 0.99. The specific growth rate μ_b = 0.7 day^{-1}

The biomass doubling time in the exponential growth phase (t_d) was:

$$t_d = \ln 2 \frac{t - t_0}{\ln B - \ln B_0} = \frac{\ln 2}{\mu_b} = \frac{0.693}{0.7} = 0.987. \quad (2)$$

Reverse doubling time (Fig. 3) was as follows:

$$\log_2 B = \frac{1}{t_d}(t - t_0) + \log_2 B_0, \qquad \frac{1}{t_d} = \frac{\mu_b}{\ln 2} = \frac{0.7}{0.693} = 1.01. \quad (3)$$

On the 5th day of the experiment, the culture reached the stationary growth phase. In this phase, the culture density remained the same (B_m = 3.3 g·L^{-1}) until the transition to the quasi-continuous mode of cultivation (Fig. 2). For 5 days of the batch cultivation, the yield was $B_b(5) = B_m - B_0$ = 3.1 g·L^{-1}. Accordingly, the average productivity of the batch culture $\overline{P}_b$ = 0.62 g·L^{-1}·day^{-1}.

Quantitative requirements for nutrients in the actively growing *C. closterium* culture were experimentally determined by us earlier [Zheleznova et al., 2015b]. Based on these data and applying formula (4), economic coefficients (Y_{ec}) were calculated for several biogenic elements (Table 2):

$$Y_{ec} = \frac{1}{Y_b}, \quad (4)$$

where Y_b is the observed requirement for a biogenic element in the batch culture.

Table 2. Observed requirements for *Cylindrotheca closterium* in the batch culture (Y_b) according to the data from [Zheleznova, Gevorgiz, 2014] and calculated values of economic coefficients (Y_{ec}) according to formula (4) for some nutrients

No.	Biogenic element	Y_b, mg·g^{-1}	Y_{ec}, g·g^{-1}
1	Nitrogen	64 ± 1	15.6
2	Silicon	38.2 ± 0.01	26.2
3	Phosphorus	17 ± 1	60.3
4	Iron	45 ± 0.2	22.2

To determine the dependence of *C. closterium* specific growth rate on the concentration of the limiting substrate in the nutrient medium, based on the data from [Zheleznova, Gevorgiz, 2014], the saturation constant (K_S) was calculated. Analyzing the composition and ratios of biogenic elements in the nutrient medium F [Guillard, 1975; Guillard, Ryther, 1962], as well as the ratio of *C. closterium* requirements from Table 2, it can be concluded as follows: when this alga is cultivated on the nutrient medium F, as was done in [Zheleznova, Gevorgiz, 2014], the limiting growth factor is the concentration of silicon in this medium. Therefore, the saturation constant was calculated precisely for silicon (Fig. 4):

$$P = P_m \frac{S}{K_S + S}, \quad P = 1.81 \frac{S}{0.028 + S}; \qquad \mu = \mu_m \frac{S}{K_S + S}, \quad \mu = \mu_m \frac{S}{0.028 + S}, \tag{5}$$

where S is the concentration of the limiting substrate (silicon) in the nutrient medium, g·L^{-1}.

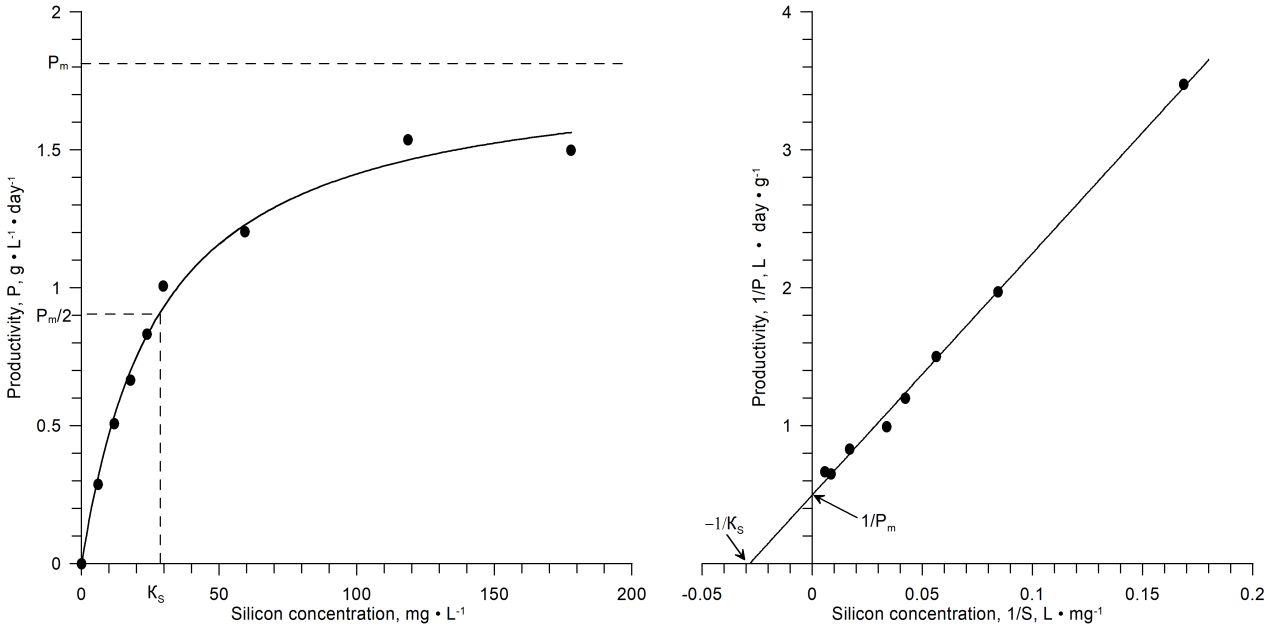

Fig. 4. Dependence of *Cylindrotheca closterium* growth rate on the silicon concentration in the nutrient medium. P_m = 1.81 g·L^{-1}·day^{-1}; K_S = 0.028 g·L^{-1}. Calculation by equation (5) according to the experimental data from [Zheleznova, Gevorgiz, 2014]

Flow culture. The chemostat theory was developed for continuous cultures of heterotrophic microorganisms in the second half of the XX century and is detailed in [Herbert et al., 1956; Maxon, 1955; Methods in Microbiology, 1970; Pirt, 1978; Theoretical and Methodological Basis of Continuous Culture of Microorganism, 1968]. In some cases, it is applicable to lower phototrophs as well. However, since their growth requires light energy, which, along with biogenic elements, can limit cell growth, the chemostat theory needs amendments and clarifications for phototrophs. This is especially true for dense cultures of microalgae, when the accumulation curve is characterized by the presence of not only an exponential growth phase, but also a long phase of growth deceleration (phase of negative growth acceleration). Of particular note is the need for significant additions and changes in the chemostat theory, when: 1) natural light is used, and a change in the growth-limiting factor is observed during the day; 2) it is difficult or impractical to organize a continuous flow of a nutrient medium; *etc.* In such a case, a batch

culture (quasi-continuous one) is often used in practice. Interestingly, the method of quasi-continuous cultivation is a certain generalization of various techniques of the flow cultivation of microorganisms. However, the publications on modeling processes in a quasi-continuous culture are quite rare [Fencl, 1968; Trenkenshu, 2005].

In our experiment, the exponential growth phase of the accumulation curve was accurately described by equation for exponential growth (see equation (1) and Fig. 3); that is, cell growth was practically not limited by light conditions. Apparently, there was no change in the growth-limiting factor in this area. This circumstance allows us to apply an approach, which is similar to that used when working with heterotrophic microorganisms, to derive equations for the density dynamics of a quasi-continuous culture. We will analyze a quasi-continuous culture in a proportional-flow single-flow multistage chemostat with the same working volume V (L) in each stage and the same volume w (L), which is withdrawn from each stage during the exchange procedure. The ratio of the algal mass in the *i*-th stage of the chemostat m_i (g) to the working volume V (L) determines the actual density of the culture in this stage (g·L^{-1}):

$$B_i = \frac{m_i}{V}. \tag{6}$$

As a result of the exchange procedure, the volume w, which contains the algal mass m_i^*, is withdrawn from the *i*-th stage of the chemostat. The remaining volume (V – w) contains the algal mass m_i^{**}. Therefore, the following equalities can be written:

$$m_i = m_i^* + m_i^{**}; \quad m_i^* = \mathrm{w} \cdot B_i; \quad m_i^{**} = V \cdot B_i - \mathrm{w} \cdot B_i = (V - \mathrm{w}) \cdot B_i. \tag{7}$$

In a multistage chemostat, after withdrawing the volume w, the *i*-th stage receives the same volume of suspension from the previous stage. So, the culture density in the *i*-th stage after the exchange ($B_i^{(-)}$) is equal to:

$$B_i^{(-)} = \frac{m_{i-1}^* + m_i^{**}}{V} = \frac{\mathrm{w} \cdot B_{i-1} + (V - \mathrm{w}) \cdot B_i}{V}, \tag{8}$$

where m_{i-1}^* is the algal mass from the previous stage, which is introduced into the current stage during the exchange;

B_{i-1} is the culture density in the previous chemostat stage.

Therefore:

$$\frac{\mathrm{w}}{V} = \frac{B_i - B_i^{(-)}}{B_i - B_{i-1}} = \frac{m_i^* - m_{i-1}^*}{m_i - m_{i-1}}; \tag{9}$$

it means that the ratio of the volume during the exchange procedure is equal to the ratio of the algal mass withdrawn during the exchange from the current stage to the difference in the algal masses in the current and previous chemostat stages.

The ratio of the culture density before and after the exchange indicates the value of the culture dilution (θ_i); it shows how many times the algal mass and the culture density decrease in the *i*-th stage:

$$\theta_i = \frac{B_i}{B_i^{(-)}} = \frac{V}{V - \mathrm{w}\left(1 - \frac{B_{i-1}}{B_i}\right)}. \tag{10}$$

Worth noting as follows: if the culture is diluted with a nutrient medium ($B_{i-1} = 0$), then, expression for the first stage of the chemostat is obtained, similar to that in the publication [Trenkenshu, 2005]:

$$\theta_1 = \frac{B_1}{B_1^{(-)}} = \frac{V}{V - \mathrm{w}}.$$

From expressions (9) and (10), it follows:

$$\frac{\mathrm{w}}{V} = \frac{B_i - B_i^{(-)}}{B_i - B_{i-1}} = \frac{B_i - \frac{1}{\theta_i} B_i}{B_i - B_{i-1}}. \tag{11}$$

In a quasi-continuous culture, the change in the algal mass (Δm_i) is determined by two processes – an increase in the mass driven by algal growth and a decrease in the mass due to the difference in inflow and outflow with a part of the suspension during the exchange procedure:

$$\underbrace{m_{i+1} - (m_{i-1}^{*} + m_i^{**})}_{\text{growth}} + \underbrace{m_{i-1}^{*}}_{\text{inflow}} - \underbrace{(m_i - m_i^{**})}_{\text{decrease with outflow}} = m_{i+1} - m_i = \Delta m_i, \tag{12}$$

where m_i is the algal mass before the exchange;

m_{i+1} is the algal mass before the exchange at the next step of the quasi-continuous cultivation;

m_{i-1}^{*} is the mass of the alga introduced into the *i*-th stage from the previous one during the exchange;

m_{i-1}^{**} is the algal mass that remains in the *i*-th stage after withdrawing a part of the suspension with volume w.

Considering (6), (7), and (8), we can write the change in the culture density (ΔB_i):

$$\underbrace{[B_{i+1} - B_i^{(-)}]}_{\text{increase}} - \underbrace{[B_i - B_i^{(-)}]}_{\text{decrease}} = B_{i+1} - B_i = \Delta B_i, \tag{13}$$

where B_i is the culture density before the exchange (current density);

$B_i^{(-)}$ is the culture density after the exchange;

B_{i+1} is the culture density before the exchange at the next step of the quasi-continuous cultivation.

In microbiological practice, the algal growth in a culture is described by two quantitative characteristics – growth rate (productivity) and relative (specific) growth rate. Over the time interval between exchange procedures Δt (days), the culture density in the *i*-th stage increases to the value B_{i+1}. Therefore, on this time interval, the average growth rate is (g·L^{-1}·day^{-1}):

$$\overline{P}_i = \frac{B_{i+1} - B_i^{(-)}}{\Delta t}, \tag{14}$$

and the average specific growth rate is (day^{-1}):

$$\overline{\mu}_i = \frac{B_{i+1} - B_i^{(-)}}{B_i^{(-)} \cdot \Delta t}. \tag{15}$$

The decrease in density is related to the dilution value of the culture, which depends on both the algal mass withdrawn from the current chemostat stage during the exchange procedure and the algal mass introduced into the working volume from the previous chemostat stage. In one exchange procedure, the volume w is withdrawn from the working volume over the time interval Δt. Therefore, the culture flow rate (F) in the current chemostat stage is equal to (L·day^{-1}):

$$F = \frac{\mathrm{w}}{\Delta t},$$

and the relative (specific) flow rate ω is equal to (day^{-1}):

$$\omega = \frac{F}{V} = \frac{\mathrm{w}}{V \cdot \Delta t}. \tag{16}$$

Taking into account (10) and (16), we can express the value of the specific flow rate of the nutrient medium for the *i*-th stage:

$$\omega \left(1 - \frac{B_{i-1}}{B_i}\right) = \left(1 - \frac{1}{\theta_i}\right) \frac{1}{\Delta t}; \qquad \omega = \frac{1 - \dfrac{1}{\theta_i}}{1 - \dfrac{B_{i-1}}{B_i}} \frac{1}{\Delta t}. \tag{17}$$

It should be kept in mind as follows: (16) allows us to calculate for the *i*-th stage the specific flow rate of the algal suspension (or a nutrient medium for the first stage), which is the same in all the chemostat stages. Expression (17) indicates what the specific flow rate will be when the culture density in the *i*-th stage decreases by θ_i times, taking into account the culture density in the previous chemostat stage.

The value of the change in the culture density (13) over the time interval Δt can be expressed in terms of the growth rate and the flow rate. From (11), (13), and (16), it follows:

$$\frac{\Delta B_i}{\Delta t} = \frac{B_{i+1} - B_i^{(-)}}{\Delta t} - \frac{B_i - B_i^{(-)}}{\Delta t} = \overline{P}_i - \omega\,(B_i - B_{i-1}). \tag{18}$$

Thus, the rate of change in the density of the quasi-continuous culture in the current chemostat stage is determined by the average growth rate ($\overline{P}_i$), the rate of introduction of the alga from the previous stage ($\omega \cdot B_{i-1}$), and the rate of withdrawal of the alga during the exchange ($\omega \cdot B_i$).

Then, we express the average growth rate $\overline{P}_i$ in units of the culture density (biomass) in the *i*-th stage of the chemostat:

$$\overline{P}_i = \tilde{\mu}_i \cdot B_i, \tag{19}$$

where $\tilde{\mu}_i$ is the coefficient reflecting the ratio of the biomass growth B_i over the time interval Δt.

At its core, this coefficient is a relative growth rate, similar to (15), with the difference that the growth rate refers not to the culture density after the exchange, but to the culture density before the exchange – to B_i. The comparison of (14), (19), and (10) allows to see that $\overline{\mu}_i = \tilde{\mu}_i \cdot \theta_i$. The closer θ_i to 1 and the shorter the time interval Δt between culture dilutions, the smaller the difference between these values.

Substituting (19) into (18), we obtain the following equation:

$$\frac{\Delta B_i}{\Delta t} = \tilde{\mu}_i \cdot B_i - \omega\,(B_i - B_{i-1}) = \left[\tilde{\mu}_i - \omega\left(1 - \frac{B_{i-1}}{B_i}\right)\right] B_i. \tag{20}$$

The solution of this equation makes it possible to describe the dynamics of the density of the quasi-continuous culture in a multistage chemostat. In a particular case, when $\Delta t \to 0$, $\tilde{\mu}_i \to \mu_i$, $\theta_i \to 1$ (a continuous flow), we obtain differential equations identical to those published in [Fencl, 1968; Pirt, 1978].

For the first stage of the chemostat, when the culture is diluted with a nutrient medium ($B_{i-1} = 0$), expression (20) is transformed into:

$$\frac{\Delta B_1}{\Delta t} = \tilde{\mu}_1 \cdot B_1 - \omega \cdot B_1 = (\tilde{\mu}_1 - \omega) B_1. \tag{21}$$

It is completely identical to expression obtained earlier for a quasi-continuous culture in a one-stage chemostat [Trenkenshu, 2005].

In our experiment, the transition processes with various changes in the flow rate of the nutrient medium lasted for a short time (Fig. 2). Accordingly, we will consider only established processes (stationary dynamic equilibrium) – when the culture density remains the same over time in each chemostat stage ($\Delta B_i = 0$). For the conditions of stationary dynamic equilibrium, from (20), expressions for the relative growth rate and culture productivity in the *i*-th stage of the chemostat follow:

$$\tilde{\mu}_i = \omega\left(1 - \frac{B_{i-1}}{B_i}\right); \qquad \overline{P}_i = \omega\,(B_i - B_{i-1}). \tag{22}$$

Whence follow the relationship of culture densities in the neighboring chemostat stages and the dilution rate in the *i*-th stage:

$$B_i = \frac{\omega}{\omega - \tilde{\mu}_i} B_{i-1}; \qquad \omega = \tilde{\mu}_i \frac{B_i}{B_i - B_{i-1}} = \frac{\overline{P}_i}{B_i - B_{i-1}}. \tag{23}$$

It is to be noted that for the conditions of stationary dynamic equilibrium, the following equalities will be valid:

$$B_i = \frac{\omega}{\omega - \tilde{\mu}_i} B_{i-1} = q_i \cdot B_{i-1}; \quad \tilde{\mu}_i = \omega\left(1 - \frac{1}{q_i}\right) = \omega \cdot \epsilon_i; \quad \tilde{\mu}_i = \frac{\epsilon_i}{\epsilon_{i-1}} \tilde{\mu}_{i-1}, \tag{24}$$

where q_i, ϵ_i, and ϵ_{i-1} are some constant values that are easily determined experimentally.

Indeed, the coefficient of relationship between the culture density in the first and second chemostat stages q_2, experimentally obtained by us, is constant at any flow rate (Fig. 5). It can be seen from the figure that even at the maximum flow rate, when a near-wall growth is recorded, the relationship between the culture density in the first and second stages is quite well described by expression (23) at $q_2 = \mathrm{tg}\alpha = 1.11$.

The expression for the culture productivity in the *i*-th stage (22) can be represented as:

$$B_i = \frac{\overline{P}_i}{\omega} + B_{i-1}. \tag{25}$$

In stationary dynamic equilibrium, a culture always has $\overline{P}_i > 0$ and $\omega > 0$. Therefore, for any mode of quasi-continuous cultivation in a multistage chemostat, $B_i > B_{i-1}$. If the culture is diluted with a nutrient medium ($B_{i-1} = 0$), it follows from expression (22):

$$\tilde{\mu}_1 = \omega; \qquad \overline{P}_1 = \omega \cdot B_1. \tag{26}$$

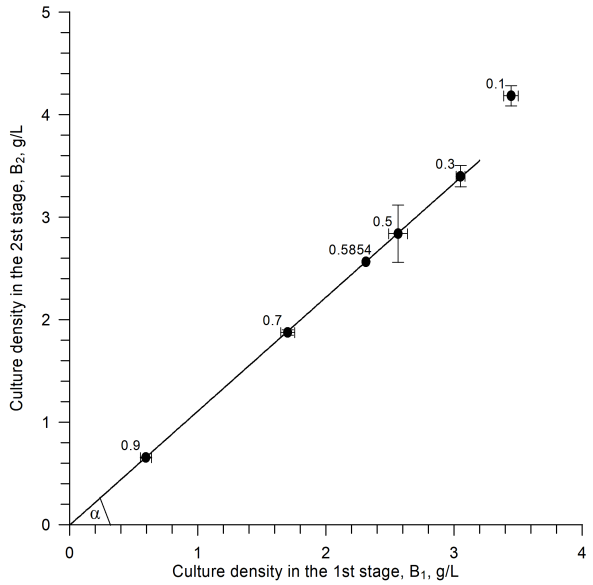

Fig. 5. The relationship between culture density in the first and second chemostat stages under conditions of stationary dynamic equilibrium, tgα = 1.11 [see expression (23)]. The dilution rate, ω, is indicated by numbers. The value for ω = 0.1 was not taken into account in the calculations due to the manifestation of cell agglutination

To determine the dependence of the concentration of the growth-limiting biogenic element in the current chemostat stage on the flow rates and the substrate consumption by cells during growth, we will follow the logic of deriving equation (20). By analogy with (7), such expressions can be written:

$$s_i = s_i^* + s_i^{**}; \quad s_i^* = \mathrm{w} \cdot S_i; \quad s_i^{**} = V \cdot S_i - \mathrm{w} \cdot S_i = (V - \mathrm{w}) \cdot S_i, \tag{27}$$

where s_i is the mass of the limiting substrate in the working volume of the *i*-th stage of the chemostat, g;

s_i^* and s_i^{**} are the masses of the limiting substrate in the withdrawn volume w during the exchange procedure and in the remaining volume (V – w), respectively;

S_i is the concentration of the limiting substrate in the *i*-th stage of the chemostat, g·L^{-1}.

The concentration of the limiting substrate in the *i*-th stage after the exchange ($S_i^{(-)}$) will be equal to:

$$S_i^{(-)} = \frac{s_{i-1}^* + s_i^{**}}{V} = \frac{\mathrm{w} \cdot S_{i-1} + (V - \mathrm{w}) \cdot S_i}{V}. \tag{28}$$

From this expression, it follows:

$$\frac{\mathrm{w}}{V} = \frac{S_i^{(-)} - S_i}{S_{i-1} - S_i} = \frac{s_{i-1}^* - s_i^*}{s_{i-1} - s_i}. \tag{29}$$

The change in the mass of the limiting substrate (Δs_i) can be expressed as follows:

$$\underbrace{s^*_{i-1}}_{\text{increase}} - \underbrace{(s_i - s^{**}_i)}_{\text{decrease with outflow}} - \underbrace{((s^*_{i-1} + s^{**}_i) - s_{i+1})}_{\text{decrease due to growth}} = s_{i+1} - s_i = \Delta s_i, \tag{30}$$

where s_i is the mass of the limiting substrate before the exchange;

s_{i+1} is the mass of the limiting substrate before the exchange at the next step of the quasi-continuous cultivation;

s^*_{i-1} is the mass of the substrate introduced into the *i*-th stage from the previous one during the exchange;

s^{**}_{i-1} is the mass of the substrate that remains in the *i*-th stage after withdrawing a part of the suspension with volume w.

Taking into account (27), (29), and (30), we write the change in the substrate concentration in the *i*-th stage of the chemostat (ΔS_i):

$$\underbrace{[S^{(-)}_i - S_i]}_{\text{increase}} - \underbrace{[S^{(-)}_i - S_{i+1}]}_{\text{decrease}} = S_{i+1} - S_i = \Delta S_i, \tag{31}$$

where S_i is the substrate concentration before the exchange procedure;

$S^{(-)}_i$ is the substrate concentration after the exchange;

S_{i+1} is the substrate concentration before the exchange at the next step of the quasi-continuous cultivation.

The value of the change in the substrate concentration (31) over the time interval Δt can be expressed in terms of the substrate consumption rate and the flow rate. From (29), (31), and (16), it follows:

$$\frac{\Delta S_i}{\Delta t} = \frac{S^{(-)}_i - S_i}{\Delta t} - \frac{S^{(-)}_i - S_{i+1}}{\Delta t} = \omega\,(S_{i-1} - S_i) - \overline{P}_{S_i}, \tag{32}$$

where $\overline{P}_{S_i}$ is the average rate of consumption of the limiting substrate by cells over the time interval Δt.

The ratio of silicon in *C. closterium* biomass varies insignificantly under different cultivation conditions. Therefore, it can be assumed that Y_b value is constant at any flow rate. In this case, the substrate consumption rate $\overline{P}_{S_i}$ will be proportional to the microalgal growth rate $\overline{P}_i$. Accordingly, taking into account (19), expression (32) is represented as:

$$\frac{\Delta S_i}{\Delta t} = \omega\,(S_{i-1} - S_i) - Y_b \cdot \tilde{\mu}_i \cdot B_i. \tag{33}$$

The solution of this equation will describe the dynamics of the concentration of the growth-limiting substrate of a quasi-continuous culture in a multistage chemostat. For a particular case (with a continuous flow of a nutrient medium), this equation is given in [Fencl, 1968; Pirt, 1978].

For the conditions of stationary dynamic equilibrium, we can express B_i from (33):

$$B_i = \frac{\omega}{\tilde{\mu}_i}\frac{(S_{i-1} - S_i)}{Y_b}; \qquad \tilde{\mu}_i = \frac{\omega}{B_i}\frac{(S_{i-1} - S_i)}{Y_b} = \omega\left(\frac{S_{i-1}}{S_i} - 1\right). \tag{34}$$

We calculate $S_i(\tilde{\mu}_i)$ from (5):

$$S_i(\tilde{\mu}_i) = \frac{K_S \cdot \tilde{\mu}_i}{\mu_m - \tilde{\mu}_i}. \tag{35}$$

Then, we substitute (24) and (35) into (34):

$$B_i = \frac{\omega}{\tilde{\mu}_i}\frac{1}{Y_b}\left(S_{i-1} - \frac{K_S \cdot \tilde{\mu}_i}{\mu_m - \tilde{\mu}_i}\right) = \frac{\omega}{\omega \cdot \epsilon_i}\frac{1}{Y_b}\left(S_{i-1} - \frac{K_S \cdot \omega \cdot \epsilon_i}{\mu_m - \omega \cdot \epsilon_i}\right). \tag{36}$$

Whence we determine the dependence of the culture density in the *i*-th stage on the dilution rate:

$$B_i(\omega) = \frac{1}{\epsilon_i}\frac{1}{Y_b}\left(S_{i-1} - \frac{K_S \cdot \omega}{\frac{1}{\epsilon_i}\mu_m - \omega}\right). \tag{37}$$

In a particular case, for the first stage of the chemostat, when the culture is diluted with a nutrient medium ($S_{i-1} = S_0$; $\epsilon_i = 1$), considering (26), we write:

$$B_1(\omega) = \frac{1}{Y_b}\left(S_0 - \frac{K_S \cdot \omega}{\mu_m - \omega}\right). \tag{38}$$

Substituting into the latter expression the numerical values of the observed requirement for silicon from Table 2, the saturation constant from (5), and silicon concentration in the nutrient medium RS S_0 = 0.115 g·L^{-1}, we calculate μ_m using the method of least squares based on the experimental data. Fig. 6 shows the correspondence between the experimental data and the theoretical curve (38) with the calculated value μ_m = 1.05 day^{-1} (R^2 = 0.97). When calculating, the value of the culture density at ω = 0.9 day^{-1} was not taken into account. As mentioned above, at the flow rate given, a near-wall growth of *C. closterium* was recorded.

Substituting the value μ_m = 1.05 day^{-1} into (38), for the conditions of our experiment, we obtain the dependence of the culture density in the first stage of the chemostat on the specific flow rate:

$$B_1(\omega) = \frac{1}{0.035}\left(0.115 - \frac{0.028 \cdot \omega}{1.05 - \omega}\right). \tag{39}$$

Worth noting as follows. Table 2 indicates the value of the observed requirement for silicon Y_b = 38.2 mg·g^{-1}. However, according to the results of our calculations, in a flow culture, the value of the observed requirement Y_{fl} = 35.0 mg·g^{-1}. The underestimation can be explained by the manifestation of autoselection in microorganisms in a flow culture [Gitelzon et al., 1973]. Accordingly, for a batch culture, the need for silicon Y_b = 38.2 mg·g^{-1}; for a flow culture, Y_{fl} = 35.0 mg·g^{-1}.

Analyzing expression (38), one can notice that at a certain critical dilution rate ω_{cr}, the value B_1 turns into zero (Fig. 6). In our experiment, the critical dilution rate (see Fig. 6) was as follows:

$$\omega_{cr}(B_1) = \mu_m \frac{S_0 - Y_{fl} \cdot B_1}{S_0 + K_S - Y_{fl} \cdot B_1}; \quad \omega_{cr}(0) = \mu_m \frac{S_0}{S_0 + K_S} = \frac{1.05 \cdot 0.115}{0.115 + 0.028} = 0.84 \text{ day}^{-1}.$$

Therefore, taking into account (26) for the conditions of our experiment, the limit value $\tilde{\mu}_1 = 0.84$ day^{-1}. In comparison with the specific growth rate $\mu_b = 0.7$ day^{-1} obtained in a batch culture [see (1)], this value is somewhat higher, which is associated with autoselection in a flow culture [Gitelzon et al., 1973].

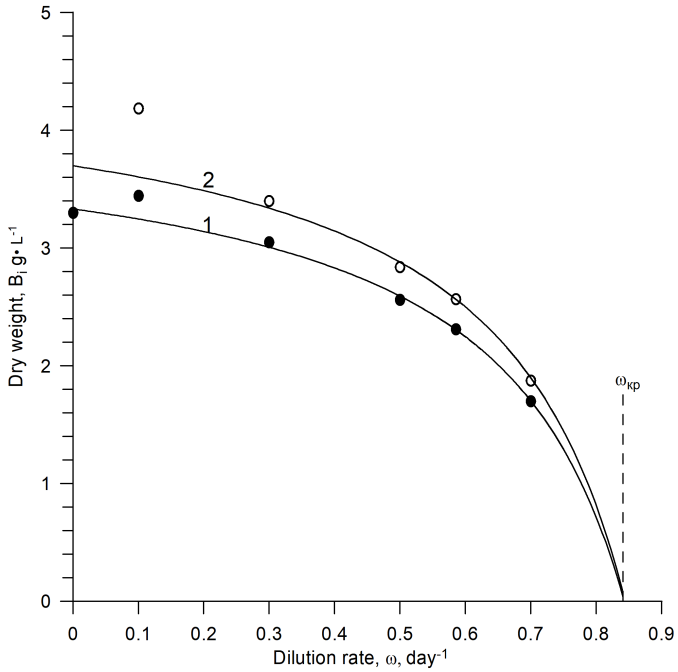

Fig. 6. The dependence of culture density on the dilution rate ω under conditions of stationary dynamic equilibrium: 1, the first stage of the chemostat, calculation according to equation (38) ($R^2 = 0.97$); 2, the second stage, calculation according to equation (45) ($R^2 = 0.96$). In the calculations, the value for $\omega = 0.9$ day^{-1} was not taken into account (see text for an explanation). The dotted line denotes the critical dilution rate $\omega_{cr} = 0.84$ day^{-1}

Thus, for the conditions of our experiment, in a batch culture, the specific growth rate $\mu_b = 0.7$ day^{-1}, its limit value in a flow culture $\tilde{\mu}_1 = 0.84$ day^{-1}, and its maximum possible value when limiting *C. closterium* growth by silicon $\mu_m = 1.05$ day^{-1}. Interestingly, the maximum value μ_m is included in expression (5) and is a certain species-specific characteristic of the substrate-dependent *C. closterium* growth (determined by the genetics of the species) when the growth is limited by silicon.

For the second stage of the chemostat, it is impossible to obtain the dependence $B_2(\omega)$ from (37) in an explicit form (as it is possible for the first stage), since $\epsilon_2 \neq 1$. To obtain the dependence $B_2(\omega)$, we use the relationship (23). When substituting (23) into (38), we get the dependence of the culture density in the second stage on ω and μ_2:

$$B_2(\omega, \mu_2) = \frac{\omega}{\omega - \tilde{\mu}_2} \frac{1}{Y_{fl}} \left(S_0 - \frac{K_S \cdot \omega}{\mu_m - \omega} \right). \tag{40}$$

Since the slope angle for q_i of the linear dependence (24) is constant and can be easily determined from the experimental data, we can write for the second stage of the chemostat:

$$B_2(\omega) = \frac{q_2}{Y_{fl}} \left(S_0 - \frac{K_S \cdot \omega}{\mu_m - \omega} \right). \tag{41}$$

Similarly for the *i*-th stage ($i \geq 2$):

$$B_i(\omega, \mu_2, \ldots \mu_i) = \frac{\omega^{i-1}}{\prod\limits_{k=2}^{i} (\omega - \tilde{\mu}_k)} \frac{1}{Y_{fl}} \left(S_0 - \frac{K_S \cdot \omega}{\mu_m - \omega} \right). \tag{42}$$

If q_i is a constant value for any pair of neighboring stages, then the product $q_2 \cdot q_3 \cdot \ldots \cdot q_i$ will be a constant value as well. Hence:

$$B_i(\omega) = \frac{\prod\limits_{k=2}^{i} q_k}{Y_{fl}} \left(S_0 - \frac{K_S \cdot \omega}{\mu_m - \omega} \right). \tag{43}$$

According to our experimental data (Fig. 5), the slope of B_2 dependence on B_1 is equal to:

$$q_2 = \frac{\omega}{\omega - \tilde{\mu}_2} = \operatorname{tg} \alpha = 1.11. \tag{44}$$

Therefore, for the conditions of our experiment, the dependence of the culture density in the second stage of the chemostat on the dilution rate can be represented as follows:

$$B_2(\omega) = 1.11 \frac{1}{Y_{fl}} \left(S_0 - \frac{K_S \cdot \omega}{\mu_m - \omega} \right) = \frac{1.11}{0.035} \left(0.115 - \frac{0.028 \cdot \omega}{1.05 - \omega} \right). \tag{45}$$

Fig. 6 shows the dependence of the culture density in the second stage of the chemostat on the specific flow rate and the correspondence between the experimental data and the theoretical curve (45).

To determine the yield value in different modes of cultivation, we calculate the total productivity of the culture in *i* chemostat stages under conditions of stationary dynamic equilibrium. As follows from expression for the productivity of the *i*-th stage (22), the total productivity of all the chemostat stages R_i (the entire cultivation system) is equal to:

$$R_i = \sum_{k=1}^{i} \overline{P}_k = \omega \cdot B_i. \tag{46}$$

Therefore, under conditions of stationary dynamic equilibrium, the yield (H_i) of a cultivation system consisting of *i* stages for a fixed period of time is (g·L^{-1}):

$$H_i(t) = R_i \cdot t = \omega \cdot B_i \cdot t, \tag{47}$$

where t is the cultivation time, day.

To determine the productivity of a multistage chemostat, we substitute expression (43) into (46):

$$R_i(\omega) = \omega \frac{\prod\limits_{k=2}^{i} q_k}{Y_{fl}} \left(S_0 - \frac{K_S \cdot \omega}{\mu_m - \omega} \right). \tag{48}$$

For a particular case, $R_1(\omega)$ and $R_2(\omega)$, we have:

$$R_1(\omega) = \omega \frac{1}{Y_{fl}} \left(S_0 - \frac{K_S \cdot \omega}{\mu_m - \omega} \right); \qquad R_2(\omega) = \omega \frac{q_2}{Y_{fl}} \left(S_0 - \frac{K_S \cdot \omega}{\mu_m - \omega} \right). \tag{49}$$

A similar expression for a one-stage chemostat was obtained in [Pirt, 1978].

Substituting the experimental values and q_2 = 1.11 [see (44)] into (49), we have:

$$R_1(\omega) = \omega \frac{1}{0.035} \left(0.115 - \frac{0.028 \cdot \omega}{1.05 - \omega} \right); \qquad R_2(\omega) = \omega \frac{1.11}{0.035} \left(0.115 - \frac{0.028 \cdot \omega}{1.05 - \omega} \right). \tag{50}$$

Thus, the dependences of the productivity of a one- and two-stage chemostat on the specific flow rate were obtained. Fig. 7 shows the correspondence between the experimental data and theoretical curves (50).

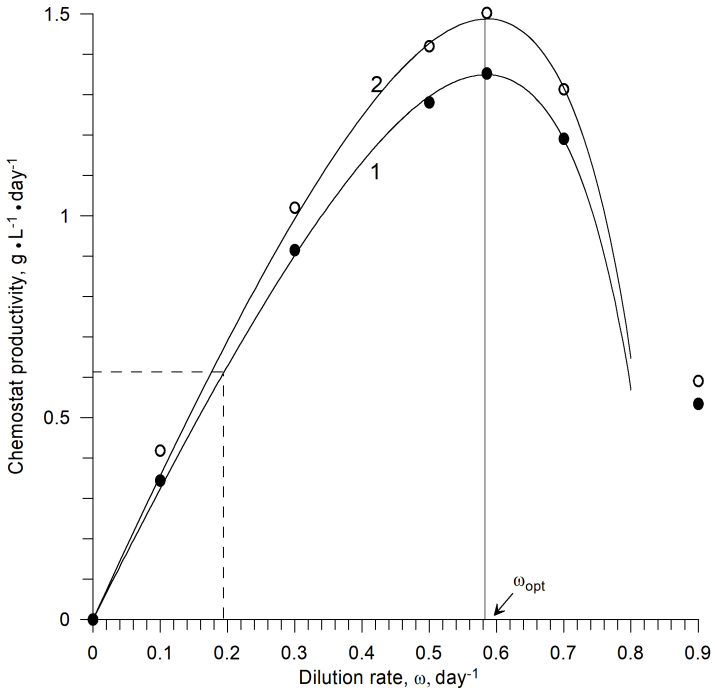

Fig. 7. Dependence of the chemostat productivity under conditions of stationary dynamic equilibrium on the dilution rate: 1 and 2 denote calculation according to equation (50) (R^2 = 0.98) for a one- and two-stage chemostat, respectively. In the calculations, the value for ω = 0.9 day^{-1} was not taken into account (see text for an explanation). The arrow indicates the optimal value of the dilution rate ω_{opt} = 0.59, at which the maximum productivity is achieved. For a comparative assessment, the dotted line shows the productivity of the batch culture [see (55) and (56)]

Then, we determine the optimal value of the specific flow rate ω_{opt}, at which the productivity of a multistage chemostat is maximum. To do this, we differentiate function (48) with respect to ω:

$$R_i'(\omega) = \frac{\prod_{k=2}^{i} q_k}{Y_{fl}} \frac{(K_S + S_0)\omega^2 - 2\mu_m\omega(K_S + S_0) + \mu_m^2 S_0}{(\mu_m - \omega)^2}. \tag{51}$$

For $R_i'(\omega) = 0$, we get a quadratic equation:

$$\omega^2 - 2\mu_m\omega + \frac{\mu_m^2 S_0}{K_S + S_0} = 0. \tag{52}$$

One of the roots of this equation has no sense, since the condition $\mu_m > \omega$ must be satisfied. Another root is the optimal value of the specific flow rate, at which the maximum productivity of the entire multistage cultivation system is achieved:

$$\omega_{opt} = \mu_m \left(1 - \sqrt{\frac{K_S}{S_0 + K_S}}\right). \tag{53}$$

It should be noted that in the latter expression, ω_{opt} value does not depend on the number of stages. So, (53) can be applied to determine the optimal specific flow rate for both a one-stage and a multistage chemostat.

Then, we calculate the optimal specific flow rate for the conditions of our experiment:

$$\omega_{opt} = 1.05 \left(1 - \sqrt{\frac{0.028}{0.115 + 0.028}}\right) = 0.59 \text{ day}^{-1}. \tag{54}$$

Moreover, using formulas (39), (45), and (50), we determine the culture density and productivity for each stage of the chemostat at ω_{opt} = 0.59 day^{-1}. Applying (47), we calculate the yield value for a one- and two-stage chemostat at the optimal flow rate for four days of cultivation. The calculation results are given in Table 3.

Let us compare the yield value obtained for a fixed period of time under conditions of batch and flow cultivation. The batch cultivation lasted five days, and we carry out our calculations for t_b = 5 days. If the batch culture at the moment of reaching the maximum density B_m (the initial moment of the stationary growth phase) is diluted down to the initial density B_0, the growth in the batch culture will continue, and the maximum density will be reached again in a period of time t_b. Under conditions when cycles of dilution of the batch culture are repeated at intervals t_b, the batch culture is involved in a flow quasi-continuous cultivation with a time interval between dilution procedures $t - t_0 = t_b$. The average productivity, relative growth rate, and yield over this period can be given as:

$$\overline{P}_b = \frac{B_m - B_0}{t - t_0} = \frac{B_b}{t_b}; \qquad \tilde{\mu}_b = \frac{1}{B_m}\frac{B_m - B_0}{t - t_0} = \frac{\overline{P}_b}{B_m}; \qquad B_b = \overline{P}_b \cdot t_b. \tag{55}$$

On the other hand, considering (46) and (47), for a quasi-continuous culture, the average productivity, relative growth rate, and yield are as follows:

$$R_i = \omega \cdot B_i; \qquad \tilde{\mu}_1 = \omega; \qquad H_{fl} = R_i \cdot t_b = \omega \cdot B_i \cdot t_b. \tag{56}$$

Comparing the productivity of two quasi-continuous cultures, (55) and (56), at the same relative flow rate under conditions of stationary dynamic equilibrium ($\omega = \tilde{\mu}_1 = \tilde{\mu}_b$), we have:

$$\frac{R_i}{\overline{P}_b} = \frac{\omega \cdot B_i}{\tilde{\mu}_b \cdot B_m} = \frac{B_i}{B_m} < 1.$$

Therefore, for the conditions $\tilde{\mu}_b = \omega$, batch cultivation is more profitable. However, with an increase in the flow rate, $\tilde{\mu}_b < \omega \le \omega_{opt}$, a flow culture becomes more profitable. Moreover, the maximum benefit of a one-stage chemostat is achieved at the optimal flow rate ω_{opt} (Fig. 7).

To calculate the productivity of the batch culture, we substitute the numerical values from our experiment into (55). As a result, we get: $\overline{P}_b$ = 0.62 g·L^{-1}·day^{-1}; $\tilde{\mu}_b$ = 0.19 day^{-1}; B = 3.1 g·L^{-1}. To determine the chemostat productivity for each of the stationary states, we apply expression (56). The results of the calculation are given in Table 3.

Table 3. *Cylindrotheca closterium* production characteristics in a one- and two-stage chemostat under stationary dynamic equilibrium conditions: ω, the dilution rate, day^{-1}; B_1, B_2, the culture density in the first and second stages, respectively, g·L^{-1}; $\tilde{\mu}_1$, $\tilde{\mu}_2$, specific growth rate in the first and second stages; R_1, R_2, productivity of a one- and two-stage chemostat, g·L^{-1}·day^{-1}; $\overline{P}_2$, productivity of the chemostat second stage; $H_1(5)$, $H_2(5)$, yield received in a one- and two-stage chemostat over a period of time t_b = 5 days, g

ω	B_1	$\tilde{\mu}_1$	R_1	$H_1(5)$	B_2	$\tilde{\mu}_2$	$\overline{P}_2 = R_2 - R_1$	R_2	$H_2(5)$
0.1	3.44	0.1	0.344	1.72	4.19	0.02	0.074	0.419	2.09
0.3	3.05	0.3	0.915	4.58	3.40	0.03	0.106	1.021	5.10
0.5	2.56	0.5	1.281	6.40	2.84	0.05	0.139	1.420	7.10
ω_{opt} = 0.59	2.29	0.59	1.348	6.76	2.54	0.06	0.150	1.498	7.51
0.7	1.70	0.7	1.191	5.95	1.88	0.07	0.123	1.314	6.57
0.9	0.59	0.9	0.534	2.67	0.66	0.09	0.057	0.591	2.96

The comparison of the calculation results shows as follows: at ω = 0.1 over a time interval t_b, the flow culture gives a lower yield than the batch one. Flow cultivation becomes profitable at higher flow rates. The yield is maximum at optimal flow rate: $R_1(0.59)$ = 1.35 g·L^{-1}·day^{-1}; $H_1(5)$ = 6.76 g·L^{-1}. Accordingly, *C. closterium* cultivation in a one-stage chemostat is 2.2 times more profitable than the batch cultivation.

Let us compare the productivity of one- and two-stage chemostat under condition that the same volume of limiting substrate enters the cultivation system *per* unit volume of the microalgal suspension. The working volume of each stage of the chemostat is equal to V; therefore, the total volume of the microalgal suspension in a two-stage chemostat is $2V$. Hence, in order to comply with the comparison condition, it is necessary to double the working volume of a one-stage chemostat or to reduce the specific flow rate by half. Taking into account (24) and (46), we write:

$$\frac{R_2}{R_1} = \frac{\omega B_2}{\frac{\omega}{2} B_1} = \frac{2B_2}{B_1} = 2 \cdot q_2 > 1.$$

Whence it follows that under the above conditions, a two-stage cultivation system is more productive than a one-stage one. The data on the productivity of a one- and two-stage chemostat are given in Table 3.

Conclusion. Our studies have shown that the culture of the diatom alga *Cylindrotheca closterium* is characterized by sufficiently high productivity rates both in batch and flow culture. In the batch culture, the specific growth rate μ_b = 0.7 day^{-1}, and the time for doubling the biomass t_d = 0.987 days. In the flow culture, at a critical dilution rate, the limit value of the specific culture growth rate $\tilde{\mu}_1$ is 0.84 day^{-1}.

For the conditions of our experiment, in a one- and two-stage chemostat, the maximum productivity is recorded at an optimal flow rate ω_{opt} = 0.59 day^{-1} (R_1 = 1.348 g·L^{-1}·day^{-1} and R_2 = 1.498 g·L^{-1}·day^{-1}, respectively). As shown experimentally, in the flow culture, *C. closterium* productivity is 2.2 times higher than in the batch one.

Based on the experimental data, two parameters of the Monod equation were determined – the maximum specific growth rate μ_m and the saturation constant K_S – with limiting *C. closterium* growth by silicon. The values were 1.05 day^{-1} and 0.028 g·L^{-1}, respectively. Moreover, the observed need of the alga for silicon in the flow culture was calculated, Y_{fl} = 35 mg·g^{-1}. As shown, the observed need for silicon in the flow culture is lower than in the batch one by 7.9%. Interestingly, μ_m, K_S, and Y_{fl} values are important physiological characteristics for the diatom *C. closterium*; those play the key role in the design of industrial systems for intensive microalgae cultivation.

This work was carried out within the framework of IBSS state research assignment "Investigation of mechanisms of controlling production processes in biotechnological complexes with the aim of developing scientific foundations for production of biologically active substances and technical products of marine genesis" (No. 121030300149-0).

REFERENCES

1. Gevorgiz R. G., Zheleznova S. N., Zozulya Yu. V., Uvarov I. P., Repkov A. P., Lelekov A. S. Industrial production technology biomass marine diatoms *Cylindrotheca closterium* (Ehrenberg) Reimann & Lewin using gas vortex photobioreactor. *Aktual'nye voprosy biologicheskoi fiziki i khimii*, 2016, no. 1–1, pp. 73–77. (in Russ.)
2. Gevorgiz R. G., Zheleznova S. N., Nikonova L. L., Bobko N. I., Nekhoroshev M. V. *Otsenka plotnosti kul'tury fototrofnykh mikroorganizmov metodom iodatnoi okislyaemosti.* Sevastopol, 2015, 31 p. (Preprint / A. O. Kovalevsky Institute of Marine Biological Research of RAS). (in Russ.). URL: https://repository.marine-research.ru/handle/299011/43
3. Gitelzon I. I., Fish A. M., Chumakova R. I., Kuznetsov A. M. Maximum reproduction rate of bacteria and the possibility of its determination. *Doklady Akademii nauk SSSR*, 1973, vol. 211, no. 6, pp. 1453–1455. (in Russ.)
4. Zheleznova S. N., Gevorgiz R. G. Intensive culture of diatom *Cylindrotheca closterium* (Ehrenb.) Reimann et Lewin. *Voprosy sovremennoi algologii*, 2014, no. 1 (5). (in Russ.). URL: http://algology.ru/474
5. Zheleznova S. N., Bobko N. I., Gevorgiz R. G., Nekhoroshev M. V. Balans zheleza v plotnoi kul'ture diatomovoi vodorosli *Cylindrotheca closterium* (Ehrenberg) Reimann & J. C. Lewin. In: *Fundamental'nye i prikladnye problemy sovremennoi eksperimental'noi biologii rastenii* : sbornik materialov Vserossiiskoi nauchnoi konferentsii s mezhdunarodnym uchastiyem i shkoly dlya molodykh uchenykh, posvyashchennykh 125-letiyu Instituta fiziologii rastenii imeni K. A. Timiryazeva RAN, Moscow, 23–27 November, 2015. Moscow : IFR RAN, 2015a, pp. 238–241. (in Russ.)
6. Zheleznova S. N., Gevorgiz R. G., Bobko N. I., Lelekov A. S. The culture medium for the intensive culture of diatomic alga *Cylindrotheca closterium* (Ehrenb.) Reimann et Lewin – promising biotech facility. *Aktual'naya biotekhnologiya*, 2015b, no. 3 (14), pp. 46–48. (in Russ.)
7. Zheleznova S. N. Production characteristics of the diatom *Cylindrotheca closterium*

(Ehrenb.) Reimann et Lewin grown in an intensive culture at various nitrogen sources in the medium. *Morskoj biologicheskij zhurnal*, 2019, vol. 4, no. 1, pp. 33–44. (in Russ.). https://doi.org/10.21072/mbj.2019.04.1.04

8. Zheleznova S. N., Gevorgiz R. G. Measurement of diatom cultures density by various methods. *Aktual'nye voprosy biologicheskoi fiziki i khimii*, 2020, vol. 5, no. 1, pp. 201–207. (in Russ.)
9. *Theoretical and Methodological Basis of Continuous Culture of Microorganisms* : transl. from Engl. / I. Málek, Z. Fencl (Eds). Moscow : Pishchevaya promyshlennost', 1968, 546 p. (in Russ.)
10. Pirt S. J. *Principles of Microbe and Cell Cultivation* / transl. from Engl. by T. A. Petrova, I. N. Pozmogova ; I. L. Rabotnova (Ed.). Moscow : Mir, 1978, 330 p. (in Russ.)
11. Trenkenshu R. P. Simplest models of microalgae growth. 2. Queasycontinuous culture. *Ekologiya morya*, 2005, iss. 67, pp. 98–110. (in Russ.). URL: https://repository.marine-research.ru/handle/299011/4659
12. Fencl Z. Theoretical analysis of continuous culture systems. In: *Theoretical and Methodological Basis of Continuous Culture of Microorganisms* : transl. from Engl. / I. Málek, Z. Fencl (Eds). Moscow : Pishchevaya promyshlennost', 1968, pp. 64–150. (in Russ.)
13. Abinandan S., Subashchandrabose S. R., Venkateswarlu K., Megharaj M. Nutrient removal and biomass production: Advances in microalgal biotechnology for wastewater treatment. *Critical Reviews in Biotechnology*, 2018, vol. 38, iss. 8, pp. 1244–1260. https://doi.org/10.1080/07388551.2018.1472066
14. Baldisserotto C., Sabia A., Ferroni L., Pancaldi S. Biological aspects and biotechnological potential of marine diatoms in relation to different light regimens. *World Journal of Microbiology and Biotechnology*, 2019, vol. 35, iss. 2, art. no. 35 (9 p.). https://doi.org/10.1007/s11274-019-2607-z
15. Bozarth A., Maier U.-G., Zauner S. Diatoms in biotechnology: Modern tools and applications. *Applied Microbiology and Biotechnology*, 2009, vol. 82, iss. 2, pp. 195–201. https://doi.org/10.1007/s00253-008-1804-8
16. de la Cuesta J. L., Manley S. L. Iodine assimilation by marine diatoms and other phytoplankton in nitrate-replete conditions. *Limnology and Oceanography*, 2009, vol. 54, iss. 5, pp. 1653–1664. https://doi.org/10.4319/lo.2009.54.5.1653
17. Creswell L. R. *Phytoplankton Culture for Aquaculture Feed.* [Stoneville, MS : Southern Regional Aquaculture Center], 2010, 13 p. (SRAC Publication ; no. 5004).
18. Guillard R. R. L., Ryther J. H. Studies of marine planktonic diatoms. I. *Cyclotella nana* Hustedt, and *Detonula confervacea* (Cleve) Gran. *Canadian Journal of Microbiology*, 1962, vol. 8, no. 2, pp. 229–239. https://doi.org/10.1139/m62-029
19. Guillard R. R. L. Culture of phytoplankton for feeding marine invertebrates. In: *Culture of Marine Invertebrates Animals* / M. L. Smith, M. H. Chanley (Eds). New York : Plenum Press, 1975, pp. 29–60. https://doi.org/10.1007/978-1-4615-8714-9_3
20. Herbert D., Elsworth R., Telling R. C. The continuous culture of bacteria; a theoretical and experimental study. *The Journal of General Microbiology*, 1956, vol. 14, iss. 3, pp. 601–622. https://doi.org/10.1099/00221287-14-3-601
21. Kiran M. T., Bhaskar M. V., Tiwari A. Phycoremediation of eutrophic lakes using diatom algae. In: *Lake Sciences and Climate Change* / M. N. Rashed (Ed).

London : IntechOpen, 2016, pp. 103–115. https://doi.org/10.5772/64111

22. Lauritano C., Andersen J. H., Hansen E., Albrigtsen M., Escalera L., Esposito F., Helland K., Hanssen K. Ø., Romano G., Ianora A. Bioactivity screening of microalgae for antioxidant, anti-inflammatory, anticancer, anti-diabetes, and antibacterial activities. *Frontiers in Marine Science*, 2016, vol. 3, art. no. 68 (12 p.). https://doi.org/10.3389/fmars.2016.00068
23. Lincoln R. A., Strupinski K., Walker J. M. Biologically active compounds from diatoms. *Diatom Research*, 1990, vol. 5, iss. 2, pp. 337–349. https://doi.org/10.1080/0269249X.1990.9705124
24. Lu X., Sun H., Zhao W., Cheng K.-W., Chen F., Liu B. A hetero-photoautotrophic two-stage cultivation process for production of fucoxanthin by the marine diatom *Nitzschia laevis*. *Marine Drugs*, 2018, vol. 16, iss. 7, art. no. 219 (13 p.). https://doi.org/10.3390/md16070219
25. Maxon W. D. Continuous fermentation: A discussion of its principles and applications. *Applied Microbiology*, 1955, vol. 3, no. 2, pp. 110–122. https://doi.org/10.1128/am.3.2.110-122.1955
26. *Methods in Microbiology* / J. R. Norris, D. W. Ribbons (Eds). London ; New York : Academic Press, 1970, vol. 2, 445 p. https://doi.org/10.1016/S0580-9517(08)70210-1
27. Minyuk G. S., Chelebieva E. S., Chubchikova I. N. Secondary carotenogenesis of the green microalga *Bracteacoccus minor* (Chodat) Petrova (Chlorophyta) in a two-stage culture. *International Journal on Algae*, 2014, vol. 16, iss. 4, pp. 354–368. https://doi.org/10.1615/InterJAlgae.v16.i4.50
28. Nagappan S., Devendran S., Tsai P.-C., Dahms H.-U., Ponnusamy V. K. Potential of two-stage cultivation in microalgae biofuel production. *Fuel*, 2019, vol. 252, pp. 339–349. https://doi.org/10.1016/j.fuel.2019.04.138
29. Patras D., Moraru C. V., Socaciu C. Screening of bioactive compounds synthesized by microalgae: A progress overview on extraction and chemical analysis. *Studia Universitatis Babeș-Bolyai, Seria Chemia*, 2018, vol. 63, iss. 1, pp. 21–35. http://dx.doi.org/10.24193/subbchem.2018.1.02
30. Salleh S., McMinn A. The effects of temperature on the photosynthetic parameters and recovery of two temperate benthic microalgae, *Amphora* cf. *coffeaeformis* and *Cocconeis* cf. *sublittoralis* (Bacillariophyceae). *Journal of Phycology*, 2011, vol. 47, iss. 6, pp. 1413–1424. https://doi.org/10.1111/j.1529-8817.2011.01079.x
31. Sathasivam R., Radhakrishnan R., Hashem A., Abd_Allah E. F. Microalgae metabolites: A rich source for food and medicine. *Saudi Journal of Biological Sciences*, 2019, vol. 26, iss. 4, pp. 709–722. https://doi.org/10.1016/j.sjbs.2017.11.003
32. Singh J., Dhar D. W. Overview of carbon capture technology: Microalgal biorefinery concept and state-of-the-art. *Frontiers in Marine Science*, 2019, vol. 6, art. no. 29 (9 p.). https://doi.org/10.3389/fmars.2019.00029
33. Stock W., Vanelslander B., Rüdiger F., Sabbe K., Vyverman W., Karsten U. Thermal niche differentiation in the benthic diatom *Cylindrotheca closterium* (Bacillariophyceae) complex. *Frontiers in Microbiology*, 2019, vol. 10, art. no. 1395 (12 p.). https://doi.org/10.3389/fmicb.2019.01395
34. Wang S., Chen J., Li Z., Wang Y., Fu B., Han X., Zheng L. Cultivation of the benthic microalga *Prorocentrum lima* for the production of diarrhetic shellfish poisoning toxins in a vertical flat photobioreactor. *Bioresource Technology*, 2015, vol. 179, pp. 243–248. https://doi.org/10.1016/j.biortech.2014.12.019

35. Wang S., Verma S. K., Said I. H., Thomsen L., Ullrich M. S., Kuhnert N. Changes in the fucoxanthin production and protein profiles in *Cylindrotheca closterium* in response to blue light-emitting diode light. *Microbial Cell Factories*, 2018, vol. 17, art. no. 110 (13 p.). https://doi.org/10.1186/s12934-018-0957-0
36. Wollmann F., Dietze S., Ackermann J.-U., Bley T., Walther T., Steingroewer J., Krujatz F. Microalgae wastewater treatment: Biological and technological approaches. *Engineering in Life Sciences*, 2019, vol. 19, iss. 12, pp. 860–871. https://doi.org/10.1002/elsc.201900071
37. Zheleznova S. N., Gevorgiz R. G., Nekhoroshev M. V. Conditions optimization of the *Cylindrotheca closterium* (Ehrenberg) Reimann et Lewin cultivation in order to obtain a high yield of fucoxanthin. In: *3rd Russian Conference on Medicinal Chemistry*, Kazan, 28 Sept. – 03 Oct., 2017 : abstr. book. Kazan : Kazan Federal University, 2017, pp. 261.

ПРОДУКЦИОННЫЕ ХАРАКТЕРИСТИКИ КУЛЬТУРЫ ДИАТОМОВОЙ ВОДОРОСЛИ *CYLINDROTHECA CLOSTERIUM* (EHRENBERG) REIMANN ET LEWIN В ДВУХСТУПЕНЧАТОМ ХЕМОСТАТЕ

Р. Г. Геворгиз[1], С. Н. Железнова[1], А. С. Малахов[2]

[1]ФГБУН ФИЦ «Институт биологии южных морей имени А. О. Ковалевского РАН», Севастополь, Российская Федерация
[2]Национальный исследовательский Томский политехнический университет, Томск, Российская Федерация
E-mail: *r.gevorgiz@yandex.ru*

В работе рассмотрены преимущества и недостатки проточного и накопительного культивирования микроводорослей. Указаны достоинства проточного культивирования, в частности в квазинепрерывном режиме в двухступенчатом хемостате. В качестве продуцента ценных веществ предложено использовать культуру бентосной диатомовой водоросли *Cylindrotheca closterium*, которая обладает многими полезными свойствами как биологического характера, так и технологического: 1) характеризуется достаточно высокими продукционными показателями; 2) эффективно утилизирует световую энергию, что снимает ограничения на размещение производства в регионах с малым количеством солнечных дней в году; 3) характеризуется довольно низким температурным оптимумом роста, что актуально для реализации промышленных технологий на территории Российской Федерации; 4) имеет удельную плотность клеток больше единицы, поэтому они достаточно быстро оседают на дно фотобиореактора при отсутствии перемешивания культуры, что упрощает отделение биомассы от культуральной среды и снижает её себестоимость. Цель работы — изучить продукционные характеристики квазинепрерывной культуры *C. closterium* в двухступенчатом хемостате. Исследования проводили при температуре (20 ± 1) °C и облучённости 150 мкмоль квантов·м$^{-2}$·с$^{-1}$. Хемостатная установка для культивирования *C. closterium* состояла из двух стеклянных фотобиореакторов плоскопараллельного типа объёмом 3 л с рабочей толщиной 5 см и рабочей поверхностью каждого фотобиореактора 0,03 м^2. Культуру выращивали на питательной среде RS. Перемешивание осуществляли посредством барботажа воздухом (скорость — 1,5 л воздуха на 1 л культуры в мин). Культуру исследовали при различных скоростях протока питательной среды — 0,1; 0,3; 0,5; 0,7; 0,9 сут$^{-1}$. Рассчитаны параметры роста накопительной культуры: удельная скорость роста $\mu_н$ = 0,7 сут$^{-1}$; время удвоения биомассы t_d = 0,987 сут.

Максимальная продуктивность одно- и двухступенчатого хемостата была отмечена при оптимальной скорости протока 0,59 сут$^{-1}$ и составила 1,348 и 1,498 г·л$^{-1}$·сут$^{-1}$ соответственно. Экспериментально показано, что в проточной культуре продуктивность *C. closterium* выше в 2,2 раза, чем в накопительной. На основе экспериментальных данных проведён расчёт максимальной удельной скорости роста μ_m и константы насыщения K_S при лимитировании роста *C. closterium* кремнием; значения составили 1,05 сут$^{-1}$ и 0,028 г·л$^{-1}$ соответственно. Показано, что наблюдаемая потребность в кремнии в проточной культуре ($Y_{\text{пр}}$ = 35 мг·г$^{-1}$) ниже на 7,9 %, чем в накопительной ($Y_{\text{н}}$ = 38 мг·г$^{-1}$). Отмечено, что величи́ны μ_m, K_S и $Y_{\text{пр}}$ являются важными физиологическими характеристиками диатомовой водоросли *C. closterium* и играют ключевую роль при проектировании промышленных систем для интенсивного культивирования микроводорослей.

Ключевые слова: *Cylindrotheca closterium*, хемостат, математическая модель

1871
ИнБЮМ – IBSS

Морской биологический журнал
Marine Biological Journal
2023, vol. 8, no. 1, pp. 51–55
https://marine-biology.ru

UDC 599.537-15:597.311

EVIDENCE OF A FAILED PREDATORY ATTEMPT BY AN ORCA, *ORCINUS ORCA* (LINNAEUS, 1758), ON A GREAT WHITE SHARK, *CARCHARODON CARCHARIAS* (LINNAEUS, 1758)

© 2023 **A. De Maddalena**

Marine Sciences, University of Milano-Bicocca, Milan, Italy
E-mail: *alessandrodemaddalena@gmail.com*

Received by the Editor 09.08.2022; after reviewing 28.09.2022;
accepted for publication 20.10.2022; published online 14.03.2023.

The first observation of a live great white shark *Carcharodon carcharias* bearing tooth rake marks by an orca *Orcinus orca* on the left flank is presented. The estimated 3.5-m shark was observed on 7 July, 2017, at Seal Island in False Bay, Western Cape, South Africa. This case provides evidence that great white sharks can survive an attack by an orca.

Keywords: great white shark, *Carcharodon carcharias*, killer whale, *Orcinus orca*, False Bay, South Africa

Orcas, or killer whales, *Orcinus orca* (Linnaeus, 1758), have been reported to feed on or attack different species of sharks, including the broadnose sevengill shark *Notorynchus cepedianus* (Péron, 1807); Pacific sleeper shark *Somniosus pacificus* Bigelow & Schroeder, 1944; whale shark *Rhincodon typus* Smith, 1828; common thresher *Alopias vulpinus* (Bonnaterre, 1788); basking shark *Cetorhinus maximus* (Gunnerus, 1765); great white shark *Carcharodon carcharias* (Linnaeus, 1758); shortfin mako *Isurus oxyrinchus* Rafinesque, 1810; tope shark *Galeorhinus galeus* (Linnaeus, 1758); grey reef shark *Carcharhinus amblyrhynchos* (Bleeker, 1856); bronze whaler, or copper shark, *Carcharhinus brachyurus* (Günther, 1870); Galapagos shark *Carcharhinus galapagensis* (Snodgrass & Heller, 1905); blue shark *Prionace glauca* (Linnaeus, 1758); scalloped hammerhead *Sphyrna lewini* (Griffith & Smith, 1834); and smooth hammerhead *Sphyrna zygaena* (Linnaeus, 1758) [Best et al., 2010, 2014; Brown, Norris, 1956; De Maddalena, Buttigieg, 2009; Engelbrecht et al., 2019; Fertl et al., 1996; Ford et al., 2011; Norris, 1958; Pyle et al., 1999; Reyes, García-Borboroglu, 2004; Sorisio et al., 2006; Ternullo et al., 1993; Towner et al., 2022; Visser, 2000a, b, 2005; Visser, Bonaccorso, 2003; Visser et al., 2000; Yukhov et al., 1975]. In the present article, the observation of a live great white shark bearing tooth rake marks by an orca is reported.

MATERIAL AND METHODS

The observation took place on 7 July, 2017, 14.8 km northeast of Simon's Town harbour, near Seal Island in False Bay, Western Cape, South Africa. The author observed the female great white shark repeatedly while cage diving off the *White Pointer II* – the 11-m boat of *Apex Shark Expeditions*. The great white

shark made several passes around the boat and the cage between 8:45 and 10:35, swimming at depths ranging from the surface to 5 m, in 10-m-deep waters. It was briefly observed at 8:45; then it was observed clearly several times between 10:22 and 10:35. At 10:35, the shark succeeded in catching the bait before it disappeared. The shark had a massive body, with a wide trunk, and it was estimated at 3.5 m in total length. Underwater visibility was about 8 m. Perhaps, the same shark was seen earlier in the morning, at 7:02, preying on a Cape fur seal, *Arctocephalus pusillus pusillus* (Schreber, 1775), in the same area, when several kelp gulls, *Larus dominicanus* Lichtenstein, 1823, were observed flying over the nearby spot attracted by the upcoming predatory event.

At least two other great white sharks were observed that morning on the same spot. One was briefly seen at 7:22 when it bit the seal-shaped decoy that was being towed behind the boat shortly after sunrise, while another one, an estimated 3-m female, was observed from the cage swimming at depths ranging from the surface to 3 m, between 10:03 and 10:04. No other species of fish were observed on that day.

In order to attract the sharks and to keep them around the cage, the crew was using a small amount of chum, made of sardines, and a few heads of salmons as the bait. It was a sunny day, with an average water temperature of +14 °C and relatively calm seas.

Photos of the sharks were taken with two cameras for subsequent analysis (Fig. 1).

Fig. 1. Estimated 3.5-m female great white shark *Carcharodon carcharias* bearing tooth rake marks by an orca *Orcinus orca* on the left side of its trunk, observed on 7 July, 2017, at Seal Island in False Bay, Western Cape, South Africa. Photos by Alessandro De Maddalena

RESULTS AND DISCUSSION

Careful observation of the photos, showing the parallel marks seen on the left posterolateral region of the trunk of the great white shark, led the author to conclude that they are consistent with tooth rake marks of an orca. This was also confirmed by following examination of a large number of photos which the author was able to take on twelve past expeditions to observe orcas in the winter season in the areas of Bodø, Kaldfjord, and Skjervoy (Norway) since January 2014. Photos published in Ford *et al.* [2000] were also useful for additional comparison. Sixteen parallel scratches can be observed. The scratches are divided into twelve on the left and four on the right, separated by a small gap. The marks could have been caused by the teeth in the lower jaw of an orca trying to grab the shark from above. Orcas have ten to twelve large, recurved teeth in each half of both jaws, which are oval in cross section [Jefferson et al., 1993]. The twelve scratches on the left match the twelve teeth in the orca's left half of the lower jaw, and the four scratches on the right match the first four teeth in the cetacean's right half of the lower jaw, while the small gap in between matches the space at the mandibular symphysis (Fig. 2). The appearance of the scratches seems to indicate that they were inflicted with significant force. It is likely, the marks were enhanced by the vigorous movement that the shark may have made in order to escape the attack of the large cetacean.

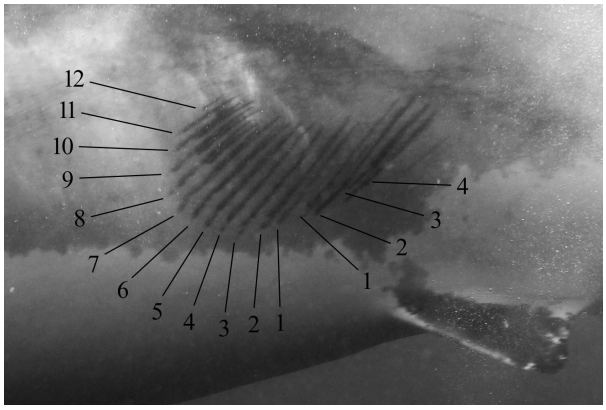

Fig. 2. Close-up of the tooth rake marks on the left side of the estimated 3.5-m female great white shark observed on 7 July, 2017, at Seal Island in False Bay, South Africa. The numbers indicate the twelve scratches on the left matching the twelve teeth in the orca's left half of the lower jaw and the four scratches matching the first four teeth in the orca's right half of the lower jaw. Photo by Alessandro De Maddalena

Predation on great white sharks by orcas is very rare. Only two cases were recorded to date outside South Africa, the first of them occurring on 4 October, 1997, at Southeast Farallon Island, California [Pyle et al., 1999], and the second occurring on 2 February, 2015, at the Neptune Islands, South Australia [Fisher, 2015]. In South Africa, a few cases have been reported. The first case was recorded on 15 March, 2002, in Plettenberg Bay [Best et al., 2010]. In 2015, a pair of male orcas, known as Port and Starboard and easily recognizable because of their collapsed dorsal fins, were recorded preying on broadnose sevengill sharks in False Bay [Engelbrecht et al., 2019]. More recently, Towner *et al.* [2022] reported five cases of predation on great white sharks by the same pair of male orcas near Gansbaai, Western Cape, South Africa, recorded between February and June in 2017. Great white sharks moved from the area following these predatory events and in response to more sightings of the same orcas and other orcas. Gansbaai is located approximately 100 km east of False Bay. The fact that the observation reported herein occurred in July 2017, immediately after the above-mentioned series of predatory events, suggests that the same pair of orcas may have attempted to prey on the great white shark described in this article, but this time without success. Apart from the rake marks, the shark appeared to be perfectly fine, swimming normally and being very active and fast.

The arrival or the departure of large predators at the top of the pyramid of biomass at any site can rapidly induce changes at lower trophic levels. Orca predation on great white sharks induces emigration of sharks from a given site. Individual great white sharks may not return for weeks or months, and in their

absence the number of other sharks, such as bronze whalers and broadnose sevengills, may temporarily increase on that site [Andrew Fox, personal communication; Jorgensen et al., 2019; Pyle et al., 1999; Towner et al., 2022].

Conclusion. To the best of the author's knowledge, the observation of a live great white shark bearing tooth rake marks by an orca described in this article is the first case of its kind reported in the scientific literature. This observation is especially interesting because it represents the evidence that great white sharks can survive an attack by an orca, and it does not necessarily have to succumb in the confrontation between the two species. We should expect more such cases to be reported from the observation area in the future.

Acknowledgement. The author wishes to thank Eric Glenn Haenni for taking the time to edit the text; Chris Fallows, Monique Fallows, the crew of *Apex Shark Expeditions*, and our guests for making it possible to observe the case reported in this article; Olav Magne Strömsholm, Pierre Robert de Latour, and the rest of the crew of *Orca Norway* for making it possible to collect the photographic documentation of orcas in Norway; Alessandra, Antonio, and Phoebe for their support and love.

REFERENCES

1. Best P. B., Meÿer M. A., Lockyer C. Killer whales in South African waters – A review of their biology. *African Journal of Marine Science*, 2010, vol. 32, iss. 2, pp. 171–186. https://doi.org/10.2989/1814232X.2010.501544
2. Best P. B., Meÿer M. A., Thornton M., Kotze P. G. H., Seakamela S. M., Hofmeyr G. J. G., Wintner S., Weland C. D., Steinke D. Confirmation of the occurrence of a second killer whale morphotype in South African waters. *African Journal of Marine Science*, 2014, vol. 36, iss. 2, pp. 215–224. https://doi.org/10.2989/1814232X.2014.923783
3. Brown D. H., Norris K. S. Observations of captive and wild cetaceans. *Journal of Mammalogy*, 1956, vol. 37, iss. 3, pp. 311–326. https://doi.org/10.2307/1376730
4. De Maddalena A., Buttigieg A. *Pesci martello / Hammerhead Sharks.* Formello : IRECO, 2009, 128 p.
5. Engelbrecht T. M., Kock A. A., O'Riain M. J. Running scared: When predators become prey. *Ecosphere*, 2019, vol. 10, iss. 1, art. no. e02531 (8 p.). https://doi.org/10.1002/ecs2.2531
6. Fertl D., Acevedo-Gutierrez A., Darby F. L. A report of killer whales (*Orcinus orca*) feeding on a carcharhinid shark in Costa Rica. *Marine Mammal Science*, 1996, vol. 12, iss. 4, pp. 606–611. http://dx.doi.org/10.1111/j.1748-7692.1996.tb00075.x
7. Fisher H. Killer whale kills great white. In: *Port Lincoln Times* : [site]. URL: https://www.portlincolntimes.com.au/story/2861721/killer-whale-kills-great-white-photos) [accessed: 19.07.2022].
8. Ford J. K. B., Ellis G. M., Balcomb K. C. *Killer Whales. The Natural History and Genealogy of Orcinus Orca in British Columbia and Washington.* 2nd edition. Vancouver, Canada : UBC Press ; Seattle, Washington : University of Washington Press, 2000, 104 p.
9. Ford J. K. B., Ellis G. M., Matkin C. O., Wetklo M. H., Barrett-Lennard L. G., Withler R. E. Shark predation and tooth wear in a population of northeastern Pacific killer whales. *Aquatic Biology*, 2011, vol. 11, no. 3, pp. 213–224. https://doi.org/10.3354/AB00307
10. Jefferson T. A., Leatherwood S., Webber M. A. *Marine Mammals of the World.* Rome : FAO, 1993, 320 p. (FAO species identification guide).
11. Jorgensen S. J., Anderson S., Ferretti F., Tietz J. R., Chapple T., Kanive P., Bradley R. W., Moxley J. H., Block B. A. Killer whales redistribute white shark foraging pressure on seals. *Scientific Reports*, 2019, vol. 9, art. no. 6153 (9 p.). https://doi.org/10.1038/s41598-019-39356-2

12. Norris K. S. Facts and tales about killer whales. *Pacific Discovery*, 1958, January, pp. 24–27.
13. Pyle P., Schramm M. J., Keiper C., Anderson S. D. Predation on a white shark (*Carcharodon carcharias*) by a killer whale (*Orcinus orca*) and a possible case of competitive displacement. *Marine Mammal Science*, 1999, vol. 15, iss. 2, pp. 563–568. https://doi.org/10.1111/j.1748-7692.1999.tb00822.x
14. Reyes L. M., García-Borboroglu P. Killer whale (*Orcinus orca*) predation on sharks in Patagonia, Argentina: A first report. *Aquatic Mammals*, 2004, vol. 30, iss. 3, pp. 376–379. http://dx.doi.org/10.1578/AM.30.3.2004.376
15. Sorisio L. S., De Maddalena A., Visser I. Interaction between killer whales (*Orcinus orca*) and hammerhead sharks (*Sphyrna* sp.) in Galápagos waters. *Latin American Journal of Aquatic Mammals*, 2006, vol. 5, no. 1, pp. 69–71. https://doi.org/10.5597/lajam00095
16. Ternullo R. L., Black N. A., Baldridge A., Shearwater D. Occurrence, distribution and predation behavior of killer whales (*Orcinus orca*) in Monterey Bay, California. In: *Tenth Biennial Conference on the Biology of Marine Mammals* : Abstracts, Galveston, Texas, U. S. A., November 11–15, 1993. Galveston : Society for Marine Mammalogy, 1993, p. 105.
17. Towner A. V., Watson R. G. A., Kock A. A., Papastamatiou Y., Sturup M., Gennari E., Baker K., Booth T., Dicken M., Chivell W., Elwen S., Kaschke T., Edwards D., Smale M. J. Fear at the top: Killer whale predation drives white shark absence at South Africa's largest aggregation site. *African Journal of Marine Science*, 2022, vol. 44, iss. 2, pp. 139–152. https://doi.org/10.2989/1814232X.2022.2066723
18. Visser I. N. Killer whale (*Orcinus orca*) interactions with longline fisheries in New Zealand waters. *Aquatic Mammals*, 2000a, vol. 26, iss. 3, pp. 241–252.
19. Visser I. N. *Orca (Orcinus Orca) in New Zealand Waters.* PhD dissertation. Auckland : University of Auckland, 2000b, 194 p.
20. Visser I. N. First observations of feeding on thresher (*Alopias vulpinus*) and hammerhead (*Sphyrna zygaena*) sharks by killer whales (*Orcinus orca*) specializing on elasmobranch prey. *Aquatic Mammals*, 2005, vol. 31, iss. 1, pp. 83–88. http://dx.doi.org/10.1578/AM.31.1.2005.83
21. Visser I. N., Bonaccorso F. J. New observations and a review of killer whale (*Orcinus orca*) sightings in Papua New Guinea waters. *Aquatic Mammals*, 2003, vol. 29, iss. 1, pp. 150–172.
22. Visser I. N., Berghan J., van Meurs R., Fertl D. Killer whale (*Orcinus orca*) predation on a shortfin mako shark (*Isurus oxyrinchus*) in New Zealand waters. *Aquatic Mammals*, 2000, vol. 26, iss. 3, pp. 229–231.
23. Yukhov V. L., Vinogradova E. K., Medvedev L. P. Ob"ekty pitaniya kosatok (*Orcinus orca* L.) v Antarktike i sopredel'nykh vodakh. In: *Morskie mlekopitayushchie* : materialy VI Vsesoyuznogo soveshchaniya, Kyiv, October, 1975 / E. G. Agarkov (Ed.). Kyiv : Naukova dumka, 1975, pt. 2, pp. 183–185.

СВИДЕТЕЛЬСТВО НЕУДАЧНОЙ АТАКИ КОСАТКОЙ *ORCINUS ORCA* (LINNAEUS, 1758) БОЛЬШОЙ БЕЛОЙ АКУЛЫ *CARCHARODON CARCHARIAS* (LINNAEUS, 1758)

А. Де Маддалена

Международная программа «Морские науки», Миланский университет Бикокка, Милан, Италия
E-mail: *alessandrodemaddalena@gmail.com*

Представлено первое наблюдение живой большой белой акулы *Carcharodon carcharias* со следами зубов косатки *Orcinus orca* на левом боку. Акула длиной около 3,5 м была замечена 7 июля 2017 г. у острова Сил, в заливе Фолс-Бей, Западный Кейп, Южная Африка. Данное наблюдение свидетельствует о том, что большие белые акулы могут пережить нападение косатки.

Ключевые слова: большая белая акула, *Carcharodon carcharias*, косатка, *Orcinus orca*, Фолс-Бей, ЮАР

1871
ИнБЮМ – IBSS

Морской биологический журнал
Marine Biological Journal
2023, vol. 8, no. 1, pp. 56–63
https://marine-biology.ru

UDC 593.161.42-113.4:547.587.11

GROWTH OF *ISOCHRYSIS GALBANA* PARKE, 1949 (HAPTOPHYTA) UNDER MIXOTROPHIC CONDITIONS USING SALICYLIC ACID

© 2023 **N. N. Kovalev, S. E. Leskova, and E. V. Mikheev**

Far Eastern State Technical Fisheries University, Vladivostok, Russian Federation
E-mail: *kovalevnn61@yandex.ru*

Received by the Editor 28.10.2021; after reviewing 27.04.2022;
accepted for publication 20.10.2022; published online 14.03.2023.

The effect of salicylic acid at different concentrations on growth dynamics of *Isochrysis galbana* Parke, 1949 in the batch culture was estimated. The cultivation was carried out in monoculture. The rise in algal biomass was evaluated by an increase in cell abundance (cells were counted in each experiment in the Goryaev chamber in triplicate under a light microscope). The experiments lasted for 7 days. As found, salicylic acid at concentrations from 2.8×10^{-7} to 5.6×10^{-7} mol·L^{-1} had a stimulating effect on the growth dynamics of *I. galbana* cells, compared with the control group. The maximum cell growth in culture was recorded with the addition of 2.8×10^{-7} mol·L^{-1} of salicylic acid, and the specific growth rate at a given concentration on the 7th day of the experiment was 1.2 times higher than in the control group. Biochemical parameters of *I. galbana* culture with salicylic acid added (2.8×10^{-7} mol·L^{-1}) during 7 days of the experiment were estimated in comparison with parameters of the control group. In the experimental group, the maximum protein content was noted on the 7th day of the experiment. A rise was 76.9% compared to the initial value. As shown, the maximum increase in the content of lipids and carbohydrates in the experimental group occurred on the 5th day. A rise in the values of these indicators was 41.7 and 87%, respectively. Chlorophyll content increased throughout the entire experiment both in the control and experimental groups, and the highest value was registered for the experimental group.

Keywords: microalgae, cultivation, *Isochrysis galbana*, phytohormones, salicylic acid

Marine microalgae play a fundamental role in fish and mollusc feeding, especially in the coastal zones. In aquaculture, one of the most widely used microalgae is *Isochrysis galbana* Parke, 1949 (Haptophyta) – due to its high content of polyunsaturated fatty acids [Sánchez et al., 2013].

I. galbana is mainly used to feed bivalve larvae and early juveniles. For most larvae, the artificial breeding occurs during periods of high temperature; this can alter the lipid composition of *I. galbana* and affect its nutritional value.

Obtaining cultures with a stable composition of nutrients is difficult because of its wide variability under the effect of both techniques and conditions of the media used. Specifically, it was noted as follows: a rise in salinity from 5 to 50 g·L^{-1} reduces the production of total lipids in *I. galbana* by 2 times [Cañavate et al., 2020]. At the same time, an increase in the time of the light regime during cultivation contributes to a rise in docosahexaenoic acid production by the alga by 1.6 times [Tzovenis et al., 1997].

However, cultivation in open water basins is unstable and requires optimization of the main parameters (pH and volume of culture, gas exchange, and flow rate), and this ultimately affects the productivity of photosynthesis [Van Bergeijk et al., 2007]. One of the ways to regulate the cultivation efficiency of microalgae and their biochemical composition is the use of phytohormones. These substances are considered as exogenous bioregulators affecting both the resistance of microalgae to environmental factors and the processes of lipid and pigment biosynthesis [Priyadarshani, Rath, 2012; Romanenko et al., 2016]. However, the effect of phytohormones on different microalgal species may differ greatly. Information on the effect of various groups of these chemical compounds on physiological and biochemical parameters of microalgae remains fragmentary; moreover, the values depend on their concentrations in different growth phases.

Investigations of microalgal phytohormones – food objects for molluscs and invertebrates – are rare and mainly concern the development of methods for their cultivation in order to extract biologically active metabolites (carotenoids and chlorophylls). The issues of the effect of exogenous growth promoters on the cultures of microalgae and their biochemical composition remain understudied. At the same time, knowledge on the physiological effects of phytohormones opens up an industrial perspective for their use on mariculture farms [Kovalev et al., 2021].

The aim of this work was to evaluate the effect of various concentrations of salicylic acid on *I. galbana* growth and biochemical composition in the batch culture.

MATERIAL AND METHODS

We used *I. galbana* culture from the collection of the Research and Production Department of Mariculture of the Far Eastern State Technical Fisheries University. The alga was grown in a batch mode on the nutrient medium f/2. This medium is prepared on the basis of filtered and sterilized seawater, with the addition of solutions of mineral salts ($NaNO_3$; $NaH_2PO_4{\cdot}H_2O$; $Na_2SiO_3{\cdot}9H_2O$), trace elements ($CuSO_4{\cdot}5H_2O$; $ZnSO_4{\cdot}7H_2O$; $CoCl_2{\cdot}6H_2O$; $MnCl_2{\cdot}4H_2O$; $Na_2MoO_4{\cdot}2H_2O$; EDTA-Na_2; $FeCl_3{\cdot}6H_2O$), and vitamins (B_1; B_7; B_{12}) [Guillard, 1975]. The algal culture was maintained under constant conditions: temperature of +21…+23 °C, irradiance of 8–10 klx, photoperiod 8 : 16 h (light : dark), and periodic stirring (4–5 times a day).

In the experiments, salicylic acid (“NevaReaktiv”, Russia) was used as a phytohormone at four concentrations: 2.8×10^{-7}; 5.6×10^{-7}; 8×10^{-7}; and 11.2×10^{-7} mol·L^{-1}. During the experiments, *I. galbana* was kept in 1-L glass heatproof conical flasks. Into sterile flasks, 400 mL of clean filtered and sterilized seawater, 2 mL of the nutrient medium, and 100 mL of algal culture were poured. In four flasks, a phytohormone was added at the beginning of the experiment. The fifth flask was a control: the alga was cultivated with no growth promoters.

The cultivation was carried out in monoculture. A rise in algal biomass was determined by an increase in cell abundance (cells were counted in each experiment in the Goryaev chamber in triplicate under a light microscope). The experiment lasted for 7 days.

To determine the content of total carbohydrates, a sample of algal suspension was subjected to acid hydrolysis. The core of this process is as follows: formed monosaccharide units are converted into furfural derivatives, which form colored compounds upon addition of L-tryptophan to the solution, and those absorb light at a wavelength of 540 nm [Laurens et al., 2012].

Sample preparation for protein determination was carried out according to [Herbert et al., 1971]. Protein content was detected by the Lowry method [Lowry et al., 1951].

Total content of lipids was determined by the method based on the color reaction of vanillin in acidic medium with lipids, with the formation of intense staining. Chromogenic groups are hydroxyl and carbonyl ones [Johnson et al., 1977].

Total chlorophyll was isolated by acetone extraction from pre-frozen algal biomass [Carneiro et al., 2019]. Quantitative chlorophyll content was determined spectrophotometrically at wavelengths of 630, 647, 664, and 750 nm. As a control, 90% acetone was used [Aminot, Ray, 2000].

The specific growth rate was calculated according to [Trenkenshu, Lelekov, 2017].

RESULTS

The effect of different concentrations of salicylic acid on *I. galbana* growth dynamics in the batch culture was analyzed.

As shown, salicylic acid at concentrations from 2.8×10^{-7} to 5.6×10^{-7} mol·L^{-1} stimulated the culture growth. This effect was the greatest at 2.8×10^{-7} mol·L^{-1}: the culture growth was 935.4%. The growth of the control culture during the same period was 744.7% (Fig. 1). Interestingly, the difference between the culture density for *I. galbana* of the control group and the experimental one, grown at 2.8×10^{-7} mol·L^{-1} salicylic acid, was 190.7%, or 1.84 million cells·mL^{-1}.

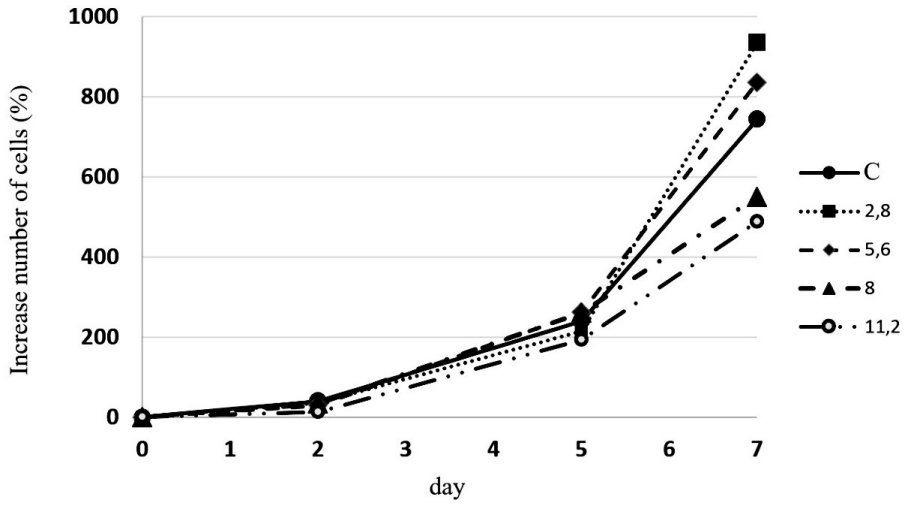

Fig. 1. Growth dynamics of *Isochrysis galbana* culture using salicylic acid ($\times 10^{-7}$ mol·L^{-1}) (C denotes control)

Positive values of the specific growth rate indirectly confirm the synthesis rate of the main biochemical components of microalgae. During the initial stages of cell culture growth, there is a shift in the biochemical composition of microalgae; in the exponential phase, the biochemical composition does not change [Trenkenshu, Lelekov, 2017].

The calculation of the specific growth rate (μ) of the microalga showed its linearity in the first 2 days of cultivation. The specific growth rate of the culture during 5 days of exposure to salicylic acid at a concentration of 2.8×10^{-7} mol·L^{-1} did not differ from that for the control group (Fig. 2).

In the experimental group of *I. galbana* cultivated using salicylic acid at 2.8×10^{-7} mol·L^{-1}, on the 7th day, the specific growth rate was 1.2 times higher compared to that for the control group (Fig. 2).

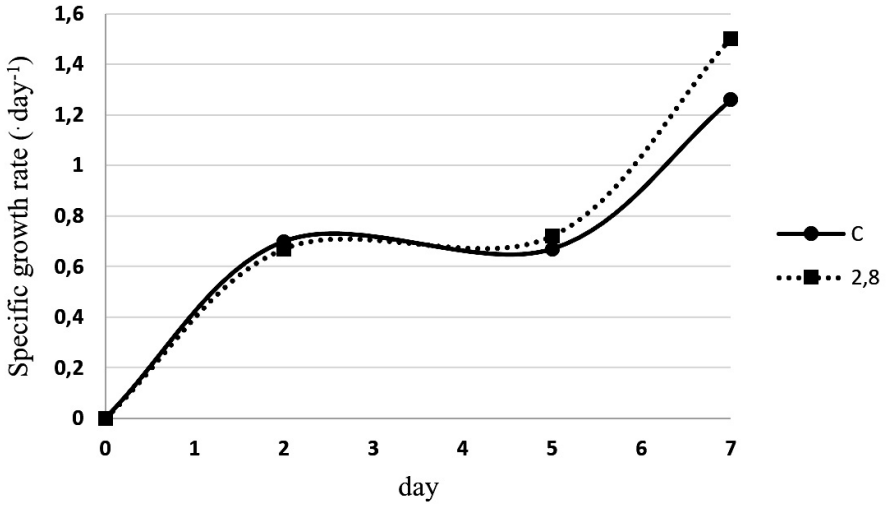

Fig. 2. Specific growth rate of *Isochrysis galbana* culture using salicylic acid (2.8×10^{-7} mol·L^{-1}) (C denotes control)

In the first 5 days of cultivation, in the control group, there was an increase in the protein content by 23%. In the experimental group (with salicylic acid added), a rise in the protein concentration was 69%. Further cultivation of the microalga (up to 7 days) led to a decrease in the protein content in the control group and to an increase by 4.5% in the experimental group (Table 1).

Table 1. Effect of salicylic acid (2.8×10^{-7} mol·L^{-1}) on *Isochrysis galbana* biochemical parameters

Parameter	Protein, μg·mL^{-1}	Carbohydrates, μg·mL^{-1}	Lipids, μg·mL^{-1}	Chlorophyll, μg·mL^{-1}	Culture density, million cells·mL^{-1}
0 days					
C	3.9	10.7	4.8	0.12	0.78
S					
5 days					
C	4.8	13.0	3.9	0.49	1.64
S	6.6	20.1	6.8	0.59	2.02
7 days					
C	4.3	11.5	4.2	0.65	1.89
S	6.9	15.5	6.1	0.76	3.73

Note: C denotes control; S denotes salicylic acid.

The dynamics of changes in the concentration of carbohydrates in culture for 5 days is similar to the dynamics of changes in the protein content. In the control group, an increase by 21.5% was noted; in the experimental group, a rise by 87.9% was recorded. Further cultivation resulted in a decrease in the concentration of carbohydrates in the control group by 11.5%; in the experimental group, there was a drop by 22.9% (Table 1).

The study showed as follows: while cultivating the control group, the content of lipids dropped; the maximum decrease was registered on the 5th day and amounted to 18.8% compared to the concentration of lipids in the initial culture. At the same time, in the culture of *I. galbana* grown with salicylic acid added, an increase in the content of lipids for 5 days was 41.7%. It should be noted that further cultivation was accompanied by a decrease in the value by 10.3% (Table 1).

Positive growth dynamics of chlorophyll content was recorded in both groups during the entire period of cultivation. The increase in chlorophyll concentration in the control group on the 5th day was 308.3%; on the 7th day, it was 441.7%. The values for the experimental group were 391.7 and 533.3%, respectively (Table 1).

DISCUSSION

I. galbana is widely used in aquaculture as a live food. The biochemical composition of microalgae may vary depending on the conditions of their cultivation (growth phase, cultivation mode, temperature, irradiance, nutrient medium composition, *etc.*). It is important to know the biochemical composition of microalgae as a live food. The growth rate and survival of bivalve larvae are known to depend on the quality of the food, and this is determined by the composition of algae – content of protein, carbohydrates, and lipids [Shields, Lupatsch, 2012].

In terms of size and biochemical parameters, the analyzed species is optimal as a part of bivalve diet. However, *I. galbana* cultivation in photobioreactor systems depends on many factors; moreover, it is expensive and unstable in terms of the quantity and quality of biomass produced [Alkhamis, Qin, 2013; Tabelskaya, Kalinina, 2021].

One of the ways to reduce production costs in marine microalgae aquaculture is the use of media supplemented with growth promoters. The use of such regulators is a new strategy for the commercial cultivation of microalgae aimed at improving growth rates and bioproduct synthesis.

Our study showed that salicylic acid stimulated the quantitative growth of *I. galbana* culture by 378%. At the same time, as established earlier, salicylic acid at a concentration of 3.75×10^{-5} mol·L^{-1} stimulated the quantitative growth of the culture of *Tetraselmis suecica* (Kylin) Butcher, 1959 (Chlorophyta) by 415%. Obviously, the physiological effects of salicylic acid on microalgae are species-specific.

During the experiments, the maximum increase in the concentration of carbohydrates and lipids was revealed on the 5th day of cultivation with the use of salicylic acid. At the same time, in the course of previous studies on *I. galbana*, it was found that the use of a medium with the addition of agricultural fertilizers and the nutrient medium f/2 led to a decrease in the content of carbohydrates and lipids during the first 5 days and to accumulation of the maximum amount of protein [Valenzuela-Espinoza et al., 2002]. Our investigations showed that further cultivation (up to 7 days) does not affect the protein concentration in the culture. Interestingly, the growth-promoting concentration of salicylic acid reduced the content of protein and lipids in *T. suecica* with a cultivation period of 14 days.

Lipids are the main source of energy during bivalve larvae development. To complete the metamorphosis of *Magallana gigas* (Thunberg, 1793), the content of lipids in the feed must reach a certain level. When oyster spat feeds on microalgae with high concentration of lipids, a higher growth rate and survival of larvae are recorded. It should be noted as follows: during *I. galbana* cultivation under mixotrophic conditions, the growth and quantitative content of lipids were stimulated by the introduction of glycerol into the medium as an additional carbon source [Danesh et al., 2019].

Chlorophyll content increased during the entire period of *I. galbana* cultivation both in the experimental and control groups. However, a more significant rise in chlorophyll concentration during *I. galbana* cultivation with the addition of salicylic acid indicates an intensifying effect of this stimulant. This, in its turn, affects the biochemical composition of microalgal biomass.

Salicylic acid derivatives stimulate biochemical processes in microalgae as well. Specifically, Madani *et al.* [2020] showed that 2,4-dichloroacetic acid at a concentration of 2 mg·L^{-1} noticeably increased the content of protein and polyunsaturated fatty acids in *I. galbana*.

The data obtained by the same researchers [Madani et al., 2021] indicate the effectiveness of improving *I. galbana* growth when using gibberellic acid at a concentration of 4 mg·L^{-1}. It is noted that an increase in phytohormone concentration from 2 to 6 mg·L^{-1} led to a rise in the concentration of lipids, but to a drop in the content of carbohydrates in terms of the dry weight of the alga. Chlorophyll concentration did not change.

Our study showed that the maximum content of protein, lipids, and carbohydrates was recorded on the 5th day of *I. galbana* cultivation with the addition of 2.8×10^{-7} mol·L^{-1} salicylic acid to the medium. The results obtained can be of practical importance in their industrial application – to optimize the microalga cultivation for mariculture purposes.

Conclusions:

1. The effect of various concentrations of salicylic acid on the growth and biochemical parameters of the mixotrophic culture of *Isochrysis galbana* was evaluated. Salicylic acid at concentrations from 2.8×10^{-7} to 5.6×10^{-7} mol·L^{-1} stimulated the quantitative growth of the microalga cells; at concentrations exceeding 8.0×10^{-7} mol·L^{-1}, it inhibited the growth.
2. The effective concentration of salicylic acid – 2.8×10^{-7} mol·L^{-1} – stimulated the accumulation of protein in the culture by 23% on the 5th day; carbohydrates, by 87.9%; and lipids, by 41.7%.
3. Cultivation of *Isochrysis galbana* culture for more than 5 days was accompanied by a decrease in the parameters of biochemical composition. This must be taken into account when the microalga is used as the feed during the cultivation of invertebrates.

This work was carried out within the framework of the state research assignment No. 121031300015-5.

REFERENCES

1. Kovalev N. N., Leskova S. E., Mikheev E. V., Pozdnyakova Yu. M., Esipenko R. V. Influence of salicylic acid on production characteristics and biochemical parameters of *Tetraselmis suecica* in enrichment culture. *Vestnik Astrakhanskogo gosudarstvennogo tekhnicheskogo universiteta. Seriya: Rybnoe khozyaistvo*, 2021, no. 1, pp. 90–99. (in Russ.). https://doi.org/10.24143/2073-5529-2021-1-90-99
2. Romanenko E. A., Kosakovskaya I. V., Romanenko P. A. Phytohormones of microalgae: Biological role and involvement in the regulation of physiological processes. Pt. II. Cytokinins and gibberellins. *Algologiya*, 2016, vol. 26, no. 2, pp. 203–229. (in Russ.). https://doi.org/10.1615/InterJAlgae.v18.i2.70
3. Tabelskaya A. S., Kalinina M. V. Growth and survival of the hatchery larvae of Pacific oyster *Crassostrea gigas* under different concentrations of microalgae and salinity in conditions of southern Primorye. *Izvestiya TINRO*, 2021, vol. 201, no. 3, pp. 723–731. (in Russ.). https://doi.org/10.26428/1606-9919-2021-201-723-734
4. Trenkenshu R. P., Lelekov A. S. *Modeling Growth of Microalgae in Culture.* Belgorod : Constanta, 2017, 152 p. (in Russ.). URL: https://repository.marine-research.ru/handle/299011/2073
5. Alkhamis Y., Qin J. G. Cultivation of *Isochrysis galbana* in phototrophic, heterotrophic, and mixotrophic conditions. *BioMed Research International*, 2013, vol. 2013, art. no. 983465 (9 p). https://doi.org/10.1155/2013/983465
6. Aminot A., Ray F. *Standard Procedure for the Determination of Chlorophyll a by Spectroscopic Methods.* Copenhagen, Denmark : International Council for the Exploration of the Sea, 2000, 17 p. (ICES Techniques in Marine Environmental Sciences).
7. Cañavate J.-P., Hachero-Cruzado I., Pérez-Gavilán C., Fernández-Díaz C. Lipid dynamics

and nutritional value of the estuarine strain *Isochrysis galbana* VLP grown from hypo to hyper salinity. *Journal of Applied Phycology*, 2020, vol. 32, iss. 6, pp. 3749–3766. https://doi.org/10.1007/s10811-020-02258-2

8. Carneiro M., Pôjo V., Malcata F. X., Otero A. Lipid accumulation in selected *Tetraselmis* strains. *Journal of Applied Phycology*, 2019, vol. 31, iss. 5, pp. 2845–2853. https://doi.org/10.1007/s10811-019-01807-8
9. Danesh A., Zilouei H., Farhadian O. The effect of glycerol and carbonate on the growth and lipid production of *Isochrysis galbana* under different cultivation modes. *Journal of Applied Phycology*, 2019, vol. 31, iss. 6, pp. 3411–3420. https://doi.org/10.1007/s10811-019-01888-5
10. Guillard R. R. L. Culture of phytoplankton for feeding marine invertebrates. In: *Culture of Marine Invertebrate Animals* / M. L. Smith, M. H. Chanley (Eds). New York ; London : Plenum Press, 1975, pp. 29–60. https://doi.org/10.1007/978-1-4615-8714-9_3
11. Herbert D., Phipps P. J., Strange R. E. Chemical analysis of microbial cells. In: *Methods in Microbiology* / J. R. Norris, D. W. Ribbons (Eds). London ; New York : Academic Press, 1971, vol. 5, pt. B, chap. 3, pp. 209–344. http://dx.doi.org/10.1016/S0580-9517(08)70641-X
12. Johnson K. R., Ellis G., Toothill C. The sulfophosphovanillin reaction for serum lipids: A reappraisal. *Clinical Chemistry*, 1977, vol. 23, iss. 9, pp. 1669–1678. https://doi.org/10.1093/CLINCHEM%2F23.9.1669
13. Laurens L. M. L., Dempster T. A., Jones H. D. T., Wolfrum E. J., Van Wychen S., McAllister J. S. P., Rencenberger M., Parchert K. J., Gloe L. M. Algal biomass constituent analysis: Method uncertainties and investigation of the underlying measuring chemistries. *Analytical Chemistry*, 2012, vol. 84, iss. 4, pp. 1879–1887. https://doi.org/10.1021/ac202668c
14. Lowry O. H., Rosebrough N. J., Farr A. L., Randall R. J. Protein measurement with the Folin phenol reagent. *Journal of Biological Chemistry*, 1951, vol. 193, iss. 1, pp. 265–275. http://doi.org/10.1016/s0021-9258(19)52451-6
15. Madani N. S. H., Hosseini Shekarabi S. P., Mehrgan M. S., Pourang N. Can 2, 4-dichlorophenoxyacetic acid alter growth performance, biochemical composition, and fatty acid profile of the marine microalga *Isochrysis galbana*? *Phycologia*, 2020, vol. 59, iss. 6, pp. 598–605. https://doi.org/10.1080/00318884.2020.1827826
16. Madani N. S. H., Shamsaie Mehrgan M., Hosseini Shekarabi S. P., Pourang N. Regulatory effect of gibberellic acid (GA_3) on the biomass productivity and some metabolites of a marine microalga, *Isochrysis galbana*. *Journal of Applied Phycology*, 2021, vol. 33, iss. 1, pp. 255–262. https://doi.org/10.1007/s10811-020-02291-1
17. Priyadarshani I., Rath B. Commercial and industrial applications of microalgae – A review. *Journal of Algal Biomass Utilization*, 2012, vol. 3, no. 4, pp. 89–100.
18. Sánchez Á., Maceiras R., Cancela Á., Pérez A. Culture aspects of *Isochrysis galbana* for biodiesel production. *Applied Energy*, 2013, vol. 101, pp. 192–197. https://doi.org/10.1016/j.apenergy.2012.03.027
19. Shields R. J., Lupatsch I. Algae for aquaculture and animal feeds. *Technikfolgenabschätzung – Theorie und Praxis*, 2012, vol. 21, no. 1, pp. 23–37.
20. Tzovenis I., De Pauw N., Sorgeloos P. Effect of different light regimes on the docosahexaenoic acid (DHA) content of *Isochrysis* aff. *galbana* (clone T-ISO). *Aquaculture International*, 1997, vol. 5, iss. 6, pp. 489–507. https://doi.org/10.1023/A:1018349131522
21. Valenzuela-Espinoza E., Millán-Núñez R., Núñez-Cebrero F. Protein, carbohydrate, lipid and chlorophyll *a* content in *Isochrysis* aff. *galbana* (clone T-Iso) cultured with a low cost alternative to the f/2 medium. *Aquacultural Engineering*, 2002, vol. 25, iss. 4, pp. 207–216. https://doi.org/10.1016/S0144-8609(01)00084-X
22. Van Bergeijk S. A., Salas-Leiton E., Cañavate J. P. Production of *Isochrysis* aff. *galbana* (T-Iso) in outdoor tubular photobioreactors. *7th European Workshop "Biotechnology of Microalgae"*, June 11–13, 2007, Nuthetal, Germany. [S. l.] : [S. n.], 2007, pp. 68–72.

РОСТ *ISOCHRYSIS GALBANA* PARKE, 1949 (HAPTOPHYTA) В МИКСОТРОФНЫХ УСЛОВИЯХ С ИСПОЛЬЗОВАНИЕМ САЛИЦИЛОВОЙ КИСЛОТЫ

Н. Н. Ковалев, С. Е. Лескова, Е. В. Михеев

Дальневосточный государственный технический рыбохозяйственный университет,
Владивосток, Российская Федерация
E-mail: *kovalevnn61@yandex.ru*

Проведена оценка влияния различных концентраций салициловой кислоты на динамику роста *Isochrysis galbana* Parke, 1949 в накопительной культуре. Культивирование осуществляли в монокультуре. Прирост биомассы водорослей находили по увеличению числа клеток, просчитанных в каждом опыте в камере Горяева в трёх повторностях под световым микроскопом. Продолжительность экспериментов составляла 7 суток. Установлено, что концентрации салициловой кислоты от $2{,}8 \times 10^{-7}$ до $5{,}6 \times 10^{-7}$ моль·л$^{-1}$ оказывали стимулирующее воздействие на динамику роста клеток *I. galbana* по сравнению с контрольной группой. Максимальный прирост клеток в культуре отмечен при добавлении салициловой кислоты в концентрации $2{,}8 \times 10^{-7}$ моль·л$^{-1}$, причём удельная скорость роста при данной концентрации на 7-е сутки эксперимента была в 1,2 раза выше, чем в контрольной группе. Проведена оценка биохимических показателей культуры водорослей *I. galbana* с добавлением салициловой кислоты в концентрации $2{,}8 \times 10^{-7}$ моль·л$^{-1}$ в течение 7 суток эксперимента в сравнении с показателями контрольной группы. Максимальное содержание белка в экспериментальной группе зарегистрировано на 7-е сутки опыта. Увеличение составляло 76,9 % по сравнению с начальным значением. Показано, что максимальный рост содержания липидов и углеводов в экспериментальной группе приходился на 5-е сутки опыта. Прирост значений по этим показателям составлял 41,7 и 87 % соответственно. Содержание хлорофилла росло на протяжении всего времени опыта как в контрольной, так и в экспериментальной группе, при этом наибольшее значение показателя отмечено для экспериментальной группы.

Ключевые слова: микроводоросли, культивирование, *Isochrysis galbana*, фитогормоны, салициловая кислота

1871
ИнБЮМ – IBSS

Морской биологический журнал
Marine Biological Journal
2023, vol. 8, no. 1, pp. 64–75
https://marine-biology.ru

UDC 582.276-15:628.4.043-022.53

INGESTION OF MICROPLASTICS BY THE HETEROTROPHIC DINOFLAGELLATE *OXYRRHIS MARINA*

© 2023 **T. V. Rauen, V. S. Mukhanov, and L. O. Aganesova**

A. O. Kovalevsky Institute of Biology of the Southern Seas of RAS, Sevastopol, Russian Federation
E-mail: *taschi@mail.ru*

Received by the Editor 05.07.2020; after reviewing 15.01.2021;
accepted for publication 20.10.2022; published online 14.03.2023.

Incorporation of microplastics (MP) into the microbial food web and its further transport to higher trophic levels have been hitherto poorly studied. In this work, the patterns of MP ingestion by the unicellular heterotrophic dinoflagellate *Oxyrrhis marina* (OXY) were analyzed. The prymnesiophycean *Isochrysis galbana* (ISO), 5.6-μm polystyrene microspheres (MS), and their mixture (ISO-MS) were used as food objects for *O. marina*. Dynamics of the abundance of microorganisms and microspheres was investigated using a flow cytometer. As shown, the heterotroph *O. marina* ingested MP even in the presence of its natural prey (microalgae), and feeding on MP did not result in a decrease in the dinoflagellate abundance. The grazing rates of "preys" in the OXY-ISO-MS mixture were (0.21 ± 0.01) MS·cell^{-1}·h^{-1} (± standard deviation) and (0.38 ± 0.01) ISO·cell^{-1}·h^{-1}. These rates were significantly lower than in the mono-diet experiments – with OXY-ISO [(1.93 ± 0.68) ISO·cell^{-1}·h^{-1}] and OXY-MS [(0.45 ± 0.04) MS·cell^{-1}·h^{-1}]. Thus, the expansion of the range of food objects led to a decrease in the grazing rate. In the mono-diet experiments, the clearance rates were (0.12 ± 0.04) and (0.19 ± 0.06) μL·cell^{-1}·h^{-1} for OXY-ISO and OXY-MS, respectively; thereby, *O. marina* spent less time on capturing ISO cells than on capturing MS. The same pattern was observed in the experiments with the OXY-ISO-MS mixture: the clearance rate for microalgae [(0.17 ± 0.02) μL·cell^{-1}·h^{-1}] was slightly lower than that for MS [(0.19 ± 0.003) μL·cell^{-1}·h^{-1}]. Since *O. marina* re-consumed MS even in the presence of its natural food object (*I. galbana*), no trophic adaptation of the dinoflagellate to MS occurred. No selective grazing of *O. marina* for any "prey" was revealed, either ISO or MS. The obtained results indicate the possibility (and high probability) of the incorporation of MP into the microbial food web and the significant role of unicellular organisms in the transport of MP to higher trophic levels.

Keywords: microplastics, ingestion, microspheres, microalgae, persistent organic pollutants, trophic transport, *Oxyrrhis marina*, *Isochrysis galbana*

The rapid development of plastics production in recent decades has led to the problem of accumulation of related waste. Marine debris is at least 60% plastic [Kozlovskii, Blinovskaia, 2015]. In the marine environment, its polymer base undergoes hydrolysis, photolysis, and microbiological redox reactions; this results in the degradation of plastic fragments [Ateia et al., 2020; Auta et al., 2017] and the formation of particles of various size, including microscopic ones (less than 5 mm), which many researchers [Barnes et al., 2009; Betts, 2008; Fendall, Sewell, 2009; Moore, 2008; Støttrup et al., 1986] consider microplastics (hereinafter MP). One of the main environmental risks associated with MP is their bioavailability to marine hydrobionts [Desforges et al., 2015; Egbeocha et al., 2018]. Having a positive or neutral buoyancy [Van Cauwenberghe et al., 2015], MP are incorporated into food webs of aquatic

biota since MP are comparable in size to phytoplankton – the initial link of a food web. By entering the gastrointestinal tract of zooplankton, MP can form aggregates; this, in turn, leads to a reduced excretion rate [Egbeocha et al., 2018; Ogonowski et al., 2016] and, consequently, to an increased probability of MP transport to higher trophic levels. In addition to physiological damage to an organism (movement disorder, false satiety, *etc.*), the negative effect of this process is related to MP vector function: MP are involved in the transport of toxic substances included in their composition (plasticizers, dyes, styrene, antimicrobials, and so on) *via* the food web [Egbeocha et al., 2018; Kwon et al., 2014; Wright et al., 2013]. During grazing, these substances can leach and accumulate in animal tissues [Batel et al., 2016; Kozlovskii, Blinovskaia, 2015]. Moreover, polymer particles adsorb hydrophobic persistent organic pollutants which are present in seawater [Ogata et al., 2009], and this increases their bioavailability for MP uptake by marine biota [Batel et al., 2016]. Concentrations of persistent organic pollutants on MP surface can be several times higher than background levels [Avio et al., 2015]. This carries a risk of the transport of toxins from animal intestinal tract to tissues [Avio et al., 2015; Koelmans, 2015; Rehse et al., 2016; Watts et al., 2014], and hydrobionts inhabiting coastal waters are most vulnerable to this adverse effect [McCormick et al., 2016].

The relationship between MP pollution and trophic processes in microorganisms that form the basis of the food web is poorly studied [Rehse et al., 2016]. In the present work, we analyzed the incorporation into the diet of a heterotrophic dinoflagellate *Oxyrrhis marina* Dujardin, 1841 – an inhabitant of the Black Sea coasts – of MP that correspond in size to cells of microalgae (the main food item of this species under natural conditions). *O. marina* was chosen as an object of study due to the fact that this dinoflagellate inhabits the coastal zone most exposed to MP pollution and, therefore, is at risk. Moreover, it is one of the main phyto- and bacterioplankton consumers in coastal marine ecosystems and the species actively involved in carbon recycling [Hansen, 1991; Roberts et al., 2010]. *O. marina* is successfully used in aquaculture production to feed copepods [Støttrup et al., 1986] – the main and highest quality feed for fish larvae [Khanaichenko, Bityukova, 1999]. Interestingly, 90% of aquaculture equipment is made of various types of plastics, and this, due to the factors described above, inevitably leads to MP pollution of the environment where hydrobionts are cultured. The possibility of MP incorporation into food webs significantly reduces the quality of final aquaculture products [Wu et al., 2020]. Thus, the heterotrophic dinoflagellate *O. marina* can serve as a model object to study plastic consumption by unicellular organisms.

The aim of this work was to study the presence/absence in *O. marina* of grazing selectivity towards MP and cells of the haptophyte microalga *Isochrysis galbana* Parke, 1949 in their food mixture and to quantify several trophic indicators of each of these food items, including the medium clearance rate (F) and grazing rate (G).

MATERIAL AND METHODS

We carried out a comparative analysis of the main indicators of cell consumption of the haptophyte *I. galbana* and plastic microspheres by the dinoflagellate *O. marina*: the clearance rate (captured volume *per* cell *per* time unit) (F); grazing rate (cell abundance *per* cell *per* time unit) (G); and selective grazing of one or another “prey” in the mixture.

In the experiment, we used *O. marina* and *I. galbana* cultures from the working collection of IBSS aquaculture and marine pharmacology department, as well as Polychromatic Red polystyrene dyed microspheres, 5.6 μm in diameter (excitation, 491 nm; manufacturer, Polysciences, Inc., the USA).

Microalgae were cultured on Walne medium [Coutteau, 1996] at (24 ± 1) °C, constant irradiance of 5,000 lux, without aeration. Aliquots of cultures were used in the exponential growth phase. *O. marina* culture was pre-adapted to the experimental conditions and maintained for a day without feed.

Experimental scheme. *I. galbana*, microspheres, and their mixture (hereinafter ISO, MS, and ISO-MS, respectively) were introduced as food items into prepared *O. marina* culture (hereinafter OXY) so that the total volume of the medium was 18 mL. The incubation in conical glass vessels lasted for 3 h under constant stirring.

To account for MS loss due to their settling and adhering to vessel walls, an additional glass vessel was placed – the one containing only nutrient medium and MS. Thus, the abundance dynamics of microorganisms and MS was studied in four types of vessels (each in three replicates): 1) OXY-ISO; 2) OXY-MS; 3) OXY-ISO-MS; and 4) MS. The initial abundance of *O. marina*, *I. galbana*, and MS in the experimental vessels was as follows: from 25×10^3 to 50×10^3 cells·mL^{-1} (OXY); from 10×10^3 to 50×10^3 cells·mL^{-1} (ISO); and from 5×10^3 to 10×10^3 MS·mL^{-1}.

Cell condition monitoring and quantification of microorganisms and MS were performed by microscopy techniques and flow cytometry. Specifically, 1 mL of a sub-sample was taken from every experimental vessel at the very beginning and then every 20 min.

The clearance rate (F) and grazing rate (G) were calculated according to [Frost, 1972], but a feeding-independent process – MS adhering to vessel walls – was taken into account as well. To study the grazing selectivity of *O. marina* with a mixture of *I. galbana* and MS (the OXY-ISO-MS experiment), the selectivity index was used [Ivlev, 1961]. It was calculated as follows: $(Ri - Pi) / (Ri + Pi)$, where R_i is the proportion of the i-th food item in the predator diet; P_i is the proportion of the i-th food item in the medium. The values of the selectivity index varied from −1 (complete avoidance) to +1 (maximum preference).

Microscopy. MS and microorganisms were microphotographed under a Nikon Eclipse TS100-F microscope equipped with a digital camera, in epifluorescence mode (a set of light filters for excitation in the blue area of the spectrum). Due to bright green fluorescence, MS were clearly visible in the nutrient medium and in *O. marina* digestive vacuoles (see Fig. 2).

Cytometric analysis. A Cytomics™ FC500 flow cytometer (Beckman Coulter, the USA), equipped with a 488-nm single-phase argon laser, and CXP software were used to study abundance dynamics of MS and abundance and size of *O. marina* and *I. galbana* cells in the experimental vessels. Total microalgae abundance was determined in unstained samples by gating a cell population on 2-parameter cytograms – forward scatter (FS) and autofluorescence in the red (FL4, 675 nm) and green (FL1, 525 nm) areas of the spectrum on dimensionless logarithmic scales (Fig. 1).

MS and microalgae concentrations were calculated from sample flow rates (15 and 60 μL·min^{-1}, respectively), time of counting (100–360 s), and the abundance of cells (or MS) recorded during this time interval (in microalgae samples, a minimum of 3,000 cells for each replicate). Measurement quality was controlled using Flow-Check™ calibration fluorospheres (Beckman Coulter) with a known concentration in the sample.

RESULTS

A rapid decline in the abundance of MS indicated high rates of their grazing by the dinoflagellate. Specifically, within the first hour of the experiment, MS abundance dropped to extremely low values (< 10^2 MS·mL^{-1}) in all vessels (see Fig. 3A, C). *O. marina* cells containing MS in their digestive

vacuoles acquired green fluorescence. As a consequence, a subcluster of points with high FL1 values was formed on the cytograms (Fig. 1).

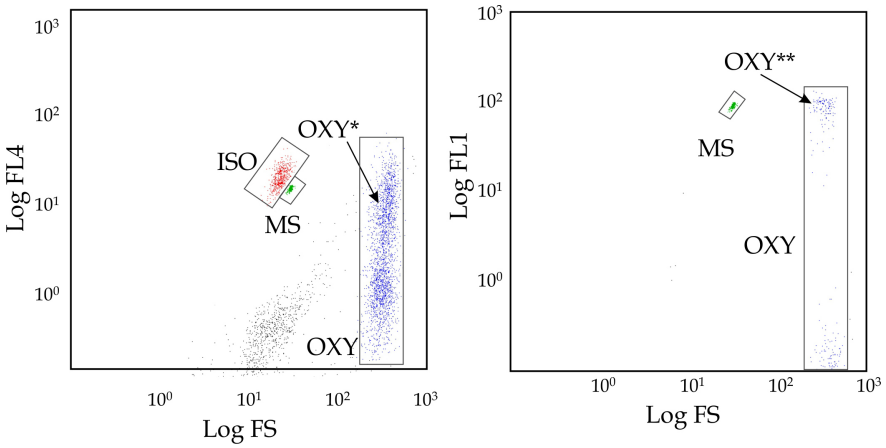

Fig. 1. Gating of the heterotrophic dinoflagellate *Oxyrrhis marina* (OXY) and its food objects [polystyrene microspheres (MS) and the haptophyte *Isochrysis galbana* (ISO)] on two-parameter cytograms – of forward scatter (FS) and of red (FL4, 675 nm) and green (FL1, 525 nm) fluorescence. OXY* denotes dinoflagellate cells grazing both *I. galbana* and microspheres; OXY**, dinoflagellate cells with microspheres in their digestive vacuoles

MS grazing by *Oxyrrhis marina* cells was recorded under a microscope as well. In some cases, up to 5–6 brightly fluorescent microspheres could be identified in digestive vacuoles of one cell (Fig. 2).

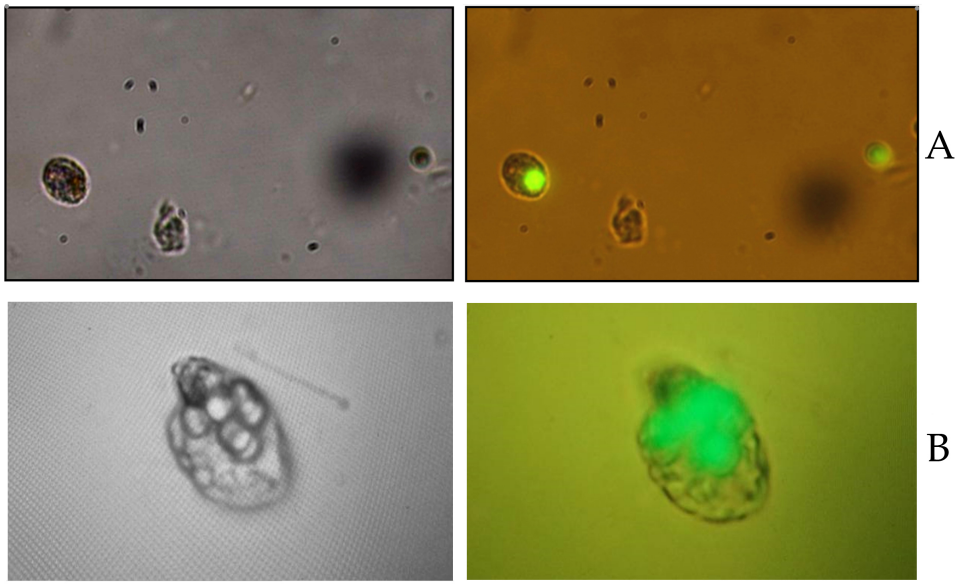

Fig. 2. Cells of the dinoflagellate *Oxyrrhis marina* with one (A) and several (B) microspheres in its digestive vacuoles in bright field (images on the left) and in epifluorescence mode (images on the right)

During the first 2 hours of the experiment, the dinoflagellate almost completely grazed *I. galbana* (Fig. 3B). MS abundance in the medium was restored with time and reached about 10^3 MS·mL^{-1} by the end of the experiment (Fig. 3A, C). Such an unusual dynamics occurs since MP cannot be digested in digestive vacuoles. An increase in MS abundance meant that the dinoflagellate excreted them back into the medium.

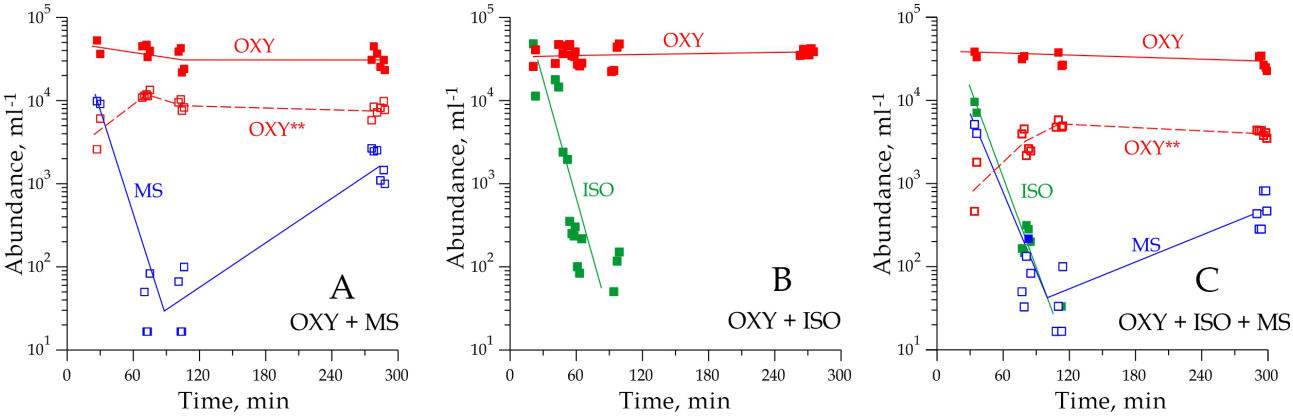

Fig. 3. Dynamics of the abundance of microspheres (MS), the haptophyte *Isochrysis galbana* (ISO), and the heterotrophic dinoflagellate *Oxyrrhis marina* (OXY) in the experimental vessels with different diets: A, microspheres only (OXY-MS); B, haptophytes only (OXY-ISO); C, the mixture (OXY-ISO-MS). Dynamics of *O. marina* cell abundance with MS in their digestive vacuoles (OXY**) is shown separately in plots A and C

Thus, a sharp drop in MS concentration in the medium at the initial stage of the experiment resulted from MS rapid grazing and their accumulation in digestive vacuoles. Then, MS were excreted back into the medium, and this led to a "compensation" of their abundance, which, however, did not reach the initial values. In accordance with this scheme of the processes, the abundance of *O. marina* cells containing MS in their vacuoles first increased and then reached a certain plateau (Fig. 3A, C).

The values of *O. marina* abundance in all series of the vessels remained almost the same throughout the experiments (Fig. 3A, B, C). This could indicate the lack of negative effect of MS on the dinoflagellate division rate. However, the duration of the experiments may have been insufficient to reveal such an effect.

Calculations of the clearance rates (F) by the dinoflagellate showed as follows. In the OXY-ISO series, the F value was (0.12 ± 0.04) μL·cells^{-1}·h^{-1}; this was lower than in the OXY-MS series [(0.19 ± 0.06) μL·cells^{-1}·h^{-1}]. So, in the first case, *O. marina* cells captured a smaller volume *per* time unit than in the second case (Fig. 4). Moreover, *O. marina* cells spent less time on capturing *I. galbana* cells than on capturing MS.

The same pattern, though to a lesser extent, was maintained in the series with the mixture of microalgae and microspheres as the feed (OXY-ISO-MS). The clearance rate calculated taking into account the haptophyte microalgae [(0.17 ± 0.02) μL·cells^{-1}·h^{-1}] was slightly lower than the value obtained for MS [(0.19 ± 0.003) μL·cells^{-1}·h^{-1}] (Fig. 4). The grazing rates (G) of these two "preys" in the OXY-ISO-MS mixture were (0.21 ± 0.01) MS·cells^{-1}·h^{-1} (± standard deviation) and (0.38 ± 0.01) ISO·cells^{-1}·h^{-1}. These values were significantly lower than in the OXY-ISO and OXY-MS mono-diet experiments [(1.93 ± 0.68) ISO·cells^{-1}·h^{-1} and (0.45 ± 0.04) MS·cells^{-1}·h^{-1}, respectively], *i. e.*, the expansion of the range of food items resulted in a decrease in the grazing rate (Fig. 4). The maximum of G was observed in the OXY-ISO experiment [(1.93 ± 0.68) ISO·cells^{-1}·h^{-1}] (Fig. 4), which means that *O. marina* consumed *I. galbana* with the highest efficiency.

However, differences in the grazing rates and clearance rates did not affect *O. marina* grazing selectivity. The values of the Ivlev selectivity index obtained for *I. galbana* and MS were close to zero (–0.03 and 0.05, respectively), which reflected the lack of grazing selectivity: the dinoflagellate ingested MP on a par with live food. This result indicated that MP could be incorporated into the food web of marine ecosystems at the lowest trophic levels.

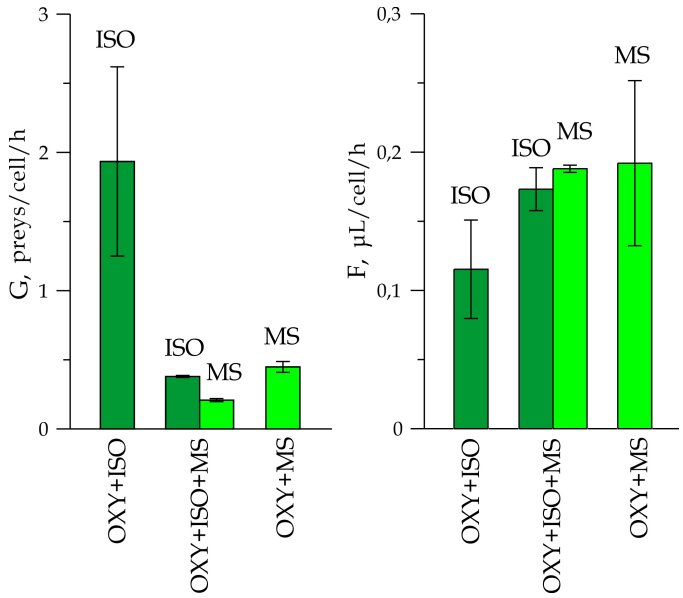

Fig. 4. Grazing rate (G) for the heterotroph *Oxyrrhis marina* (OXY) [the "preys" are the haptophyte *Isochrysis galbana* (ISO) and polystyrene microspheres (MS)] and clearance rate (F) for *O. marina* cells in the experimental vessels with different diets: OXY-MS, microspheres only; OXY-ISO, microalgae only; OXY-ISO-MS, the mixture of microalgae and microspheres

DISCUSSION

To date, reports on MP consumption by multicellular hydrobionts (detritophages, *Artemia*, copepods, mussels, crabs, *etc.*) are quite numerous [Batel et al., 2016; Egbeocha et al., 2018; Procter et al., 2019; Watts et al., 2014; Wu et al., 2020], whereas the incorporation of artificial particles into the diet of unicellular organisms has been studied poorly [Christaki et al., 1998; Rillig, Bonkowski, 2018]. Our results fill this gap to some extent by demonstrating the ability of marine protists to actively consume MP. However, we had to question the ability of the heterotrophic dinoflagellate *O. marina* to distinguish artificial particles from its normal food items – unicellular microorganisms.

The ideas of chemotactic or other warning signals in heterotrophic protists, which enable them to recognize plastic particles and prevent their phagocytosis, remain rather controversial. Specifically, *O. marina* is known for size-selective grazing [Hansen et al., 1996]. It has also been noted in several studies that *O. marina* may reject certain types of food items after capturing prey, at the stage of grazing [Flynn et al., 1996; Hansen et al., 1996; Wolfe et al., 1997]. Moreover, it was established that *O. marina* has receptors on the cell surface, with which it recognizes a prey [Martel, 2009]. According to preliminary experimental data [Hartz, 2010], *O. marina* plasma membrane contains rhodopsin, which makes this heterotroph capable of recognizing photoautotroph cells by red chlorophyll autofluorescence. The presence of such a prey recognition mechanism indicates *O. marina* ability to distinguish microalgae from other, non-pigmented food objects, *inter alia* MP.

Only three experimental studies are known in which artificial particles were incorporated into *O. marina* diet. Specifically, E. Wootton *et al.* [2007] established a new biochemical mechanism for prey recognition in unicellular protists, including *O. marina*. The core of this mechanism is in the presence of a special receptor – mannose-binding lectin – on the predator cell surface. As found, blocking this receptor significantly inhibited *O. marina* feeding on the microalga *I. galbana*, and application of mannose to the surface of plastic microspheres doubled the grazing rate. Pre-incubation of the dinoflagellate with mannose

solution completely deprived it of the ability to identify any plastic particles coated with a polysaccharide layer. The characteristic feature of this study was that plastic microspheres were used in experiments only after a special treatment – application of sugars on their surface [Wootton et al., 2007]. Thus, the results presented by the authors did not allow making a confident conclusion on the ability of *O. marina* to consume MP.

In the second investigation [Hammer et al., 1999], artificial particles (silicon and plastic microspheres, albumin microbeads, *etc.*) were offered to the heterotrophic dinoflagellate as prey along with its natural food items (live phytoplankton). *O. marina* was found to confidently consume artificial particles, but the rate was significantly lower than when feeding on regular food. The authors explained this selectivity by the magnitude of a charge on the surface of a prey: a more negative potential of an artificial particle prevented its capture by the predator. Differences between surface charges for *O. marina* and its prey increased the probability of collision and duration of their contact; consequently, the grazing rate rose [Hammer et al., 1999]. The initiation of the capture of the prey with a more negative surface charge occurred at a shorter distance from the prey (only 0.5 to 2 μm), whereas that with a higher potential occurred at significantly greater distance (6 to 10 μm), which increased the capture probability [Hammer et al., 1999]. In any case, this study established the incorporation of artificial particles into *O. marina* diet. However, the ability of the dinoflagellate to identify these food items was shown as well, which contradicts our results.

Finally, D. Lyakurwa [2017] demonstrated in his experiment that *O. marina* ingested plastic microspheres just as intensively as a natural prey – the cryptophyte alga *Rhodomonas baltica* Karsten, 1898. These observations are fully consistent with our results. In both cases, *O. marina* did not reject the plastic microspheres proposed. Equally high grazing rates by the heterotrophic dinoflagellate both of artificial and natural food items suggested a very limited ability of these protist to distinguish MP from its natural prey. We can only assume that selective grazing failed to be revealed both by us and [Lyakurwa, 2017] due to rapid adsorption of biopolymers (microalgae exometabolites and bacteria) on MP surface, which are abundant in the experimental medium. “Packaging” microspheres in an organic “film” disguised them as an “edible” prey and thus could hinder their identification by the predator.

The sorption properties of plastic particles have recently become the subject of much research attention as they determine their vector function – the ability to accumulate and transport organic pollutants [Ateia et al., 2020]. We believe that a thin organic film on MP surface, the same as a bacterial film or fouling community, increases MP bioavailability and facilitates their incorporation into trophic processes. At the same time, “taste quality” of particles may depend on the rate of formation of an organic film and its chemical composition. These characteristics are difficult to control even under experimental conditions since they can vary greatly in different nutrient media and cultured microorganisms. Accordingly, the phagocytosis rate of MP is an unpredictable value. This hypothesis well explains, on the one hand, the fact of MP consumption by predatory protists and, on the other hand, contradictory data on the ability of protists to distinguish MP from food items.

Interestingly, in the OXY-ISO series, where *O. marina* fed on *I. galbana* cells only, the grazing rate was higher than that for MS in the OXY-MS series (Fig. 4). This may be due to the fact that MP, having entered *O. marina* digestive vacuoles, stayed in the predator cell for a longer time as they could not be digested. Therefore, the grazing rate decreased in this case. *I. galbana* cells were rapidly digested, which allowed the predator to maintain a high rate of food consumption. The mobility of *I. galbana* cells could also increase their attractiveness to *O. marina*.

The abundance dynamics of *O. marina* cells with microspheres inside (Fig. 3A, C) indicated recaptures of MS after their excretion. This occurred both in the absence of an alternative food source (*I. galbana*) in the OXY-MS series and in its presence in the OXY-ISO-MS series. It can be assumed that *O. marina* did not identify MP upon re-encounter as a less suitable food object and captured them for the second time on a par with *I. galbana* cells. So, no trophic adaptation occurred. At the same time, MS consumption had no negative effect on the dinoflagellate: there were no significant differences in *O. marina* abundance in all experimental series within the time range studied (Fig. 3A, B, C). The same result was obtained in another experiments [Lyakurwa, 2017]. The negative effect of MS consumption could be manifested over longer exposure time; this assumption requires further experimental verification.

It should be noted that microspheres used in the experiment were microgranules of polystyrene, which is a major contributor to the chemical composition of microplastic pollution in marine coastal waters [Cordova et al., 2019]. This type of plastic is widely used in various human activities and is an unstable product [Cooper, Corcoran, 2010; Koelmans, 2015]. Thus, under solar radiation, its brittleness increases; at high temperatures, the polymer disintegrates to form a monomer [Cooper, Corcoran, 2010]. So, we can argue that polystyrene microgranules are capable of incorporating into the microbial food web, being food items even for unicellular organisms. The results obtained in this work highlight the need for further study of MP incorporation into trophic webs, MP effect on the physiological state of the smallest hydrobionts, and the possibility of biomagnification of persistent organic pollutants by planktonic organisms.

Conclusions:

1. The heterotrophic dinoflagellate *Oxyrrhis marina* ingests plastic microspheres even in the presence of alternative food objects from its natural diet.
2. Consumption rates of *Isochrysis galbana* cells and microspheres by the dinoflagellate in the OXY-ISO-MS mixture were significantly lower than in the OXY-ISO and OXY-MS mono-diet experiments, *i. e.*, the expansion of the range of food items led to a decrease in the grazing rate.
3. The high clearance rate when the dinoflagellate fed on live prey (*I. galbana*) indicated that it takes less time for the predator to capture microalga cells than to capture plastic microspheres.
4. The values of the Ivlev selectivity index obtained for *I. galbana* and microspheres indicated the lack of selective grazing in *O. marina*. This confirms the possibility of incorporation of microplastics into the microbial food web.
5. Trophic adaptation of *O. marina* cells to microplastics did not occur: cells consumed polystyrene microspheres for the second time even in the presence of an alternative food item.
6. No significant differences in the dynamics of *O. marina* abundance when feeding on live prey (*I. galbana*) and microplastics were revealed. Thus, there was no negative effect of microplastics on the predator, at least on the time scale of the experiment (hours).

This work was carried out within the framework of IBSS state research assignment "Investigation of mechanisms of controlling production processes in biotechnological complexes with the aim of developing scientific foundations for production of biologically active substances and technical products of marine genesis" (No. 121030300149-0) and "Structural and functional organization, productivity, and sustainability of marine pelagic ecosystems" (No. 121040600178-6).

REFERENCES

1. Kozlovskii N. V., Blinovskaia J. Y. Microplastic is World Ocean macroproblem. *Mezhdunarodnyi zhurnal prikladnykh i fundamental'nykh issledovanii*, 2015, vol. 10-1, pp. 159–162. (in Russ.)
2. Khanaichenko A. N., Bityukova Y. E. Black Sea turbot larvae feeding selectivity and choice of feeding strategy. *Ekologiya morya*, 1999, iss. 3, pp. 63–67. (in Russ.). URL: https://repository.marine-research.ru/handle/299011/4212
3. Ateia M., Zheng T., Calace S., Tharayil N., Pilla S., Karanfil T. Sorption behavior of real microplastics (MPs): Insights for organic micropollutants adsorption on a large set of well-characterized MPs. *Science of The Total Environment*, 2020, vol. 720, art. no. 137634 (7 p.). https://doi.org/10.1016/j.scitotenv.2020.137634
4. Auta H. S., Emenike C. U., Fauziah S. H. Distribution and importance of microplastics in the marine environment: A review of the sources, fate, effects, and potential solutions. *Environment International*, 2017, vol. 102, pp. 165–176. https://doi.org/10.1016/j.envint.2017.02.013
5. Avio C. G., Gorbi S., Milan M., Benedetti M., Fattorini D., d'Errico G., Pauletto M., Bargelloni L., Regoli F. Pollutants bioavailability and toxicological risk from microplastics to marine mussels. *Environmental Pollution*, 2015, vol. 198, pp. 211–222. https://doi.org/10.1016/j.envpol.2014.12.021
6. Barnes D. K. A., Galgani F., Thompson R. C., Barlaz M. Accumulation and fragmentation of plastic debris in global environments. *Philosophical Transactions of the Royal Society B*, 2009, vol. 364, iss. 1526, pp. 1985–1998. https://doi.org/10.1098/rstb.2008.0205
7. Batel A., Linti F., Scherer M., Erdinger L., Braunbeck Th. Transfer of benzo[*a*]pyrene from microplastics to *Artemia* nauplii and further to zebrafish *via* a trophic food web experiment: CYP1A induction and visual tracking of persistent organic pollutants. *Environmental Toxicology and Chemistry*, 2016, vol. 35, iss. 7, pp. 1656–1666. https://doi.org/10.1002/etc.3361
8. Betts K. Why small plastic particles may pose a big problem in the oceans. *Environmental Science and Technology*, 2008, vol. 42, iss. 24, pp. 8995. https://doi.org/10.1021/es802970v
9. Christaki U., Dolan J. R., Pelegri S., Rassoulzadegan F. Consumption of picoplankton-size particles by marine ciliates: Effects of physiological state of the ciliate and particle quality. *Limnology and Oceanography*, 1998, vol. 43, iss. 3, pp. 458–464. https://doi.org/10.4319/lo.1998.43.3.0458
10. Cooper D. A., Corcoran P. L. Effects of mechanical and chemical processes on the degradation of plastic beach debris on the island of Kauai, Hawaii. *Marine Pollution Bulletin*, 2010, vol. 60, iss. 5, pp. 650–654. https://doi.org/10.1016/j.marpolbul.2009.12.026
11. Cordova M. R., Purwiyanto A. I. S., Suteja Y. Abundance and characteristics of microplastics in the northern coastal waters of Surabaya, Indonesia. *Marine Pollution Bulletin*, 2019, vol. 142, pp. 183–188. https://doi.org/10.1016/j.marpolbul.2019.03.040
12. Coutteau P. Micro-Algae. In: *Manual on the Production and Use of Live Food for Aquaculture* / P. Lavens, P. Sorgeloos (Eds). Rome : FAO, 1996, pp. 7–48. (FAO Fisheries Technical Paper ; no. 361).
13. Desforges J. W., Galbraith M., Ross P. S. Ingestion of microplastics by zooplankton in the northeast Pacific Ocean. *Archives of Environmental Contamination and Toxicology*, 2015, vol. 69, iss. 3, pp. 320–330. https://doi.org/10.1007/s00244-015-0172-5
14. Egbeocha C. O., Malek S., Emenike C. U., Milow P. Feasting on microplastics ingestion by and effects on marine organisms. *Aquatic Biology*, 2018, vol. 27, pp. 93–106. https://doi.org/10.3354/ab00701
15. Fendall L. S., Sewell M. A. Contributing to marine pollution by washing your face: Microplastics in facial cleansers. *Marine Pollution Bulletin*, 2009, vol. 58, iss. 8, pp. 1225–1228. https://doi.org/10.1016/j.marpolbul.2009.04.025

16. Flynn K. J., Davidson K., Cunningham A. Prey selection and rejection by a microflagellate; implications for the study and operation of microbial food webs. *Journal of Experimental Marine Biology and Ecology*, 1996, vol. 196, iss. 1–2, pp. 357–372. https://doi.org/10.1016/0022-0981(95)00140-9
17. Frost B. W. Effects of size and concentration of food particles on the feeding behavior of the marine planktonic copepod *Calanus pacificus*. *Limnology and Oceanography*, 1972, vol. 17, iss. 6, pp. 805–815. https://doi.org/10.4319/lo.1972.17.6.0805
18. Hansen P. J. Quantitative importance and trophic role of heterotrophic dinoflagellates in a coastal pelagial food web. *Marine Ecology Progress Series*, 1991, vol. 73, no. 2/3, pp. 253–261. http://doi.org/10.3354/meps073253
19. Hansen F. C., Witte H. J., Passarge J. Grazing in the heterotrophic dinoflagellate *Oxyrrhis marina*: Size selectivity and preference for calcified *Emiliania huxleyi* cells. *Aquatic Microbial Ecology*, 1996, vol. 10, iss. 3, pp. 307–313. https://doi.org/10.3354/ame010307
20. Hammer A., Grüttner C., Schumann R. The effect of electrostatic charge of food particles on capture efficiency by *Oxyrrhis marina* Dujardin (Dinoflagellate). *Protist*, 1999, vol. 150, iss. 4, pp. 375–382. https://doi.org/10.1016/s1434-4610(99)70039-8
21. Hartz A. J. *Investigating the Ecological Role of Cell Signaling in Free-living Marine Heterotrophic Protists.* PhD thesis / Oregon State University. Oregon, 2010, 182 p.
22. Ivlev V. S. *Experimental Ecology of the Feeding of Fishes.* New Haven : Yale University Press, 1961, 302 p.
23. Koelmans A. A. Modeling the role of microplastics in bioaccumulation of organic chemicals to marine aquatic organisms. A critical review. In: *Marine Anthropogenic Litter* / M. Bergmann, L. Gutow, M. Klages (Eds). Berlin : Springer, 2015, pp. 309–324. https://doi.org/10.1007/978-3-319-16510-3_11
24. Kwon B. G., Saido K., Koizumi K., Sato H., Ogawa N., Chung S. Y., Kusui T., Kodera Y., Kogure K. Regional distribution of styrene analogues generated from polystyrene degradation along the coastlines of the North-East Pacific Ocean and Hawaii. *Environmental Pollution*, 2014, vol. 188, pp. 45–49. https://doi.org/10.1016/j.envpol.2014.01.019
25. Lyakurwa D. J. Uptake and effects of microplastic particles in selected marine microalgae species; *Oxyrrhis marina* and *Rhodomonas baltica*. PhD thesis / Norwegian University of Science and Technology. Trondheim, 2017, 51 p.
26. Martel C. M. Conceptual bases for prey biorecognition and feeding selectivity in the microplanktonic marine phagotroph *Oxyrrhis marina*. *Microbial Ecology*, 2009, vol. 57, iss. 4, pp. 589–597. https://doi.org/10.1007/s00248-008-9421-8
27. McCormick A. R., Hoellein T. J., London M. G., Hittie J., Scott J. W., Kelly J. J. Microplastic in surface waters of urban rivers: Concentration, sources, and associated bacterial assemblages. *Ecosphere*, 2016, vol. 7, iss. 11, art. no. e01556 (22 p.). https://doi.org/10.1002/ecs2.1556
28. Moore C. J. Synthetic polymers in the marine environment: A rapidly increasing, long-term threat. *Environmental Research*, 2008, vol. 108, iss. 2, pp. 131–139. https://doi.org/10.1016/j.envres.2008.07.025
29. Ogata Y., Takada H., Mizukawa K., Hirai H., Iwasa S., Endo S., Mato Y., Saha M., Okuda K., Nakashima A., Murakami M., Zurcher N., Booyatumanondo R., Zakaria M. P., Dung L. Q., Gordon M., Miguez C., Suzuki S., Moore Ch., Karapanagioti H. K., Weerts S., McClurg T., Burres E., Smith W., Van Velkenburg M., Lang J. S., Lang R. C., Laursen D., Danner B., Stewardson N., Thompson R. C. International Pellet Watch: Global monitoring of persistent organic pollutants (POPs) in coastal waters. 1. Initial phase data on PCBs, DDTs, and HCHs. *Marine Pollution Bulletin*, 2009, vol. 58, iss. 10, pp. 1437–1446. https://doi.org/10.1016/j.marpolbul.2009.06.014
30. Ogonowski M., Schür C., Jarsén A., Gorokhova E. The effects of natural and anthropogenic microparticles on individual fitness in *Daphnia magna*. *PLoS One*, 2016, vol. 11, iss. 5, art. no. e0155063 (20 p.). https://doi.org/10.1371/journal.pone.0155063

31. Procter J., Hopkins F. E., Fileman E. S., Lindeque P. K. Smells good enough to eat: Dimethyl sulfide (DMS) enhances copepod ingestion of microplastics. *Marine Pollution Bulletin*, 2019, vol. 138, pp. 1–6. https://doi.org/10.1016/j.marpolbul.2018.11.014
32. Rehse S., Kloas W., Zarfl C. Short-term exposure with high concentrations of pristine microplastic particles leads to immobilisation of *Daphnia magna*. *Chemosphere*, 2016, vol. 153, pp. 91–99. https://doi.org/10.1016/j.chemosphere.2016.02.133
33. Rillig M. C., Bonkowski M. Microplastic and soil protists: A call for research. *Environmental Pollution*, 2018, vol. 241, pp. 1128–1131. https://doi.org/10.1016/j.envpol.2018.04.147
34. Roberts E. C., Wootton E. C., Davidson K., Jeong H. J., Lowe C. D., Montagnes D. J. Feeding in the dinoflagellate *Oxyrrhis marina*: Linking behaviour with mechanisms. *Journal of Plankton Research*, 2010, vol. 33, iss. 4, pp. 603–614. https://doi.org/10.1093/plankt/fbq118
35. Støttrup J. G., Richardson K., Kirkegaard E., Pihl N. J. The cultivation of *Acartia tonsa* Dana for use as a live food source for marine fish larvae. *Aquaculture*, 1986, vol. 52, iss. 2, pp. 87–96. https://doi.org/10.1016/0044-8486(86)90028-1
36. Van Cauwenberghe L., Claessens M., Vandegehuchte M. B., Janssen C. R. Microplastics are taken up by mussels (*Mytilus edulis*) and lugworms (*Arenicola marina*) living in natural habitats. *Environmental Pollution*, 2015, vol. 199, pp. 10–17. https://doi.org/10.1016/j.envpol.2015.01.008
37. Watts A. J. R., Lewis C., Goodhead R. M., Beckett S. J., Moger J., Tyler Ch. R., Galloway T. S. Uptake and retention of microplastics by the shore crab *Carcinus maenas*. *Environmental Science and Technology*, 2014, vol. 48, iss. 15, pp. 8823–8830. https://doi.org/10.1021/es501090e
38. Wolfe G. V., Steinke M., Kirst G. O. Grazing-activated chemical defence in a unicellular marine alga. *Nature*, 1997, vol. 387, pp. 894–897. https://doi.org/10.1038/43168
39. Wootton E., Zubkov M., Jones D., Jones R., Martel C., Thornton C., Roberts E. Biochemical prey recognition by planktonic protozoa. *Environmental Microbiology*, 2007, vol. 9, iss. 1, pp. 216–222. https://doi.org/10.1111/j.1462-2920.2006.01130.x
40. Wright S. L., Thompson R. C., Galloway T. S. The physical impacts of microplastics on marine organisms: A review. *Environmental Pollution*, 2013, vol. 178, pp. 483–492. https://doi.org/10.1016/j.envpol.2013.02.031
41. Wu F., Wang Y., Leung J. Y. S., Huang W., Zeng J., Tang Y., Chen J., Shi A., Yu X., Xu X., Zhang H., Cao L. Accumulation of microplastics in typical commercial aquatic species: A case study at a productive aquaculture site in China. *Science of the Total Environment*, 2020, vol. 708, art. no. 135432 (11 p.). https://doi.org/10.1016/j.scitotenv.2019.135432

ПОТРЕБЛЕНИЕ ЧАСТИЦ МИКРОПЛАСТИКА ГЕТЕРОТРОФНОЙ ДИНОФЛАГЕЛЛЯТОЙ *OXYRRHIS MARINA*

Т. В. Рауэн, В. С. Муханов, Л. О. Аганесова

ФГБУН ФИЦ «Институт биологии южных морей имени А. О. Ковалевского РАН»,
Севастополь, Российская Федерация
E-mail: *taschi@mail.ru*

Включение частиц микропластика (МП) в микробную пищевую цепь и их дальнейшая передача на более высокие трофические уровни практически не исследованы. В данной работе закономерности поглощения МП одноклеточными организмами анализировали в культуре гетеротрофной динофлагелляты *Oxyrrhis marina* (OXY). В качестве пищевых объектов для *O. marina*

использовали гаптофитовую микроводоросль *Isochrysis galbana* (ISO), полистирольные микросферы (MS) размером 5,6 мкм, а также их смесь (ISO-MS). Динамику численности микроорганизмов и микросфер изучали с помощью проточного цитометра. Показано, что гетеротроф *O. marina* потреблял частицы МП даже в условиях наличия своих обычных жертв — микроводорослей; при этом МП не оказывал на него негативного влияния. Скорости выедания «жертв» в смеси OXY-ISO-MS составили (0,21 ± 0,01) MS·кл$^{-1}$·ч$^{-1}$ (± стандартное отклонение) и (0,38 ± 0,01) ISO·кл$^{-1}$·ч$^{-1}$ и были достоверно ниже, чем в экспериментах с монодиетами OXY-ISO [(1,93 ± 0,68) ISO·кл$^{-1}$·ч$^{-1}$] и OXY-MS [(0,45 ± 0,04) MS·кл$^{-1}$·ч$^{-1}$], то есть усложнение состава (расширение спектра) пищевых объектов вело к снижению скорости их потребления. Скорость осветления среды динофлагеллятой *O. marina* в экспериментах с монодиетами составила (0,12 ± 0,04) и (0,19 ± 0,06) мкл·кл$^{-1}$·ч$^{-1}$ для OXY-ISO и OXY-MS соответственно, а значит, на поимку клеток ISO динофлагеллята *O. marina* затрачивала меньше времени, чем на поимку MS. Эту же закономерность наблюдали и в экспериментах со смесью пищевых объектов (OXY-ISO-MS): скорость осветления среды в сосудах с ISO [(0,17 ± 0,02) мкл·кл$^{-1}$·ч$^{-1}$] была незначительно ниже, чем в сосудах с MS [(0,19 ± 0,003) мкл·кл$^{-1}$·ч$^{-1}$]. Трофической адаптации *O. marina* к MS не происходило, на что указывал факт их вторичного потребления даже в условиях наличия альтернативного кормового объекта — *I. galbana*. Не была выявлена и селективность питания *O. marina* ни к одной из «жертв», будь то *I. galbana* или пластиковые микросферы. Полученные результаты указывают на возможность (и высокую вероятность) включения МП в микробную пищевую цепь и на важную роль одноклеточных организмов в передаче МП на более высокие трофические уровни.

Ключевые слова: микропластик, поглощение, микросферы, микроводоросли, стойкие органические загрязнители, трофический перенос, *Oxyrrhis marina*, *Isochrysis galbana*

1871
ИнБЮМ – IBSS

Морской биологический журнал
Marine Biological Journal
2023, vol. 8, no. 1, pp. 76–92
https://marine-biology.ru

UDC 594.124(265.54.04)

FEATURES OF SPATIAL DISTRIBUTION OF *CRENOMYTILUS GRAYANUS* AND *MODIOLUS KURILENSIS* (BIVALVIA, MYTILIDAE) IN PETER THE GREAT BAY (THE SEA OF JAPAN)

© 2023 **L. G. Sedova and D. A. Sokolenko**

Pacific branch of "VNIRO" ("TINRO"), Vladivostok, Russian Federation
E-mail: *ludmila.sedova@tinro-center.ru*

Received by the Editor 14.10.2021; after reviewing 24.03.2022;
accepted for publication 20.10.2022; published online 14.03.2023.

The bivalves of the family Mytilidae – *Crenomytilus grayanus* (Dunker, 1853) and *Modiolus kurilensis* Bernard, 1983 – are Pacific, Asian species and mass representatives of upper sublittoral epifauna in coastal waters of Peter the Great Bay (the Sea of Japan). *C. grayanus* is a traditional commercial species, and *M. kurilensis* is a promising one; resources of both molluscs are significant. The aim of the work is the comparative analysis of spatial distribution and biomass of *C. grayanus* and *M. kurilensis* on different types of bottom sediments and habitat depths in Peter the Great Bay. The investigation was carried out in 2007–2019 by scuba diving hydrobiological techniques at depths of down to 20 m. The data were analyzed for 5,911 stations; Mytilidae representatives were found at 1,635 stations. For mytilids, vital mass of each individual was determined, and mean biomass was estimated. The landscape diversity of Peter the Great Bay bottom determines an almost ubiquitous distribution of *C. grayanus* and *M. kurilensis*, and this reflects good adaptation of molluscs to conditions typical for this part of their area. Monospecific aggregations of *C. grayanus* prevailed both on hard and soft bottom sediments (78.6 and 38.2% of total stations with Mytilidae, respectively), while mixed aggregations of both species prevailed on soft bottom sediments (38.3%). On soft bottom sediments, monospecific aggregations of *M. kurilensis* were more common (23.5%) than on hard ones (8.1%). In Peter the Great Bay, mean biomass of *C. grayanus* on hard bottom sediments was (728 ± 47) g·m^{-2} varying from 524 g·m^{-2} (the Amur Bay) to 922 g·m^{-2} (eastern Peter the Great Bay). The value for mean biomass of *C. grayanus* on soft bottom sediments was (491 ± 51) g·m^{-2} varying from 228 g·m^{-2} (the Ussuri Bay) to 829 g·m^{-2} (the Amur Bay), except for southwestern Peter the Great Bay and Boisman Bay, where the value was below 50 g·m^{-2}. Mean biomass of *M. kurilensis* on hard bottom sediments was (370 ± 74) g·m^{-2} varying from 18 g·m^{-2} (Baklan Bay) to 656 g·m^{-2} (the Empress Eugénie Archipelago water areas). The value for mean biomass of *M. kurilensis* on soft bottom sediments was (335 ± 37) g·m^{-2} varying from 77 g·m^{-2} (southwestern Peter the Great Bay) to 456 g·m^{-2} (the Amur Bay), except for Boisman and Baklan bays where the species was rare. In Peter the Great Bay, maximum values of the mean biomass for both species were recorded at depths of 1–10 m (*C. grayanus*, 664–805 g·m^{-2}; *M. kurilensis*, 347–485 g·m^{-2}); with increasing habitat depth, the abundance of both species decreased. The mean biomass of *C. grayanus* inhabiting hard bottom sediments at 10–20 m was quite high as well – 431–507 g·m^{-2}. On soft bottom sediments, with a shift in depth from 10–15 to 15–20 m, its mean biomass decreased from (204 ± 33) to (27 ± 11) g·m^{-2}. The mean biomass of *M. kurilensis* inhabiting both types of bottom sediments at 10–15 m was 121–194 g·m^{-2}, and at 15–20 m, the value was 11–60 g·m^{-2}.

Keywords: mytilids, Mytilidae, Gray mussel, *Crenomytilus grayanus*, horsemussel, *Modiolus kurilensis*, biomass, distribution, bottom sediments, habitat depth, Peter the Great Bay, Sea of Japan

The bivalves of the family Mytilidae – the Gray mussel *Crenomytilus grayanus* (Dunker, 1853) and horsemussel *Modiolus kurilensis* Bernard, 1983 – are Pacific, Asiatic species and mass representatives of upper sublittoral epifauna in coastal waters of the Peter the Great Bay (hereinafter the PGB), the Sea of Japan. *C. grayanus* is a low-boreal species capable of entering subtropical waters, while *M. kurilensis* is a subtropical boreal species [Golikov, Skarlato, 1967; Skarlato, 1981]. Low-boreal species tend to inhabit bays and open shelf areas; warm-water (subtropical) species prefer the warmest areas of bays. *C. grayanus* and *M. kurilensis* coexistence in the PGB is due to the location of the bay at the junction of two climatic zones: there, waters of the cold Primorsky Current, which mostly affects this area, meet waters of the East Korea Warm Current [Zuenko, 2008]. During winter, the PGB waters have the characteristics of Arctic ones; during summer, of subtropical ones [Manuilov, 1990].

Off the coast of Primorsky Krai, the Gray mussel is a traditional commercial species [Razin, 1934; Sedova, 2020], while the horsemussel is a promising one. The resources of these species in the PGB are significant: *C. grayanus*, 54.8 thousand tons; *M. kurilensis*, 27.1 thousand tons [Sedova, Sokolenko, 2019, 2021a]. At present, these species are often not separated when harvesting the Gray mussel: visually, their shells and sizes are similar, as well as their taste qualities. However, there are several differences (Fig. 1).

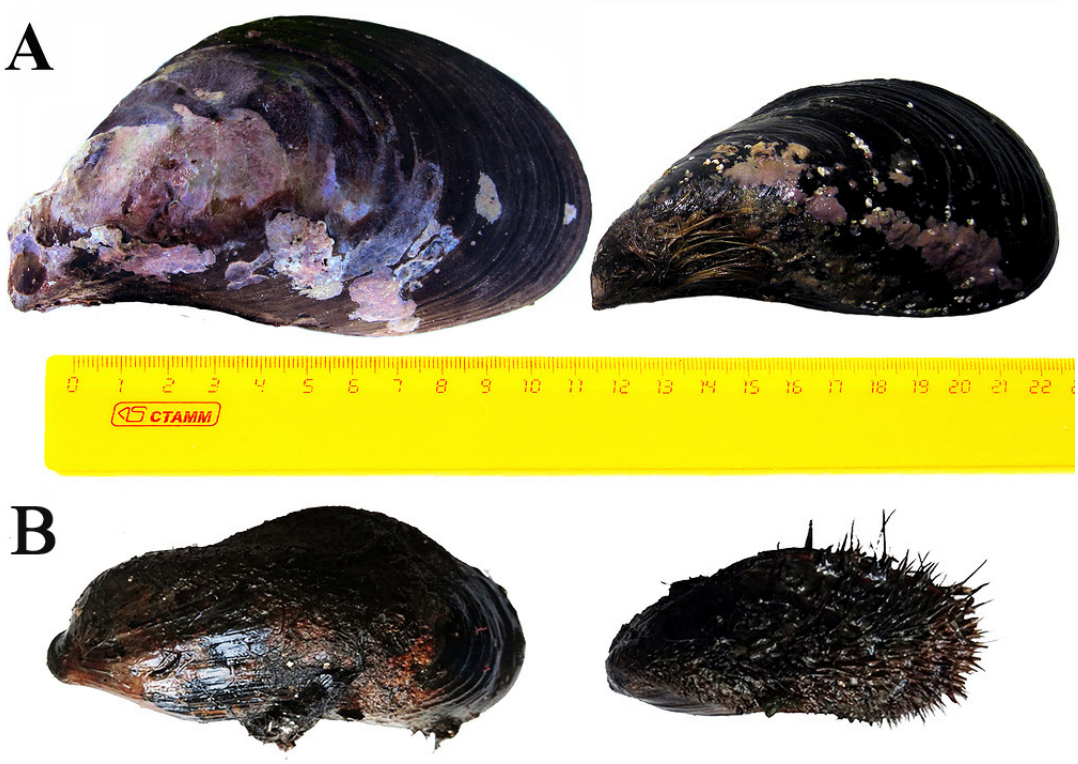

Fig. 1. *Crenomytilus grayanus* (A) and *Modiolus kurilensis* (B)

In *C. grayanus*, the upper edge of the shell is arcuate, and the lower is usually concave. The vertex is pulled down; the shell surface is smooth. In *M. kurilensis*, the front of the shell protrudes in front of the vertexes. The valves are covered with black and brown periostracum, with its brush-shaped setae being long and thick, which is more pronounced in younger molluscs [Volova, Skarlato, 1980]. With the same length, *C. grayanus* has a more massive shell.

Mytilidae are rarely found as single individuals; they usually form druses (Fig. 2) consisting of molluscs fastened with byssus filaments (the abundance of mussels can reach tens or even hundreds). Sometimes, druses form “brushes” of significant length or “banks.”

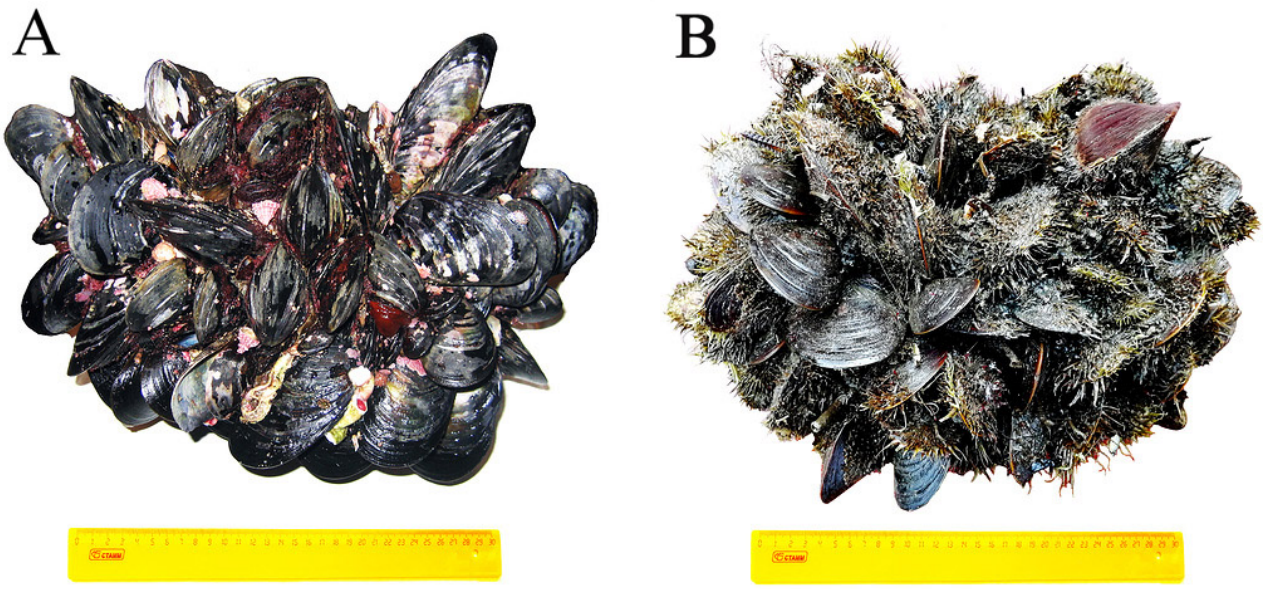

Fig. 2. Aggregations (druses) of *Crenomytilus grayanus* (A) and *Modiolus kurilensis* (B)

C. grayanus and *M. kurilensis* distribution in the PGB depends on both the variety of bottom sediments in the coastal area and hydrological conditions [Manuilov, 1990; Preobrazhensky et al., 2000; Razin, 1934; Skarlato, 1981]. An essential factor determining the composition of bottom sediments is the isolation of water areas which results from the indentation of the PGB coastline with secondary bays and adjacent islands. Due to different abilities of *C. grayanus* and *M. kurilensis* to inhabit hard and soft substrates, these species usually occur in different biotopes; however, they can form monospecific and mixed settlements on various types of bottom sediments [Kutishchev, Gogolev, 1983; Sedova, Sokolenko, 2018a, b, c, 2020a, b, 2021b; Selin, 2018a; Selin, Vekhova, 2002]. In the published works, Mytilidae settlement are considered only in certain PGB areas. To date, there is no complete picture of *C. grayanus* and *M. kurilensis* distribution throughout the PGB depending on the type of bottom sediments and the habitat depths. Interestingly, this is of great practical importance for organizing rational harvesting and planning measures to preserve Mytilidae resources.

The aim of this work is to conduct a comparative analysis of *C. grayanus* and *M. kurilensis* spatial distribution and abundance on different types of bottom sediments and habitat depth in the Peter the Great Bay.

MATERIAL AND METHODS

The work is based on the results of regular research carried out on the RV “Ubezhdenny” of the TINRO Base of Research Fleet in August–October 2007–2019 in different PGB sections by scuba diving. Mytilidae settlements that have an attached lifestyle maintain for a long time their spatial structure and abundance in the absence of unfavorable abiotic conditions, anthropogenic load, and intensive harvesting [Sedova, Sokolenko, 2019].

The bay was conditionally divided into following sections: 1, the southwestern PGB (from the Tumen River mouth to Cape Suslov); 2, Posyet Bay (from Cape Suslov to Cape Gamov); 3, Boisman Bay; 4, Baklan Bay; 5, the Amur Bay (the southern border is a line connecting the Cape Bruce and the Zheltukhin Island); 6, the Empress Eugénie Archipelago water areas (Russky, Shkot, Popov, Reyneke, and Rikord islands, as well as adjacent smaller islands); 7, the Ussuri Bay (the southern border is a line connecting southern tips of the Zheltukhin and Askold islands); 8, the eastern PGB (from the Cape Sysoev to the Cape Povorotny, including water areas of Putyatin and Askold islands) [Lotsiya severo-zapadnogo berega Yaponskogo morya, 1984] (Fig. 3).

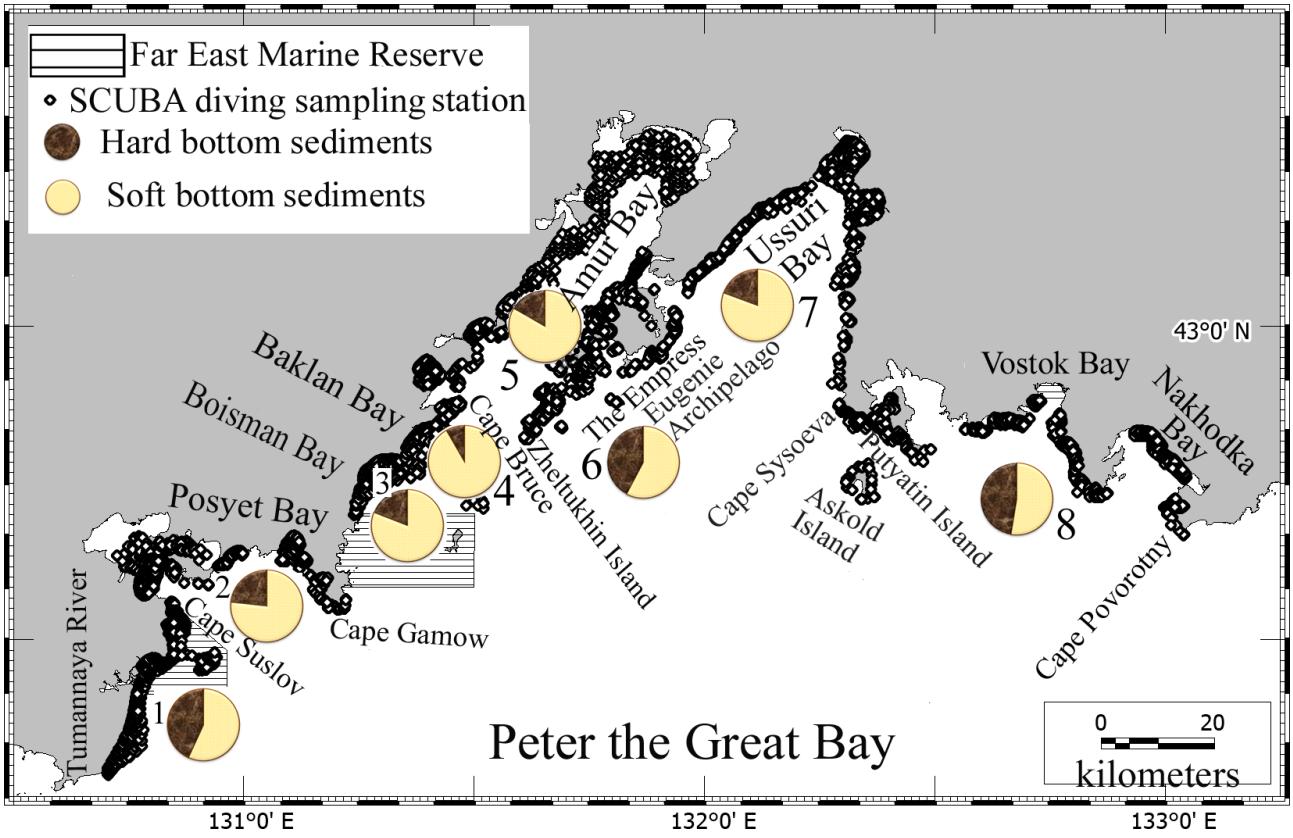

Fig. 3. Map of the research and sampling area; ratio of hard and soft bottom sediments in Peter the Great Bay (the Sea of Japan)

Standard scuba diving hydrobiological techniques were applied to obtain data on spatial distribution and abundance of molluscs. Depending on the orography and nature of bottom landscapes, the distance between the stations on the cuts perpendicular to the coastline was of 100–500 m [Sedova, Sokolenko, 2019]. In the vast areas of the relative flat bottom of bays, a regular grid of stations was used. Considering this and taking into account the areas of the studied spots at depths of 1–20 m, a different number of stations was carried out (Table 1). In total, the data from 5,911 stations located along the entire coast of the PGB were analyzed, except for areas prohibited for navigation (Fig. 3).

In areas with dense mollusc settlements, the diver used for sampling a measuring frame from one m^2 (in three replicates). In sparse settlements, the transect method was applied: the calculation and periodic sampling of animals were carried out in the field of view on a certain bottom area. The type of bottom sediments was determined visually. Sandy, silty-sand, and silty substrates were attributed

to soft bottom sediments. Rocks, blocks, boulders, stones, and pebbles were attributed to hard bottom sediments. In total, 1,708 stations were carried out on hard bottom sediments, and 4,203 were carried out on soft ones (Table 1).

All sampled hydrobionts were analyzed onboard the RV. Druses were disassembled, the species composition of molluscs was determined, and lifetime mass of each mytilid was established. The mean Mytilidae biomass was determined considering the stations where the mussels were found (Table 1). Then, live molluscs were released back to the spots of sampling. *C. grayanus* and *M. kurilensis* were recorded at 1,635 stations (Table 1).

To prepare cartographic material, GIS MapInfo Pro software (https://mapinfo.ru/product/mapinfo-professional) was used. The obtained data were statistically processed in Microsoft Excel and Statistica (http://statsoft.ru/). The mean values of indicators, standard deviation, and standard error of the mean (*SEM*) with a significance level of 0.05 were determined. The ratio of Mytilidae biomass was evaluated by the two-sample independent *t*-test. To compare biomass of *C. grayanus* and *M. kurilensis* living under different conditions, Mann–Whitney *U* test was used – a non-parametric analogue of the *t*-test [Borovikov, 2003]. The null hypothesis was rejected at a significance level of 0.05 ($p \leq 0.05$).

RESULTS

***C. grayanus* and *M. kurilensis* spatial distribution depending on the type of bottom sediments.** The PGB stretches from the Tumen River mouth in the west to the Cape Povorotny in the east in the northwestern Sea of Japan [Lotsiya severo-zapadnogo berega Yaponskogo morya, 1984] (Fig. 3). Bottom sediments in the bay are very diverse. Rocks, blocks, and boulders are common off the steep shores and capes at depths of down to 10–14 m. With an increase in depth, those are replaced by pebbles or sandy, silty-sand, or silty substrates. In the tops of the bays, soft bottom sediments prevail – sand, silty-sand, and silt. The bottom sediment composition for each PGB section is described in detail in our previous publications [Sedova, Sokolenko, 2018a, b, c, 2020a, b, 2021b]. Throughout the PGB at depths of down to 20 m, the prevalence of soft bottom sediments was noted: on them, 71.1% of stations were carried out (on hard bottom sediments, 28.9%, respectively) (Table 1). For individual PGB sections, this ratio varied. Hard bottom sediments were most represented (42.3–47.4%) in the southwestern and eastern PGB and in the Empress Eugénie Archipelago water areas (Table 1, Fig. 3).

In other PGB sections, the number of stations carried out on hard bottom sediments varied from 8.3% (Baklan Bay) to 23.3% (Posyet Bay). Mytilidae were found at 27.7% of all the surveyed stations (Table 1). There were both monospecific and mixed druses of molluscs.

In different PGB sections on hard bottom sediments (rocks, boulders, stones, and pebbles), monospecific druses of the Gray mussel accounted for 47.4–90.7%; for monospecific druses of the horsemussel, the value ranged within 2.7–13.7% (except for Baklan Bay); mixed druses accounted for 1.7–18.6%; and in Baklan Bay, the value was 52.6% (Table 2). The occurrence of monospecific druses of the Gray mussel on soft bottom sediments was 25.0–73.1%; monospecific druses of the horsemussel, 9.7–50.0%; and mixed druses, 7.7–48.7%. On both types of bottom sediments, monospecific druses of the Gray mussel prevailed in the southwestern PGB and the Amur and Ussuri bays; monospecific druses of the horsemussel prevailed on soft substrates in Boisman Bay and the eastern PGB (Table 2). Mixed druses prevailed on soft bottom sediments in Posyet Bay and the Empress Eugénie Archipelago water areas, as well as on hard substrates in Baklan Bay.

Table 1. Number of stations surveyed and Mytilidae biomass in Peter the Great Bay (2007–2019)

Section	Area, km^2	Number of stations, in parentheses, percentage of stations surveyed				Mean Mytilidae biomass ± *SEM*, in parentheses, standard deviation, below the line, range of values, g·m^{-2}	
		surveyed	hard bottom sediments	soft bottom sediments	on which Mytilidae were found	*C. grayanus*	*M. kurilensis*
Peter the Great Bay	1,005.8	5,911	1,708 (28.9%)	4,203 (71.1%)	1,635 (27.7%)	645 ± 36 (1,333) 0.1–14,120	347 ± 35 (869) 0.1–8,512
1. Southwestern PGB	70.2	475	205 (43.2%)	270 (56.8%)	133 (28.0%)	628 ± 141 (1,519) 3.5–14,120	84 ± 20 (71) 1.2–242
2. Posyet Bay	129.2	1,164	271 (23.3%)	893 (76.7%)	352 (30.2%)	563 ± 59 (1,017) 0.3–6,000	252 ± 57 (729) 0.5–6,000
3. Boisman Bay	41.1	440	84 (19.1%)	356 (80.9%)	67 (15.2%)	593 ± 129 (954) 0.6–4,555	46 ± 39 (153) 0.4–600
4. Baklan Bay	40.9	240	20 (8.3%)	220 (91.7%)	27 (11.2%)	660 ± 156 (767) 1–2,600	14 ± 11 (41) 0.5–150
5. Amur Bay	348.7	934	156 (16.7%)	778 (83.3%)	194 (20.8%)	671 ± 122 (1,508) 0.1–9,610	350 ± 118 (1,062) 0.1–8,000
6. Empress Eugénie Archipelago water areas	109.9	1,043	441 (42.3%)	602 (57.7%)	504 (48.3%)	597 ± 61 (1,272) 0.2–11,180	493 ± 67 (1,023) 0.3–8,512
7. Ussuri Bay	168.1	837	162 (19.4%)	675 (80.6%)	156 (18.6%)	739 ± 111 (1,356) 0.1–9,500	344 ± 100 (560) 0.2–2,360
8. Eastern PGB	97.7	778	369 (47.4%)	409 (52.6%)	202 (26.0%)	832 ± 135 (1,754) 0.1–11,448	228 ± 71 (533) 0.1–3,018

In total for the PGB (Fig. 4), the prevalence of monospecific druses of the Gray mussel was revealed at 783 stations (79% of the total stations with Mytilidae) on hard bottom sediments which this species prefers; the prevalence of mixed druses was recorded on soft substrates. These differences are statistically significant ($p = 0.001$ and $p = 0.002$, respectively). There were no noticeable differences in *M. kurilensis* distribution on hard and soft bottom sediments ($p = 0.341$).

Table 2. Ratio of stations with monospecific and mixed aggregations of Mytilidae and biomass values for *Crenomytilus grayanus* and *Modiolus kurilensis* on hard and soft bottom sediments in Peter the Great Bay

Section	Number of stations, in parentheses, percentage of stations with Mytilidae			Mean Mytilidae biomass ± *SEM*, in parentheses, standard deviation, below the line, range of values, $g \cdot m^{-2}$	
	C. grayanus	*M. kurilensis*	*C. grayanus* + *M. kurilensis*	*C. grayanus*	*M. kurilensis*
Hard bottom sediments					
1. Southwestern PGB	97 (90.7%)	7 (6.5%)	3 (2.8%)	743 ± 166 (1,637) 4–14,120	88 ± 21 (56) 1–121
2. Posyet Bay	133 (76.0%)	18 (10.3%)	24 (13.7%)	731 ± 87 (1,085) 0.1–6,000	393 ± 185 (1,197) 1–6,000
3. Boisman Bay	50 (84.7%)	8 (13.6%)	1 (1.7%)	639 ± 137 (976) 1–4,555	77 ± 65 (196) 0.1–600
4. Baklan Bay	9 (47.4%)	0	10 (52.6%)	743 ± 196 (832) 1–2,600	18 ± 15 (46) 1–150
5. Amur Bay	70 (73.7%)	13 (13.7%)	12 (12.6%)	524 ± 147 (1,309) 0.1–9,610	115 ± 30 (148) 0.1–580
6. Empress Eugénie Archipelago water areas	202 (73.7%)	21 (7.7%)	51 (18.6%)	614 ± 84 (1,336) 0.1–11,180	656 ± 177 (1,498) 0.1–8,512
7. Ussuri Bay	97 (84.3%)	3 (2.7%)	15 (13.0%)	907 ± 140 (1,477) 1–9,500	362 ± 119 (506) 0.1–1,940
8. Eastern PGB	125 (85.2%)	11 (7.2%)	16 (10.6%)	922 ± 158 (1,874) 0.1–11,448	113 ± 77 (402) 0.1–2,068
Soft bottom sediments					
1. Southwestern PGB	19 (73.1%)	5 (19.2%)	2 (7.7%)	41 ± 20 (86) 4–353	77 ± 43 (95) 12–242
2. Posyet Bay	57 (32.2%)	38 (21.5%)	82 (46.3%)	374 ± 76 (901) 0.1–5,040	203 ± 42 (464) 1–3,110
3. Boisman Bay	2 (25.0%)	4 (50.0%)	2 (25.0%)	3.3 ± 1.1 (2.1) 1–5	1.3 ± 0.2 (0.4) 1–2
4. Baklan Bay	5 (62.5%)	2 (25.0%)	1 (12.5%)	411 ± 204 (500) 2–1,199	1.8 ± 0.6 (1.1) 1–3
5. Amur Bay	43 (43.4%)	26 (26.3%)	30 (30.3%)	829 ± 198 (1,692) 0.1–8,000	456 ± 169 (1,263) 1–8,000
6. Empress Eugénie Archipelago water areas	69 (30.0%)	49 (21.3%)	112 (48.7%)	575 ± 88 (1,180) 0.1–7,252	420 ± 56 (710) 0.1–3,762
7. Ussuri Bay	28 (68.3%)	4 (9.7%)	9 (22.0%)	228 ± 114 (692) 0.1–3,870	320 ± 180 (649) 1–2,360
8. Eastern PGB	21 (42.0%)	22 (44.0%)	7 (14.0%)	379 ± 155 (823) 2–3,843	334 ± 115 (620) 1–3,018

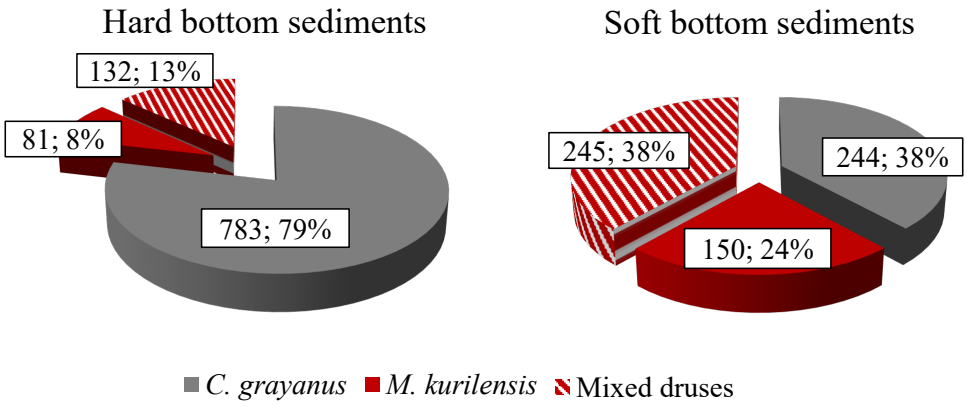

Fig. 4. Ratio of monospecific and mixed aggregations of *Crenomytilus grayanus* and *Modiolus kurilensis* on hard and soft bottom sediments in Peter the Great Bay (number of stations; percentage of total stations with Mytilidae)

The values of *C. grayanus* and *M. kurilensis* biomass in individual PGB sections, as well as ratios of hard and soft bottom sediments there, differed (Fig. 3, Tables 1, 2). On hard bottom sediments, the mean value of *C. grayanus* biomass varied from 524 g·m^{-2} in the Amur Bay to 922 g·m^{-2} in the eastern PGB (Table 2). On soft substrates, the highest value of the mean biomass of *C. grayanus* was recorded in the Amur Bay (829 g·m^{-2}), while the lowest ones (< 50 g·m^{-2}) were registered in Boisman Bay and the southwestern PGB. On hard bottom sediments, the mean biomass of *M. kurilensis* varied from 18 g·m^{-2} (Baklan Bay) to 656 g·m^{-2} (the Empress Eugénie Archipelago water areas); on soft bottom sediments, the value varied from 77 g·m^{-2} (the southwestern PGB) to 456 g·m^{-2} (the Amur Bay), except for open Boisman and Baklan bays, where the species was rare (Table 2). In the Amur, Posyet, and Ussuri bays, the Empress Eugénie Archipelago water areas, and the eastern PGB, the mean biomass of each of two species was > 100 g·m^{-2} both on hard and soft bottom sediments.

In the PGB, the mean values of the biomass of *C. grayanus* and *M. kurilensis* were statistically significantly different ($p = 0.0004$), amounting to 645 and 347 g·m^{-2}, respectively (Table 1). Comparison of species biomass values separately on hard and soft bottom sediments showed noticeable differences as well ($p = 0.001$ and $p = 0.019$, respectively). The values of the mean biomass of *C. grayanus* inhabiting hard and soft substrates differed significantly ($p = 0.001$), amounting to 728 and 491 g·m^{-2}, respectively. Interestingly, there were no noticeable differences in the values for *M. kurilensis* – 370 and 335 g·m^{-2} ($p = 0.643$) (Table 3).

Table 3. Mean Mytilidae biomass on hard and soft bottom sediments in Peter the Great Bay, g·m^{-2}

Bottom sediments	*C. grayanus*			*M. kurilensis*		
	Mean biomass ± *SEM*	Standard deviation	Range of values	Mean biomass ± *SEM*	Standard deviation	Range of values
Hard	728 ± 47	1,422	0.1–14,120	370 ± 74	1,070	0.1–8,512
Soft	491 ± 51	1,134	0.1–8,000	335 ± 37	741	0.1–8,000

Vertical distribution. On hard bottom sediments in the southwestern PGB, Posyet Bay, and Boisman Bay, higher values of the mean biomass for *C. grayanus* were recorded at depths of 1–14.9 m; in Baklan Bay, at 1–20 m; in the Empress Eugénie Archipelago water areas and the eastern PGB, at 1–9.9

and 15–20 m; and in the Ussuri Bay, at 1–9.9 m (Table 4). On soft bottom sediments, *C. grayanus* was not registered at all in the southwestern PGB and Boisman and Baklan bays at depths of down to 5 m. In Ussuri Bay and the eastern PGB, the biomass of the Gray mussel was low. Higher values were noted at depths of 1–9.9 m in the Amur and Posyet bays and in the Empress Eugénie Archipelago water areas, as well as at depths of 5–9.9 m in Baklan Bay and the eastern PGB (Table 4). On hard bottom sediments, *M. kurilensis* settlements with the biomass of > 300 g·m^{-2} were found at depths of down to 10 m in Posyet Bay and the Empress Eugénie Archipelago water areas, as well as at depths of 10–14.9 m in Boisman Bay. On soft bottom sediments, those were registered at depths of 5–9.9 m in the Amur Bay and the eastern PGB, as well as at 1–10 m in the Empress Eugénie Archipelago water areas (Table 5).

Table 4. Distribution of mean biomass of *Crenomytilus grayanus* on hard and soft bottom sediments depending on the habitat depth in Peter the Great Bay, g·m^{-2}

Depth / Section	1–4.9 m	5–9.9 m	10–14.9 m	15–20 m
	Mean biomass ± *SEM*; in parentheses, standard deviation; below the line, range of values			
Hard bottom sediments				
1.Southwestern PGB	767 ± 161 (992) 4–3,530	791 ± 394 (2,367) 4–14,120	800 ± 302 (1,209) 4–3,883	239 ± 155 (409) 4–1,059
2. Posyet Bay	610 ± 104 (849) 0.3–3,900	856 ± 168 (1,232) 0.3–6,000	930 ± 278 (1,390) 1–5,100	395 ± 220 (731) 1–2,500
3. Boisman Bay	480 ± 191 (787) 1–2,615	862 ± 259 (1,217) 1–4,555	545 ± 216 (683) 1–2,070	3 ± 2 (3) 1–5
4. Baklan Bay	592 ± 405 (993) 1–2,592	613 ± 124 (351) 190–1,098	977 ± 813 (1,408) 80–2,600	1,000
5. Amur Bay	639 ± 234 (1,533) 0.2–9,610	418 ± 177 (1,019) 0.7–5,760	58 ± 46 (80) 3.4–150	0
6. Empress Eugénie Archipelago water areas	858 ± 158 (1,661) 1–11,180	483 ± 119 (1,109) 1–7,854	278 ± 103 (654) 0.4–2,882	479 ± 241 (965) 2–2,892
7. Ussuri Bay	506 ± 210 (1,092) 0.6–5,325	994 ± 326 (1,459) 1–5,000	325 ± 169 (478) 1–1,320	282 ± 278 (393) 3–560
8. Eastern PGB	964 ± 225 (1,770) 0.1–9,562	1,162 ± 310 (2,280) 1–11,448	200 ± 138 (572) 0.1–2,336	502 ± 333 (941) 1.2–2,450
Soft bottom sediments				
1. Southwestern PGB	0	107 ± 82 (165) 4–353	4	34 ± 17 (55) 4–177
2. Posyet Bay	555 ± 208 (1,247) 0.3–5,040	392 ± 119 (916) 0.3–5,000	248 ± 71 (421) 0.7–1,582	29 ± 20 (61) 0.6–189
3. Boisman Bay	0	0.6	2.5	5
4. Baklan Bay	0	493 ± 296 (591) 2–1,199	247 ± 245 (347) 2–492	0
5. Amur Bay	693 ± 305 (1,139) 0.9–4,000	1,045 ± 302 (2,026) 0.9–8,000	290 ± 115 (414) 0.1–1,200	80
6. Empress Eugénie Archipelago water areas	1,012 ± 280 (1,731) 1–7,252	736 ± 147 (1,246) 0.2–7,200	218 ± 57 (408) 0.2–2,060	32 ± 25 (104) 0.5–436
7. Ussuri Bay	77 ± 63 (166) 0.2–450	221 ± 146 (506) 0.1–1,800	8 ± 3 (8) 1.5–22	0.8 ± 0.3 (0.4) 0.5–1.1
8. Eastern PGB	13 ± 10 (14) 3–22	1,030 ± 475 (1,344) 2–3,842	194 ± 74 (257) 3–744	3 ± 0.4 (0.9) 1.6–3.7

Analyzing the entire PGB, it has to be noted that *C. grayanus* forms settlements with the highest biomass at depths of 1–20 m on hard substrates (mean value is 431–805 g·m^{-2}) and at depths of down to 10 m on soft ones (Fig. 5). At the same time, mean biomass values at depths of 1–4.9 and 5–9.9 m did not differ significantly for *C. grayanus* inhabiting both types of bottom sediments (p = 0.495 and p = 0.425, respectively). There were no noticeable differences in these indicators (Fig. 5) in molluscs inhabiting hard substrates at depths of 10–14.9 and 15–20 m as well (p = 0.920). Interestingly, mean biomass values for *C. grayanus* inhabiting soft bottom sediments at same depths were significantly different (p = 0.0002).

Table 5. Distribution of mean biomass of *Modiolus kurilensis* on hard and soft bottom sediments depending on the habitat depth in Peter the Great Bay, g·m^{-2}

Depth / Section	1–4.9 m	5–9.9 m	10–14.9 m	15–20 m
	Mean biomass ± *SEM*; in parentheses, standard deviation; below the line, range of values			
Hard bottom sediments				
1. Southwestern PGB	81 ± 40 (69) 1–121	121	121	12
2. Posyet Bay	341 ± 216 (1,146) 1–6,000	860 ± 507 (1,717) 1–5,048	22 ± 14 (24) 6–50	2.4 ± 0.4 (0.8) 2–3.3
3. Boisman Bay	14 ± 1 (2) 12–15	15 ± 1 (1) 14–17	301 ± 299 (423) 2–600	0.4
4. Baklan Bay	5 ± 4 (8) 1–15	24 ± 21 (56) 1–150	0	0
5. Amur Bay	132 ± 54 (179) 0.1–580	128 ± 38 (127) 0.2–350	1.3 ± 0.4 (0.6) 0.8–2	0
6. Empress Eugénie Archipelago water areas	1,002 ± 369 (2,055) 0.4–8,512	490 ± 174 (936) 1–4,204	155 ± 59 (166) 1–417	182 ± 180 (360) 0.5–722
7. Ussuri Bay	40	29 ± 14 (24) 2–50	190 ± 187 (266) 2–378	0
8. Eastern PGB	205 ± 186 (618) 0.7–2,068	57 ± 53 (151) 0.1–432	85 ± 82 (143) 2–250	18 ± 17 (39) 0.7–88
Soft bottom sediments				
1. Southwestern PGB	242	61	0	28 ± 16 (28) 12–61
2. Posyet Bay	267 ± 83 (557) 0.5–3,110	205 ± 68 (467) 0.6–2,496	116 ± 50 (229) 0.5–900	7 ± 2 (6) 1–16
3. Boisman Bay	0	0.7	1.4	1.5
4. Baklan Bay	0	1.1	1.2	3.0
5. Amur Bay	271 ± 127 (458) 0.5–1,640	615 ± 280 (1,609) 0.9–8,000	235 ± 71 (188) 2–500	18 ± 15 (27) 2–50
6. Empress Eugénie Archipelago water areas	668 ± 185 (1,095) 1.6–3,762	464 ± 68 (584) 0.3–2,738	254 ± 82 (506) 0.3–1,933	13 ± 10 (36) 0.6–126
7. Ussuri Bay	0	157 ± 87 (150) 1–300	8	1.4 ± 0.3 (0.5) 1.1–1.8
8. Eastern PGB	219 ± 68 (205) 1–532	609 ± 276 (917) 1–3,018	168 ± 136 (332) 1–834	1.2 ± 0.03 (0.05) 1.2–1.3

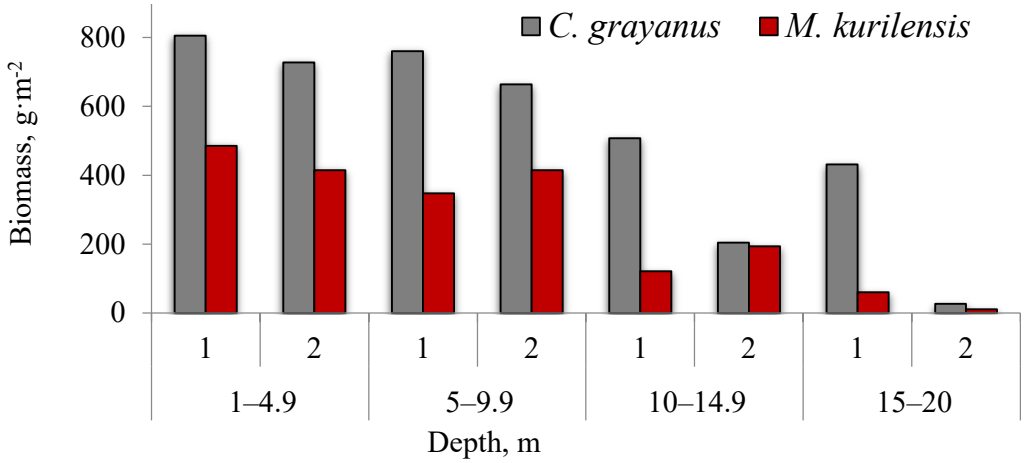

Species	Mean biomass ± *SEM*; in parentheses, standard deviation; below the line, range of values, g·m^{-2}			
1, hard bottom sediments				
C. grayanus	805 ± 72 (1,460) 0.1–11,180	760 ± 88 (1,579) 0.1–14,120	507 ± 85 (952) 0.1–5,100	431 ± 118 (806) 1–2,892
M. kurilensis	485 ± 136 (1,357) 0.1–8,512	347 ± 98 (842) 0.1–5,048	121 ± 37 (175) 1–600	60 ± 51 (192) 0.1–722
2, soft bottom sediments				
C. grayanus	727 ± 141 (1,418) 0.1–7,252	664 ± 94 (1,348) 0.1–8,000	204 ± 33 (374) 0.1–2,060	27 ± 11 (72) 1–436
M. kurilensis	415 ± 76 (787) 1–3,762	415 ± 66 (874) 0.1–8,000	194 ± 44 (392) 0.1–1,933	11 ± 4 (25) 1–126

Fig. 5. Distribution of mean biomass of *Crenomytilus grayanus* and *Modiolus kurilensis* depending on the habitat depth in Peter the Great Bay

M. kurilensis prevailed at depths of 1–10 m on both types of bottom sediments (Fig. 5). There were no significant differences in mean biomass values for *M. kurilensis* inhabiting both hard and soft substrates at depths of 1–4.9 and 5–9.9 m ($p = 0.508$ and $p = 0.985$, respectively), while at 10–14.9 and 15–20 m, mean biomass values for this species were noticeably different ($p = 0.019$ and $p = 0.001$, respectively).

DISCUSSION

The results of the study and analysis of literary sources confirmed the existence of both monospecific and mixed settlements of *C. grayanus* and *M. kurilensis*. According to the data obtained, in the PGB, monospecific druses of *C. grayanus* prevailed both on hard and soft bottom sediments, while mixed druses prevailed on soft substrates (Fig. 4). Similar studies on spatial distribution of Mytilidae on different types of bottom sediments throughout the PGB have not been carried out earlier.

The stable position of mytilids on bottom sediments is ensured by their byssus filaments which reduce unfavorable hydrodynamic load of the environment [Vekhova, 2007]. *C. grayanus* is known to attach more successfully to hard bottom sediments, while *M. kurilensis*, to soft ones [Rees et al., 2008; Selin, 2018b; Selin, Vekhova, 2002, 2004; Vekhova, 2013, 2019]. It is related to the morphology and size of byssus filaments. The Gray mussel – with its streamlined mytiloid-shaped shell and strong attachment

to substrates with the help of a powerful byssus apparatus – prefers to settle on hard rocky and boulder sediments in coastal areas with moderate wave action [Skarlato, 1981]. On soft bottom sediments, the Gray mussel can form settlements only when it finds a hard base: rare boulders, stone-strewn area, or mollusc shells [Selin, Vekhova, 2004]. The horsemussel – with its wide and light shell with periostracum setae and numerous long and thin byssus filaments (those are capable of penetrating deep into bottom sediment, thereby facilitating the mollusc staying on its surface) – usually inhabits deeper areas of bay bottom sheltered from waves [Selin, 2018a; Vekhova, 2007]. When a single horsemussel tries to attach to hard substrates, the thickness of its byssus filaments does not allow either to stay on their surface or to form druses.

The formation of mixed druses is due to the fact that *C. grayanus* and *M. kurilensis* larvae can settle on druses of both species; this allows molluscs to inhabit unusual biotopes [Kutishchev, Gogolev, 1983; Lindenbaum et al., 2008; Selin, 1977, 2018a; Tsuchiya, 2002]. According to the literature data, in mixed druses formed on hard substrates, the structure of *C. grayanus* druses is usually preserved; on soft bottom sediments, the structure of *M. kurilensis* druses is preserved. More stable aggregations are formed mainly on hard substrates (rocks, blocks, boulders, and stones) and consist of medium and large druses with a dense spatial structure, which increases the efficiency of Mytilidae larvae settling [Kutishchev, Gogolev, 1983; Vigman, 1983]. In mixed druses on hard substrates, the horsemussel can live due to the compensation of its attachment by a more powerful byssus apparatus of the Gray mussel.

C. grayanus and *M. kurilensis* larvae settle on bottom settlements of adult mussels. After the metamorphosis is complete, those attach with their byssus filaments to a shell surface, to byssus filaments of larger Mytilidae, or among the periostracum setae of the horsemussel [Selin, 2018a]. However, on soft bottom sediments, the conditions for juvenile settling are hampered by the fact that adults are contaminated with silty sand (therefore, the larvae settle less than on hard substrates). Settling of *C. grayanus* larvae on *M. kurilensis* druses occurs annually; when the horsemussel specimens are displaced from mixed druses, the Gray mussel can form monospecific druses on soft bottom sediments [Selin, 1991]. Under favorable conditions of hydrodynamic load, *C. grayanus* can form extensive settlements on soft substrates as well [Selin, 2018a; Selin, Vekhova, 2003; Skarlato et al., 1967]. The successful coexistence of Mytilidae on different types of bottom sediments was shown by N. Selin [2018a] for a local area of Vostok Bay (the PGB).

The ratio of *C. grayanus* biomass (of the total biomass of two species) in different PGB sections ranged within 54.8–97.9%, averaging 76.9% throughout the bay. On hard substrates, the value was higher (79.0%); on soft ones, it was lower (61.0%). The lower mean values of *M. kurilensis* biomass, compared to that of *C. grayanus* (Table 3), can be explained by its subtropical origin as well, since the water area of most of the PGB is suitable for the habitat of low-boreal species, while subtropical boreal species inhabit mainly shallow coastal areas, which are well warmed up during summer, and sheltered bays [Golikov, Skarlato, 1967; Skarlato, 1981].

At depths of 1–10 m, the biomass of the studied species in the PGB, both on hard and soft substrates, mostly reached its highest values; at depths of 10–20 m, only *C. grayanus* biomass on hard bottom sediments reached its maximum (Fig. 5). This is consistent with the literature data. As known, with increasing depth, there is a decrease in the occurrence and biomass of almost all benthic species, except for boreal-Arctic ones [Golikov, Skarlato, 1967]. As a rule, subtropical species inhabit the depths of down to 5 m; deeper (down to 20 m), low-boreal species prevail [Skarlato et al., 1967].

In the southwestern PGB, as well as in Posyet, Boisman, and Baklan bays, the highest biomass of the Gray mussel on hard bottom sediments was recorded at depths of down to 15 m; in other sections, down to 10 m; on soft substrates in the Amur and Posyet bays, down to 10 m; and in Baklan Bay and the eastern PGB, at depths of 5–10 m (Table 4). The highest biomass of the horsemussel was registered at depths of down to 10 m in Posyet Bay on hard bottom sediments; in the Empress Eugénie Archipelago water areas on both types of bottom sediments; and at depths of 5–10 m in the Amur Bay and the eastern PGB on soft substrates (Table 5).

Conclusion. The landscape diversity of the bottom of the Peter the Great Bay (the Sea of Japan) is the reason for the almost ubiquitous distribution of *C. grayanus* and *M. kurilensis*, and this reflects good adaptation of molluscs to the conditions typical for this part of their area. *C. grayanus* and *M. kurilensis* abundance in different sections of the bay varies widely. However, the mean biomass of the Gray mussel on hard bottom sediments exceeds its value for soft substrates by 1.5 times, and the biomass of the horsemussel, both on hard and soft bottom sediments, by 2 times. There was no difference in mean biomass values of *M. kurilensis* on hard and soft substrates. Both on hard and soft bottom sediments, monospecific druses of the Gray mussel prevail; on soft substrates, mixed druses prevail.

When planning Mytilidae harvesting in the Peter the Great Bay, it should be taken into account as follows: both species form settlements with a maximum biomass at depths of down to 10 m (*C. grayanus*, on hard bottom sediments; *M. kurilensis*, on soft substrates). This makes it possible to collect molluscs by diving.

Acknowledgement. The authors are sincerely grateful to the anonymous reviewers for their constructive comments and recommendations, which were taken into account when preparing this article for publication.

REFERENCES

1. Borovikov V. P. *STATISTICA. Iskusstvo analiza dannykh na komp'yutere.* 2nd ed. Moscow [et al.] : Piter, 2003, 668 p. (in Russ.)
2. Vekhova E. E. Comparative morphology of byssal threads in three Mytilidae (Bivalvia) species from the Sea of Japan. *Zoologicheskii zhurnal*, 2007, vol. 86, no. 2, pp. 154–162. (in Russ.)
3. Vekhova E. E. The peculiarities of growth and shell morphology of three Mytilidae (Bivalvia) species from the Sea of Japan. *Zoologicheskii zhurnal*, 2013, vol. 92, no. 4, pp. 399–408. (in Russ.). https://doi.org/10.7868/S0044513413040181
4. Vekhova E. E. Byssus adaptive morphology in *Mytilus coruscus*, *Crenomytilus grayanus* and *Modiolus modiolus* (Mytilidae, Bivalvia) from the Sea of Japan. *Zoologicheskii zhurnal*, 2019, vol. 98, no. 3, pp. 245–259. (in Russ.). https://doi.org/10.1134/S0044513419020193
5. Vigman E. P. Structure of Gray's mussel clumps. In: *Biologiya midii Greya*. Moscow : Nauka, 1983, pp. 88–108. (in Russ.)
6. Volova G. N., Skarlato O. A. *Dvustvorchatye mollyuski zaliva Petra Velikogo.* Vladivostok : Dal'nevostochnoe knizhnoe izdatel'stvo, 1980, 95 p. (in Russ.)
7. Golikov A. N., Skarlato O. A. Molluscs of the Possiet Bay (the Sea of Japan) and their ecology. *Trudy Zoologicheskogo instituta AN SSSR*, 1967, vol. 42, pp. 5–154. (in Russ.)
8. Zuenko Yu. I. *Promyslovaya okeanologiya Yaponskogo morya.* Vladivostok : TINRO-Tsentr, 2008, 227 p. (in Russ.)
9. Kutishchev A. A., Gogolev A. Yu. Interaction of *Crenomytilus grayanus* and *Modiolus*

difficilis mussel species under different ecological conditions. In: *Biologiya midii Greya*. Moscow : Nauka, 1983, pp. 115–118. (in Russ.)

10. *Lotsiya severo-zapadnogo berega Yaponskogo morya. Ot reki Tumannaya do mysa Belkina.* Saint Petersburg : Gl. upr. navig. i okeanogr., 1984, 319 p. (in Russ.)
11. Manuilov V. A. *Podvodnye landshafty zaliva Petra Velikogo.* Vladivostok : Izdatel'stvo Dal'nevostochnogo universiteta, 1990, 168 p. (in Russ.)
12. Preobrazhensky B. V., Zharikov V. V., Dubeikovsky L. V. *Basics of Underwater Landscape Studies. Management of Marine Ecosystems.* Vladivostok : Dal'nauka, 2000, 352 p. (in Russ.)
13. Razin A. I. *Morskie promyslovye mollyuski yuzhnogo Primor'ya* : Predvaritel'nye rezul'taty Yaponomorskoi ekspeditsii TIPKha po izucheniyu promyslovykh mollyuskov v 1931–32 gg. / V. V. Zaostrovskii (Ed.). Moscow ; Khabarovsk : Dal'nevostochnoe kraev. izd-vo, 1934, 106 p. (Izvestiya / Tikhookeansk. nauch. inst. rybnogo khozyaistva ; vol. 8). (in Russ.)
14. Sedova L. G. Bivalve mollusks fishery and resources at the coast area of Primorsky Krai (Japan Sea). In: *Prirodnye resursy, ikh sovremennoe sostoyanie, okhrana, promyslovoe i tekhnicheskoe ispol'zovanie* : materialy XI Natsional'noi (vserossiiskoi) nauchno-prakticheskoi konferentsii, 24–25 March, 2020. Petropavlovsk-Kamchatsky : KamchatGTU, 2020, pp. 54–58. (in Russ.)
15. Sedova L. G., Sokolenko D. A. Distribution and resources of mussel *Crenomytilus grayanus* and horsemussel *Modiolus kurilensis* in the Amur Bay (Peter the Great Bay, Sea of Japan). In: *Urgent Problems of the World Ocean Biological Resources Development* : proceedings of the V International scientific & technical conference, Vladivostok, 22–24 May, 2018 : [in 2 pt.]. Vladivostok : Dal'rybvtuz, 2018a, pt. 1, pp. 184–189. (in Russ.)
16. Sedova L. G., Sokolenko D. A. Distribution of mussel *Crenomytilus grayanus* and horsemussel *Modiolus kurilensis* in the Posyet Bay (Peter the Great Bay, Sea of Japan). In: *Prirodnye resursy, ikh sovremennoe sostoyanie, okhrana, promyslovoe i tekhnicheskoe ispol'zovanie* : materialy IX Vserossiiskoi nauchno-prakticheskoi konferentsii, 20–22 March, 2018. Petropavlovsk-Kamchatsky : KamchatGTU, 2018b, pp. 88–92. (in Russ.)
17. Sedova L. G., Sokolenko D. A. Stock and distribution of mussel *Crenomytilus grayanus* and horse mussel *Modiolus kurilensis* in the Boysman and Baklan bays (Peter the Great Gulf, the Sea of Japan). In: *Aktual'nye voprosy rybolovstva, rybovodstva (akvakul'tury) i ekologicheskogo monitoringa vodnykh ekosistem* : materialy Mezhdunarodnoi nauchno-prakticheskoi konferentsii, posvyashchennoi 90-letiyu Azovskogo nauchno-issledovatel'skogo instituta rybnogo khozyaistva, 11–12 December, 2018. Rostov-on-Don : AzNIIRKh, 2018c, pp. 215–219. (in Russ.)
18. Sedova L. G., Sokolenko D. A. State of settlements, resources and fishery of Gray mussel *Crenomytilus grayanus* at the coast of Primorsky Region (Japan Sea). *Izvestiya TINRO*, 2019, vol. 198, pp. 33–45. (in Russ.). https://doi.org/10.26428/1606-9919-2019-198-33-45
19. Sedova L. G., Sokolenko D. A. Distribution and resources of mussel *Crenomytilus grayanus* and horsemussel *Modiolus kurilensis* in the Ussuri Bay (Peter the Great Bay, Sea of Japan). In: *Promyslovye bespozvonochnye* : materialy IX Vserossiiskoi nauchnoi konferentsii, Kerch, 30 September – 2 October, 2020.

Simferopol : ARIAL, 2020a, pp. 102–107. (in Russ.)

20. Sedova L. G., Sokolenko D. A. Distribution of mussel *Crenomytilus grayanus* and horse-mussel *Modiolus kurilensis* in the north-eastern Peter the Great Bay (Sea of Japan). In: *Biologicheskoe raznoobrazie: izuchenie, sokhranenie, vosstanovlenie, ratsional'noe ispol'zovanie* : materialy II Mezhdunarodnoi nauchno-prakticheskoi konferentsii, Kerch, 27–30 May, 2020. Simferopol : ARIAL, 2020b, pp. 436–441. (in Russ.)
21. Sedova L. G., Sokolenko D. A. Resources and structure of horsemussel *Modiolus kurilensis* settlements in Peter the Great Bay (the Sea of Japan). *Morskoj biologicheskij zhurnal*, 2021a, vol. 6, no. 2, pp. 83–94. (in Russ.). https://doi.org/10.21072/mbj.2021.06.2.06
22. Sedova L. G., Sokolenko D. A. Distribution of mussel *Crenomytilus grayanus* and horse-mussel *Modiolus kurilensis* in the waters of Archipelago of Empress Eugenia (Peter the Great Bay, Japan Sea). In: *Prirodnye resursy, ikh sovremennoe sostoyanie, okhrana, promyslovoe i tekhnicheskoe ispol'zovanie* : materialy XII Natsional'noi (vserossiiskoi) nauchno-prakticheskoi konferentsii, 28–29 April, 2021 : [in 2 pt.]. Petropavlovsk-Kamchatsky : KamchatGTU, 2021b, pt. I, pp. 71–75. (in Russ.)
23. Selin N. I. Stroenie druz midii Graiana na zailennykh gruntakh. In: *Vsesoyuznaya konferentsiya po ispol'zovaniyu promyslovykh bespozvonochnykh na pishchevye, kormovye i tekhnicheskiye tseli*, Odesa, 22–25 November, 1977 : tezisy dokladov. Moscow : [s. n.], pp. 83–84. (in Russ.)
24. Selin N. I. Population structure and growth of the mussel *Crenomytilus grayanus* in the subtidal zone of the Sea of Japan. *Biologiya morya*, 1991, no. 2, pp. 55–63. (in Russ.)
25. Selin N. I. The composition and structure of a mixed population of *Crenomytilus grayanus* (Dunker, 1853) and *Modiolus kurilensis* (Bernard, 1983) (Bivalvia: Mytilidae) in Peter the Great Bay, Sea of Japan. *Biologiya morya*, 2018a, vol. 44, no. 5, pp. 307–316. (in Russ.). https://doi.org/10.1134/S0134347518050029
26. Selin N. I. Ontogenetic variation in byssal attachment strength of *Modiolus kurilensis* F. R. Bernard, 1983 (Bivalvia: Mytilidae) in connection with spatial organization in druses. *Biologiya morya*, 2018b, vol. 44, no. 6, pp. 418–420. (in Russ.). https://doi.org/10.1134/S106307401806010X
27. Selin N. I., Vekhova E. E. Morphology of the bivalve mollusks *Crenomytilus grayanus* and *Mytilus coruscus* in relation to their spatial distribution in the upper subtidal zone. *Biologiya morya*, 2002, vol. 28, no. 3, pp. 228–232. (in Russ.). https://doi.org/10.1023/A:1016809823033
28. Selin N. I., Vekhova E. E. Morphological adaptations of the mussel *Crenomitilus grayanus* (Bivalvia) to attached life. *Biologiya morya*, 2003, vol. 29, no. 4, pp. 262–267. (in Russ.). https://doi.org/10.1023/A:1025480725601
29. Selin N. I., Vekhova E. E. Dynamics of byssal thread production in *Crenomytilus grayanus* and *Modiolus modiolus* (Bivalvia) upon reattachment to substrate. *Biologiya morya*, 2004, vol. 30, no. 6, pp. 476–478. (in Russ.). https://doi.org/10.1007/s11179-005-0008-7
30. Skarlato O. A. *Dvustvorchatye mollyuski umerennykh shirot zapadnoi chasti Tikhogo okeana.* Leningrad : Nauka, 1981, 480 p. (Opredeliteli po faune SSSR, izdavaemye Zool. in-tom AN SSSR ; iss. 126). (in Russ.)
31. Skarlato O. A., Golikov A. N., Vasilenko S. V., Tsvetkova N. L., Gruzov E. N., Nesis K. N. Composition, structure and distribution of bottom biocoenoses

in the coastal waters of the Possjet Bay (the Sea of Japan). In: *Explorations of the Fauna of the Seas*, 1967, vol. 5 (13), pp. 5–61. (in Russ.)

32. Lindenbaum C., Bennell J. D., Rees E. I. S., McClean D., Cook W., Wheeler A. J., Sanderson W. G. Small-scale variation within a *Modiolus modiolus* (Mollusca: Bivalvia) reef in the Irish Sea: I. Seabed mapping and reef morphology. *Journal of the Marine Biological Association of the United Kingdom*, 2008, vol. 88, iss. 1, pp. 133–141. https://doi.org/10.1017/S0025315408000374
33. Rees E. I. S., Sanderson W. G., Mackie A. S. Y., Holt R. H. F. Small-scale variation within a *Modiolus modiolus* (Mollusca: Bivalvia) reef in the Irish Sea. III. Crevice, sediment infauna and epifauna from targeted cores. *Journal of the Marine Biological Association of the United Kingdom*, 2008, vol. 88, iss. 1, pp. 151–156. https://doi.org/10.1017/S0025315408000052
34. Tsuchiya M. Faunal structures associated with patches of mussels on East Asian coasts. *Helgoland Marine Research*, 2002, vol. 56, pp. 31–36. https://doi.org/10.1007/s10152-001-0099-2

ОСОБЕННОСТИ ПРОСТРАНСТВЕННОГО РАСПРЕДЕЛЕНИЯ *CRENOMYTILUS GRAYANUS* И *MODIOLUS KURILENSIS* (BIVALVIA, MYTILIDAE) В ЗАЛИВЕ ПЕТРА ВЕЛИКОГО (ЯПОНСКОЕ МОРЕ)

Л. Г. Седова, Д. А. Соколенко

Тихоокеанский филиал ФГБНУ «ВНИРО» («ТИНРО»), Владивосток, Российская Федерация
E-mail: *ludmila.sedova@tinro-center.ru*

Двустворчатые моллюски семейства Mytilidae — мидия Грея *Crenomytilus grayanus* (Dunker, 1853) и модиолус курильский *Modiolus kurilensis* Bernard, 1983 — тихоокеанские, приазиатские виды, массовые представители эпифауны верхней сублиторали прибрежных вод залива Петра Великого Японского моря. Мидия Грея является традиционным, а модиолус — перспективным объектом промысла; оба вида имеют значительные ресурсы. Цель работы — выполнить сравнительный анализ пространственного распределения и обилия *C. grayanus* и *M. kurilensis* на разных типах грунта и глубинах обитания в заливе Петра Великого. Исследования проводили в 2007–2019 гг. с использованием стандартных водолазных гидробиологических методов на глубинах до 20 м. Выполнено 5911 станций; на 1635 из них обнаружены митилиды. У митилид определяли прижизненную массу каждой особи и среднюю биомассу. Ландшафтное разнообразие дна залива Петра Великого обуславливает почти повсеместное распространение *C. grayanus* и *M. kurilensis*, что отражает хорошую адаптацию моллюсков к условиям, характерным для этой части их ареала. Моновидовые друзы *C. grayanus* преобладали как на твёрдых, так и на мягких субстратах (78,6 и 38,2 % от общего количества станций с митилидами соответственно), а смешанные друзы обоих видов — на мягких грунтах (38,3 %). Моновидовые друзы *M. kurilensis* на мягких субстратах встречались чаще (23,5 %), чем на твёрдых (8,1 %). В заливе Петра Великого средняя биомасса *C. grayanus* на твёрдых грунтах составляла (728 ± 47) г·м$^{-2}$, варьируя от 524 г·м$^{-2}$ (Амурский залив) до 922 г·м$^{-2}$ (восточная часть залива Петра Великого); на мягких грунтах — (491 ± 51) г·м$^{-2}$, изменяясь от 228 г·м$^{-2}$ (Уссурийский залив) до 829 г·м$^{-2}$ (Амурский залив), за исключением юго-западной части залива Петра Великого и бухты Бойсмана, где значение было ниже 50 г·м$^{-2}$. Средняя биомасса *M. kurilensis* на твёрдых грунтах составляла (370 ± 74) г·м$^{-2}$, варьируя от 18 г·м$^{-2}$ (бухта Баклан) до 656 г·м$^{-2}$ (акватории архипелага Императрицы Евгении); на мягких грунтах — (335 ± 37) г·м$^{-2}$, изменяясь от 77 г·м$^{-2}$ (юго-западная часть залива Петра Великого) до 456 г·м$^{-2}$ (Амурский залив), за исключением бухт Бойсмана и Баклан, где вид встречался единично. В заливе Петра Великого максимальные значения средней биомассы

обоих видов отмечены на глубинах 1–10 м (*C. grayanus* — 664–805 г·м$^{-2}$, *M. kurilensis* — 347–485 г·м$^{-2}$); с возрастанием глубины их обилие снижалось. Значения средней биомассы *C. grayanus*, обитающей на глубинах от 10 до 20 м на твёрдых субстратах, также достаточно высоки — 431–507 г·м$^{-2}$. На мягких грунтах с изменением глубины от 10–15 до 15–20 м её средняя биомасса уменьшалась от (204 ± 33) до (27 ± 11) г·м$^{-2}$. Средняя биомасса *M. kurilensis* на глубинах 10–15 м составляла 121–194 г·м$^{-2}$, а на глубинах 15–20 м — 11–60 г·м$^{-2}$ на обоих типах грунта.

Ключевые слова: митилиды, Mytilidae, мидия Грея, *Crenomytilus grayanus*, модиолус курильский, *Modiolus kurilensis*, биомасса, распределение, грунт, глубина обитания, залив Петра Великого, Японское море

1871
ИнБЮМ – IBSS

Морской биологический журнал
Marine Biological Journal
2023, vol. 8, no. 1, pp. 93–98
https://marine-biology.ru

UDC 595.384.2(262.5)

DETECTION OF AN ALIEN SPECIES OF THE PILUMNIDAE FAMILY OFF THE COAST OF SEVASTOPOL (BLACK SEA)

© 2023 **S. V. Statkevich[1] and A. B. Ershov[2]**

[1]A. O. Kovalevsky Institute of Biology of the Southern Seas of RAS, Sevastopol, Russian Federation
[2]Sevastopol Marine Aquarium Museum, Sevastopol, Russian Federation
E-mail: *statkevich.svetlana@mail.ru*

Received by the Editor 21.04.2020; after reviewing 03.02.2021;
accepted for publication 20.10.2022; published online 14.03.2023.

In July 2018, during Black Sea hydrobionts sampling, a crab of the family Pilumnidae was detected in the coastal area of the southwestern Crimea. Bottom sediments in the spot of crab finding are represented by a solid substrate. At the time of sampling, the water temperature was +24 °C, and the salinity was 18.0‰. According to morphological characteristics, the specimen we found was classified as a hairy crab *Pilumnus* cf. *vespertilio* (Fabricius, 1793) – a representative of the Indo-Pacific. In the work, photographs of alive and fixed crab are given.

Keywords: crab, alien species, Pilumnidae, *Pilumnus* cf. *vespertilio*, Black Sea

Over the last century, a marked intensification in all areas of human activity throughout the world resulted in sharp transformation of local ecosystems and distribution of alien species. For modern ecology, their introduction has become one of the global problems.

Out of decapods, crabs account for the highest number of alien species detected. About 7,100 species of crabs and craboids (representatives of the orders Brachyura and Anomura) have been recorded worldwide; out of them, 73 species are regarded as invasive [Brockerhoff, McLay, 2011]. These hydrobionts penetrate mainly with ship ballast water and ship-bottom fouling.

To date, there are 5 species of alien crabs in the Sea of Azov–Black Sea basin: *Rhithropanopeus harrisii* (Gould, 1841), *Callinectes sapidus* Rathbun, 1896, *Eriocheir sinensis* H. Milne Edwards, 1853, *Dyspanopeus sayi* (Smith, 1869), and *Hemigrapsus sanguineus* (De Haan, 1835) [in De Haan, 1833–1850] [Zalota, 2017; Guchmanidze et al., 2017]. Out of them, one species, *Rh. harrisii*, can be classified as fully naturalized in this area [Slynko et al., 2017; Zalota et al., 2016]. The crab *C. sapidus* is caught regularly [Gül et al., 2021]. For *E. sinensis*, several records are described in the Sea of Azov and Black Sea [Murina, Antonovsky, 2001]. Crabs *D. sayi* and *H. sanguineus* are known due to their single findings in the Black Sea waters (Romanian coast) [Micu et al., 2010a, b].

The detection of another crab species, which is an inhabitant of the Indo-Pacific and was not previously recorded in the Mediterranean basin, in the Black Sea off the Crimean coast is interesting and unusual. For the Black Sea, the Mediterranean basin is often a donor of new species [Boltachev, Karpova, 2014; Galil et al., 2002].

MATERIAL AND METHODS

The material for the study was a crab specimen caught in July 2018 in the southwestern Crimea area (Sevastopol, Karantinnaya Bay) (Fig. 1) during the sampling of Black Sea hydrobionts. The crab was transported alive to the Sevastopol Marine Aquarium Museum and lived there until April 2020.

The dimensional characteristics of the crab were determined using a caliper with an accuracy of 0.1 mm. The individual weight was measured in an electronic balance with an accuracy of 0.01 g. The detected specimen was identified according to the species guides [Awaad et al., 2019; Emmerson, 2016; Naderloo, 2017]. The crab specimen fixed in 96% ethanol is stored in the World Ocean hydrobionts collection at IBSS.

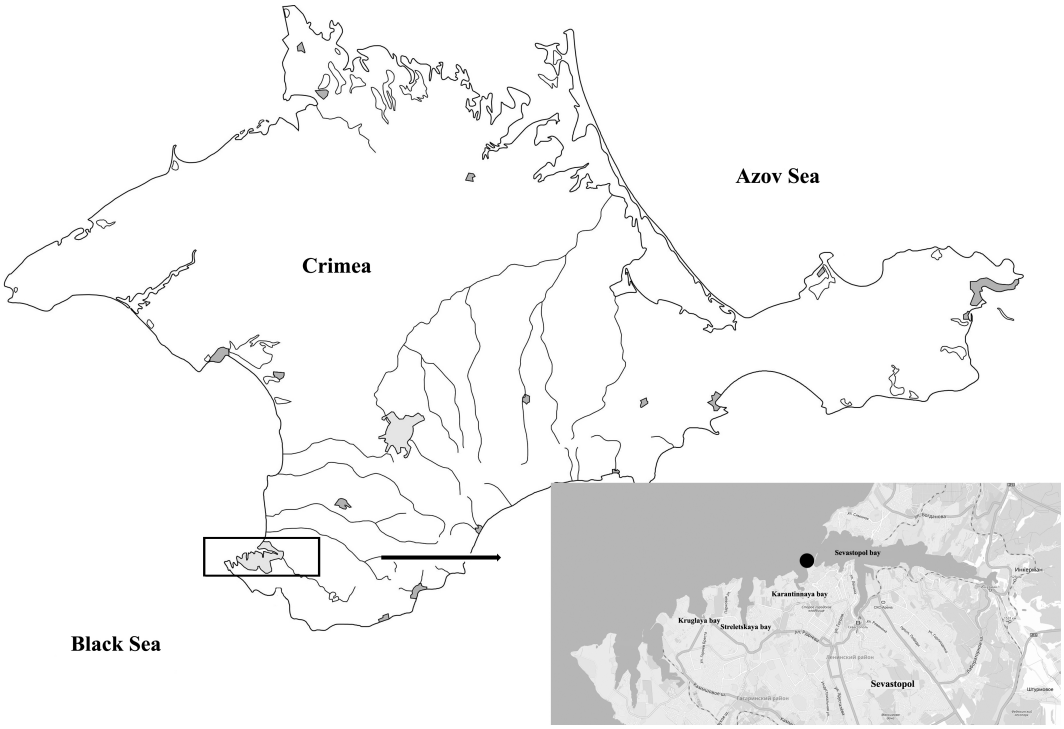

Fig. 1. Map of the crab finding spot (the location is marked with a black dot)

RESULTS AND DISCUSSION

Material. The crab was detected on 11.07.2018 in the coastal area of the southwestern Crimea near Sevastopol (44°37′02.12″N, 33°30′12.38″E) on a rocky bottom among thickets of seagrasses and algae. The water temperature at the time of sampling was +24 °C, and the water salinity was about 18.00‰. The crab specimen found is a mature female (Fig. 2a, b), with a carapace width of 39.4 mm and a length of 27.2 mm, with a total weight of 31.7 g.

Description. The carapace is hexagonal, with rounded edges (Fig. 2c, d). Its front is convex; the back is flatter. The width of the carapace is about 1.4 times the length. The body surface is densely covered with setae of various length, with longer ones at margins. The frontal lobe is divided by a medial notch into two parts, with each having a distinct supraorbital angle. The eye orbits are small, with two notches on the dorsal margin. The anterolateral margin is slightly shorter than the posterolateral margin and is armed with three teeth (without an external orbital).

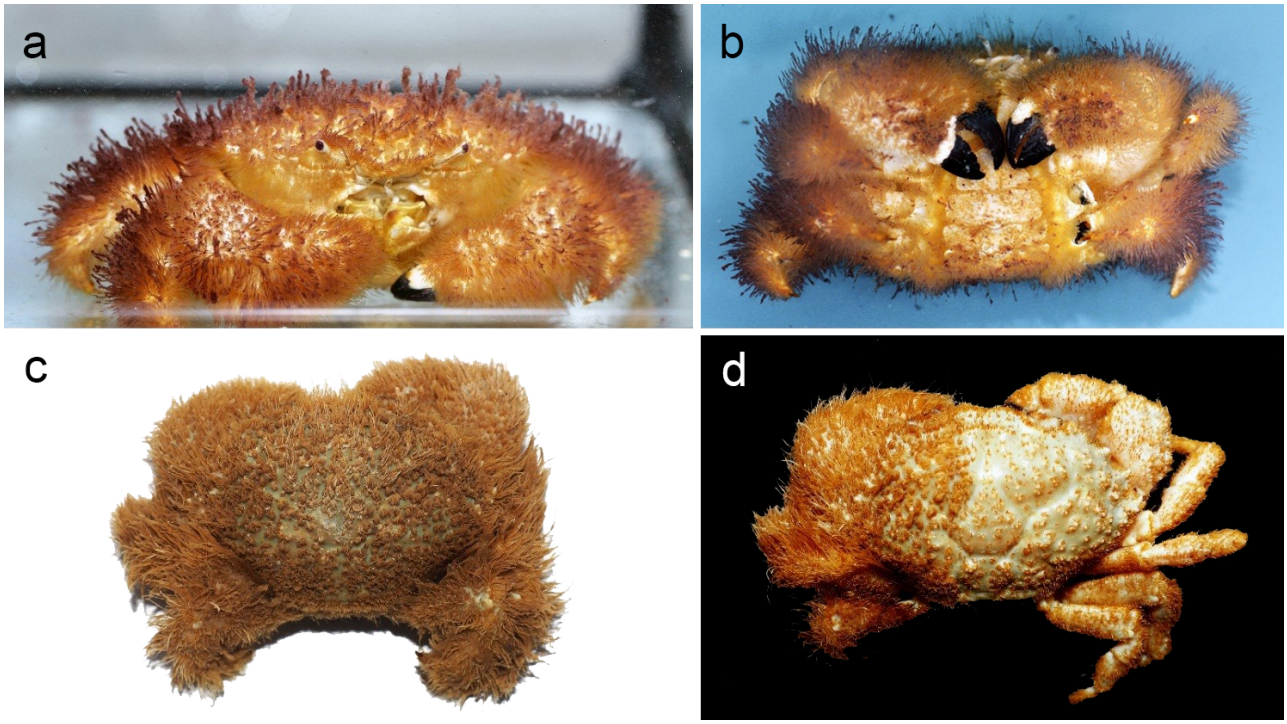

Fig. 2. Hairy crab: a, general view; b, ventral side; c, d, dorsal side

Chelipeds are asymmetrical, with long setae (Fig. 2b). Claw fingers are black, with blunt teeth along the cutting edge. II–V pairs of walking limbs are flattened, abundantly covered with setae (Fig. 2d). The setae are brown to golden yellow.

The caught specimen belongs to the genus *Pilumnus* Leach, 1816 (hairy crabs), the family Pilumnidae. Among the representatives of this genus, there are several species with similar morphological structure and setae coverage.

The detected specimen was classified by us as the hairy crab *Pilumnus* cf. *vespertilio* (Fabricius, 1793) based on the following peculiarities:

- The only representative of the family in the Black Sea – *Pilumnus hirtellus* (Linnaeus, 1761) – has short club-shaped setae on the dorsal surface of the carapace, while the caught crab has the carapace densely covered with even setae of different length. In *P. hirtellus*, the anterolateral margin of the carapace is armed with four teeth (without an external orbital); in *P. vespertilio*, there are three teeth (without an external orbital).
- From the closely related species *Pilumnus minutus* De Haan, 1835 [in De Haan, 1833–1850], the found specimen differs in a longer setae coverage, maximum size, and some structural features. Unlike *P. vespertilio*, the crab *P. minutus* is a small species, with a carapace length of about 10 mm; moreover, it has thin, elongated pereopods [Galil et al., 2002; *Pilumnus minutus*, 2020].
- Another representative of the genus – *Pilumnus scabriusculus* Adams & White, 1849 – also has a dense setae coverage; its carapace is covered with long yellowish hairs. In *P. scabriusculus*, the anterolateral margins of the carapace have three rounded low teeth (the first and second are almost equal, and the third is the smallest, triangle-shaped). In *P.* cf. *vespertilio*, the lateral margins have three teeth; out of them, the first is triangle-shaped, and the second and third are sharp (the last tooth is sharper) [Ng, Clark, 1849].

The crab *P. scabriusculus* inhabits the coast of Australia, New Guinea, the Philippines, and the Seychelles; moreover, it was registered for the Sea of Japan. The crab *P. vespertilio* is widely distributed in the warm-water areas of the Indo-Pacific; it is found from the coast of East Africa to the Philippines [Awaad et al., 2019; Emmerson, 2016; Kyomo, 2002], recorded off the coast of Australia and Singapore [Siddiqui, Tirmizi, 1992], and detected in New Caledonia [Emmerson, 2016]. Also, this species was registered in the Red Sea, the Gulf of Suez, and the Suez Canal [Awaad et al., 2019], and this makes the detection of the crab off the Crimean coast possible.

P. vespertilio is an inhabitant of sublittoral rocky areas and mangroves. It occurs in the coastal areas from the water edge to a depth of 10 m, under stones, in crevices, and among coral fragments. This crab, due to its dense setae coverage, becomes almost invisible on the substrate. It spends most of time in burrows, which it builds on both hard and soft bottoms [Emmerson, 2016; Kyomo, 1999, 2001]. It is most active at night. The name of the crab species was inspired by the name of the genus of bats *Vespertilio* Linnaeus, 1758 – due to external similarity of the setae coverage of these animals [Emmerson, 2016].

Males are larger than females and can reach 25.5–30.8 mm in width and 18.0–25.5 mm in length; females are up to 25 mm in width and 18.1 mm in length [Dai, Yang, 1991]. Some individuals can reach 40.1 mm in length [Teddy bear crab, 2020]. They are continuous breeders, with maximum activity during summer months [Kyomo, 1999; Litulo, 2005]. In temperate latitudes, the breeding season is shorter and lasts May to October [Kyomo, 1999]. In the coastal area near Okinawa Island (Japan), the duration of embryogenesis for hairy crabs averages 21.2 days [Kyomo, 2002]. This species has four larval stages – three zoeal and one megalope [Clark, Paula, 2003; Siddiqui, Tirmizi, 1992]. Off the coast of Japan, the hairy crab mainly feeds on algae, most often red *Gelidium pusillum* (Stackhouse) Le Jolis, 1863 (Rhodophyta), and on small invertebrates [Kyomo, 1999]. Moreover, *P. vespertilio* can feed on toxic Zoantharia (coral polyps), and the poisons accumulated while feeding on these coral polyps make the crabs toxic [*Pilumnus vespertilio* – Hairy crab, 2021]. Interestingly, when catching the specimen considered, the second author of the article suffered burns to his fingers.

The occurrence of the hairy crab in the Black Sea can be explained by economic activity. Specifically, larvae (planktonic stage of crab development) could be transferred through ballast water. An indirect confirmation of this fact is that the crab was detected in the immediate vicinity of the Sevastopol Bay mouth, where various ships are based for many years.

The studies were carried out under the RFBR grant No. 18-44-920016 "Dynamics and consequences of the introduction of alien species of fish and invertebrates into biocenoses of Sevastopol coast and bays" and partially within the framework of IBSS state research assignment No. 121040600178-6 "Structural and functional organization, productivity, and sustainability of marine pelagic ecosystems."

REFERENCES

1. Zalota A. K. *Chuzherodnye vidy desyatinogikh rakoobraznykh (Crustacea Decapoda) v moryakh Rossii i sopredel'nykh vodakh.* [dissertation]. Moscow, 2017, 234 p. (in Russ.)
2. Murina V. V., Antonovsky A. G. Chinese crab, *Eriocheir sinensis* is an invader into the basin of the Sea of Azov. *Ekologiya morya*, 2001, iss. 55, pp. 37–39. (in Russ.). URL: https://repository.marine-research.ru/handle/299011/4382
3. Awaad A. M. E., Abdullah M. A., Mohamed A. A., Mostafa H. S. Revision of superfamily Pilumnoidea from the Egyptian Red Sea coasts, Gulfs of Aqaba and Suez,

Egypt. *Egyptian Journal of Aquatic Biology & Fisheries*, 2019, vol. 23 (5), pp. 137–166. https://doi.org/10.21608/EJABF.2019.62493

4. Boltachev A. R., Karpova E. P. Faunistic revision of alien fish species in the Black Sea. *Russian Journal of Biological Invasions*, 2014, vol. 5, no. 4, pp. 225–241. https://doi.org/10.1134/S2075111714040018
5. Brockerhoff A., McLay C. Human-mediated spread of alien crabs. In: *In the Wrong Place – Alien Marine Crustaceans: Distribution, Biology and Impacts* / B. S. Galil, P. F. Clark, J. T. Carlton (Eds). Dordrecht ; Heidelberg ; London ; New York : Springer, 2011, pp. 27–105. (Invading Nature – Springer Series in Invasion Ecology ; vol. 6). https://doi.org/10.1007/978-94-007-0591-3_2
6. Clark P. F., Paula J. Descriptions of ten xanthoidean (Crustacea: Decapoda: Brachyura) first stage zoeas from Inhaca Island, Mozambique. *The Raffles Bulletin of Zoology*, 2003, vol. 51, no. 2, pp. 323–378.
7. Dai A., Yang S. *Crabs of the China Seas.* Beijing ; Berlin ; Heidelberg ; New York ; Tokyo : China Ocean Press : Springer-Verlag, 1991, 608 p.
8. Emmerson W. D. *A Guide to, and Checklist for, the Decapoda of Namibia, South Africa and Mozambique.* [In 3 vols]. Newcastle upon Tyne, UK : Cambridge Scholars Publishing, 2016, vol. 3, 720 p.
9. Galil B., Froglia C., Noël P. *CIESM Atlas of Exotic Species in the Mediterranean.* Vol. 2. *Crustaceans: Decapods and Stomatopods.* Monaco : CIESM Publishers, 2002, 192 p.
10. Guchmanidze A., Statkevich S. V., Boltachev A. R. The first record of prawn *Penaeus semisulcatus* De Haan, 1844 (Decapoda, Penaeidae) near the coast of Georgia. *Russian Journal of Biological Invasions*, 2017, vol. 8, no. 1, pp. 14–17. https://doi.org/10.1134/S2075111717010039
11. Gül M., Bodur B., Aydin M. First record of gravid female American blue crab (*Callinectes sapidus* Rathbun, 1986) from the Black Sea. *Marine Science and Technology Bulletin*, 2021, vol. 10, iss. 3, pp. 224–227. https://doi.org/10.33714/masteb.795884
12. Kyomo J. Feeding patterns, habits and food storage in *Pilumnus vespertilio* (Brachyura: Xanthidae). *Bulletin of Marine Science*, 1999, vol. 65, no. 2, pp. 381–389.
13. Kyomo J. Reproductive behavior of the play-dead hairy *Pilumnus vespertilio* (Crustacea: Brachyura: Pilumnidae) with respect to carapace size. *Bulletin of Marine Science*, 2001, vol. 68, no. 1, pp. 37–46.
14. Kyomo J. Timing and synchronization of the breeding period in *Pilumnus vespertilio* (Crustacea: Pilumnidae) in subtropical Okinawa, Japan. *Pacific Science*, 2002, vol. 56, no. 3, pp. 317–328. https://doi.org/10.1353/psc.2002.0025
15. Litulo C. Population structure and breeding biology of the hairy crab *Pilumnus vespertilio* (Fabricius, 1793) (Crustacea: Brachyura: Pilumnidae) in southern Mozambique. *Journal of Natural History*, 2005, vol. 39, iss. 17, pp. 1359–1366. https://doi.org/10.1080/00222930400010070
16. Micu D., Niţă V., Todorova V. First record of the Japanese shore crab *Hemigrapsus sanguineus* (de Haan, 1835) (Brachyura: Grapsoidea: Varunidae) from the Black Sea. *Aquatic Invasions Magazine*, 2010a, vol. 5, suppl. 1, pp. S1–S4. https://doi.org/10.3391/ai.2010.5.S1.001
17. Micu D., Niţă V., Todorova V. First record of Say's mud crab *Dyspanopeus sayi* (Brachyura: Xanthoidea: Panopeidae) from the Black Sea. *Marine Biodiversity Records*, 2010b, vol. 3, art. no. 30 (6 p.). https://doi.org/10.1017/S1755267210000308
18. Naderloo R. *Atlas of Crabs of the Persian Gulf.* Cham, Switzerland : Springer, 2017, 444 p. https://doi.org/10.1007/978-3-319-49374-9
19. Ng P. K. L., Clark P. F. The Indo-West Pacific Pilumnidae XVIII: On the taxonomy of *Pilumnus scabriusculus* Adams and White, 1849, and *P. sluiteri* De Man, 1892, with a note on *Cancer incanus* Forskål, 1775 (Brachyura: Xanthoidea). *Zootaxa*, 2005, vol. 841, no. 1, pp. 1–14. https://doi.org/10.11646/zootaxa.841.1.1
20. *Pilumnus minutus.* In: *Crabs of Japan / Linnaeus Naturalis Biodiversity Center* : [site]. URL: https://crabs-japan.linnaeus.naturalis.nl/linnaeus_ng/app/views/species/taxon.php?id=34082&cat=69&epi=32 [accessed: 10.12.2020].

21. Siddiqui F., Tirmizi N. M. The complete larval development, including the first crab stage of *Pilumnus kempi* Deb, 1987 (Crustacea: Decapoda: Brachyura: Pilumnidae) reared in the laboratory. *Raffles Bulletin of Zoology*, 1992, vol. 40 (2), pp. 229–244.
22. Slynko Y. V., Pakunova E. N., Statkevich S. V., Slynko E. E. Genetic diversity of invasive populations of the Florida crab (*Rhithropanopeus harrisii* (Gould, 1841): (Decapoda, Panopidae)). *Russian Journal of Genetics*, 2017, vol. 53, no. 5, pp. 623–629. https://doi.org/10.1134/S1022795417050106
23. Teddy bear crab (*Pilumnus vespertilio*). In: *Dr. Lee's Gallery Museum* : [site]. URL: http://leechitse66.blogspot.com/2011/02/pilumnus-vespertilio-401mm.html [accessed: 10.12.2020].
24. *Pilumnus vespertilio* – Hairy crab. In: *Wiki.nus* / National University of Singapore : [site]. URL: https://wiki.nus.edu.sg/display/TAX/Pilumnus+vespertilio+-+Hairy+crab [accessed: 30.01.2021].
25. Zalota A. K., Spiridonov V. A., Kolyuchkina G. A. *In situ* observations and census of invasive mud crab *Rhithropanopeus harrisii* (Crustacea: Decapoda: Panopeidae) applied in the Black Sea and the Sea of Azov. *Arthropoda Selecta*, 2016, vol. 25, no. 1, pp. 39–62. https://doi.org/10.15298/arthsel.25.1.04

ОБНАРУЖЕНИЕ ЧУЖЕРОДНОГО ВИДА КРАБА СЕМЕЙСТВА PILUMNIDAE У БЕРЕГОВ СЕВАСТОПОЛЯ (ЧЁРНОЕ МОРЕ)

С. В. Статкевич[1], А. Б. Ершов[2]

[1]ФГБУН ФИЦ «Институт биологии южных морей имени А. О. Ковалевского РАН», Севастополь, Российская Федерация

[2]Севастопольский морской аквариум-музей, Севастополь, Российская Федерация

E-mail: *statkevich.svetlana@mail.ru*

В июле 2018 г. в прибрежной зоне Юго-Западного Крыма во время сбора образцов черноморских гидробионтов обнаружен краб семейства Pilumnidae. Донные отложения в районе поимки краба представлены твёрдым субстратом. На момент сбора материала температура воды составляла +24 °С, солёность — 18,0 ‰. Пойманный экземпляр по морфологическому строению был идентифицирован нами как волосатый краб *Pilumnus* cf. *vespertilio* (Fabricius, 1793), представитель Индо-Тихоокеанского региона. В работе приведены фотографии живого и фиксированного краба.

Keywords: crab, alien species, Pilumnidae, *Pilumnus* cf. *vespertilio*, Black Sea

1871
ИнБЮМ – IBSS

Морской биологический журнал
Marine Biological Journal
2023, vol. 8, no. 1, pp. 99–108
https://marine-biology.ru

UDC [581.526.325:577.31]:519.22

RELATIONSHIP BETWEEN GROWTH CHARACTERISTICS OF MICROALGAE CULTURE AND AGE-SPECIFIC CELL STATE IN ONTOGENESIS (PROBABILISTIC MODEL)

© 2023 **R. P. Trenkenshu**

A. O. Kovalevsky Institute of Biology of the Southern Seas of RAS, Sevastopol, Russian Federation
E-mail: *r.trenkenshu@rambler.ru*

Received by the Editor 27.01.2021; after reviewing 27.01.2021;
accepted for publication 20.10.2022; published online 14.03.2023.

The article presents a quantitative model of the dependence of the morphological structure of the continuous microalgae culture on external lighting and species-specific cell parameters. The modeling is based on the concept of two main phases that make up the cell life cycle – interphase and division phase. The interphase is regarded as a light-dependent process during which cell biomass increases. The division phase does not depend on light and occurs when a cell reaches a certain mass equal to (or higher than) the sum of masses of daughter cells. The division stage ends with cytokinesis: a cell splits into daughter cells. The age-specific microalgae cell state is characterized by the value of its biomass, while transitions from one state to another are characterized by the activity (growth and division). The model is represented by a system of differential equations that fully describe the dynamics of ontogenesis. A particular solution of the model for dynamically equilibrium growth of microalgae in the culture at different light intensity is analyzed. As shown, in the continuous microalgae culture under photolithotrophic conditions, the specific growth rate is related to the morphological structure of the cell population by simple directly proportional equations with species-specific coefficients. These coefficients are the maximum growth rate in the interphase (at saturating light intensity) and cell division activity in mitosis.

Keywords: microalgae, ontogenesis, age-specific cell state, interphase, mitosis, probabilistic model, growth rate, morphological structure of culture

Considering a microalgae monoculture as a population of individual cells, one can speak about the age population structure, or rather morphological population structure, which is determined by the relationship of age groups (the same as in all plants). The difference between microalgae and higher plants is as follows: in the strict sense, there is no age concept for individual microalgae cells in a population. To characterize age groups and individual cells, the concept of an age-specific state, or ontogenetic state, is applied. The transition from one state to another is one-sided and directed towards growth; it can occur at the same or different rate depending on the actual ontogenetic state and the cell environment.

The microalgae growth in culture is directly related to the growth of each individual cell and the rate of division, *i. e.*, to cell cycle, the duration of which is determined by the properties of the cell environment. The study of ontogenesis of individual microalgae cells is a difficult task since they are microscopic in size. Ideally, ontogenetic investigations can be carried out with a coeval cell population [Helmstetter, 2015]. Methodically, it can be done; the possibility is connected with occurrence of light-dependent

and light-independent phases of microalgae cell development in ontogenesis [Tsoglin, Klyachko-Gurvich, 1980]. By establishing the relationship between durations of light and dark regimes for a particular microalgae culture, the age-specific state for all cells in culture can be synchronized [Tsoglin, 1996; Tsoglin, Klyachko-Gurvich, 1980]. Significant progress in the work with synchronous *Chlorella* cultures is reflected in publications of the researchers [Tsoglin, 1996; Tsoglin, Pronina, 2012].

To date, there are many papers concerning the study of the eukaryotic cell cycle, *inter alia* early works [Winter, 1835] and recent large reviews, such as [Cvrčková, 2018]. The latter publication emphasizes that current understanding of the processes leading to cell division is based on a limited range of concepts, although a lot of hypotheses were proposed earlier.

A similar situation is observed when constructing mathematical models for describing the age-specific cell state in ontogenesis or the cell size distribution within a microbial population [Karlin, 1968; Riznichenko, 2011; Stepanova, 1980]. The most developed kinetic models of eukaryotic regulation of the cell cycle are based on the concept of cyclin-dependent kinases and cyclins [Novák et al., 1999; Sasabe, Machida, 2014]. However, this refers mostly to the very fact of division and is not directly related to the growth processes of an individual cell, especially at the initial stage of the life cycle [Wang, Levin, 2009; Wilkins, Holliday, 2009]. Moreover, the proposed kinetic models include a large number of differential equations, and this ultimately leads to the need for reducing the systems of equations to a small amount [Sible, Tyson, 2007; Tyson, Novák, 2001, 2015].

To establish the relationship between the microalgae growth characteristics in culture and its morphological structure, it is necessary to know the effect of the environment on the life cycle (the age-specific state of individual cells). This relationship can be quantified in various ways. In this work, the age-specific cell state and its transitions during the life cycle are modeled by probabilistic methods.

Basic provisions. The life cycle of a microalgae cell, or cell cycle, consists of several periods, which are combined into two distinct phases – interphase and mitosis or meiosis [Cvrčková, 2018; Tyson, Novák, 2015]. During the interphase, a cell grows; then, the processes of DNA replication begin, and a cell enters the division stage; it ends with cytokinesis – a cell splits into daughter cells. During mitosis, two distinct daughter cells are formed. During meiosis, which can be considered as a sequence of several mitoses (or autospores), cytokinesis ends with the formation of several daughter cells [Tsoglin, Pronina, 2012; Wilkins, Holliday, 2009], with their abundance depending on the quantity of mitoses according to an exponential law.

To characterize the age-specific cell state, various parameters can be applied. Cell biomass (b) can be considered as the most appropriate quantitative characteristic of the age-specific microalgae cell state. Indeed: in order for a cell to divide into daughter cells (d), its biomass in the interphase must increase to a value (b_m) higher than or equal to the sum of masses of daughter cells (b_0):

$$b_m \geq db_0,\ d = 2, 4, 8, 16...$$

This inequality may be due to the fact that the process of cell division is accompanied by the internal energy consumption and, consequently, by the mass loss [Pederson, 2003; Tsoglin, 1996]. Moreover, the mass loss can result from a cell wall destruction, flagella shedding, *etc.*

The cell biomass structural form seems to be a more accurate characteristic [Trenkenshu et al., 2018] if we consider the mass loss during division to be insignificant. In this case, it becomes possible to assess the biomass structural form by measuring chlorophyl concentration, which is proportional to the cell

biomass structural form [Trenkenshu et al., 2018]. At the same time, a key point in terms of methodology is the ability to measure pigments and biomass optically – without damage to the cell structural integrity.

The growth of microalgae in culture is characterized by the rate of change in its density (biomass B or cell abundance N) over time t. For relatively long constant external conditions, the specific growth rate μ remains constant:

$$\mu = \frac{dB}{Bdt} = \frac{dN}{Ndt}.$$

If, as a result of cytokinesis, an individual cell is divided into d daughter cells, the duration of the life cycle is related to the specific growth rate of the culture by a simple ratio:

$$\tau_z = \frac{\ln d}{\mu}.$$

Distinguishing two time periods in the life cycle [the growth stage (interphase τ_g) and the division stage (mitosis τ_m)], we state that their sum is equal to the duration of the life cycle:

$$\tau_z = \tau_g + \tau_m.$$

Probabilistic model of ontogenesis. The life cycle of an individual microalgae cell can be represented as a graph of the age-specific states in which the cell can be. To do this, we express the probability that a cell is in one of its growth states through $\theta_g(t)$, and the probability that it is in the division stage, through $\theta_m(t)$.

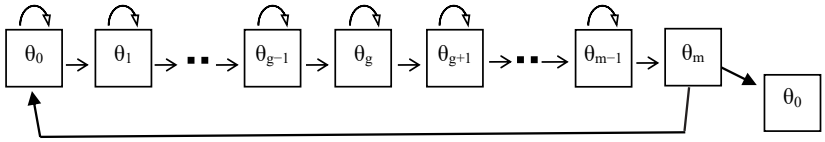

We denote the activity of transitions from one state to another with subscripts corresponding to the probabilities from which the transition occurs. Thus, the growth transition activity is μ_g ($0 \le g \le m - 1$), and the activity of complete cell division into daughter cells is μ_m. Analytically, such a graph can be outlined by a system of differential equations that completely describes the change in the cell state over time:

$$\begin{cases} \frac{d\theta_0(t)}{dt} = -\mu_0\theta_0(t) + \mu_m\theta_m(t), \\ \frac{d\theta_1(t)}{dt} = -\mu_1\theta_1(t) + \mu_0\theta_0(t), \\ \ldots\ldots\ldots\ldots \\ \frac{d\theta_g(t)}{dt} = -\mu_r\theta_g(t) + \mu_{g-1}\theta_{g-1}(t);\ [0 \le g \le m-1], \\ \ldots\ldots\ldots\ldots \\ \frac{d\theta_m(t)}{dt} = -\mu_m\theta_m(t) + \mu_{m-1}\theta_{m-1}(t). \end{cases}$$

Normalization condition for all the states is as follows:

$$\theta_m + \sum_{g=0}^{m-1} \theta_g = 1.$$

By integrating the obtained system of equations, one can completely describe the dynamics of cell ontogenesis for any moment of time. However, an exact formal description of cyclic graphs is mathematically difficult due to integration problems [Karlin, 1968]. Nevertheless, some particular solutions are possible, and those can be used in assessing the morphological structure of microalgae populations.

Stationary case. Of particular interest is the solution of the system of equations for the stationary case. In a stationary (dynamically equilibrium) process, the state probabilities are equal to their limits:

$$\lim_{\Delta t\to 0}\theta_g(t)=\theta_g;\ 0\le g\le m-1),\ \lim_{\Delta t\to 0}\theta_m(t)=\theta_m,$$

and the derivatives of the probabilities in terms of time are equal to zero:

$$\frac{d\theta_g(t)}{dt}=0;\ (0\le\ g\le\ m-1),\ \frac{d\theta_m(t)}{dt}=0.$$

The system of differential equations turns into an algebraic one:

$$\begin{cases}\frac{d\theta_0}{dt}=0=-\mu_0\theta_0+\mu_m\theta_m,\\ \frac{d\theta_1}{dt}=0=-\mu_1\theta_1+\mu_0\theta_0,\\ \ldots\ldots\ldots\\ \frac{d\theta_g}{dt}=0=-\mu_g\theta_g+\mu_{g-1}\theta_{g-1};\ [0\le g\le m-1],\\ \ldots\ldots\ldots\\ \frac{d\theta_m}{dt}=0=-\mu_m\theta_m+\mu_{m-1}\theta_{m-1}.\end{cases}$$

We express the required probabilities for the interphase in terms of the probability of the initial state:

$$\theta_1=\frac{\mu_0}{\mu_1}\theta_0,\ \theta_2=\frac{\mu_0}{\mu_2}\theta_1=\frac{\mu_0}{\mu_2}\frac{\mu_0}{\mu_1}\theta_0,\ \ldots,\ \theta_g=\frac{(\mu_0)^g}{\prod_{g=0}^{m-1}\mu_g}\theta_0.$$

The probability of the age-specific cell state in the division stage is as follows:

$$\theta_m=\frac{\mu_0}{\mu_m}\theta_0.$$

Condition for normalization over all the states is:

$$\frac{\mu_0}{\mu_m}\theta_0+\sum_{g=0}^{m-1}\frac{(\mu_0)^g}{\prod_{g=0}^{m-1}\mu_g}\theta_0=1.$$

Hence, we obtain the dependences of the probability density of cell being in the growth state (Θ_g) and in the division stage (Θ_m):

$$\Theta_g=\frac{\theta_g}{\frac{\mu_0}{\mu_m}\theta_0+\sum_{g=0}^{m-1}\frac{(\mu_0)^g}{\prod_{g=0}^{m-1}\mu_g}\theta_0}=\frac{\frac{(\mu_0)^g}{\prod_{g=0}^{m-1}\mu_g}}{\frac{\mu_0}{\mu_m}+\sum_{g=0}^{m-1}\frac{(\mu_0)^g}{\prod_{g=0}^{m-1}\mu_g}};$$

$$\Theta_m = \frac{\theta_m}{\frac{\mu_0}{\mu_m}\theta_0 + \sum_{g=0}^{m-1} \frac{(\mu_o)^g}{\prod_{g=0}^{m-1}\mu_g}\theta_0} = \frac{\frac{\mu_0}{\mu_m}}{\frac{\mu_0}{\mu_m} + \sum_{g=0}^{m-1} \frac{(\mu_0)^g}{\prod_{g=0}^{m-1}\mu_g}}.$$

It is possible to use the model obtained for describing age or size cell distribution in a microalgae culture, only if we know the relationship between the probabilistic coefficients of the ontogenesis model and the kinetic characteristics of the culture. First of all, we take into account that the last equations were obtained for continuous dynamically equilibrium conditions. Thus, the equations can be applied to continuous microalgae cultures. This means that probability densities of cells being in a growth state and division stage will show the quantitative ratio of growing cells (n_g/N) and the ratio of dividing cells (n_m/N) in their total abundance (N):

$$n_g + n_m = N,$$

$$\frac{n_g}{N} = \Theta_g = \frac{\frac{(\mu_0)^g}{\prod_{g=0}^{m-1}\mu_g}}{\frac{\mu_0}{\mu_m} + \sum_{g=0}^{m-1} \frac{(\mu_0)^g}{\prod_{g=0}^{m-1}\mu_g}}; \frac{n_m}{N} = \Theta_m = \frac{\frac{\mu_0}{\mu_m}}{\frac{\mu_0}{\mu_m} + \sum_{g=0}^{m-1} \frac{(\mu_0)^g}{\prod_{g=0}^{m-1}\mu_g}}.$$

The ontogenetic state of cells is described by a set of probabilistic coefficients that determine transitions from one state to another. Interestingly, this process is cyclic: in the interphase, it is directed towards growth; in the division phase, it returns the cell to its initial state. The rate of transitions is taken into account by activity factors which generally determine the life cycle. As established, there are two phases in the microalgae life cycle – light-dependent and light-independent [Tsoglin, Klyachko-Gurvich, 1980; Tsoglin, Pronina, 2012]. The first relates to the interphase while the second relates to mitosis.

The continuity of growth, both for a microalgae culture and an individual cell, is characterized by a constant specific rate, in other words, by an exponential increase in the culture density (biomass concentration) and the cell biomass. The continuity of biomass growth under constant light allows simplifying the equation for the probability density of cell being in the growth state and mitosis:

$$\mu_0 = \mu_g = \text{const}, \ \mu_m = \text{const},$$

$$\Theta_g = \frac{\theta_g}{\frac{\mu_g}{\mu_m} + \sum_{g=0}^{m-1} \frac{(\mu_g)^g}{\prod_{g=0}^{m-1}\mu_g}} = \frac{1}{1+\mu_g/\mu_m}, \ \Theta_m = \frac{\theta_m}{\frac{\mu_g}{\mu_m} + \sum_{g=0}^{m-1} \frac{(\mu_g)^g}{\prod_{g=0}^{m-1}\mu_g}} = \frac{\mu_g/\mu_m}{1+\mu_g/\mu_m},$$

$$\Theta_g = \frac{\mu_m}{\mu_g+\mu_m}, \ \Theta_m = \frac{\mu_g}{\mu_g+\mu_m}.$$

The effect of light on the age-specific cell state. With continuous photolithotrophic [Stukolova, Trenkenshu, 2020] microalgae growth, the duration of the interphase depends on a light intensity at which cell grows. This means that the activity of transitions of age-specific states in the interphase is also dependent on light conditions under which the cell is. The effect of light on the biomass specific growth rate in the interphase can be described by the equation [Lelekov, Trenkenshu, 2019]:

$$\mu_g = \begin{cases} \mu_{gmax}(i - i_{cp}), \ i_{cp} \le i \le 1; \\ \mu_{gmax}, \ i - i_{cp} \ge 1. \end{cases}$$

There, μ_{gmax} is the maximum specific rate of the cell mass growth at saturating light intensity;

i is the light intensity normalized relative to saturating one;

i_{cp} is the compensation point of photosynthesis in normalized units.

As a result, the probability density of cell being in the growth state or mitosis will depend on non-saturating light intensity according to the equation:

$$\Theta_g = \frac{\mu_m}{\mu_{gmax}(i - i_{cp}) + \mu_m},\ (i_{cp} \le i \le 1);\ \Theta_m = \frac{\mu_{gmax}(i - i_{cp})}{\mu_{gmax}(i - i_{cp}) + \mu_m},\ (i_{cp} \le i \le 1).$$

At light intensities equal to or higher than saturating intensity:

$$\Theta_g = \frac{\mu_m}{\mu_{gmax} + \mu_m}, (i - i_{cp}) \ge 1;\ \Theta_m = \frac{\mu_{gmax}}{\mu_{gmax} + \mu_m}, (i - i_{cp}) \ge 1.$$

Given that the maximum transition activities during growth and division are species-specific constants, their ratio (μ_{gmax}/μ_m) is also a species-specific constant. This allows writing the above equations in the form:

$$\begin{cases} \Theta_g = \frac{1}{1+\mu_{gmax}(i-i_{cp})/\mu_m},\ (i_{cp} \le i \le 1);\ \Theta_m = \frac{\mu_{gmax}(i-i_{cp})/\mu_m}{1+\mu_{gmax}(i-i_{cp})/\mu_m},\ (i_{cp} \le i \le 1), \\ \Theta_g = \frac{1}{1+\mu_{gmax}/\mu_m},\ (i - i_{cp}) \ge 1;\ \Theta_m = \frac{\mu_{gmax}/\mu_m}{1+\mu_{gmax}/\mu_m},\ (i - i_{cp}) \ge 1. \end{cases}$$

The obtained equations are graphically illustrated in Fig. 1.

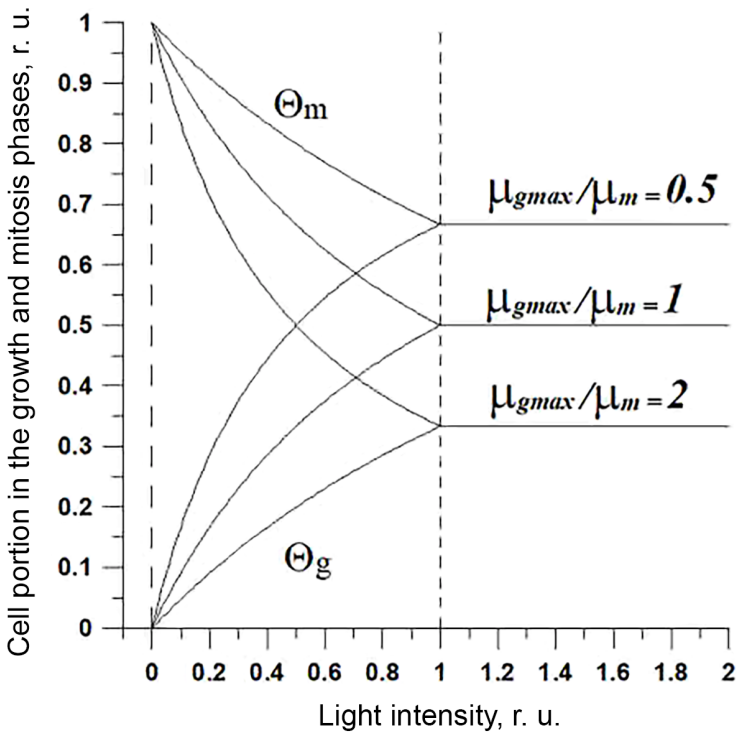

Fig. 1. Dependence of the cell proportion in the interphase (Θ_g) and in the mitosis phase (Θ_m) on light intensity at different species-specific ratios (shown by numbers) of specific growth rate of the cell mass and mitosis rate (μ_{gmax}/μ_m)

Fig. 2 clearly shows how the morphological structure of the microalgae population at saturating light intensity depends on the species-specific ratio μ_{gmax}/μ_m.

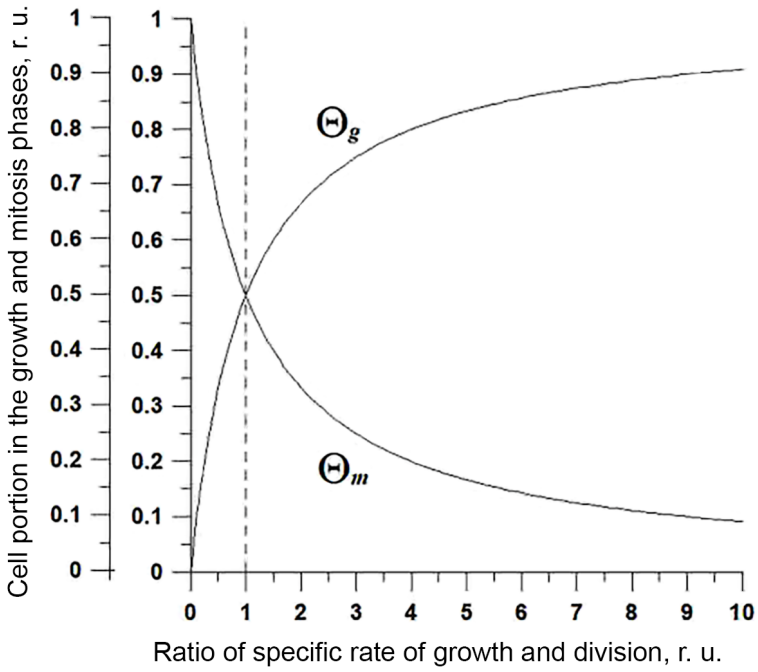

Fig. 2. Dependence of the cell proportion in the interphase (Θ_g) and in the mitosis phase (Θ_m) on the species-specific ratio of specific growth rate of the cell mass and mitosis rate (μ_{gmax}/μ_m) at saturating light intensity

There is an important corollary of the obtained equations. As the last equation shows, it is possible to experimentally find the quantitative value of the species-specific ratio μ_{gmax}/μ_m. To do this, it is necessary to identify the distribution of growing or dividing cells in a continuous microalgae culture at saturating light intensity:

$$(i - i_{cp}) \geq 1,$$

$$\frac{\mu_{gmax}}{\mu_m} = \frac{1 - \Theta_g}{\Theta_g}; \; \frac{\mu_{gmax}}{\mu_m} = \frac{\Theta_m}{1 - \Theta_m}.$$

Relationship between specific growth rate in a culture and probability density of the age-specific cell state. First, we determine the relationship between the specific growth rate and the activities of cell transitions from one state to another. This requires some transformations:

$$\tau_z = \tau_g + \tau_m, \;\; \frac{\ln d}{\mu} = \frac{\ln d}{\mu_g} + \frac{\ln d}{\mu_m}, \;\; \frac{1}{\mu} = \frac{1}{\mu_g} + \frac{1}{\mu_m}, \;\; \mu = \frac{\mu_g \mu_m}{\mu_g + \mu_m}.$$

Comparing this result with the obtained probability density of age-specific cell states, we finally get:

$$\Theta_g = \frac{\mu_m}{\mu_g + \mu_m}, \;\; \Theta_m = \frac{\mu_g}{\mu_g + \mu_m},$$

$$\mu = \frac{\mu_g \mu_m}{\mu_g + \mu_m} = \mu_g \Theta_g = \mu_m \Theta_m.$$

The obtained relationship equations allow assessing the morphological structure of a microalgae cell population at different specific growth rates of a microalgae culture. This value is determined by a simple formula:

$$\frac{n_g}{N} = \Theta_g = \frac{\mu}{\mu_g};\ \frac{n_m}{N} = \Theta_m = \frac{\mu}{\mu_m}.$$

Conclusion. Based on the concept of two main phases that make up the cell life cycle – interphase and division phase, a probabilistic model of the dynamics of changes in the age-specific microalgae cell state in ontogenesis is developed.

The age-specific microalgae cell state is characterized by its biomass value, while transitions from one state to another are characterized by the activity of growth and division. For photolithotrophic conditions of microalgae cultivating, the interphase is regarded as a light-dependent process during which cell biomass grows. The division phase does not depend on light and starts after a cell reaches a certain mass.

A particular solution of the model is found for the dynamically equilibrium microalgae growth in culture at different light intensities. As shown, the activities of cell transitions from the growth state to the cytokinesis stage are species-specific microalgae culture parameters, and their quantitative ratio is constant at saturating light intensity.

It is shown that in a continuous microalgae culture under photolithotrophic conditions, the specific growth rate is related to the morphological structure of a cell population by simple directly proportional equations with species-specific coefficients. These coefficients are the maximum growth rate in the interphase (at saturating light intensity) and cell division activity in mitosis.

This work was carried out within the framework of IBSS state research assignment "Investigation of mechanisms of controlling production processes in biotechnological complexes with the aim of developing scientific foundations for production of biologically active substances and technical products of marine genesis" (No. 121030300149-0).

REFERENCES

1. Karlin S. Determinirovannyi rost populyatsii s raspredeleniem po vozrastam. In: Karlin S. *Osnovy teorii sluchainykh protsessov*. Moscow : Mir, 1968, pp. 387–395. (in Russ.)
2. Lelekov A. S., Trenkenshu R. P. Modeling of photosynthesis light curves by linear splines. *Ekologiya gidrosfery*, 2019, no. 2 (4), pp. 20–29. (in Russ.). https://doi.org/10.33624/2587-9367-2019-2(4)-20-29
3. Riznichenko G. Yu. *Lektsii po matematicheskim modelyam v biologii.* Moscow : Izd-vo RKhD, 2011, 560 p. (in Russ.)
4. Stepanova N. V. Matematicheskie modeli nepreryvnoi kul'tury mikroorganizmov, raspredelennykh po vozrastam i razmeram. In: *Matematicheskie modeli v ekologii*. Gorky : Izd-vo GGU, 1980, pp. 95–113. (in Russ.)
5. Stukolova I. V., Trenkenshu R. P. The main types of algae nutrition (short glossary). *Voprosy sovremennoi algologii*, 2020, no. 1 (22), pp. 34–38. (in Russ.). https://doi.org/10.33624/2311-0147-2020-1(22)-34-38
6. Trenkenshu R. P., Lelekov A. S., Novikova T. M. Linear growth of marine microalgae culture. *Morskoj biologicheskij zhurnal*, 2018, vol. 3, no. 1, pp. 53–60. (in Russ.). https://doi.org/10.21072/mbj.2018.03.1.06
7. Tsoglin L. N. *Tsikly razvitiya kletok i fiziologicheskie svoistva populyatsii mikrovodoroslei* : avtoref. dis. … d-ra biol. nauk : 03.00.12. Moscow, 1996, 77 p. (in Russ.)
8. Tsoglin L. N., Klyachko-Gurvich G. L. Changes in functional activity of the chloroplast in the chlorella cell cycle. *Fiziologiya rastenii*, 1980, vol. 27, no. 6, pp. 1172–1179. (in Russ.)
9. Tsoglin L. N., Pronina N. A. *Biotekhnologiya mikrovodoroslei.* Moscow : Nauchnyi mir, 2012, 184 p. (in Russ.)

10. Cvrčková F. A brief history of eukaryotic cell cycle research. In: *Concepts in Cell Biology – History and Evolution* / V. P. Sahi, F. Baluška (Eds). Cham, Switzerland : Springer, 2018, pp. 67–93. (Plant Cell Monographs (CELLMONO ; vol. 23)). https://doi.org/10.1007/978-3-319-69944-8_4
11. Helmstetter Ch. E. A ten-year search for synchronous cells: Obstacles, solutions, and practical applications. *Frontiers in Microbiology*, 2015, vol. 6, art. no. 238 (10 p.). https://doi.org/10.3389/fmicb.2015.00238
12. Novák B., Tóth A., Csikász-Nagy A., Györffy B., Tyson J. J., Nasmyth K. Finishing the cell cycle. *Journal of Theoretical Biology*, 1999, vol. 99, iss. 2, pp. 223–233. https://doi.org/10.1006/jtbi.1999.0956
13. Pederson T. Historical review: An energy reservoir for mitosis, and its productive wake. *Trends in Biochemical Sciences*, 2003, vol. 28, iss. 3, pp. 125–129. https://doi.org/10.1016/s0968-0004(03)00030-6
14. Sasabe M., Machida Y. Signaling pathway that controls plant cytokinesis. In: *Signaling Pathways in Plants* / Y. Machida, C. Lin, F. Tamanoi (Eds). London ; San Diego ; Oxford : Academic Press, 2014, chap. 6, pp. 145–165. (The Enzymes ; vol. 35). https://doi.org/10.1016/B978-0-12-801922-1.00006-3
15. Sible J. C., Tyson J. J. Mathematical modeling as a tool for investigating cell cycle control networks. *Methods*, 2007, vol. 41, iss. 2, pp. 238–247. https://doi.org/10.1016/j.ymeth.2006.08.003
16. Tyson J. J., Novák B. Regulation of the eukaryotic cell cycle: Molecular antagonism, hysteresis, and irreversible transitions. *Journal of Theoretical Biology*, 2001, vol. 210, iss. 2, pp. 249–263. https://doi.org/10.1006/jtbi.2001.2293
17. Tyson J. J., Novák B. Temporal organization of the cell cycle. *Current Biology*, 2008, vol. 18, iss. 17, pp. R759–R768. https://doi.org/10.1016/j.cub.2008.07.001
18. Tyson J. J., Novák B. Models in biology: Lessons from modeling regulation of the eukaryotic cell cycle. *BMC Biology*, 2015, vol. 13, iss. 1, art. no. 46 (10 p.). https://doi.org/10.1186/s12915-015-0158-9
19. Wang J. D., Levin P. A. Metabolism, cell growth and the bacterial cell cycle. *Nature Reviews Microbiology*, 2009, vol. 7, iss. 11, pp. 822–827. https://doi.org/10.1038/nrmicro2202
20. Wilkins A. S., Holliday R. The evolution of meiosis from mitosis. *Genetics*, 2009, vol. 181, iss. 1, pp. 3–12. https://doi.org/10.1534/genetics.108.099762
21. Winter A. W. Ueber die Vermehrung der Pflanzen-Zellen durch Theilung. [dissertation]. Tübingen : L. F. Fues, 1835. 20 S.

СВЯЗЬ РОСТОВЫХ ХАРАКТЕРИСТИК КУЛЬТУР МИКРОВОДОРОСЛЕЙ С ВОЗРАСТНЫМ СОСТОЯНИЕМ КЛЕТОК В ОНТОГЕНЕЗЕ (ВЕРОЯТНОСТНАЯ МОДЕЛЬ)

Р. П. Тренкеншу

ФГБУН ФИЦ «Институт биологии южных морей имени А. О. Ковалевского РАН»,
Севастополь, Российская Федерация
E-mail: *r.trenkenshu@rambler.ru*

В работе представлена количественная модель зависимости морфологической структуры непрерывной культуры микроводорослей от внешнего освещения и видоспецифических параметров клеток. В основе моделирования лежит представление о двух ключевых фазах, составляющих жизненный цикл клетки, — интерфазе и фазе деления. Интерфаза рассматривается как светозависимый процесс, при котором происходит рост биомассы клетки. Фаза деления не зависит от света и наступает после достижения клеткой определённой массы, равной (или большей) сумме масс дочерних клеток. Заканчивается стадия деления цитокинезом — полным разделением клетки на дочерние. Возрастное состояние микроводорослевой клетки характеризуется

величиной её биомассы, а переходы из одного состояния в другое — активностью (роста и деления). Модель представлена системой дифференциальных уравнений, полностью описывающих динамику процесса онтогенеза. Проанализировано частное решение модели для динамически равновесного роста микроводорослей в культуре при различной интенсивности света. Показано, что в непрерывной культуре микроводорослей, растущей фотолитотрофно, удельная скорость роста связана с морфологической структурой популяции клеток простыми прямо пропорциональными уравнениями с видоспецифическими коэффициентами — максимальной скоростью роста в интерфазе (при насыщающей интенсивности света) и активностью деления клеток при митозе.

Ключевые слова: микроводоросли, онтогенез, возрастное состояние, интерфаза, митоз, вероятностная модель, скорость роста, морфологическая структура культуры

1871
ИнБЮМ – IBSS

Морской биологический журнал
Marine Biological Journal
2023, vol. 8, no. 1, pp. 109–112
https://marine-biology.ru

NOTES

UDC [582.273:581.9](265.2/.5)

ON THE DISTRIBUTION OF MARINE ALGA *LUKINIA DISSECTA* PERESTENKO (RHODYMENIACEAE, RHODYMENIALES) IN THE NORTHERN PACIFIC

© 2023 **O. N. Selivanova and G. G. Zhigadlova**

Kamchatka Branch of the Pacific Geographical Institute, Far Eastern Branch
of the Russian Academy of Sciences, Petropavlovsk-Kamchatsky, Russian Federation
E-mail: *oselivanova@mail.ru*

Received by the Editor 05.04.2022; after reviewing 08.06.2022;
accepted for publication 20.10.2022; published online 14.03.2023.

The red alga *Lukinia dissecta*, previously found in a laboratory marine aquarium containing water and substrate (bottom stones and broken shells) from the Avacha Bay (the Southeastern Kamchatka), was first discovered in natural conditions in the Eastern Kamchatka waters. This significantly broadens the concept of the range of the species, which was previously considered disjunctive and exclusively insular. Based on new findings, the species range is reported as extended and, apparently, continuous. The availability of *L. dissecta* samples from Alaska (USA) in the authors' possession made it possible to consider the species as a boreal interzonal pan-Pacific one.

Keywords: *Lukinia*, Kamchatka, range, pan-Pacific species

The species *Lukinia dissecta* Perestenko, 1996 (Rhodophyta), described by L. Perestenko [1994] and assigned by her to the order Gigartinales, long remained a taxon with an unclear systematic position at the family level. However, recently, the researchers from the Far East [Shibneva et al., 2022] carried out a radical review of *L. dissecta* status and came to an unambiguous conclusion that the species belongs to the family Rhodymeniaceae within the order Rhodymeniales.

During our studies in a laboratory marine aquarium containing substrate and water from the Avacha Bay (the Southeastern Kamchatka), algae new to this region were found, including *L. dissecta* [Selivanova, Zhigadlova, 2022]. We suggested that the presence of unusual algae in the aquarium may indicate their occurrence in the Avacha Bay water, and it was justified in terms of *L. dissecta*: the species was soon discovered in the Kamchatka water area. The data on the findings are shown in Figs 1 and 2 (water areas 2 and 3).

The aim of this work was to clarify the range of *L. dissecta* taking into account all currently known data on the distribution of this algae.

MATERIAL AND METHODS

Aquarium and natural algae sampled near the Southeastern Kamchatka were identified under an Olympus CX31 light microscope. When identifying the material, a comparison was made with the original taxon description and data from other publications on this species [Klochkova et al., 2009; Lopatina, Klochkova, 2016; Perestenko, 1994; Shibneva et al., 2022]. The samples were photographed with an Olympus SZ-20 digital camera. The studied material is stored in the laboratory of hydrobiology of the Kamchatka Branch of the Pacific Geographical Institute.

RESULTS AND DISCUSSION

The study of our *L. dissecta* samples showed their close morphological similarity with representatives of the genera *Palmaria* Stackhouse, 1802 and *Sparlingia* G. W. Saunders, I. W. Strachan et Kraft, 1999. *L. dissecta* also has a narrow wedge-shaped base and a lamellar part widened upwards with varying degree of the apex dissection (the apex from almost non-dissected to deeply dissected). The polymorphic appearance of plants is shown in Fig. 1. However, *L. dissecta* differs from representatives of closely related genera in the structure of subcortical and medulla cells, as well as in the structure of the cystocarp [Lopatina, Klochkova, 2016; Shibneva et al., 2022]. This allows to reliably distinguish its specimens from closely related ones.

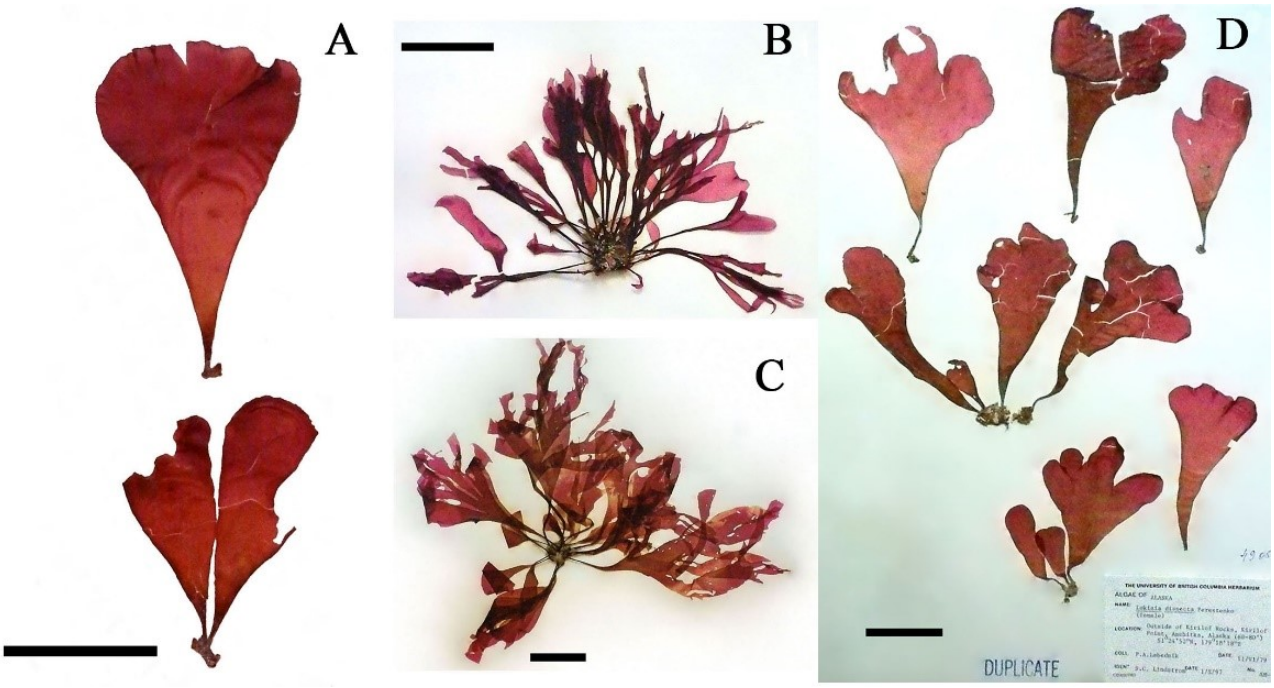

Fig. 1. *Lukinia dissecta* from different habitats: sampled at the Commander Islands (A), at Cape Baraniy (B), in Vestnik Bay (C), and at Amchitka Island (D). Scale: A, D, 4.5 cm; B, C, 3 cm

Our information on *L. dissecta* distribution differs from the data obtained earlier. Specifically, it was considered that *L. dissecta* occurs in Russian waters of the Far East alone and, in addition to the Commander Islands (its typical habitat), is distributed near Sakhalin and the Kuril Islands [Klochkova et al., 2009; Lopatina, Klochkova, 2016; Perestenko, 1994]. However, *L. dissecta* findings first in the laboratory

marine aquarium containing bottom sediments and water from the Avacha Bay [the Southeastern Kamchatka] [Selivanova, Zhigadlova, 2022] and then in the Eastern Kamchatka water area [Cape Baraniy (the Avacha Bay) and Vestnik Bay (the Southeastern Kamchatka) (Fig. 2, water areas 2 and 3, respectively)] significantly expanded the understanding of its range. It is quite natural that *Lukinia* described from the Commander Islands and then found much further south, on Sakhalin and Kuriles, could only get there through the Kamchatka water area. Moreover, our herbarium specimens of this alga, kindly sent by Dr. Sandra C. Lindstrom (University of British Columbia, Canada), sampled in Alaska (USA) (Fig. 2, water area 6), allowed us to assume an even more extended and continuous range of *L. dissecta* in the northern Pacific Ocean [Selivanova, Zhigadlova, 2022]. This is shown in Fig. 2.

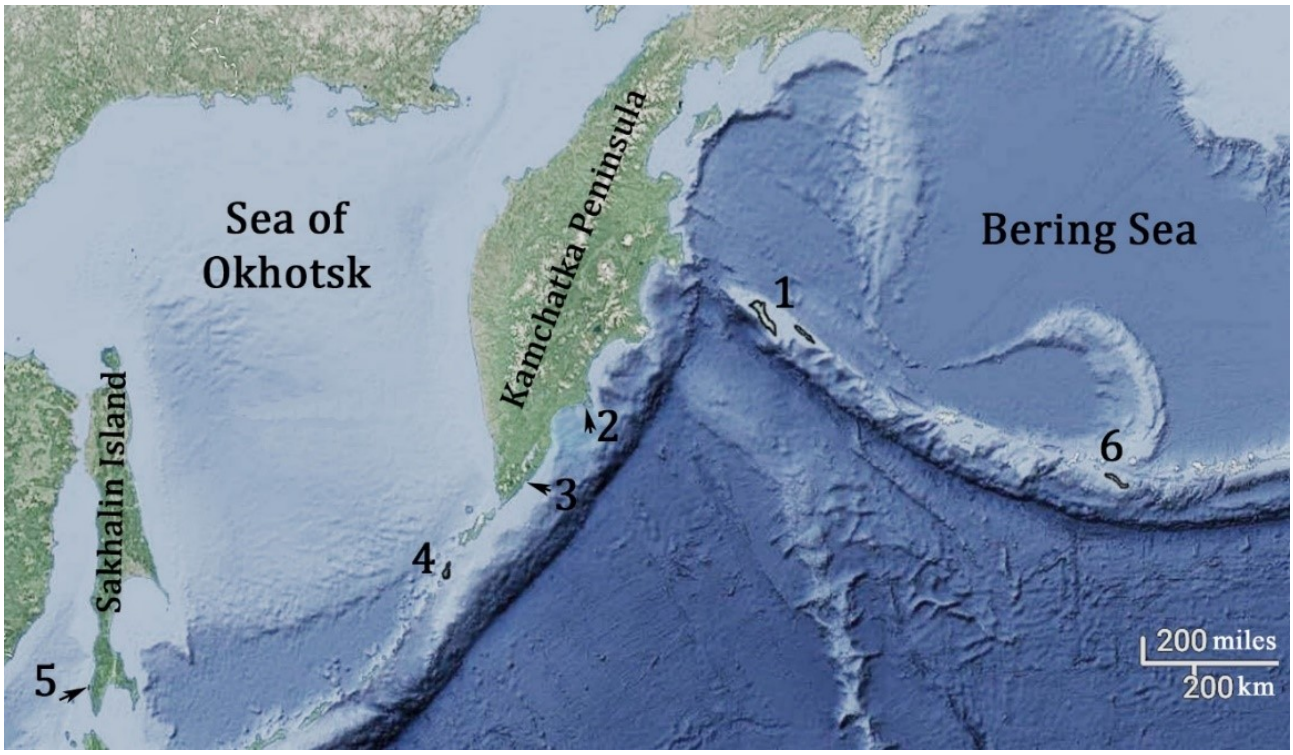

Fig. 2. Location map of *Lukinia dissecta* in the Northern Pacific. Russian water area: the Commander Islands (1); Cape Baraniy (the Avacha Bay) (2); Vestnik Bay (the Southeastern Kamchatka) (3); the Onekotan Island (the Northern Kuriles) (4); Cape Lopatin (the Sakhalin Island) (5). American sector: Amchitka Island (the Aleutian Islands, Alaska, USA) (6)

Conclusion. The study of *Lukinia dissecta* from the Avacha Bay showed that this species has an extended range in the Northern Pacific (from the Commander Islands to Sakhalin and the Kuriles through the Eastern Kamchatka), though it was previously considered disjunctive and exclusively insular. The occurrence of *L. dissecta* in Alaska led to the conclusion that this species is even more widespread in the Pacific Ocean and should be considered as a boreal interzonal pan-Pacific (also found in the American sector).

Acknowledgement. We thank our colleagues for their participation in the algae sampling and Sandra C. Lindstrom (Canada) for providing alga herbarium specimens.

REFERENCES

1. Klochkova N. G., Koroleva T. N., Kusidi A. E. *Marine Algae of Kamchatka and Surrounding Areas.* Vol. 2. *Red Seaweeds.* Petropavlovsk-Kamchatsky : KamchatNIRO Publishing, 2009, 303 p. (in Russ.)
2. Lopatina N. A., Klochkova N. G. The genus *Lukinia* (Rhodophyta: Gigartinales) in the Far-Eastern seas of Russia. *Vestnik Kamchatskogo gosudarstvennogo tekhnicheskogo universiteta*, 2016, no. 36, pp. 74–78. (in Russ.). https://doi.org/10.17217/2079-0333-2016-36-74-78
3. Perestenko L. P. *Red Algae of the Far-Eastern Seas of Russia.* Saint Petersburg : Olga, 1994, 331 p. (in Russ.)
4. Selivanova O. N., Zhigadlova G. G. On the finding of algae new to Southeastern Kamchatka in a laboratory marine aquarium. *Biologya morya*, 2022, vol. 48, no. 2, pp. 129–134. (in Russ.). https://doi.org/10.1134/S1063074022020092
5. Shibneva S. Yu., Skriptsova A. V., Semenchenko A. A. Molecularly assisted taxonomic studies of marine red algae from the north-western Pacific: Establishing the ordinal and family positions of the genus *Lukinia* and the monospecific status of the genus *Sparlingia* (Rhodymeniales). *Phycologia*, 2022, vol. 61, iss. 1, pp. 37–44. https://doi.org/10.1080/00318884.2021.1988488

О РАСПРОСТРАНЕНИИ МОРСКОЙ ВОДОРОСЛИ *LUKINIA DISSECTA* PERESTENKO (RHODYMENIACEAE, RHODYMENIALES) В СЕВЕРНОЙ ПАЦИФИКЕ

О. Н. Селиванова, Г. Г. Жигадлова

Камчатский филиал Тихоокеанского института географии ДВО РАН,
Петропавловск-Камчатский, Российская Федерация
E-mail: *oselivanova@mail.ru*

Красная водоросль *Lukinia dissecta*, которую ранее нашли в лабораторном морском аквариуме, содержащем грунт и воду из Авачинского залива (Юго-Восточная Камчатка), впервые обнаружена в природных условиях в акватории Восточной Камчатки. Это значительно расширяет представления об ареале вида, который ранее считали дизъюнктивным и исключительно островным. На основании новых находок ареал вида признан протяжённым и, по-видимому, непрерывным, а наличие у авторов образцов *L. dissecta* с Аляски (США) позволило рассматривать вид как бореальный интерзональный панпацифический.

Ключевые слова: *Lukinia*, Камчатка, ареал, панпацифический вид

1871
ИнБЮМ – IBSS

Морской биологический журнал
Marine Biological Journal
2023, vol. 8, no. 1, pp. 113–118
https://marine-biology.ru

CHRONICLE AND INFORMATION

UDC 574.5(091)

OUTSTANDING RUSSIAN ZOOLOGIST AND HYDROBIOLOGIST VLADISLAV KHLEBOVICH, ON HIS 90th BIRTHDAY

© 2023 **N. V. Shadrin[1], M. I. Orlova[2,3], E. V. Anufriieva[1], and A. O. Smurov[3]**

[1]A. O. Kovalevsky Institute of Biology of the Southern Seas of RAS, Sevastopol, Russian Federation
[2]Saint Petersburg Research Center of the Russian Academy of Sciences, Saint Petersburg, Russian Federation
[3]Zoological Institute of Russian Academy of Sciences, Saint Petersburg, Russian Federation
E-mail: *lena_anufriieva@mail.ru*

Received by the Editor 14.01.2023; after reviewing 14.01.2023;
accepted for publication 20.10.2022; published online 14.03.2023.

In 2022, Professor Vladislav Khlebovich, a prominent zoologist and hydrobiologist, turned 90. This essay is a brief review of his diverse activity and contribution to science.

Keywords: Khlebovich, main results, salinity, evolution, ecology

"Without emotions, without passion,
there can be no science."
S. Korolev
(cited from: [Khlebovich, 2017d])

The results of research by D. Sc., Professor Vladislav Khlebovich are reflected in scientific publications that have become classics [Khlebovich, 1974, 1981, 1996], in the articles published in the last decade [Smirnov et al., 2015; Khlebovich, 2013a, b, c, 2014a, b, 2015a, b, c, d, e, f, 2016, 2017a, b, c, 2018, 2019, 2020, Khlebovich, Ivanov, 2018], and in memoirs. All these works form a whole layer in understanding the physiological, ecological, and evolutionary role of the salinity factor, autecology [Khlebovich, 2015d], and fine mechanisms of physiological and behavioral reactions of aquatic invertebrates [Khlebovich, 2015b] inhabiting marine and continental waters, especially the most variable aquatic systems – estuaries [Khlebovich, 2019]. His interests are so diverse that it is hard to set the boundaries. In 2022, V. Khlebovich turned 90.

Photo from http://casp-geo.ru/

An outstanding Russian zoologist was born on 27 February, 1932, in Voronezh. He spent his first years in the Voronezh Natural Reserve, where his father, Vilgelm Khlebovich, worked in 1933–1939 as deputy director for science, and his mother, Vera, was a weather observer. In the autobiography [2017d], Vladislav Khlebovich recalls: "When I was a child, the world of the forest cut by the Usmanka River (in Tatar, *beauty*) seemed endless… Because of the reserve, I have always wanted to be a biologist and became one." In 1939, his father began working at the Voronezh University as an associate professor at the zoology department, which was headed by his teacher – Konstantin Saint-Hilaire[1]. In the same year, the future biologist went to a Voronezh school. In the years of the war, the family was evacuated to the Voronezh Nature Reserve (1942). His father joined the militia.

In 1945, the family moved to the city of Braslav (Western Belarus), to the father's homeland. In 1949, V. Khlebovich graduated from a Braslav school with a silver medal and realized his dream – entered the biology and soil faculty of the Leningrad State University and chose the invertebrate zoology department. His studies at the university began with the lectures of Valentin Dogiel[2] – the author of *Zoology of Invertebrates*. With this textbook, the university life of most Soviet biology students (belonging to the generations of the authors of this article) usually began, both in leading and provincial universities. In 2022, V. Dogiel would have turned 110.

In 1954, Vladislav Khlebovich graduated with honors from the university. His project was focused on polychaetes. He entered the PhD graduate school at the Zoological Institute of the Academy of Sciences of the Soviet Union and continued studying polychaetes under the guidance of Pavel Ushakov (1903–1992). He always talks about his teacher with gratitude and great respect [2017d]. In 1959, he defended his PhD thesis *Polychaeta Worms of the Littoral of the Kuril Islands*. After a vacation spent at the Kaliningrad Biological Station, even *prior* to defending his PhD thesis, V. Khlebovich, as he uses to say, "fell ill": "It was at this ornithological station that I got the virus of my main scientific interests – Nereididae and the salinity factor." These interests led him to a series of discoveries and generalizations that brought fame and respect among colleagues all over the world. His monograph on polychaetes was published in the *Fauna of Russia* series [Khlebovich, 1996].

In 1960, he began his research on salinity adaptations; later, he developed the concept of critical salinity of biological processes [Khlebovich, 1974], which received wide international recognition and was further deepen in his works [Smirnov et al., 2015; Khlebovich, 2014a, 2015c]. In 1971, he defended his D. Sc. dissertation *The Concept of Critical Salinity in Zoology*. In three years, Vladislav Khlebovich published the monograph *The Critical Salinity of Biological Processes* [1974]. The development of ideas and the acquisition of new data resulted in the publication of another scientific work – *The Acclimation of Animal Organisms* [1981]. In 2008, he was awarded the prestigious prize for biologists "for a series of works on the topic *The Salinity Factor in Zoology*" – Pavlovsky Prize of the Russian Academy of Sciences.

[1]K. Saint-Hilaire (1866–1941), Russian and Soviet zoologist, hydrobiologist, organizer of the first biological station in the Russian Empire [in the Kandalaksha Bay of the White Sea (Kovda)], Professor at the Yuryev and Voronezh universities.

[2]V. Dogiel (1882–1955), Russian and Soviet zoologist, corresponding member of the Academy of Sciences of the Soviet Union (1939), D. Sc., Professor, the Lenin Prize winner.

One of the results of his work in this direction was the creation of a scientific school recognized by the scientific community: he brought up a whole generation of researchers, *inter alia* PhD and D. Sc. Analyzing salinity adaptations and osmoregulation in hydrobionts, he substantiated the concepts of physiologically freshwater animals of marine origin [Khlebovich, Komendantov, 1985]. At present, his concepts are developed by numerous students and followers, including the authors of this article.

It is impossible not to recall many years of his interest in the issues of phenotypic adaptations and the theory of evolution in general. Assuming that an individual should be considered as an indivisible quantum of life, V. Khlebovich is focused on the ecology of individuals [2012]. He experimentally showed that modification variability is often based on the inclusion by the environment of alternative hereditary programs (those are present in the genotype of an individual). He established that one of the ways of diversification is the formation of species *via* sequential creation and "falling out" of alternative norms of gene expression. To date, this is confirmed by the works of molecular geneticists.

He was an active participant and organizer of several expeditions aimed at studying the Far Eastern and Arctic coastal regions of our country. I remember, for example, 1971 (N. Sh.): the Barents Sea, in the scientific village of Dalnie Zelentsy, on a used hunting schooner, two expeditions of the Zoological Institute live and work – *Freshwater Life* (headed by not yet an Academician A. Alimov) and *Salty Distances* (headed by V. Khlebovich). In 1993 and 1994, he headed the Russian–American expeditions aimed at studying the Arctic estuaries. In his life, there was the Chernobyl period as well. Specifically, for many years, Vladislav Khlebovich was a member of a complex radioecological expedition in the ecology section of the integrated program to eliminate the consequences of the disaster at the Chernobyl nuclear power plant. In 1987, he was awarded a diploma. In 1997, he was awarded the medal *For Saving the Dying*.

Speaking of V. Khlebovich, it is impossible not to mention the versatility of his talents. According to him, after the famous ornithologist Aleksey Malchevskiy[3], he was the best bird impersonator in Leningrad. He is an outstanding organizer of science as well: for 12 years, he headed the Belomorsk Biological Station of the Zoological Institute and made it the best in the USSR. He wrote the book *Kartesh and Around* [2007] about this. Is it worth listing everything that this amazing person has done and continues to do? He has his own vision of many things that go far beyond the scope of his professional scientific activity. He is an incredibly interesting speaker. He became the author of several popular science books [Khlebovich, 1987, 1991, 2015g]. Through the prism of biology, he is not afraid to consider human problems, and this is confirmed by his articles in the literary magazine *Zarya* (no. 5, 2002) *This Is Our Beginningless World… Biological Models of Human Societies* and in the newspaper *Novaya Gazeta* (15.06.2005) *In the Structure of the Brain, There Is No President*. Moreover, he is one of the creators of public aquariums in Saint Petersburg.

The concept of active creative longevity is strongly associated with Vladislav Khlebovich. Having celebrated his 80th birthday, which we wrote about as well [Shadrin et al., 2012], he published a series of interesting papers on the role of potassium in animal evolution. Developing the ideas of his co-author,

[3] A. Malchevskiy (1915–1985), one of the leading Soviet ornithologists, dean of the biology and soil faculty of the Leningrad State University (1969–1973).

friend, and peer, Academician of the Russian Academy of Sciences Yury Natochin[4], he convincingly showed that life originated in the potassium environment, and Na^+/K^+-ATPase played a key role in animal evolution. An insight on the fundamental works, on activity aimed at popularizing scientific knowledge, and on philosophical reflections of V. Khlebovich in the decade between two jubilees can be gained from the reference list at the end of this article.

Vladislav Khlebovich is in creative search, and we – his friends, followers, and students – wish him strong health and success!

REFERENCES

1. Smirnov A. V., Khlebovich V. V. Marine biologist V. V. Kuznetsov: All life at the front line. *Priroda*, 2015, no. 5 (1197), pp. 80–84. (in Russ.)
2. Khlebovich V. V. *The Critical Salinity of Biological Processes.* Leningrad : Nauka, 1974, 236 p. (in Russ.)
3. Khlebovich V. V. *Akklimatsiya zhivotnykh organizmov.* Leningrad : Nauka, 1981, 136 p. (in Russ.)
4. Khlebovich V. V. *Poka eshche ne domashnie.* Moscow : Agropromizdat, 1987, 160 p. (in Russ.)
5. Khlebovich V. V. *Agrozoologiya.* Moscow : Agropromizdat, 1991, 172 p. (in Russ.)
6. Khlebovich V. V. *Mnogoshchetinkovye chervi semeistva Nereidae morei Rossii i sopredel'nykh vod.* Saint-Petersburg : Nauka, 1996, 223 p. (Fauna of Russia and neighbouring countries ; vol. 22). (in Russ.)
7. Khlebovich V. V. *Kartesh i okolo.* Moscow : WWF Rossii, 2007, 72 p. (in Russ.)
8. Khlebovich V. V. *Ekologiya osobi (ocherki fenotipicheskikh adaptatsii zhivotnykh).* Saint Petersburg : ZIN RAN, 2012, 143 p. (in Russ.)
9. Khlebovich V. V. The experience in the graphs analysis of the experimental and field hydrobiological data. *Astrakhanskii vestnik ekologicheskogo obrazovaniya*, 2013a, no. 2 (24), pp. 71–81. (in Russ.)
10. Khlebovich V. V. Critical salinity – homeostasis – sustainable development. *Proceedings of the Zoological Institute RAS*, 2013b, vol. 317, suppl. 3, pp. 3–6. (in Russ.)
11. Khlebovich V. V. To the 75th anniversary of BBS [Nikolai Pertsov White Sea Biological Station] MGU. *Priroda*, 2013c, no. 4 (1172), pp. 42–43. (in Russ.)
12. Khlebovich V. V. Milestones and principles of evolution of water–salt relationships in living organisms. *Biosfera*, 2014a, vol. 6, no. 2, pp. 170–175. (in Russ.)
13. Khlebovich V. V. Sketches of protoevolution. *Priroda*, 2014b, no. 8 (1188), pp. 93–94. (in Russ.)
14. Khlebovich V. V. Critical salinity as a marker of transition from the potassium to sodium stage of life development. *Uspekhi sovremennoi biologii*, 2015a, vol. 135, no. 1, pp. 18–20. (in Russ.)
15. Khlebovich V. V. Applied aspects of the concept of critical salinity. *Uspekhi sovremennoi biologii*, 2015b, vol. 135, no. 3, pp. 272–278. (in Russ.)
16. Khlebovich V. V. Presumption of the marine beginning in the animal physiology and ecology. *Proceedings of the Zoological*

[4]Yu. Natochin (born 1932), Soviet and Russian scientist, physiologist, and evolutionist, Academician of the Russian Academy of Sciences, D. Sc.

Institute RAS, 2015c, vol. 319, no. 4, pp. 536–544. (in Russ.)
17. Khlebovich V. V. Origin of life and animals. *Priroda*, 2015d, no. 6 (1198), pp. 69–71. (in Russ.)
18. Khlebovich V. V. Individual as a quantum of life. *Russkii ornitologicheskii zhurnal*, 2015e, vol. 24, no. 1188, pp. 3265–3273. (in Russ.)
19. Khlebovich V. V. New window to epigenetics. *Russkii ornitologicheskii zhurnal*, 2015f, vol. 24, no. 1231, pp. 4639–4653. (in Russ.)
20. Khlebovich V. V. *Zhivotnye i my.* Moscow : KDU, 2015g, 49 p. (in Russ.)
21. Khlebovich V. V. On predator–prey taxocenes. *Biosfera*, 2016, vol. 8, no. 2, pp. 151–154. (in Russ.)
22. Khlebovich V. V. Memoirs of Vladimir Lvovich Wagin. *Uchenye zapiski Kazanskogo universiteta. Seriya Estestvennye nauki*, 2017a, vol. 159, no. 3, pp. 361–366. (in Russ.)
23. Khlebovich V. V. Adaptivnye reaktsii organizma v menyayushcheisya srede. *Nauka – shkole* : sbornik nauchnykh publikatsii / Rossiiskaya akademiya nauk, Sankt-Peterburgskii nauchnyi tsentr. Saint Petersburg : Art-Ekspress, 2017b, iss. 6, pp. 33–46. (in Russ.)
24. Khlebovich V. V. Acclimation of animal organisms: Basic theory and applied aspects. *Uspekhi sovremennoi biologii*, 2017c, vol. 137, no. 1, pp. 20–28. (in Russ.)
25. Khlebovich V. *Kadry iz zhizni odnogo zoologa. Vospominaniya.* Moscow : Novyi khronograf, 2017d, 336 p. (in Russ.)
26. Khlebovich V. V. On strategic solutions of living nature. *Uspekhi sovremennoi biologii*, 2018, vol. 138, no. 6, pp. 627–630. (in Russ.)
27. Khlebovich V. V., Ivanov V. V. Estuarine ecosystems and their place in natural river mouth complexes of the Arctic (by the example of the Yenisey mouth area). *Uspekhi sovremennoi biologii*, 2018, vol. 138, no. 2, pp. 218–224. (in Russ.)
28. Khlebovich V. V. About the origin and fate of extraterrestrial civilizations. *Uspekhi sovremennoi biologii*, 2019, vol. 139, no. 2, pp. 206–208. (in Russ.)
29. Khlebovich V. V. The Tree of Life – animals – man – science. *Russkii ornitologicheskii zhurnal*, 2020, vol. 29, no. 1923, pp. 2192–2195. (in Russ.)
30. Khlebovich V. V., Komendantov A. Yu. On physiologically freshwater invertebrates of marine origin. *Zhurnal obshchei biologii*, 1985, vol. 46, no. 3, pp. 331–335. (in Russ.)
31. Shadrin N. V., Shulman G. E., Zaika V. E., Aladin N. V., Plotnikov I. S., Smurov A. O. Jubilee of DS (biol.), Prof. Vladislav Vil'hel'movich Khlebovich. *Morskoj ekologicheskij zhurnal*, 2012, vol. 11, no. 4, pp. 108–109. (in Russ.)

ВЫДАЮЩИЙСЯ ОТЕЧЕСТВЕННЫЙ ЗООЛОГ И ГИДРОБИОЛОГ ВЛАДИСЛАВ ВИЛЬГЕЛЬМОВИЧ ХЛЕБОВИЧ, К 90-ЛЕТИЮ

Н. В. Шадрин[1], М. И. Орлова[2,3], Е. В. Ануфриева[1], А. О. Смуров[3]

[1]ФГБУН ФИЦ «Институт биологии южных морей имени А. О. Ковалевского РАН»,
Севастополь, Российская Федерация

[2]Санкт-Петербургский научный центр Российской академии наук,
Санкт-Петербург, Российская Федерация

[3]Зоологический институт Российской академии наук, Санкт-Петербург, Российская Федерация
E-mail: *lena_anufriieva@mail.ru*

В 2022 г. исполнилось 90 лет выдающемуся зоологу и гидробиологу — профессору Владиславу Вильгельмовичу Хлебовичу. Очерк представляет собой краткий обзор его многогранной деятельности и вклада в науку.

Keywords: Khlebovich, main results, salinity, evolution, ecology

1871
ИнБЮМ – IBSS

Морской биологический журнал
Marine Biological Journal
2023, vol. 8, no. 1, pp. 119–120
https://marine-biology.ru

ON THE ANNIVERSARY OF D. SC., PROF. ALEKSANDER SOLDATOV

On 31 October, 2022, the outstanding hydrobiologist Aleksander Soldatov celebrated his 65th birthday – D. Sc., Prof., chief researcher, and head of IBSS animal physiology and biochemistry department.

A. Soldatov has devoted more than 30 years to work at the institute. He has been working at the animal physiology and biochemistry department for more than 20 years and has headed it since 2008.

Aleksander Soldatov is a highly qualified specialist in ecological physiology and biochemistry of hydrobionts who enjoys a well-deserved reputation both in Russia and abroad. He is the author of more than 270 publications, *inter alia* 3 collective monographs.

He is the supervisor of six successfully defended PhD theses and leads many research projects. His scientific activity is diverse. It was he who proposed a classification of hypoxic conditions for hydrobionts, determined the mechanisms of short- and long-term regulation of tissue partial pressure of oxygen in marine fish, and studied the significance of tissue lipid level in correcting the diffusion capacity of skeletal muscles in terms of oxygen. Moreover, he established the fact of low diffusion capacity of the histo-hematic barrier in lower vertebrates.

A. Soldatov deeply studied hematopoiesis processes in teleost fish. For the first time, he established the fact of monocycles in the functioning of the erythroid germ of the hematopoietic tissue during the annual cycle and showed its relationship with spawning. He discovered and described colony-forming units in the hematopoietic tissue (anterior kidneys, spleen). Under experimental conditions, he analyzed the effect of hypoxia and hypothermia on hematopoiesis. He reported the process of balanced inhibition of membrane and metabolic functions (metabolic arrest) in fish red blood cells during adaptation to extreme external conditions. Also, he determined the morphological and functional characteristics of erythroid blood elements during cellular differentiation.

He described the functional effects of the use of anesthetics on teleost fish. Moreover, he developed a methodology for applying urethane anesthesia during experimental studies.

Under the leadership of Aleksander Soldatov, complex field and experimental research was carried out: functional, metabolic, and molecular bases of adaptation of representatives of the Black Sea malacofauna to existence under conditions of extreme ecotopes (hypoxia (anoxia), hydrogen sulfide load,

and hypo- and hyperosmotic environments) were studied. Within the framework of these investigations, the results were obtained that reflect the state of cellular systems and antioxidant enzymatic complex; qualitative and quantitative composition of carotenoids was determined.

A. Soldatov is a talented scientist and an outstanding mentor generously sharing his experience with new generations of researchers. For more than 20 years, he has been teaching at the Sevastopol State University (department of technogenic safety and metrology) and in several other universities in Sevastopol, and he is one of the best lecturers in the city in hydrobiology, physiology, and ecology. Currently, he supervises the work of four postgraduate students and serves as a professor of IBSS postgraduate department. At SevSU, he graduated about 15 masters and 30 bachelors.

To date, Aleksander Soldatov is a member of the expert council of the Higher Attestation Commission and chairman of IBSS scientific council. Moreover, he serves on editorial boards of several scientific journals, as well as dissertation councils of our institute and V. I. Vernadsky Crimean Federal University. For some years, he was involved in activity of program committees of key scientific conferences in hydrobiology and physiology.

For the work done, he was awarded the titles of Honorary Worker of Science and High Technologies (Ministry of Science and Higher Education of the Russian Federation, 2021) and Professor of the Year (Russian Professors' Meeting, 2021).

A. Soldatov is a helpful person and a wonderful family man. This eminent hydrobiologist is a true enthusiast of his work, who inspires with his passion and instills a love for science in young researchers.

On behalf of all colleagues, friends, and grateful students, we congratulate dear Aleksander Soldatov on his anniversary! We wish success in further work, new discoveries, great accomplishments, happiness, and prosperity!

Team of IBSS animal physiology and biochemistry department

К ЮБИЛЕЮ ДОКТОРА БИОЛОГИЧЕСКИХ НАУК, ПРОФЕССОРА АЛЕКСАНДРА АЛЕКСАНДРОВИЧА СОЛДАТОВА

31 октября 2022 г. исполнилось 65 лет Александру Александровичу Солдатову — д. б. н., проф., руководителю отдела физиологии животных и биохимии ФИЦ ИнБЮМ. Александр Александрович является специалистом в области экологической физиологии и биохимии морских организмов, автором более чем 270 научных публикаций, председателем учёного совета ФИЦ ИнБЮМ и заместителем главного редактора «Морского биологического журнала».

ISSN 2499-9768 23001
9 772499 976005 >

Вниманию читателей!

Институт биологии южных морей имени А. О. Ковалевского РАН, Зоологический институт РАН

издают научный журнал

Морской биологический журнал
Marine Biological Journal

- МБЖ — периодическое издание открытого доступа. Подаваемые материалы проходят независимое двойное слепое рецензирование. Журнал публикует обзорные и оригинальные научные статьи, краткие сообщения и заметки, содержащие новые данные теоретических и экспериментальных исследований в области морской биологии, материалы по разнообразию морских организмов, их популяций и сообществ, закономерностям распределения живых организмов в Мировом океане, результаты комплексного изучения морских и океанических экосистем, антропогенного воздействия на морские организмы и экосистемы.
- Целевая аудитория: биологи, экологи, биофизики, гидро- и радиобиологи, океанологи, географы, учёные других смежных специальностей, аспиранты и студенты соответствующих научных и отраслевых профилей.
- Статьи публикуются на русском и английском языках.
- Периодичность — четыре раза в год.
- Подписной индекс в каталоге «Пресса России» — Е38872. Цена свободная.

Заказать журнал

можно в научно-информационном отделе ИнБЮМ. Адрес: ФГБУН ФИЦ «Институт биологии южных морей имени А. О. Ковалевского РАН», пр-т Нахимова, 2, г. Севастополь, 299011, Российская Федерация.
Тел.: +7 8692 54-06-49.
E-mail: *mbj@imbr-ras.ru*.

A. O. Kovalevsky Institute of Biology of the Southern Seas of RAS, Zoological Institute of RAS

publish scientific journal

Морской биологический журнал
Marine Biological Journal

- MBJ is an open access, peer reviewed (double-blind) journal. The journal publishes original articles as well as reviews and brief reports and notes focused on new data of theoretical and experimental research in the fields of marine biology, diversity of marine organisms and their populations and communities, patterns of distribution of animals and plants in the World Ocean, the results of a comprehensive studies of marine and oceanic ecosystems, anthropogenic impact on marine organisms and on the ecosystems.
- Intended audience: biologists, ecologists, biophysicists, hydrobiologists, radiobiologists, oceanologists, geographers, scientists of other related specialties, graduate students, and students of relevant scientific profiles.
- The articles are published in Russian and English.
- The journal is published four times a year.
- The subscription index in the “Russian Press” catalogue is E38872. The price is free.

You may order the journal

in the scientific information department of IBSS. Address: A. O. Kovalevsky Institute of Biology of the Southern Seas of RAS, 2 Nakhimov avenue, Sevastopol, 299011, Russian Federation.
Tel.: +7 8692 54-06-49.
E-mail: *mbj@imbr-ras.ru*.